THE UNIVERSITY *of* EDINBURGH

ANALYSIS OF THE EXPRESSION AND FUNCTION OF MAMMALIAN CSP ISOFORMS

Oforiwa Afi Gorleku

A thesis presented for the degree of Doctor of Philosophy in Biomedical Sciences

The University of Edinburgh

April 2011

Abstract

Exocytosis, the fusion of intracellular vesicles with the plasma membrane, is fundamental to intercellular communication in multicellular organisms. This pathway facilitates the release or secretion of molecules from the cell. In addition, exocytosis is essential for delivery of resident proteins to the plasma membrane. There are two different pathways of exocytosis, constitutive and regulated exocytosis. Constitutive exocytosis occurs without regulation, e.g. pathways regulating the delivery of lipids and 'house-keeping' proteins to the plasma membrane or the secretion of antibodies and extra-cellular matrix components from the cell. In contrast, regulated exocytosis facilitates the controlled release of extra-cellular molecules or insertion of new membrane components only in response to a physiological signal. The most common signal for regulated exocytosis is an increase in intracellular Ca^{2+} concentration.

Several proteins function in exocytosis, and the membrane fusion step is widely believed to result from an interaction between SNARE (SNAP receptor) proteins on the vesicle membrane and plasma membrane. In neuroendocrine cells, these SNARE proteins are VAMP2, which is bound to vesicle membranes and syntaxin1A and SNAP25, which are associated with the plasma membrane. Several proteins have been implicated as SNARE regulators, such as NSF (N-ethylmaleimide-sensitive factor) and its cofactor α-SNAP, Munc18 and synaptotagmin. Another possible SNARE regulator is the cysteine string protein (CSP).

CSPα was first identified in *Drosophila melanogaster* and was later identified in *Torpedo* as a possible Ca^{2+}-channel regulator. Inactivation of the CSPα gene in *Drosophila* is lethal at an embryonic stage and in embryos synaptic vesicle exocytosis was decreased by ~50% at 22°C and was abolished at higher temperatures. These results provided strong evidence that CSPα has an important role in presynaptic neurotransmission. However, more recent work on CSPα null mice uncovered an important neuroprotective function for CSPα in brain, but also challenged the proposed function of CSPα in neuronal exocytosis, as no defect in this pathway was evident, at least in young animals. The only reported developmental abnormality of CSPα null mice was bilateral cryptorchidism, a failure of testicular descent during development. Interestingly, two additional CSP isoforms

were recently identified in mouse and human testis, CSPβ and CSPγ. One consequence of the identification of CSPβ and CSPγ is that they may complicate analysis of CSPα knockout mice.

Here, we have used a combination of techniques, cell systems and human brain samples to examine the function of CSPα in exocytosis, the expression of novel CSPα isoforms in testis, and expression changes of CSPα and its partner proteins in neurological disorders. Furthermore, we have initiated studies to examine how CSPα function is linked to cryptorchidism at the molecular level. My results show that CSPα depletion perturbs regulated exocytosis in neuroendocrine cells, but has no consistent effect on constitutive exocytosis. CSPα has been reported to have an important neuroprotective function; however, no significant changes in CSPα expression were detected in brain samples for schizophrenia, depression and bipolar disorder. Nevertheless the expression of specific CSPα binding partners was found to be significantly changed in some of these disorders. In addition to these studies focussing on CSPα function and expression in neuronal and neuroendocrine cells, studies were undertaken to analyse expression profiles of CSP isoforms in testis. This analysis found that CSPβ and CSPγ are exclusively expressed in testis, and that mRNA transcription of both isoforms is initiated with sexual maturation. Furthermore expression of both isoforms is restricted to germ cells, whereas CSPα is expressed throughout testes. Previous work has shown that the secretory hormone INSL3, which is exclusively expressed in testicular Leydig cells, is involved in the development of cryptorchidism. Confocal microscopic analysis revealed that CSPα and INSL3 colocalise on vesicles in Leydig cells, suggesting the intriguing possibility that CSPα inactivation might cause cryptorchidism due to a loss of INSL3 secretion.

Table of Contents

Abstract I

Table of Contents III

List of Figures VIII

List of Tables XI

Acknowledgments XII

Author's Declaration XIII

Abbreviations XIV

Publications XX

CHAPTER ONE: INTRODUCTION ..... - 1 -

1.1 The secretory pathway ..... - 2 -

1.2 Exocytosis ..... - 2 -

1.2.1 Exocytosis pathways occurring in testis ..... - 4 -

1.2.2 Vesicle cycling and endocytosis ..... - 7 -

1.3 SNARE proteins: regulators of membrane fusion ..... - 8 -

1.3.1 VAMP2 (Synaptobrevin 2) ..... - 10 -

1.3.2 Syntaxin 1A ..... - 11 -

1.3.3 SNAP25 ..... - 13 -

1.4 SNARE protein regulators ..... - 14 -

1.4.1 NSF and α-SNAP ..... - 14 -

1.4.2 Synaptotagmin ..... - 15 -

1.4.3 Munc18 ..... - 16 -

1.4.4 Complexins ..... - 17 -

1.4.5 Rab proteins ..... - 18 -

1.5 Cysteine String Protein (CSP) ..... - 19 -

1.5.1 Discovery of CSP ..... - 19 -

1.5.2 Intracellular distribution of CSP ..... - 23 -

1.5.3 The role of CSP in exocytosis and as possible Ca^{2+}-regulator..... - 24 -
1.5.4 Protein interactions of CSP ..... - 30 -
1.5.4.1 Heat-shock proteins and co-chaperones..... - 30 -
1.5.4.2 Ca^{2+} channels ..... - 33 -
1.5.4.3 VAMP ..... - 35 -
1.5.4.4 Syntaxin ..... - 36 -
1.5.4.5 SNAP25 ..... - 37 -
1.5.4.6 Synaptotagmin ..... - 38 -
1.5.4.7 Homomeric interactions of CSP..... - 39 -
1.5.5 Phospho-regulation of CSP ..... - 39 -
1.5.6 CSP domains important for regulated exocytosis ..... - 40 -
1.5.7 Additional functions of CSP ..... - 43 -
1.5.8 Palmitoylation and membrane-association of CSP ..... - 44 -
1.5.9 Phenotype of CSP null mice ..... - 46 -
1.5.10 Mammalian CSP isoforms ..... - 53 -
1.6 Aims and hypothesis ..... - 57 -

CHAPTER TWO: MATERIAL AND METHODS ..... - 59 -
2.1 Material and suppliers..... - 60 -
2.1.1 Chemicals..... - 60 -
2.1.2 Molecular biology reagents..... - 60 -
2.1.3 Small interference RNA..... - 61 -
2.1.4 Primers ..... - 61 -
2.1.4.1 PCR primers..... - 61 -
2.1.5 Plasmids ..... - 64 -
2.1.6 Cell culture plastics and media ..... - 64 -
2.1.7 Antibodies ..... - 65 -
2.1.7.1 Primary antibodies ..... - 65 -

2.1.7.2 Secondary antibodies ..... - 68 -
2.1.8 Radioactive materials ..... - 68 -
2.1.9 Animal tissues ..... - 68 -
2.1.10 Mammalian cell lines ..... - 68 -
2.2 Animal dissection ..... - 69 -
2.2.1 Sperm isolation ..... - 69 -
2.2.2 Collection of rat-tail collagen ..... - 69 -
2.3 Molecular biology ..... - 70 -
2.3.1 Standard molecular biology protocols ..... - 70 -
2.3.2 DNA amplification by polymerase chain reaction (PCR) ..... - 70 -
2.3.3 Amplification of CSPβ, CSPγ and INSL3 from rat testis ..... - 71 -
2.3.3.1 RNA purification ..... - 71 -
2.3.3.2 Reverse transcription (RT) PCR of CSPβ,CSP γ and INSL3 ..... - 72 -
2.3.3.3 Cloning of CSPβ, CSPγ and INSL3 into pQE30 and eGFP-C2 vectors ..... - 72 -
2.3.4 RT-PCR analysis of CSP isoforms mRNA expression in mammalian tissues ..... - 73 -
2.3.5 Site-directed mutagenesis ..... - 74 -
2.3.6 Quantitative real-time PCR ..... - 74 -
2.3.7 Agarose gel electrophoresis ..... - 75 -
2.3.8 DNA purification from agarose gels ..... - 75 -
2.3.9 Restriction endonuclease digestion of DNA ..... - 76 -
2.3.10 Ligation of insert DNA with plasmid vector ..... - 76 -
2.3.11 Transformation of competent bacterial cells ..... - 77 -
2.3.12 Small-scale (miniprep) plasmid purification ..... - 77 -
2.3.13 Large-scale (maxiprep) plasmid purification ..... - 78 -
2.3.14 Glycerol stocks ..... - 80 -
2.3.15 Spectrophotometric quantification of DNA and RNA ..... - 80 -
2.3.16 DNA sequencing ..... - 80 -

2.4 Mammalian cell culture ..... - 81 -
2.4.1 Storage and reuse of mammalian cells ..... - 81 -
2.4.2 Culturing mammalian cells ..... - 81 -
2.4.3 Small interference RNA transfection into mammalian cells ..... - 82 -
2.4.4 Plasmid DNA transfection into mammalian cells ..... - 83 -
2.5 Purification of recombinant CSP proteins ..... - 83 -
2.6 Protein biochemistry ..... - 85 -
2.6.1 Sodium dodecyl sulphate polyacrylamide gel electrophoresis (SDS-PAGE) ..... - 85 -
2.6.2 Coomassie blue staining ..... - 86 -
2.6.3 Immunoblotting ..... - 86 -
2.6.4 Protein cross-linking ..... - 88 -
2.6.5 Lysis of mammalian tissues ..... - 88 -
2.6.6 Bicinchoninic acid (BCA) assay ..... - 88 -
2.6.7 Fractionation ..... - 89 -
2.6.7.1 Fractionation of mammalian tissues ..... - 89 -
2.6.7.2 Fractionation of mammalian cell lines ..... - 90 -
2.6.8 Isolation of Leydig, germ and Sertoli cells from rat testis ..... - 90 -
2.6.9 Chemical depalmitoylation of palmitoylated proteins ..... - 92 -
2.6.10 Constitutive exocytosis assay ..... - 92 -
2.6.11 Exocytosis assay ..... - 93 -
2.6.12 [^{3}H]-dopamine assay ..... - 93 -
2.6.13 Human growth hormone (hGH) assay ..... - 94 -
2.7 Indirect immunofluorescence ..... - 95 -
2.8 Immunohistochemistry ..... - 96 -
2.8.1 Fixation, paraffin embedding and sectioning of testis ..... - 96 -
2.8.2 Immunolabelling of testis sections ..... - 97 -
2.9 Optical microscopy ..... - 98 -
2.9.1 Widefield microscopy ..... - 98 -

2.9.2 Confocal microscopy ..... - 98 -

2.10 Data analysis ..... - 99 -

CHAPTER THREE: ANALYSIS OF CSPα FUNCTION IN EXOCYTOSIS BY SIRNA-MEDIATED KNOCKDOWN ..... - 100 -

3.1 Introduction ..... - 101 -

3.2 Results ..... - 103 -

3.2.1 Successful knock down of CSPα in PC12 cells ..... - 103 -

3.2.2 CSPα depletion results in a decreased secretion of ^{3}H-dopamine and human growth hormone from PC12 cells ..... - 105 -

3.2.3 Chemical cross-linking experiments reveal that CSPα participates in distinct protein-protein interaction following elevation of $[Ca^{2+}]_i$ ..... - 114 -

3.2.4 Expression of CSPα in cell types that do not have defined regulated exocytosis pathways ..... - 116 -

3.2.5 CSPα depletion in HeLa-C1 cells shows inconsistent results for constitutive exocytosis ..... - 118 -

3.3 Discussion ..... - 125 -

CHAPTER FOUR: ANALYSIS OF EXPRESSION LEVELS OF CSPα AND INTERACTING PARTNERS IN POST-MORTEM BRAIN SAMPLES FROM PATIENTS WITH BIPOLAR DISORDER, MAJOR DEPRESSION AND SCHIZOPHRENIA ..... - 129 -

4.1 Introduction ..... - 130 -

4.2 Results ..... - 134 -

4.2.1 Human post-mortem samples ..... - 134 -

4.2.2 Samples from patients with major depression displayed a significant reduction of syntaxin expression in cortex compared with controls ..... - 140 -

4.2.3 Patients with schizophrenia showed no significant change in protein expression levels compared with controls ..... - 140 -

4.2.4 Significant changes in HSP70 and syntaxin expression in bipolar disorder ..... - 150 -

4.3 Discussion ..... - 150 -

CHAPTER FIVE: EXPRESSION AND LOCALISATION OF THE CYSTEINE STRING PROTEIN ISOFORMS CSPβ AND CSPγ ..... - 162 -

5.1 Introduction ..... - 163 -

5.2 Result ..... - 164 -

5.2.1 Characterisation of CSP isoform-specific antibodies ..... - 164 -

5.2.2 Membrane-association and palmitoylation of CSPβ ..... - 168 -

5.2.3 Localisation of CSPβ and CSPγ in germ cells ..... - 176 -

5.3 Discussion ..... - 183 -

CHAPTER SIX: LOCALISATION AND MEMBRANE TARGETING OF CSPα IN LEYDIG CELLS ..... - 188 -

6.1 Introduction ..... - 189 -

6.2 Results ..... - 190 -

6.2.1 Colocalisation of CSPα and INSL3 in R2C Leydig cells ..... - 190 -

6.2.2 Analysis of targeting signals in CSPα ..... - 193 -

6.2.3 Successful depletion of CSPα in R2C cells ..... - 196 -

6.3 Discussion ..... - 196 -

CHAPTER SEVEN: CONCLUSION ..... - 201 -

BIBLIOGRAPHY ..... - 208 -

List of Figures

Figure 1.1: Schematic diagram of the domains of mammalian Cysteine String Protein (CSP) ..... - 21 -

Figure 1.2: Alignment of CSP in a section of vertebrates. ..... - 22 -

Figure 1.3: Alignment of rat CSP isoforms. ..... - 54 -

Figure 1.4: Alignment and phylogenetic tree of CSPβ in a section of vertebrates - 56 -

Figure 3.1: siRNA-mediated depletion of CSPα in PC12 cells. ..... - 104 -

Figure 3.2: CSPα depletion with siRNA and quantification of knock down efficiency. ..... - 106 -

Figure 3.3: SNARE protein levels in CSPα-depleted cells. ..... - 107 -

Figure 3.4: Reduced CSPα expression levels correlates with a decreased level of Ca^{2+}-stimulated exocytosis in PC12 cells. ..... - 109 -

Figure 3.5 Effect of CSPα siRNAs on dopamine accumulation in PC12 cells. . - 112 -

Figure 3.6: Growth Hormone secretion from PC12 cells treated with CSPα siRNA... - 113 -

Figure 3.7: Chemical cross-linking of CSPα in PC12 cells. ..... - 115 -

Figure 3.8: Expression of CSPα in mammalian cell lines. ..... - 117 -

Figure 3.9: Visualisation of Constitutive Secretion in HeLa-C1 cells. ..... - 119 -

Figure 3.10: Quantitative measurement of constitutive secretion by immunoblotting. - 120 -

Figure 3.11: siRNA-mediated depletion of CSPα in HeLa cells. ..... - 122 -

Figure 3.12: Quantitation of constitutive exocytosis in HeLa-C1 cells treated with CSPα siRNA. ..... - 123 -

Figure 4.1: Protein expression in Cerebellum in depression disorder ..... - 141 -

Figure 4.2: Protein expression in Cortex in depression disorder. ..... - 143 -

Figure 4.3: Protein expression in Hippocampus in depression disorder. ..... - 144 -

Figure 4.4: Protein expression in Thalamus in depression disorder. ..... - 145 -

Figure 4.5: Protein expression in Cerebellum in schizophrenia disorder. ..... - 146 -

Figure 4.6: Protein expression in Cortex in schizophrenia disorder. ..... - 147 -

Figure 4.7: Protein expression in Hippocampus in Schizophrenia disorder. ..... - 148 -

Figure 4.8: Protein expression in Thalamus in Schizophrenia disorder..... - 149 -

Figure 4.9: Protein expression in Cerebellum in Bipolar disorder..... - 151 -

Figure 4.10: Protein expression in Cortex in Bipolar disorder. ..... - 153 -

Figure 4.11: Protein expression in Hippocampus in Bipolar disorder. ..... - 155 -

Figure 4.12: Protein expression in Cortex in Bipolar disorder. ..... - 157 -

Figure 5.1: Analysis of CSP isoform-specific antibodies ..... - 165 -

Figure 5.2: Tissue distribution of CSP isoforms. ..... - 167 -

Figure 5.3: CSP expression in brain regions. ..... - 169 -

Figure 5.4: Membrane binding and palmitoylation of CSPα ..... - 171 -

Figure 5.5: Palmitoylation and membrane binding of GFP-tagged CSP isoforms…… ..... - 172 -

Figure 5.6: Membrane binding and palmitoylation of GFP-tagged CSPα and CSPβ chimeric constructs ..... - 175 -

Figure 5.7: Expression of CSP isoforms during testicular maturation. ..... - 177 -

Figure 5.8: Expression of CSP isoforms in sperm ..... - 178 -

Figure 5.9: Detection of CSP isoforms in Testis cell types. ..... - 179 -

Figure 5.10: Localisation of CSPα in testis slices. ..... - 181 -

Figure 5.11: Effect of busulphan treatment on CSP expression levels. ..... - 182 -

Figure 5.12: Localisation of CSP isoforms in germ cell populations. ..... - 184 -

Figure 6.1: Detection of endogenous and over-expressed GFP-tagged CSPα in testis cell types. ..... - 191 -

Figure 6.2: CSPα and INSL3 localisation on moving vesicles in R2C Leydig cells…. ..... - 192 -

Figure 6.3: Analysis of CSPα targeting in R2C Leydig cells. ..... - 195 -

Figure 6.4: Targeting of CSPα cysteine-string domain mutants in R2C Leydig cells... ..... - 197 -

Figure 6.5: siRNA-mediated depletion of CSPα in Leydig cells. ..... - 198 -

List of Tables

Table 1.1: Effects of CSP over-expression. ..... - 28 -

Table 1.2: Effects of CSP mutations on exocytosis in relation to over-expression of wild type CSP, which has an inhibitory effect on exocytosis. ..... - 42 -

Table 2.1: Small interference RNA oligonucleotides (5'>3') for rat CSPα in rat - 61 -

Table 2.2: Small interference RNA oligonucleotides (5'>3') for human CSPα .. - 61 -

Table 2.3: Oligonucleotide primers (5'>3') for DNA amplification of CSP isoforms and INSL3 from mammalian tissues ..... - 61 -

Table 2.4: Oligonucleotide primers (5'>3') for CSPβ and CSPγ having HindIII (AAGCTT) and BamHI (GGATCC) restriction sites incorporated, which allowed the amplified DNA to be inserted into pQE30 and pEGFP-C2 vectors ..... - 62 -

Table 2.5: Oligonucleotide primers (5'>3') used to generate CSPα N-terminal truncation mutants incorporating HindIII (AAGCTT) and BamHI (GGATCC) restriction sites, which allowed the amplified DNA to be inserted into the pEGFP-C2 vector ..... - 62 -

Table 2.6: Oligonucleotide primers (5'>3') to generate CSPα– and CSPβ–chimeras incorporating or deleting EcoRI (GAATTC) restriction sites through site-directed mutagenesis ..... - 63 -

Table 2.7: Oligonucleotide primers (5'>3') used for quantitative real-time PCR in rat testicular cells samples ..... - 63 -

Table 2.8: Oligonucleotide primers (5'>3') used for quantitative real-time PCR in mouse testicular cells ..... - 64 -

Table 4.1: Summary of neuropsychiatric disorder characteristics. ..... - 132 -

Table 4.2: Anonymised details of the human post-mortem control patients. ..... - 135 -

Table 4.3: Anonymised details of the human post-mortem depression patients. - 136 -

Table 4.4: Anonymised details of the human post-mortem schizophrenia patients……- 137 -

Table 4.5: Anonymised details of the human post-mortem bipolar patients. ..... - 138 -

Table 4.6: Average age, gender ratio and PMI (post mortem interval (hours)) of human post-mortem depression, schizophrenia and bipolar samples. ..... - 139 -

Acknowledgments

Firstly I would like to thank Dr Luke Chamberlain for picking me as his PhD student, not knowing what he got himself into. It was a delight working with you and having you as my supervisor. I was able to joke around with you and you made me laugh all the time. But to get back to work, I was always able to come to your office at any time and discuss my work with you. You guided and encouraged me all the time. Even if the project looked pretty doomed, you somehow got me working harder and finish the project.

I would like to thank Jenny who is a great colleague and became a really good friend. Oh my god, what would I have done without the Queen of Site-Directed-Mutagenisis. However, you were not only useful for mutagenesis, it was good to have you around and talk 'occasionaly' about non scientific, girly things.

Furthermore I would like to thank Giselle, Sarah, Annya and Ali who also became really good friends. We were able to talk about our little problems in the lab, but most important were our conversations outside work. Always very amusing!

A big thank you to my family and friends, who are distributed all over the world. Though we are so far apart, we always managed to support each other. Most of you did not understand what my work was about and especially what I was complaining about, but you always took your time and listened. You all know exactly how hard it was for me and how much a miss you all, but you always reminded me why I was here, who I am and gave me my strength and confidence back, that I lost from time to time. This just shows that I've got the best family and friends in the world.

Last but not least I would like to thank my parents, Albert and Baaba, and my brother Kwaku, who always support me whatever I'm doing. I am so grateful that you always trusted my decisions, though I sometimes didn't know myself what exactly I am doing. The last four years were not always easy for me and I was always able to call you at any time and you were always there for me. At this point I want to say that i love you very much and I am very proud that we are a very close family.

Author's Declaration

The contents of this thesis and the investigations presented herein, unless otherwise stated, were conducted by the author. No part of this work has been, or is being, submitted for any other degree or qualification at the University of Edinburgh or at any other institution:

……..

Oforiwa Afi Gorleku

April 2011

Abbreviations

%	percent
°C	degrees Celsius
µg	microgram
µl	microlitre
^{3}H	Tritium
A	alanine
A	ampere
ADP	adenosine diphosphate
APS	ammonium persulfate
ATP	adenosine triphosphate
BCA	bicinchoninic acid
BoNT	botulinum toxin
bp	base pair
BSA	bovine serum albumin
C	Carbon
C-	carboxy-(terminus)
C	cysteine
C. elegans	*Caenorhabditis elegans*
Ca^{2+}	calcium
$CaCl_2$	calcium chloride
cAMP	cyclic adenosine monophosphate
cDNA	complementary DNA
CFTR	cystic fibrosis transmembrane conductance regulator
cm^2	square metre
CNS	Central nervous system
CO_2	carbon dioxide gas
CSP	cysteine string protein

D	aspartate
DEPC	diethylpyrocarbonate
dH_2O	distilled water
DMSO	dimethyl sulphoxide
DNA	desoxyribonucleic acid
dNTP	2'-deoxynucleoside 5'triphosphate
Drosophila	*Drosophila melanogaster*
DTT	dithio-1,4-threitol
E	glutamic acid
E. coli	*Escherichia coli*
ECL	enhanced chemiluminescence
EDTA	Ethylenediaminetetraacetic acid
EGFP	enhanced green fluorescence protein
ER	endoplasmic reticulum
FBS	foetal bovine serum
FLIM	Fluorescence lifetime imaging microscopy
FRET	Förster resonance energy transfer
FSH	follicle-stimulating hormone
G protein	guanine nucleotide-binding protein
g	gram
g	gravitational force
GABA	gamma-aminobutyric acid
GAPDH	glyceraldehydes 3-phosphate dehydrogenase
GDP	guanosine diphosphate
GEF	guanine nucleotide exchange factor
GLUT	glucose transporter
GST	glutathione S-tranferase
GTP	guanosine triphosphate

H	histidine
H_2O	water
HA	haemagglutinin
HA	hydroxylamine
HCl	hydrochloric acid
HEK293	human embryonic kidney 293 cells
HeLa	Henrietta Lacks cells
HEPES	4-(2-hydroxyethyl)-1-piperazineethanesulphonic acid
hGH	human growth hormone
HS	horse serum
HSC70	heat shock cognate protein of 70 kDa
HSP40	heat shock protein of 40 kDa
HSP60	heat shock protein of 60 kDa
HSP70	heat shock protein of 70 kDa
HSP90	heat shock protein of 90 kDa
Hz	Hertz
I	isoleucine
INSL3	insulin-like hormone 3
K	lysine
K	lysine
kb	kilo-base pair
KCl	potassium chloride
kDa	kiloDalton
KH_2PO_4	potassium dihydrogen phosphate
KO	knock out
L	leucine
L	litre
LDCV	large dense core vesicle

LH	luteinizing hormone
MBq	mega becquerel
mg	milligram
$MgCl_2$	magnesium chloride
min	minute
ml	millilitre
mm	millimetre
mM	millimolar
mRNA	messenger RNA
N-	amino-(terminus)
N	asparagine
n	statistical sample
Na_2HPO_4	disodium hydrogen phosphate
NaCl	sodium chloride
NaOH	sodium hydroxide
ng	nanogram
nm	nanometre
NMJ	Neuromuscular junction
NSF	N-ethylmaleimide-sensitive factor
p	post-natal
P	proline
P	proline
PAGE	polyacrylamide gel electrophorese
PBS	phosphate-buffered saline solution
PC12	pheochromocytoma cells
PCR	polymerase chain reaction
Pfu	*pyrococcus furiosis*
pg	pictogram

PK	protein kinase
PM	plasma membrane
Q	glutamine
qRT PCR	quantitative real-time PCR
R	arginine
RNA	ribonucleic acid
Rnase	ribonuclease
RT	reverse transcription
S	serine
S	sulphate
SCAMP1	secretory carrier-associated membrane protein 1
SDS	sodium dodecyl sulphate
SDS-PAGE	sodium dodecyl sulphate polyacrylamide electrophorese
SEM	standard error of mean
SGT	small glutamine-rich tetratricopeptide repeat containing protein
siRNA	small interference RNA
SNAP	soluble NSF attachment protein
SNAP23	synaptosomal-associated protein of 23 kDa
SNAP25	synaptosomal-associated protein of 25 kDa
SNARE	soluble-N-ethylmaleimid-sensitive factor attachment protein receptor
SV	synaptic vesicle
T	threonine
Taq	*Thermus aquaticus*
TeTx	tetanus toxin
TGN	trans Golgi network
Torpedo	*Torpedo californica*
TTX	tetrodotoxin
U	uracil

UV	ultraviolet
V	valine
V	volt
v/v	volume per volume
VAMP	vesicle-associated membrane protein
VGAT	vesicular GABA transporter
VGCC	voltage-gated calcium channels
w/v	weight per volume
Y	tyrosine
Δ	Delta
α	alpha
β	beta
γ	gamma

Publications

The following papers were published during the course of this thesis:

Gorleku, O.A., and Chamberlain, L.H. (2010). Palmitoylation and Testis-Enriched Expression of the Cysteine-String Protein Beta Isoform. Biochemistry *49* (25), 5308-5313

Greaves, J., Gorleku, O.A., Salaun, C., and Chamberlain, L.H. (2010). Palmitoylation of the SNAP25 protein family: specificity and regulation by DHHC palmitoyl transferases. J Biol Chem *285* (32), 24629-24638.

CHAPTER ONE: INTRODUCTION

1.1 The secretory pathway

The invention of the electron microscope facilitated a detailed characterisation of compartmentalisation in eukaryotic cells. Seminal work from George Palade (1975) paved the way for a description of the 'secretory pathway' (Palade, 1975). Proteins destined to be secreted from cells are translocated across the endoplasmic reticulum (ER) membrane, and their correct folding and maturation begins at this stage. The proteins are then packaged into membrane–bound vesicles that bud out from the ER membrane and subsequently fuse with Golgi membranes. In the Golgi, secretory proteins may undergo additional processing steps, such as glycosylation. Classical secretion models suggest that proteins then move through the Golgi stacks in a directed fashion (cis → medial → trans) (Rothman and Orci, 1992). Budding of membrane vesicles from the trans Golgi is followed by fusion with the plasma membrane, which releases or 'secretes' soluble proteins to the cell exterior. This secretory pathway is not only a mechanism to deliver proteins to the cell exterior, but also functions to transport membrane proteins to various locations in the cell including Golgi, endosomes, lysosomes and the plasma membrane (Rothman and Orci, 1992).

The secretory pathway is fundamental to generate and maintain subcellular compartments and organelles, and for cell growth and division. Genetic and biochemical analyses have demonstrated that many of the components of the secretory pathway are universal and highly conserved from yeast to humans (Rothman and Orci, 1992).

1.2 Exocytosis

Exocytosis occurs when an intracellular membrane-bound organelle fuses with the plasma membrane. Exocytosis is a fundamental process that allows insertion of proteins into the plasma membrane, and mediates the secretion of soluble cargo to the cell exterior (Kelly, 1985). Fusion with the plasma membrane occurs in all cell types without temporal regulation; this particular type of fusion is called constitutive

exocytosis. Constitutive exocytosis mediates the delivery of newly-synthesised 'housekeeping' proteins to the plasma membrane and mediates the secretion of molecules such as plasma proteins, antibodies and extracellular matrix components. In specialised cells, such as neurons, neuroendocrine, endocrine and exocrine cells, sperm and eggs, an additional form of exocytosis occurs, termed 'regulated exocytosis' (Burgoyne and Morgan, 2003). This process ensures the controlled release of vesicle/granule contents following a physiological signal. Most commonly this signal is a rise in intracellular calcium concentrations (Llinas *et al.*, 1981; Adler *et al.*, 1991; Neher and Sakaba, 2008).

Two main types of vesicles typically undergo regulated exocytosis. On one hand there are so-called secretory granules, which contain mostly larger molecules, such as polypeptides, hormones or proteins. Secretory granules are typically > 100 nm in diameter and may contain a mixture of molecules. Upon a signal almost the entire pool of storage granules might be emptied, allowing sustained secretion for seconds or minutes. Secretory granules containing protein cargo form at the trans Golgi network (Tooze *et al.*, 2001). Another type of vesicles are smaller secretory vesicles, such as synaptic vesicles, which typically have a clear morphology when visualised by electron microscopy (Katz, 1969). These vesicles are generally < 50 nm in diameter. After nerve terminal depolarisation, synaptic vesicles release their content almost instantly (Bruns and Jahn, 1995). In neurons, synaptic vesicles are thought to form distinct pools: the ready-releasable pool, where vesicles are docked at the plasma membrane and are immediately ready for release, and the reserve pool (Schweizer and Ryan, 2006).

Although secretory vesicles and granules display distinct kinetics of fusion, both types of vesicle undergo similar steps in exocytosis. 'Priming', which is dependent on ATP hydrolysis, is a poorly-defined process that may involve reorganisation of the actin cytoskeleton (Roth and Burgoyne, 1994) to recruit vesicles to the plasmalemmal space, and also the modification of SNARE proteins by α-SNAP and NSF (Chamberlain *et al.*, 1995; Banerjee *et al.*, 1996) (see 1.4.1). Dependent upon the specific system of regulated exocytosis, priming may occur before or after vesicle 'docking', the term used to describe vesicles that are physically attached to the

plasma membrane. Docked vesicles likely undergo several maturation steps (priming) before they fuse with the plasma membrane following an increase in intracellular calcium concentration. This is suggested because only a subset of docked synaptic vesicles exocytose in response to nerve terminal depolarisation (Schikorski and Stevens, 2001). The fusion of vesicles occurs by the formation of fusion pores that can open transiently and reclose rapidly (termed 'kiss and run'), or the fusion pore can expand and lead to full exocytosis where the vesicle completely collapses into the plasma membrane (Valtorta *et al.*, 2001). These different kinds of fusion events allow a controlled amount of release that occurs per secretory granule/vesicle. There is considerable controversy in the field over how prevalent 'kiss-and-run' exocytosis is, particularly for synaptic vesicle fusion (Rizzoli and Jahn, 2007).

A very large number of proteins have been shown to function in exocytosis, and the membrane fusion step is widely believed to result from an interaction between SNARE (SNAP receptor) proteins on the vesicle membrane and plasma membrane (Jahn and Scheller, 2006)(see 1.3).

1.2.1 Exocytosis pathways occurring in testis

Testes execute two basic functions, sperm production and testosterone secretion. Three major cell types are located in testis; germ, sertoli and leydig cells. The adult mammalian testis contains several types of germ cells. Spermatogonial stem cells are located at the luminal side of the basal membrane, where they undergo mitotic divisions to become spermatogonia and primary spermatocytes. After further rounds of meiotic divisions, haploid spermatids are produced, which eventually form spermatozoa. Sertoli cells are essential to organise and orchestrate spermatogenesis during puberty (Mruk and Cheng, 2004). Depletion and loss of function of Sertoli cells lead to massive degeneration of haploid cells and an almost complete loss of germ cells (Russell *et al.*, 2001) and the number of Sertoli cells present in the testis determines the number of sperm produced in adulthood. Leydig cells secrete

testosterone, which is required for the development of internal and external male genitalia, and is essential for male sexual differentiation (Shalet, 2009).

Endocrine control of testicular function is mediated by the hypothalamic-pituitary-testicular axis. The hypothalamus secretes gonadotrophin-releasing hormone, which stimulates the pituitary gland to release luteinizing-hormone (LH) and follicle-stimulating hormone (FSH). FSH accelerates the rate of Sertoli cell proliferation. LH stimulates testosterone biosynthesis, by binding to the luteinizing-hormone receptor (LHR) (Dufau, 1998; Scott *et al.*, 2009). This activates adenylate cyclase, leading to an increased production of intracellular cAMP (Dufau, 1988) and mediates the transport of cholesterol to the inner mitochondrial membrane, where the first enzyme is localised that initiates the conversion pathway from cholesterol to testosterone. The initial step is the conversion of C_{27} cholesterol to the C_{21} steroid, pregnenolone, which is catalysed by the cytochrome P450 enzyme cholesterol side chain cleavage ($P450_{SCC}$). Pregnenolone diffuses across the mitochondrial membranes and is further metabolised by enzymes associated with the smooth endoplasmic reticulum. Pregnenolone is catalysed to progesterone by 3β-hydroxysteroid dehydrogenase/Δ^5-Δ^4-isomerase (3βHSD). The next enzyme, cytochrome P450 enzyme 17α-hydroxylase/C_{17-20} lyase ($P450_{17\alpha}$), catalyses two distinct reactions; the hydroxylation of progesterone at C_{17} and subsequent cleavage of the two-carbon side-chain to obtain the C_{19} steroid androstenedione. The final reaction is the reduction of the 17-ketone of androstenedione by 17-ketosteroid reductase to form testosterone (Payne and Youngblood, 1995). The level of testosterone secreted from Leydig cells is thought to be directly correlated with the level of synthesis (Shalet, 2009). Testosterone interaction with the androgen receptor expressed on Sertoli cells activates meiosis and maintains spermatogenesis.

Failures in testes development can cause infertility or expose the individual to risks of germ cell tumours. Cryptorchidism is a failure of one or two testes to descend into the scrotum (Jocelyn and Setchell, 1972) and is one of the most frequent congenital abnormalities in humans, occurring in 2-12 % of male births (Hutson *et al.*, 1994). Testicular descent from abdomen to scrotum occurs in two distinct phases; the trans

abdominal phase and inguino-scrotal phase (Hutson, 1985; Hutson *et al.*, 1994; Satokata *et al.*, 1995).

It has previously been shown that null mutations in Leydig cell insulin-like hormone (INSL3) cause the testes to be visibly absent at the scrotum, indicating bilateral cryptorchidism. The testicular size of $INSL3^{-/-}$ adult mice was also decreased, although at birth $INSL3^{+/+}$, $INSL3^{+/-}$ and $INSL3^{-/-}$ testes did not differ in size. Histological analysis revealed that the cryptorchid testes were normal at P0 but degenerated rapidly and progressively. The number of primary spermatocytes was also reduced and no spermatozoa were identified, indicating that INSL3 may be required for normal mature testicular function in addition to testicular descent. Serum analysis showed that testosterone levels in $INSL3^{-/-}$ mice were similar to wild type mice and $INSL3^{-/-}$ male mice exhibited androgen-dependent behaviour, such as normal mounting and copulatory behaviour. Furthermore, after copulation with female mice ejaculate was found in female vaginal plugs, indicating that INSL3 is not involved in androgen production. Scanning electron microscopy (SEM) showed that $INSL3^{-/-}$ neonate testes remained adjacent to the lower pole of kidneys compared to wild type mice, in which testes descend and are located caudal to the bladder neck in the inguinal region. The wild type gubernaculae in male mice, which are embryonic structures that attach to the caudal end of the gonads, have a large bulb and a thick cord, however, $INSL3^{-/-}$ male mice had flat gubernaculae with a thin bulb and an elongated cord, which is similar to that found in females. Overall, the results from analysis of $INSL3^{-/-}$ mice are consistent with the notion that Leydig cells of the testes secrete INSL3, and that the gubernacular bulb is the target organ; furthermore the results revealed a key requirement of $INSL3^{-/-}$ for testicular descent. Similar to testosterone secretion, very little is known about the mechanisms of INSL3 secretion.

In contrast to $INSL3^{-/-}$ male mice, $INSL3^{-/-}$ females were morphologically normal, but showed impaired fertility with 22 % of the mutant females being infertile.

1.2.2 Vesicle cycling and endocytosis

Synaptic vesicle exocytosis has been extensively investigated. The central nervous system contains in the region of 100-200 vesicles in each synaptic terminal, and a mechanism is required to maintain this number of vesicles, particularly during sustained action potential firing. After fusion with the presynaptic plasma membrane, vesicles are recycled by endocytosis into a vesicle cluster at the active zone (Ceccarelli *et al.*, 1973; Ales *et al.*, 1999). Clathrin-dependent endocytosis is the major mechanism of synaptic vesicle retrieval, which involves a number of molecules, including clathrin, clathrin adaptors and dynamin (Murthy and De Camilli, 2003; Royle and Lagnado, 2003). Following retrieval, clathrin coated vesicles are uncoated, refilled with transmitter and returned to the active pool of cycling vesicles. In addition to conventional clathrin-mediated endocytosis, vesicle retrieval can also be achieved by bulk endocytosis. This type of endocytosis occurs only during intense neuronal activity (Cousin, 2009), and does not retrieve a single synaptic vesicle, but rather recruits a large area of the plasma membrane, which then forms new vesicles by budding from this bulk endosome compartment (Richards *et al.*, 2000; Evans and Cousin, 2007).

Physiological stimulation promotes the fusion of only a small number of vesicles located at the presynaptic terminal. These fusion-ready vesicles were identified as being morphologically ‘docked’ at the plasma membrane, and were termed the readily releasable pool (Schikorski and Stevens, 2001). Further experiments at the NMJ demonstrated that vesicles previously labelled by FM1-43 (indicating previous exocytosis) were released preferentially during subsequent stimulation, indicating the existence of a distinct recycling vesicle pool. After strong stimulation (5–10 Hz in frog NMJ, 30 Hz in *Drosophila* larval NMJ or prolonged high potassium application at the Calyx of Held) and FM1-43 uptake, only a subset of the vesicles are labelled, whereas others are resilient to labelling; these non-labelled vesicles are classified as belonging to the non-recycling pool (also termed ‘reserve’ pool) (Rizzoli and Betz, 2005).

1.3 SNARE proteins: regulators of membrane fusion

The driving force and key elements behind membrane fusion are widely believed to be the SNARE proteins (soluble-N-ethylmaleimide-sensitive factor attachment protein receptor).

The consensus view of membrane fusion is that SNARE proteins localised on opposing membranes drive fusion by using the free energy that is released during the formation of the highly stable four-helix SNARE bundle (Jahn and Scheller, 2006). The formation of the four helical bundle, which occurs as a zip starting from the N-termini towards the C-terminal membrane anchors, forms a tight connection between the plasma membrane and the vesicle, and formation of this complex is sufficient to drive fusion of lipid bilayers in vitro (Sutton *et al.*, 1998; Weber *et al.*, 1998).

SNARE proteins are found in all eukaryotes from yeast (e.g. *Saccharomyces cerevisae*), over plants (e.g. *Arabidopsis thaliana*) to humans. All SNARE proteins have a highly conserved SNARE motif in common, which is stretched over 60-70 amino acids in heptad repeats (Chapman *et al.*, 1994). Heptad repeats are composed of 7 amino acids where positions 1 and 4 are occupied by hydrophobic residues. When these heptad repeats form a helical secondary structure, the hydrophobic amino acids align on one face of the helix. The core SNARE complex is a coiled coil bundle of four such helices, with the centre of the bundle containing 16 stacked layers of interacting side chains (Sutton *et al.*, 1998). These layers are predominantly stabilised by hydrophobic interactions, but the central or '0' layer contains three highly conserved glutamine (Q) residues and one highly conserved arginine (R) residue (each provided by a different SNARE motif).

The majority of SNARE proteins have a single C-terminal transmembrane domain, however SNARE proteins can also be attached to membranes via post-translational lipidation. Originally the SNARE proteins were classified based upon their localisation. v-SNAREs were present on vesicle ('donor') membranes, and t-SNAREs were associated with acceptor (or target) membrane compartments. However, certain SNAREs function in several membrane fusion pathways and also with different interacting partners, and some fusion reactions involve identical membrane compartments ('homotypic') and thus the use of 'v' and 't' SNARE was not always appropriate. Thus, it was proposed that SNAREs be re-classified

dependent upon the amino acid they have at this zero layer position (Fasshauer *et al.*, 1998).

Seminal work from Rothman's group first proposed that idea that the interactions between SNARE proteins on opposing membranes were important for membrane fusion. Sollner *et al.* (1993a,b) identified a complex containing syntaxin 1 (Q-SNARE), SNAP25 (Q-SNARE) and VAMP (R-SNARE) which associated with α-SNAP and NSF (see 1.4.1), proteins that had already been identified as performing a key function in intracellular fusion pathways (Sollner *et al.*, 1993b). The syntaxin : SNAP25 : VAMP complex was isolated from brain and Rothman proposed that this specific SNARE complex was required for synaptic vesicle exocytosis. In support of this idea, work around the same time found that these three SNARE proteins were specifically cleaved by botulinum (BoNT) and tetanus neurotoxins (TeNT) (Blasi *et al.*, 1993a; Blasi *et al.*, 1993b; Schiavo *et al.*, 1993). BoNTs penetrate motor neurons at the neuromuscular junction and are inhibitors of acetylcholine release (Simpson, 1989). Schiavo *et al*. (1993) discovered that BoNT B and BoNT F, as well as tetanus toxin (TeTx) specifically cleave VAMP in rat brain homogenates. Botulinum neurotoxins A and E were shown to cleave SNAP25 near the C-terminus (Blasi *et al.*, 1993a; Schiavo *et al.*, 1993). In the same year it was also detected that BoNT C1 directly and selectively proteolyse syntaxin, which led to an inhibition of neurotransmission (Blasi *et al.*, 1993b). The potent inhibitory effects of these toxins on synaptic vesicle fusion pathways is strong evidence that SNAREs are essential for membrane fusion (Sollner *et al.*, 1993a; Sollner *et al.*, 1993b).

Rothman initially proposed that synaptic vesicles dock when vesicle-localised VAMP binds to its complementary Q-SNARE (syntaxin and SNAP25) at the plasma membrane. Indeed specific interactions mediated by SNAREs were proposed to determine the specificity of intracellular membrane fusion pathways (Sollner *et al.*, 1993a; Sollner *et al.*, 1993b). Interestingly, Sollner *et al.* (1993a,b) also identified synaptotagmin binding to SNARE complexes; this interaction was mutually exclusive with α-SNAP binding to the SNARE complex. Thus, a model for membrane fusion was proposed whereby vesicles dock at membranes by virtue of SNARE complex formation. Synaptotagmin binding to the complex was suggested to act as a clamp and prevent the vesicle from fusing with the membrane. Following

stimulation, Ca^{2+} binding to synaptotagmin was suggested to dissociate it from the complex allowing SNAP to bind recruit NSF (N-ethylmaleimide-sensitive factor). Subsequent ATP hydrolysis by NSF, which drives dissociation of the SNARE proteins, was proposed to drive membrane fusion (Sollner *et al.*, 1993b). However, this model was inconsistent with several reports published around the same time showing that membrane fusion/exocytosis could be triggered by Ca^{2+} in the absence of ATP, as long as previous 'priming' in the presence of ATP had occurred (Holz *et al.*, 1989). Indeed, later work demonstrated that R- (VAMP) and Q-SNAREs (syntaxin and SNAP25) were sufficient to drive fusion of membrane vesicles *in vitro* (Weber *et al.*, 1998). It was assumed that R- and Q-SNAREs might exist in a thermodynamically metastable state and that SNARE assembly leads to a lower energy status. The remaining energy could therefore be used for fusion. Current models now place NSF/SNAP action in SNARE disassembly and reactivation of SNAREs following membrane fusion (Jahn and Scheller, 2006).

1.3.1 VAMP2 (Synaptobrevin 2)

Vesicle-associated membrane protein (VAMP; also termed synaptobrevin) was initially isolated from a cDNA expression library from *Torpedo californica* electromotor nucleus mRNA and was found to be neuron specific (Trimble *et al.*, 1988; Sudhof *et al.*, 1989). Among several identified VAMP isoforms which function as R-SNAREs in membrane fusion, VAMP2 has been shown to be involved in regulated secretion in neuronal and neuroendocrine cells (Baumert *et al.*, 1989). VAMP2 is composed of 118 amino acids arranged into a short N-terminal proline rich sequence, a central SNARE motif and a C-terminal transmembrane region (Jahn and Sudhof, 1999). BoNT B and BoNT F, which specifically cleave VAMP (Link *et al.*, 1992; Schiavo *et al.*, 1992), penetrate motor neurons at the neuromuscular junction and block acetylcholine release, but some residual fusion is still observed (David *et al.*, 1998; Ashton and Dolly, 2000). It was not clear whether this remaining fusion was due to compensation by related R-SNAREs or if a low level of fusion events could occur independently of SNARE proteins. VAMP2 knock out mice ($VAMP2^{-/-}$) (Schoch *et al.*, 2001) die immediately after birth with the newborn mice

exhibiting a rounded appearance and a shoulder hump, with this striking body shape possibly indicating a function for VAMP2 in endocrine and fat cells (Lowe *et al.*, 1988; Baumert *et al.*, 1990; Olson *et al.*, 1997; Foran *et al.*, 1999). No changes were observed in expression of other synaptic proteins or the closely related isoforms VAMP1 and cellubrevin (VAMP3). In VAMP2$^{-/-}$ mice fast Ca^{2+}-triggered fusion of synaptic vesicles with the presynaptic membrane was decreased more than 100-fold in knockout cultures, confirming a key role for VAMP2 in synaptic transmission. However, spontaneous miniature excitatory currents showed only a 15 % reduction in frequency in mutant mice compared to control. This suggested that the synaptic release apparatus was still present, working at a lower efficiency, which was also observed previously in *Drosophila* and *C. elegans* VAMP2 null mutants (Deitcher *et al.*, 1998; Nonet *et al.*, 1998). These results suggested that VAMP2 may not be absolutely essential for vesicle fusion, but is a key player that controls the rate of fusion, especially for the fast Ca^{2+}-triggered fusion. Quantification of the rate of RRP (ready releasable pool) refilling in neurons in VAMP2$^{-/-}$ mice, revealed that depletion of VAMP2 showed a delay in refilling of the pool, perhaps also highlighting a function for this protein in synaptic vesicle endocytosis and recycling (Deak *et al.*, 2004). The defects shown in VAMP$^{-/-}$ mice indicate that VAMP2 may be an important component in the tight coupling of exocytosis and endocytosis. The differential effects of VAMP2 knock out on evoked and spontaneous release might suggest that these fusion events are not identical at the molecular level.

1.3.2 Syntaxin 1A

Syntaxin 1 was first identified by its co-immunoprecipitation from rat brain with a monoclonal antibody to the protein p65 (synaptotagmin) (Bennett *et al.*, 1992). Amino acid analysis identified a hydrophobic site at the C-terminus, which was proposed to be a possible membrane anchor. Further immunoprecipitation, fractionation, and indirect immunofluorescence experiments indicated that syntaxin 1 is an integral membrane protein localised on the plasma membrane site and oriented towards the cytoplasm (Bennett *et al.*, 1993). Two syntaxin 1 isoforms, syntaxin 1A

and syntaxin 1B were described, and syntaxin 1A has been the most thoroughly investigated of these isoforms. Syntaxin 1A is composed of 288 amino acids, with the SNARE motif flanked by an independently folded N-terminal domain (Habc) and a single transmembrane domain at the C-terminus (Inoue *et al.*, 1992). There are 15 members of the syntaxin family in mammals; all isoforms display a broad tissue distribution and are targeted to different subcellular compartments (Bennett *et al.*, 1993; Teng *et al.*, 2001).

The N-terminal Habc domain of syntaxin appears as a flexible arm in electron micrographs (Hanson *et al.*, 1997) and is common throughout the syntaxin family (Fasshauer *et al.*, 1999). Syntaxin interacts intramolecularly by folding its N-terminal domain onto the SNARE motif, resulting in a 'closed' conformation which inhibits SNARE assembly (Calakos *et al.*, 1994; Nicholson *et al.*, 1998; Dulubova *et al.*, 1999; Fiebig *et al.*, 1999). Munc13 and Munc18 have been shown to bind to the N-terminal domain of syntaxin (Pevsner *et al.*, 1994; Betz *et al.*, 1997).

Microinjection of the monoclonal antibody against syntaxin (HPC-1) in PC12 cells, demonstrated a reduction in Ca^{2+}-regulated secretion (Bennett *et al.*, 1993), confirming that syntaxin plays a role in regulated secretion. Surprisingly however, syntaxin 1A knock out mice ($Syx1A^{-/-}$), in which the protein was deleted at exons 9 and 10, unexpectedly exhibited normal glutamatergic and GABAergic fast synaptic transmission (Fujiwara *et al.*, 2006), but fear memory was impaired, suggesting that syntaxin 1A may be involved in synaptic plasticity. However, more recent work showed that syntaxin 1A knockout, by deletion of exon 3, resulted in embryonic lethality (McRory *et al.*, 2008). Four out of 204 offspring were born, and these $Syx1A^{-/-}$ mice showed only mild behavioural deficiencies, but were reduced in body weight, suggesting that syntaxin 1A might be important in embryonic development and not essential for brain function in post-natal mice.

1.3.3 SNAP25

To investigate the expression and developmental regulation of neuronal specific genes, the cDNA clone pMuBr8 (Branks and Wilson, 1986) was used to screen an adult mouse hippocampal cDNA library (Oyler *et al.*, 1989). One clone, which contained nearly the full-length DNA, was isolated, subcloned and sequenced. This clone encoded for a 206 amino acid protein and immunoblotting experiments recognised a 25 kDa synaptosomal protein (SNAP25) (Oyler *et al.*, 1989). SNAP25 is an unusual SNARE protein in that it contains two SNARE motifs on its C- and N-terminal domains, which are separated by a linker region (Hong, 2005). Electron microscopy revealed that SNAP25 is a presynaptic protein found throughout the CNS. SNAP25 is a hydrophilic protein and, in contrast to VAMP and syntaxin, lacks a transmembrane domain; SNAP25 is palmitoylated at cysteine residues in the linker domain which facilitates membrane attachment (Hess *et al.*, 1992). Two distinct SNAP25 isoforms have been identified, termed SNAP25A and SNAP25B (Bark and Wilson, 1994). These isoforms are splice variants, which differ only in 9 amino acids, but appear to have distinct functions (Sorensen *et al.*, 2003).

SNAP25 interacts with sxyntaxin1A and VAMP2 in neurons and neuroendocrine cells to promote membrane fusion (Sutton *et al.*, 1998). It was also shown that SNAP25 association with synaptotagmin 1 and 9 during Ca^{2+}-dependent exocytosis seems to be essential for triggering membrane fusion (Zhang *et al.*, 2002b; Rickman *et al.*, 2006).

Deletion of SNAP25 ($SNAP25^{-/-}$) in mice caused immediate death after birth (Washbourne *et al.*, 2002). Homozygous $SNAP25^{-/-}$ mutants were smaller in size than their wild type littermates at E18.5. It was observed that the mutant mice failed to exhibit either spontaneous movement or sensorimotor reflexes in response to mechanical stimuli, which indicated a loss of neuromuscular function. The $SNAP25^{-/-}$ foetus showed no EPPs (end-plate potentials) nor evoked contraction, however, surprisingly spontaneous mEPPs could be constantly recorded. Other work also showed that replacing SNAP25B with an extra copy of SNAP25A led to developmental abnormalities, seizures and early death, demonstrating that expression of both isoforms is important (Johansson *et al.*, 2008).

1.4 SNARE protein regulators

1.4.1 NSF and α-SNAP

NSF (N-ethylmaleimide-sensitive factor) was originally identified as a factor that reconstituted intra-Golgi vesicular transport after inactivation of membranes with the alkylating agent N-ethylmaleimide (NEM) (Block *et al.*, 1988; Beckers *et al.*, 1989). NSF contains two homologous AAA domains, which are signature modules of AAA (ATPases Associated with diverse cellular Activities) ATPases (White and Lauring, 2007). NSF is a soluble protein that forms hexamers (Fleming *et al.*, 1998).

It was shown that NSF required a membrane protein adaptor to bind to Golgi membranes and stimulate its ATPase activity (Weidman *et al.*, 1989; Clary *et al.*, 1990; Clary and Rothman, 1990; Morgan *et al.*, 1994). This protein was identified as SNAP (soluble NSF attachment protein), comprising three isoforms, α-, β- and γ-SNAP (Whiteheart *et al.*, 1993). The first nine α-helices of α-SNAP form an N-terminal sheet whose positively charged residues interact with the surface of the SNARE complex (Marz *et al.*, 2003). A role for NSF and SNAPs in neurotransmitter release was first indicated by their binding to SNARE proteins (Sollner *et al.*, 1993b; Jahn *et al.*, 1995; Poulain *et al.*, 1995). α-SNAP binds to the syntaxin/SNAP25 heterodimer, and association of VAMP with syntaxin/SNAP25 generates a third binding site for α-SNAP which induces the interaction with the hexameric NSF and forms a transient 20 S complex (Hanson *et al.*, 1995; Hayashi *et al.*, 1995; Wimmer *et al.*, 2001). NSF then drives the disassembly of the SNARE complex through ATP hydrolysis (Sollner *et al.*, 1993a). Binding to α-SNAP increases the ATPase activity of NSF to promote complex disassembly (Barnard *et al.*, 1997). NSF/SNAP action induce a conformational change in syntaxin (Hanson *et al.*, 1995), but are also capable of large conformational motions that may drive SNARE complex disassembly (Neuwald, 1999; Yu *et al.*, 1999). It is generally believed that NSF and SNAP may act as molecular chaperones, regulating the conformation of SNARE complexes by dissociating cis-SNARE complexes (Morgan and Burgoyne, 1995a); in contrast, trans-SNARE complexes were suggested to become functionally resistant to NSF/SNAP (Weber *et al.*, 2000).

Presynaptic injection of inhibitory NSF peptides into the squid giant synapse reduced nerve-evoked neurotransmitter release in an activity-dependent manner, and increased the number of docked vesicles, suggesting a post-docking pre-fusion role for NSF in exocytosis (Schweizer *et al.*, 1998). Similarly in PC12 NSF has been proposed to function in the priming stage (Banerjee *et al.*, 1996). Deletion of α-SNAP is embryonic lethal (Chae *et al.*, 2004; Hong *et al.*, 2004) but other experiments revealed that presynaptic injection of recombinant α-SNAP into squid giant synapse increased transmitter release, however injection of peptides which mimic α-SNAP inhibited release and reduced the number of cytoplasmic vesicles, indicating a requirement of SNAP in replenishing this vesicle pool (Chamberlain *et al.*, 1995; DeBello *et al.*, 1995; Morgan and Burgoyne, 1995b; Poulain *et al.*, 1995; Kibble *et al.*, 1996; He *et al.*, 1999; Xu *et al.*, 1999). These studies showed that the defects obtained with α-SNAP were similar to the effects seen with NSF (see above), suggesting again that both proteins act cooperatively in exocytosis.

1.4.2 Synaptotagmin

The calcium sensor synaptotagmin was identified by two different monoclonal antibodies as a 65 kDa protein (Matthew *et al.*, 1981). Immune competition experiments showed that synaptotagmin is expressed throughout neuronal and neuroendocrine cells on synaptic vesicles (Matthew *et al.*, 1981), and so far 16 members have been identified in vertebrates (Craxton, 2004). Synaptotagmin contains a single N-terminal transmembrane domain and two cytoplasmic repeats that are homologous to the C_2 domain of Ca^{2+}/phospholipid-dependent protein kinase; the C_2 domains in synaptotagmin are termed C_2A and C_2B (Perin *et al.*, 1990). Later work demonstrated that synaptotagmin binds to calcium and phospholipids in a ternary complex (Brose *et al.*, 1992; Davletov and Sudhof, 1993), suggesting that synaptotagmin may be involved in Ca^{2+}-triggered neurotransmitter release. This assumption was confirmed by microinjection of synaptotagmin mutants into neuronal cells, *Drosophila* (DiAntonio *et al.*, 1993; Littleton *et al.*, 1993) and *C.*

elegans (Nonet *et al.*, 1993), demonstrating an impaired function in neurotransmitter release.

Synaptotagmin I has been shown to display both Ca^{2+}-dependent and -independent interactions with SNARE proteins (Tucker *et al.*, 2003; Bowen *et al.*, 2005; Dai *et al.*, 2007), and these interactions together with lipid and Ca^{2+} binding are likely to be at the heart of synaptotagmin function in exocytosis. More recent work has also suggested a role for synaptotagmin-SNAP25 binding in vesicle docking (de Wit *et al.*, 2009).

Synaptotagmin null mice die within 48 hour after birth (Geppert *et al.*, 1994a) and analysis of neurotransmitter release in preparations from these animals revealed that Ca^{2+}-dependent exocytosis was decreased, whereas spontaneous synaptic activity was unaffected. Synaptotagmins are the prime candidates to couple intracellular increases in free calcium upon an action potential to exocytosis of synaptic vesicles (Geppert *et al.*, 1994b; Fernandez-Chacon *et al.*, 2001; Bai and Chapman, 2004); indeed mutations that decrease the Ca^{2+} affinity of synaptotagmin lead to an increased level of Ca^{2+} being required to stimulate synaptic vesicle exocytosis (Fernandez-Chacon *et al.*, 2001).

1.4.3 Munc18

Munc18 belongs to the family of cytosolic SM (Sec1p/Munc18) proteins which were initially discovered during genetic screens for mutants in yeast and *C. elegans* showing defects in membrane traffic and secretion (Brenner, 1974). Mutations in the yeast SM protein Sec1p and the *C. elegans* homologue Unc18 led to deficits in secretion (Brenner, 1974; Novick and Schekman, 1979; Novick *et al.*, 1980); other identified genetic alterations in these proteins also showed deficits in membrane fusion (Cowles *et al.*, 1994; Harrison *et al.*, 1994; Schulze *et al.*, 1994; Verhage *et al.*, 2000; Voets *et al.*, 2001).

A major focus has been on the interaction of Munc18 with syntaxin, and this interaction was originally demonstrated to inhibit the ability of syntaxin to form the ternary SNARE complex (Pevsner *et al.*, 1994). Munc 18 is composed of three domains that form an arch-shaped molecule with a central cleft (Misura *et al.*, 2000), and Munc18 is thought to prevent SNARE complex assembly by wrapping around syntaxin and holding it in a 'closed' conformation. However, more recent work has shown that Munc18 also binds by a different mode to short region of the N-terminal domain of syntaxin (Chen *et al.*, 2008). The interaction with syntaxin in its 'closed' conformation has been termed mode 1 and interaction with the N-terminal motif of syntaxin has been termed mode 2/3 (Burgoyne and Morgan, 2007; Dulubova *et al.*, 2007; Rickman *et al.*, 2007; Shen *et al.*, 2007). Mode 1 binding masks the SNARE motif of syntaxin (Burkhardt *et al.*, 2008), suggesting that this mode might be important to shield syntaxin from forming inappropriate SNARE interactions as it traffics through the ER and Golgi to reach the plasma membrane following its biosynthesis (Medine *et al.*, 2007). It has been also shown that binding of Munc18 to syntaxin in the 2/3 mode increases the rate of membrane fusion and SNARE complex formation *in vitro* (Khvotchev *et al.*, 2007; Shen *et al.*, 2007).

Knockout of Munc18 expression in mice resulted in a normally developed nervous system, but there was a complete loss of both spontaneous and stimulated secretion (Verhage *et al.*, 2000).

1.4.4 Complexins

Complexins are a family of four proteins in mammals (Reim *et al.*, 2005) and were identified as proteins which bind to SNARE complexes in a 1:1 stoichiometry (Ishizuka *et al.*, 1995; McMahon *et al.*, 1995; Ishizuka *et al.*, 1997; Chen *et al.*, 2002). Complexins interact through a central α-helical domain with the assembled four helix bundle of SNARE complexes, binding to the groove between the VAMP and syntaxin helices (McMahon *et al.*, 1995; Pabst *et al.*, 2000; Bracher *et al.*, 2002; Chen *et al.*, 2002). Complexin-1 is expressed specifically in the central nervous

system, complexin-2 is also expressed in non-neuronal tissues and complexin-3 and -4 are predominantly expressed in retina (Reim *et al.*, 2005).

Complexin-1/complexin-2 double knock out mice die shortly after birth and further analyses suggested that these proteins regulate a late post-priming step in synaptic vesicle release, possibly by stabilising assembled SNARE complexes (Reim *et al.*, 2001; Xue *et al.*, 2007; Xue *et al.*, 2008). It has also been suggested that complexins act as a pre-fusion clamp that arrests SNARE complexes to prevent fusion (Giraudo *et al.*, 2006; Carr and Munson, 2007; Melia, 2007). This hypothesis was supported, since spontaneous fusion of cells expressing flipped SNARE components was blocked by soluble and membrane anchored complexin-1. The block was reversed by Ca^{2+} in the presence of synaptotagmin (Giraudo *et al.*, 2006; Schaub *et al.*, 2006; Tang *et al.*, 2006; Huntwork and Littleton, 2007). It should be noted however that other studies have indicated a positive role for complexins in the fusion process (Cai *et al.*, 2008) and thus the precise function of these proteins in membrane fusion remains to be determined.

1.4.5 Rab proteins

Rab proteins are small (20-29 kDa) ubiquitously expressed monomeric GTPases, which belong to the Ras GTPase superfamily (Grosshans *et al.*, 2006; Lee *et al.*, 2009). So far 11 members are known in yeast and more that 60 have been identified in mammalian cells (Schultz *et al.*, 2000; Pereira-Leal and Seabra, 2001; Seabra *et al.*, 2002). Rab proteins cycle between the cytosol and the membrane of the trafficking organelle, controlled by conformational changes that are regulated by guanine-nucleotides. Rab proteins are also termed ‘molecular switches’, with the membrane bound GTP form being ‘on’ and the GDP-form being ‘off’ (Pfeffer, 2001; Segev, 2001; Lee *et al.*, 2009). GTP-Rabs bind to proteins named effectors, which only recognise Rabs in their GTP-bound state (Pereira-Leal and Seabra, 2001; Eathiraj *et al.*, 2005; Pfeffer, 2005; Lee *et al.*, 2009) and are specific for a single Rab or a small subset of Rabs (Shirane and Nakayama, 2006).

Fusion can only occur if membrane contact is established and there has been evidence that contacts are engineered by Rabs, regulating SNARE-dependent membrane docking and fusion (Grosshans *et al.*, 2006). Rab3A, one of the most abundant synaptic Rab proteins, is vesicle bound and undergoes a synaptic vesicle association and dissociation cycle coupled to calcium stimulated exocytosis and recovery. Geppert *et al*. (1994) showed that Rab3A knock out mice were viable, fertile and showed no abnormalities in synaptic transmission, however synaptic depression was significantly increased after reiterating stimuli and the Rab3A binding partner rabphilin was decreased by 70 %. The results suggested a key role for Rab3A and its effectors in supplying fusion-competent vesicles during repetitive stimulations (Geppert *et al.*, 1994a).

1.5 Cysteine String Protein (CSP)

1.5.1 Discovery of CSP

A molecular understanding of synaptic function has been driven by the identification and characterisation of key synaptic proteins in mammals and model organisms. Cysteine-string protein (CSP) was first identified from the use of hybridoma libraries generated against *Drosophila* heads. The antibodies from these libraries were thus used for screening cDNA expression libraries to identify clones coding for brain proteins. Zinsmaier *et al.*, 1990 used one monoclonal antibody (mab) "mab49" derived from the hybridoma library to identify, through immunohistochemical staining, novel proteins expressed in the adult nervous system of *Drosophila*. This antibody selectively bound strongly to all neuropil regions, motor neurons and synaptic terminals of all neurons. In-situ hybridisation to *Drosophila* brain also demonstrated specific hybridisation to retina and the brain cellular rind. Through western blot analyses of homogenised *Drosophila* brain, two proteins were recognised at the sizes of 29 kDa and 32 kDa. To detect the cDNA sequences that code for the antigen, a lambda gt11 head cDNA expression library was screened

using the mab49 antibody. cDNAs encoding for two different proteins of 249 and 223 amino acids in length were identified. Interestingly, both proteins had a conspicuous feature, the presence of 11 cysteine residues in a span of 22 amino acids. For this reason these proteins were named 'cysteine-string protein' (abbreviated to CSP); the *Drosophila* proteins were designated CSP-29 and CSP-32, according to the size of the protein bands detected by immunoblotting.

Interestingly, a homologous protein to *Drosophila* CSPs was independently discovered in *Torpedo californica* (Gundersen and Umbach, 1992). The aim of this study was to identify subunits or regulators of presynaptic Ca^{2+}-channels through a suppression cloning technique. For this, *Xenopus* oocytes were injected with mRNA from the Torpedo electric lobe, which resulted in the expression of a novel Ca^{2+}-channel current that could be differentiated from endogenous currents. The suppression cloning technique employed antisense copy (c)RNA to block the *Torpedo* ω-conotoxin GVIA (ω-CgTx)-sensitive Ca^{2+} currents in *Xenopus* oocytes. This approach led to the identification of a 1.55 kb cDNA with a 585 nucleotide open reading frame, and the encoded protein was termed candidate Ca^{2+} channel subunit 1 ($CCCS_1$). The authors also noted a local abundance of 13 cysteine residues, and *in vitro* translation and labelling with ^{35}S cysteine revealed a single protein band of 27 kDa. The *Torpedo* $CCCS_1$ protein is 69 % - 70 % identical at the amino acid level to the two CSPs expressed in *Drosophila*. Hydropathy analysis suggested that $CCCS_1$ may have a single membrane spanning domain centred around the cysteine-string region and flanked by lysine residues, and that most of the cysteine residues might be embedded in the lipid environment of the membrane. Due to its linkage to Ca^{2+}-channels it was also proposed that CCCS1 might be involved in regulated exocytosis (see 1.5.3).

The high abundance of cysteine residues in the cysteine-string domain (Figure 1.1) was of particular interest to researchers and it was suggested that these residues may be important for post-translational modification of the protein. Indeed, SDS-PAGE analysis of ^{35}S-cysteine labelled T-CSP revealed a band at 27 kDa, as expected, but

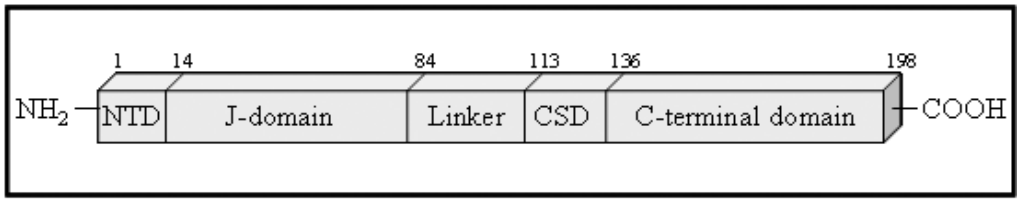

Figure 1.1: Schematic diagram of the domains of mammalian Cysteine String Protein (CSP). The amino acid numbers corresponding to domain boundaries are indicated.

also a second band at 34 kDa, suggestive of a modified form of the protein (Gundersen *et al.*, 1994). Fractionation of homogenised Xenopus oocytes revealed that the 34 kDa band associated with membrane fractions, whereas the 27 kDa CSP was entirely cytosolic. As the higher molecular weight form of T-CSP was membrane-associated it was suggested that CSP might be modified with hydrophobic fatty acids. To test this idea, membrane fractions containing the 34 kDa T-CSP were treated with hydroxylamine or methanolic KOH, which cleave thioester-linked fatty acids from cysteines. Both treatments converted the 34 kDa T-CSP to a 27 kDa form, the same size as cytosolic CSP. Furthermore, T-CSP was shown to incorporate [^{3}H]-palmitate, and the mass of [^{3}H]-palmitate-labelled T-CSP was similar to endogenous 34 kDa T-CSP. A time course of hydroxylamine treatment of T-CSP disclosed that the majority of (12 out of 13) cysteine residues were palmitoylated.

Subsequent work identified expression of an homologous CSP protein in mammalian species (Figure 1.2) (Braun and Scheller, 1995; Mastrogiacomo and Gundersen, 1995; Chamberlain and Burgoyne, 1996). In addition, a second CSP isoform with a truncated C-terminus was identified (Chamberlain and Burgoyne, 1996). These proteins were termed CSP1 and CSP2 (CSP isoforms are discussed in more detail in section 1.5.10). Although CSP1 is enriched in brain in mammals, it is expressed in all tissues that have been examined (Chamberlain and Burgoyne, 1996).

In addition to the cysteine-string domain another defining feature of CSP is the J-domain (Figure 1.1) (Silver and Way, 1993), an ~ 70 amino acid region located at the N-terminus of the protein. The J-domain is the signature motif of the DnaJ family of co-chaperones, a group of proteins that function in concert with HSC70 (Heat-Shock Cognate protein of 70 kDa) and its homologs to regulate many cellular processes.

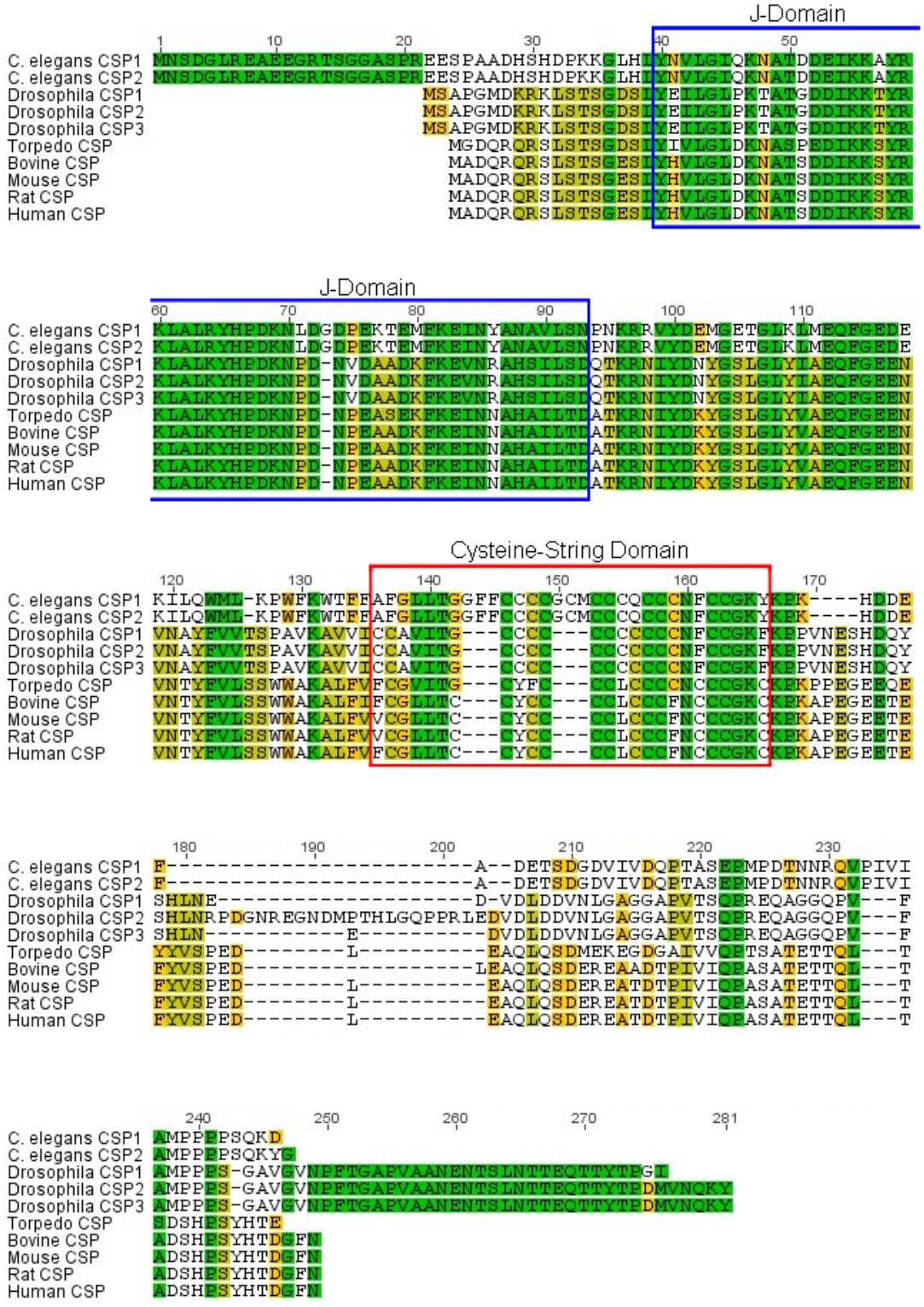

Figure 1.2: Alignment of CSP in a section of vertebrates. Amino acid sequences of CSP from several species (as noted in the figure) were aligned. Conserved amino acids present in all species are highlighted green, conserved residues present in 80 % of the species are coloured light green and conserved residues presenting 60 % of the species are coloured yellow. The blue box highlights the highly conserved J-domain and the red box the highly conserved cysteine string domain.

Subsequent work showed that the J domain mediates binding of CSP to HSC70 and activates the ATPase activity of HSC70 several-fold (Braun *et al.*, 1996; Chamberlain and Burgoyne, 1997a; Zhang *et al.*, 1999). Other domains of CSP include the short N-terminal region that precedes the J-domain and the "linker" domain, which lies between the J-domain and the cysteine string (Figure 1.1). Important functions of these domains have also been suggested by mutational studies (Zhang *et al.*, 1999; Arnold *et al.*, 2004). In section 1.5.6 all domains and their proposed functions will be discussed in more detail.

1.5.2 Intracellular distribution of CSP

As *Torpedo* CSP was proposed to be an essential subunit or regulator of presynaptic calcium channels (Gundersen and Umbach, 1992), it was expected that this protein would be localised to the plasma membrane. To examine T-CSP intracellular distribution, electric organ was fractionated into cytosol and membrane fractions (Mastrogiacomo *et al.*, 1994a). T-CSP was mainly detected in the membrane fraction. Consistent with this membrane localisation, 80 % of T-CSP separated into Triton X-114 detergent phase suggesting that endogenous T-CSP has a high hydrophobicity. Surprisingly however, CSP was found to be associated with synaptic vesicles following subcellular fractionation of *Torpedo* electric organ (Mastrogiacomo *et al.*, 1994b). In agreement with this observation, a subsequent study showed that CSP was also enriched in a synaptic vesicle fraction purified from rat brain (Braun and Scheller, 1995).

Subsequent studies in different cell types confirmed that CSP localised predominantly to vesicular structures. CSP was enriched in a zymogen granule fraction from rat pancreas (Braun and Scheller, 1995), and associated with chromaffin granules in adrenal medullary chromaffin cells as determined by a range of approaches including cell fractionation, immunofluorescence and electron microscopy (Chamberlain and Burgoyne, 1996). CSP is also present on insulin-containing granules in pancreatic beta cells (Zhang *et al.*, 1998). The neurohypophysis holds two types of vesicles, small synaptic vesicles (SSVs), which

store glutamate, actylcholine and GABA, and large dense core vesicles (LDCVs), which secrete peptides and hormones. CSP was shown to be localised to SSVs in peptidergic terminals of the neurohypophysis, and was also detected in fractions containing arginine vasopressin (AVP), which is found in LDCVs, following fractionation of neurohypophyseal nerve endings (Pupier *et al.*, 1997). However, in contrast to the vesicular/granular localisation observed for CSP in several cell types, CSP associated with the plasma membrane in 3T3-L1 adipocytes (Chamberlain *et al.*, 2001). This observation was surprising as adipocytes contain a well-defined regulated exocytosis pathway involving the fusion of vesicles containing the glucose transporter GLUT4 with the plasma membrane in response to insulin stimulation (Bryant *et al.*, 2002). CSP was not detected on these vesicles.

1.5.3 The role of CSP in exocytosis and as possible Ca^{2+}-regulator

Drosphila CSP was detected presynaptically at larval and adult neuromuscular junctions (NMJ) and also in synaptic boutons, suggesting an important function at presynaptic regions (Zinsmaier *et al.*, 1990; Zinsmaier *et al.*, 1994). To examine the function of CSP in *Drosophila*, a site-selected P-element mutagenesis was performed to target the CSP gene and induce its mutational inactivation (Zinsmaier *et al.*, 1994). The resultant mutants showed a semilethal embryonic phenotype and only 4 % survived to adulthood and died within four to five days at 22°C. When the mutants were exposed to higher temperature (29°C) they presented increasingly sluggish behaviour, intense spasmic jumping, uncoordinated locomotion, paralysis and died soon thereafter. To further investigate the CSP mutant, the csp^{x1} mutant was used, which showed some residual expression of CSP. Electroretinograms of wild type and CSP mutant flies were compared at increasing temperatures ranging from 19°C to 38°C. At higher temperatures it was observed that the mutants lost their on/off transient which was rescued by returning to low temperatures. This transient is dependent on synaptic transmission from photoreceptor terminals to lamina neurons. Electromicroscopic comparison of synaptic regions in lamina revealed that synaptic vesicles in the mutant were barely visible; terminals were filled with electron dense

debris, which might have been caused by neuronal degeneration. These results suggested that CSP might have a role in presynaptic neurotransmitter release or synaptic vesicle cycling. To examine this at the cellular level, neuromuscular transmission was studied in *csp* null mutant larvae, flies rescued by P-element transformation and wild type *Drosophila* via electrophysiological experiments (Umbach *et al.*, 1994). The nerve-evoked excitatory junctional potentials (EJPs) of mutants were found to be reduced by a half at 22°C and almost completely abolished at 29°C. There was also a decline detected in the spontaneous excitatory junctional potential (MEJP) amplitude in the mutant flies compared to rescued and wild type flies. In summary, these studies indicated that CSP might play a specific role in regulated exocytosis (Schwarz, 1994; Umbach *et al.*, 1994; Broadie, 1995; Poage *et al.*, 1999). Independently from Zinsmaier's work, CSP was discovered as a possible subunit or regulator of presynaptic Ca^{2+}-channels (Gundersen and Umbach, 1992). However, as CSP was found on synaptic vesicles (Mastrogiacomo *et al.*, 1994b) it was proposed that shortly after vesicle docking at the plasma membrane CSP activates presynaptic calcium channels, enhancing calcium-secretion coupling.

As neurotransmission in CSP null mutant *Drosophila* only failed completely at higher temperatures, it was subsequently examined if there were any differences in evoked release at low 'permissive' temperatures of 16°C-18°C in CSP mutant flies (Heckmann *et al.*, 1997). Here it was seen that the quantal content was normal, whereas the time course of release is disturbed at 'permissive' temperatures in CSP mutant flies. These findings confirmed that CSP is involved in neurotransmitter release and that impairment of neurotransmitter release is not specifically present only at higher temperatures, but already at permissive temperatures. A review published around this time hypothesised CSP to be involved in synaptic vesicle recycling (Sudhof, 1995), and this hypothesis was investigated (Umbach and Gundersen, 1997; Ranjan *et al.*, 1998). Stimulation at 21°C and 32°C by α-Latrotoxin, which forms ion-permeable pores in the membrane, released a sizable pool of quanta in wild type flies and in CSP null mutants. Shibire mutant flies on the other hand, which are known to be defective in endocytosis due to dynamin inactivation, did not retain abundant releasable quanta (Umbach and Gundersen, 1997). An intact endocytotic machinery was also elegantly verified by a study

demonstrating that CSP mutant *Drosophila* neurons were able to effectively take up FM1-43 dye at 22°C, as an indicator of endocytosis (Ranjan *et al.*, 1998). In contrast, subsequent release of FM1-43 (indicative of exocytosis) was blocked at 32°C, further confirming a selective loss of exocytosis in CSP null *Drosophila*.

Umbach and Gundersen (1997) suggested that the failure of quantal secretion in CSP mutants might occur due to an inhibition of presynaptic calcium channels activity. This observation was experimentally supported, given that high external Ca^{2+} concentrations, potassium concentrations and nerve stimulations failed to restore evoked responses, whereas Ca^{2+} ionophores where reported to bypass the block of transmitter release in CSP null mutant *Drosophila*. It was therefore suggested that CSP regulates an important step in calcium-secretion-coupling (Umbach and Gundersen, 1997). However, it is important to note that there have been conflicting experimental evidence concerning the role of CSP in modulating presynaptic Ca^{2+}-channel activity in fast neurotransmitter release. On one hand, Ca Crimson was used to monitor stimulus dependent changes in cytosolic Ca^{2+} at motor nerve terminals of CSP null mutant *Drosophila* (Umbach *et al.*, 1998). Here it was shown that the inhibition of neuromuscular transmission is correlated with a block of Ca^{2+} ion entry at nerve endings in CSP null mutants, which would support the hypothesis of CSP mediating a regulatory interaction between synaptic vesicles and presynaptic calcium channels. Then again, the same hypothesis was tested using the calcium indicator fluo-4 AM in neuromuscular junctions in *Drosophila* CSP null mutants (Dawson-Scully *et al.*, 2000). This study reported that in control and CSP mutant flies, loaded with fluo-4 AM or Ca Crimson, presynaptic calcium signals firmly increased following stimulation at temperatures above 30°C. Indeed, mutant boutons displayed a slower time course of decay for calcium signals, especially at higher temperatures. This suggested that CSP null mutant boutons are physiologically less able to cope with calcium loads than control boutons. Indeed, further experiments disclosed that the relative increase in intraterminal calcium is generally larger in CSP null mutants than in controls and that the reduction in neurotransmitter release in these mutants cannot therefore be explained by a loss of calcium entry into nerve terminals. One possible explanation for the defect in calcium triggered exocytosis in CSP null mutants might be that the resting calcium concentration is actually lower in these

mutants, but measurements of the resting values of calcium concentrations revealed no differences between control and mutant flies at room temperature, with the exception that the resting level was higher in mutant flies at 34°C. This study concluded that the loss of neurotransmitter release in CSP null mutants is primarily caused by a defect of a direct step in calcium regulated exocytosis and not as a result of a defect in Ca^{2+} channel activation.

Overall the study by Zinsmaier's group supported the findings of Chamberlain and Burgoyne, 1998, who reported a direct function of CSP in exocytosis in PC12 cells. CSP over-expression (~ 13-fold) (see Table 1.1) caused an ~50 % increase in Ca^{2+}-stimulated [^{3}H] dopamine secretion, with no difference could be seen in cytosolic Ca^{2+} channel levels in resting cells or following stimulation. Importantly, CSP over-expression enhanced secretion in permeabilised cells independently of any Ca^{2+} channel requirement. Thus, this work demonstrated that CSP directly functions in regulated exocytosis. Over-expression of CSP in INS-1 pancreatic beta cells also impacted insulin secretion; in this case over-expression of CSP inhibited release (see Table 1.1) (Brown *et al.*, 1998). Moreover, it was examined whether CSP over-expression had any effect on voltage-dependent Ca^{2+}-channels in these cells, by using the whole cell configuration of the patch-clamp technique. No difference was detected in Ca^{2+}-channel activity in control cells and cells over-expressing CSP. This work suggested that CSP is not a modulator or a subunit of Ca^{2+}-channels and must play an alternative role in regulated secretion (Morales *et al.*, 1999).

The role of CSP in exocytosis was more accurately analysed by examining the effect of CSP over-expression of dense-core granules exocytosis in single adrenal chromaffin cells using amperometric recordings to detect released catecholamines (see Table 1.1) (Graham and Burgoyne, 2000). CSP over-expression caused a reduction in amperometric spike number after stimulation, indicating a decrease in fusion events leading to a reduction in catecholamine release by ~ 82 %. The mean spike amplitude was unaffected by CSP over-expression, but closer examination of spike parameters revealed that the total charge per spike was significantly increased (half-width increased ~ 60 %), and there was a deceleration in the rate of the spike rise. These results indicated that CSP is important for fusion pore formation or even controls fusion pore opening.

Table 1.1: Effects of CSP over-expression.

Organism/Cell Type	Method of Analysis/Stable or Transient Over-expression	Effect	Reference
INS-1 pancreatic beta cells	Insulin ELISA Transient over-expression	Inhibition of exocytosis	(Brown *et al.*, 1998; Boal *et al.*, 2004)
PC12 cells	[^{3}H] dopamine assay Stable over-expression	Increase in exocytosis	(Chamberlain and Burgoyne, 1998)
Adrenal chromaffin cells	Amperometric recordings Transient over-expression	Inhibition of exocytosis	(Graham and Burgoyne, 2000)
Drosophila	Electrophysiology Stable over-expression	Rough eyes, crumpled wings; inhibition of exocytosis	(Nie *et al.*, 1999; Arnold *et al.*, 2004)
Airway epithelial cell	Co-immunoprecipitation Transient over-expression	Increased amount of HSC70 co-immunuprecipitated with CFTR	(Schmidt *et al.*, 2009)
KIM-2 cells	Growth hormone assay Transient over-expression	No effect on constitutive exocytosis	(Gleave *et al.*, 2001)
Xenopus oocytes (CSPβ)	Secretion of cortical granule lectin Transient over-expression	Block of cortical granule exocytosis	(Gundersen *et al.*, 2010)

The idea that CSP does not regulate activity of voltage-gated Ca^{2+}-channels is in agreement with previous work of Pupier *et al.*, 1997, where the interaction of CSP with presynaptic calcium channels was examined by assessing the ability of CSP antibodies to immunoprecipitate N-type Ca^{2+}-channels solubilised from peptidergic terminals of the neurohypophysis or brain P2 membranes labelled with a specific radioligand [^{125}I]-ωGVIA. The CSP antibody could not capture more Ca^{2+}-channels than non-immuno IgG, which concluded that CSP does not form a complex with these Ca^{2+}-channels (Pupier *et al.*, 1997). However, subsequent work suggested that CSP does interact with the N-type calcium channel (Magga *et al.*, 2000). In this work it was examined whether the protein-protein interaction between CSP and the $G_{\beta\gamma}$ subunit of the G protein complex influences calcium channel activity. CSP was co-expressed with the N-type (α_{1B}, β_{1b} and α_2-δ) Ca^{2+}-channels in tsa-201 cells and its function was assessed via whole cell patch clamping. Compared to the typically N-type Ca^{2+}-channel current waveform, the channels co-expressed with CSP exhibited a slowed current waveform and the densities appeared reduced by ~2-fold. This led to the assumption that CSP has a strong inhibitory effect on these channels. It was proposed if the inhibitory effect of G protein on N-type Ca^{2+}-channel activity is dependent on the physical interaction between CSP and the channel, then a reduction of CSP binding should be simultaneous with a reduction in the G protein effect. Thus CSP, N-type Ca^{2+}-channel and the α_{1B}II-III linker synprint region of N-type Ca^{2+}-channel were co-expressed in tsa-201 cells. Whole cell patch clamping revealed a dramatic reduction in prepulse facilitation induced by CSP, which indicates $G_{\beta\gamma}$ modulation of voltage-gated Ca^{2+}-channels. Compendious the results showed that interactions between CSP and N-type calcium channels result in a robust inhibition of channel activity by G protein βγ subunits.

It was investigated whether huntingtin mutants, which have expanded polyglutamine repeats, alter the association of G proteins with CSP (Miller *et al.*, 2003). The huntingtin protein is an essential protein of unknown function. Mutations in its gene cause Huntington's disease. The initial pathological target in Huntington's disease is the degeneration of the striatal medium spiny GABAergic neuron. The huntingtin protein mutant contains 36-250 polyglutamine repeats in exon1, compared to the wild type protein with 6 to 39 repeats. It has been observed that proteins with

expanded polyglutamine repeats interfere with the chaperone balance of the cell. *In vitro* binding assays were used to analyse the effect of the normal huntingtin protein exon1 (HDQ20) and the protein with the expanded polyglutamine repeats in exon1 (HDQ53). HDQ53 reduced the interaction between CSP and G proteins and it was also shown that HDQ53 directly bound to CSP. HDQ53 tended to aggregate after some time. CSP chaperone function on HDQ53 could be excluded. Despite that, further experiments revealed that the Huntington's disease protein (HDQ53) blocked the CSP modulation of G protein inhibition of calcium channel activity.

1.5.4 Protein interactions of CSP

1.5.4.1 Heat-shock proteins and co-chaperones

One defining domain of CSP is the J-domain, a 70 amino acid region, which is a conserved motif of the DnaJ family of co-chaperones identified in *Escherichia coli*. DnaJ proteins function in conjunction with HSC70 (Heat-Shock Cognate protein of 70 kDa, homolog to DnaK in bacteria) to regulate many cellular processes.

HSC70 is a ubiquitously expressed molecular chaperone that regulates substrate proteins by several mechanisms, including the stabilisation of unfolded proteins, promotion of correct protein folding and assembly/disassembly of multimeric protein complexes (Beckmann *et al.*, 1990; Langer *et al.*, 1992). The binding and release kinetics of HSC70 proteins are controlled by an ATPase activity, which is subject to regulation by cofactors including DnaJ proteins. It was shown that CSP binds to both HSC70 and HSP70 (heat-shock inducible isoform) and stimulates their ATPase activity by ~ 13-fold (Braun *et al.*, 1996; Chamberlain and Burgoyne, 1997a, b). In contrast, synaptotagmin (vesicle protein) and α-SNAP (NSF activator) were not able to activate HSC70 (Braun *et al.*, 1996).

The conserved tripeptide, histidine-proline-aspartate (HPD), is present in all J domains and has been shown to play an important role in the interaction between DnaJ proteins and HSC70/DnaK (Wall *et al.*, 1994; Tsai and Douglas, 1996). Mutations in the HPD motif of CSP (H43Q or D45A) completely inhibited activation of HSC70 ATPase activity (Chamberlain and Burgoyne, 1997a). Furthermore,

competition-binding assays with these two mutants and wild type CSP suggested that the mutants were unable to bind to HSC70. In agreement, tryptic digestion confirmed that unlike wild type CSP, the CSP(H43Q) and CSP(D45A) mutants were unable to promote conformational changes in HSC70 (Chamberlain and Burgoyne, 1997a).

As other HSC70/DnaJ protein pairs have been shown to regulate protein folding/aggregation, it was examined if CSP/HSC70 could prevent aggregation of heat-denatured firefly luciferase (Chamberlain and Burgoyne, 1997a). Prevention of protein aggregation by binding to exposed hydrophobic regions of denatured proteins is a classical assay for chaperone activity. Wild type CSP as well as the HPD mutants (CSP(H43Q) and CSP(D45A)) were able to act as molecular chaperones by blocking luciferase aggregation. In contrast, HSC70 was ineffective at preventing aggregation, whereas CSP and HSC70 together functioned synergistically to prevent luciferase aggregation, suggesting that they form a chaperone 'machine'.

Subsequent work built upon these earlier studies by showing that CSP/HSC70 form a complex with a third chaperone protein, αSGT (Small glutamine-rich tetratricopeptide repeat-containing protein alpha) (Tobaben *et al.*, 2001). The trimeric complex formed in the presence of ADP and was disassembled by Mg^{2+}-ATP. αSGT has a tetratricopeptide repeat (TPR) motif, which is known to be a protein-protein interaction module. Furthermore, most TPR-containing proteins are associated with multiprotein complexes, and there is evidence indicating that TPR motifs are important to the functioning of chaperones, cell-cycle, transcription, and protein transport complexes (Blatch and Lassle, 1999). αSGT has also been shown, together with HSP70/HSP90, to promote cytoplasmic retention of the androgen receptor and to be a determinant of the sensitivity and specificity of androgen receptor activation (Buchanan *et al.*, 2007; Goodarzi *et al.*, 2008).

It was shown that αSGT and CSP intensely activate the HSC70 ATPase (~19-fold), compared to CSP (~12-fold) or SGT (~3-fold) alone, thus it was assessed whether this trimeric complex behaves as a chaperone-complex; to approach this, denatured firefly luciferase was used as a substrate. The results demonstrated that CSP, αSGT or HSC70 alone were not able to re-fold denatured luciferase, and that CSP/HSC70 only achieved a low level of luciferase reactivation, however all three proteins together renatured ~60 % of denatured luciferase in the presence of ATP, indicating

that SGT increases the efficiency of CSP/HSC70 chaperone activity. The CSP/HSC70/αSGT-complex is also likely to be important *in vivo* as the proteins interact in cells as revealed by co-precipitation of αSGT from purified vesicles with CSP and HSC70. Indeed CSP regulates αSGT association with synaptic vesicles, as SGT was decreased in this fraction from CSP knockout mice (Fernandez-Chacon *et al.*, 2004).

β-small glutamine-rich TPR protein (βSGT) is an isoform of αSGT expressed exclusively in brain, which shares approximately 60 % amino acid sequence identity with the αSGT isoform (Tobaben *et al.*, 2003). Both α- and βSGT incorporate the defining tetratricopeptide repeats (TPRs) motif, which is known to bind to the C-terminus of HSC70 (Liu *et al.*, 1999; Scheufler *et al.*, 2000; Tobaben *et al.*, 2001). The TRPs of βSGT were shown to bind to the cysteine string domain of CSP (Tobaben *et al.*, 2003), as truncation of 6 of the 14 cysteine residues in CSP blocked this interaction. The interaction of βSGT with the cysteine-string domain may be via hydrophobic interactions, as mutations of all cysteines to hydrophilic serines abolished binding, whereas mutation of the cysteines to alanine had less of an effect on binding.

Chemical cross-linking experiments revealed that CSP/HSC70 also bind to a complex containing αGDP-dissociation inhibitor (αGDI) and HSP90 (heat-shock protein of 90 kDa) (Sakisaka *et al.*, 2002). αGDI regulates membrane release and recycling of Rab GTPases and HSP90 is a specialised chaperone that is known for its role in stabilising intermediates of molecules in signalling pathways. This suggested that a major component of a membrane-associated complex containing αGDI is likely to include HSP90 tethered to synaptic vesicles through CSP/HSC70 and possibly other factors. As Rab proteins play key roles in membrane fusion pathways, this interaction of CSP may be relevant to its function in exocytosis, however, no further work on this area has been forthcoming.

The J-domain is clearly important for the function of CSP in exocytosis as point mutations in the HPD motif (CSP(H43Q) and CSP(D45N)) reduced the inhibitory effect of CSP over-expression on secretion of human insulin C-peptide from HIT-T15 cells (Zhang *et al.*, 1999). Furthermore the J-domain is also important for the function of *Drosophila* CSP at neuromuscular junctions (Bronk *et al.*, 2005). Two

defined mutants, ΔJ-CSP (deletion of the J-domain) and CSP(H45Q) (point mutation in the conserved HPD tripeptide motif) were unable to reverse the lethal phenotype of Drosophila CSP null mutants. Indeed, expression of both J-domain mutants even enhanced the temperature sensitive lethality of CSP null *Drosophila*. However, the J-domain is not required for every function of CSP. For example, the number of synaptic boutons is reduced in CSP null mutants and this was reversed by expression of either wild type CSP, ΔJ-CSP or CSP(H45Q). Wild type CSP increased the number of boutons to 186 % of wild-type controls, whereas the mutants reversed the decrease of synaptic boutons in *csp* null flies to 74 % - 80 % of wild type controls. In addition it was observed that expression of ΔJ-CSP in motor neurons increased the excitatory junction potential (EJP) amplitudes at 22°C in the mutant, however normal transmission functions were not restored (Bronk *et al.*, 2005; Weng *et al.*, 2009). Thus, the J-domain seems to be essential for only a subset of the synaptic functions of CSP. Finally, although some functions of CSP might proceed in the absence of HSC70 interaction, it is important to note that mutation of HSC70 in *Drosophila* caused a ~50 % reduction of nerve-evoked neurotransmitter release at 23°C and was abolished at 30°C (Bronk *et al.*, 2001). The loss of nerve-evoked neurotransmitter secretion was caused by reduced Ca^{2+}-sensitivity of exocytosis downstream of Ca^{2+} entry, which could be rescued by increasing internal and external calcium. The results indicated that HSC70 and CSP might act in mutual pathways, as CSP mutant *Drosophila* displayed similar temperature sensitive effects (Zinsmaier *et al.*, 1994), homozygous HSC70-CSP double mutants showed a similar loss of evoked release, and CSP and HSC70 have been shown to interact with each other *in vitro* and *in vivo* (Chamberlain and Burgoyne, 1997b, a; Bronk *et al.*, 2001; Tobaben *et al.*, 2001). These results suggested that CSP and HSC70 cooperatively enhance release by increasing the calcium sensitivity of vesicle fusion (Bronk *et al.*, 2001).

1.5.4.2 Ca^{2+} channels

CSP was identified in one study as a subunit or modulator of Ca^{2+}-channel subunits in *Torpedo* (Gundersen and Umbach, 1992) and it has been repeatedly suggested that CSP might regulate Ca^{2+}-channel activity (Umbach and Gundersen, 1997).

Neurotransmitter release in the central and peripheral nervous system is regulated by Ca^{2+} entry through voltage-gated Ca^{2+} channels (VGCCs). VGCCs also regulate secretion from chromaffin and pancreatic beta cells. Different VGCCs are important for regulated exocytosis in different cell types. For example L-type VGCCs regulate secretion from pancreatic beta cells, whereas N-type and P/Q-type VGCCs are localised at presynaptic terminals and are important for neurotransmitter release.

To assess if CSP interacts with P/Q-type calcium channels, *in vitro* binding assays were performed (Leveque *et al.*, 1998). P/Q-type calcium channels consists of several subunits, α_1, $\alpha_2\delta$, $\beta_{1\text{-}4}$, and γ. The α_1 subunit has 24 transmembrane domains and forms the ion conducting pore and consists of the characteristic four homologous I-IV domains containing six transmembrane α-helices each (Dolphin, 2006). The domains II and III are linked through an intracellular loop in the α_1A subunit of the P/Q calcium channel (Sheng *et al.*, 1998). A GST-tagged form of this II-III linker region of the P/Q calcium channel α_1A subunit (GST-II-III_A) immobilised on glutathione-sepharose beads was shown to interact with *in vitro* translated ^{35}S-labelled CSP (Leveque *et al.*, 1998). Furthermore, endogenous (and hence palmitoylated) CSP was also able to associate with the GST-II-III_A fusion protein. This direct association of CSP with P/Q-type channel α_1A subunits suggested that CSP might indeed regulate calcium channel activity by binding to and modulating the II-III linker region of the α_1A subunit (Leveque *et al.*, 1998).

The activity of VGCCs can also be regulated by heterotrimeric G proteins. It has been demonstrated that syntaxin 1A physically binds to both the N-type calcium channel domain II–III linker and to the $G_{\beta\gamma}$ subunit (Jarvis *et al.*, 2000; Lu *et al.*, 2001). The protein complex facilitates G protein interactions with the channel leading to channel inhibition. Cleavage of syntaxin 1A with botulinum toxin C (BoNT C) removes the syntaxin 1A-mediated enhancement of G protein modulation and reduces the probability of interactions between the channel and $G_{\beta\gamma}$. In a separate study, Magga *et al.* (2000) examined the possibility that CSP might also regulate VGCC function indirectly via interaction with regulatory pathways. This hypothesis was initially tested by examining the interaction of CSP with heterotrimeric G protein subunits. GST-tagged CSP or a mutant truncated after the J-domain (CSP(1-82)) were coupled to glutathione agarose beads and incubated with a rat hippocampal

homogenate. Western Blot analysis revealed that the $G_{\beta\gamma}$ subunits of the G protein complex associated with recombinant full-length CSP in vitro, but not with the CSP(1-82) construct. This indicated that $G_{\beta\gamma}$ complex interacts with the linker region, cysteine-string domain or C-terminus of CSP or that the complete structure of CSP is required for binding. Further analysis of interactions between these proteins revealed co-precipitation of CSP with anti-syntaxin and anti-Ca^{2+} channel β1 subunit antibodies. Hence, direct binding of $G_{\beta\gamma}$ to CSP and/or syntaxin may be linked with regulation of VGCCs. Interestingly, analysis of the G_{α} subunit of the trimeric GTP binding proteins via western blotting revealed that this subunit bound to CSP(1-82) in an ATP dependent manner. This finding may suggest the intriguing possibility that CSP chaperones the $G_{\alpha}/G_{\beta\gamma}$ interaction in addition to $G_{\beta\gamma}$/VGCC (Magga *et al.*, 2000).

Further analysis of the CSP/G_{α} interaction demonstrated that the J-domain and linker region of CSP also associate with the inactive GDP-bound conformation of G_{α} (Natochin *et al.*, 2005). The CSP(1-112) mutant increased the initial rate of GTPγS binding to $G_{\alpha s}$ but not $G_{\alpha i}$. Moreover, transiently expressed CSP enhanced $G_{\alpha s}$-mediated signalling and therefore increased intracellular cAMP levels. These data suggested that CSP modulates G protein function by targeting the inactive GDP-bound form of $G_{\alpha s}$ and promoting GDP/GTP exchange. It was suggested that upon activation by HSC70/SGT, CSP is a direct guanine nucleotide exchange factor (GEF), however there is no experimental evidence to support this statement. Thus, biochemical studies are consistent with the notion that CSP might regulate Ca^{2+} channel function directly or indirectly via effects on heterotrimeric G proteins. However, there is a lack of strong evidence that CSP regulates VGCC in vivo and additional work is clearly required to determine precisely how any such regulation is achieved.

1.5.4.3 VAMP

The SNARE protein VAMP (synaptobrevin) is a key component of the exocytosis machinery. Pairing between VAMP on secretory vesicles and syntaxin/SNAP25 on

the plasma membrane forces the vesicle membrane and the plasma membrane into close contact and promotes membrane fusion (Weber *et al.*, 1998; Wang and Tang, 2006). The first report of an interaction between CSP and VAMP by Leveque *et al.* (1998) indicated coimmunoprecipitation of CSP and VAMP from solubilised synaptosomes. However Leveque and colleagues were unable to show an interaction between the recombinant forms of VAMP and CSP, suggesting that the interaction might be indirect. A subsequent study reported that CSP1, but not CSP2, coimmunopreciptated with both VAMP2 and VAMP7 under stimulating conditions (high Ca^{2+}-levels) from HIT-T15 cell extracts. Importantly, these interactions were verified using recombinant proteins, showing that the interaction is direct. As CSP1 and CSP2 are identical except that CSP2 has a truncated C-terminal domain, this work showed the importance of the C-terminus of CSP for VAMP2 interaction (Boal *et al.*, 2004). In contrast, analysis of binding to CSP truncation mutants suggested that VAMP8 binds to the linker domain and/or cysteine-string region (Weng *et al.*, 2009).

There is currently no data available that indicates that a CSP-VAMP interaction regulates exocytosis. In pancreatic beta cells, the inhibitory effect of CSP2 over-expression in exocytosis was less than that of CSP1, indicating some function of the extreme C-terminus of CSP in exocytosis; subsequent work should examine whether this difference reflects an important role for CSP-VAMP2 binding. By analysing more CSP truncation mutants/point mutants it should be possible to map the minimal region of CSP required for VAMP binding. This will allow the effects of more defined CSP mutants on exocytosis to be examined, and more directly correlate changes in VAMP2 affinity and exocytotic function of CSP.

1.5.4.4 Syntaxin

It was suggested that CSP might facilitate VGCC activation by promoting the dissociation of the plasma membrane associated SNARE protein syntaxin (Seagar *et al.*, 1999). To investigate if there was an association between the functions of CSP and syntaxin, it was examined whether co-expression of syntaxin 1A suppresses the

phenotype associated with CSP over-expression in *Drosophila* (Nie *et al.*, 1999). The results revealed that co-expression of syntaxin 1A partially suppressed the CSP over-expression phenotype (crumpled wings and rough eyes; see Table 1.1). Moreover syntaxin immunopurified with CSP from Drosophila protein extracts, indicating that the two proteins interact. It was subsequently shown that His_6-CSP1 interacts with GST-syntaxin 1A *in vitro*, demonstrating a direct interaction (Chamberlain *et al.*, 2001). The fusion of GLUT4 vesicles with the plasma membrane in adipocytes is regulated by syntaxin 4. Interestingly immobilised His_6-CSP pulled down syntaxin 4 from a lysate of 3T3-LI adipocytes. This observation was important as adipocytes do not express VGCCs, suggesting that the CSP-syntaxin 4 interaction is not related to Ca^{2+} channel regulation. Subsequent *in vitro* binding assays examining interactions between CSP1/CSP2 and syntaxin 1/4 reported that both CSP1 and CSP2 bound to syntaxin 1A whereas syntaxin 4 only interacted with CSP1. These results are reminiscent of analysis of VAMP2/VAMP7 binding to CSP, and suggest that syntaxin 1 and syntaxin 4 bind to different regions of CSP.

1.5.4.5 SNAP25

Deletion of CSP in mice resulted in a decrease in the expression level of the SNARE protein SNAP25 (Chandra *et al.*, 2005), suggesting a possible chaperone role for CSP (see 1.5.9).

To map protein interaction of CSP in hormone secretion of pancreatic β cells, pull-down experiments were carried out with immobilised CSP1 and extracts of clonal β cells (Boal *et al.*, 2011). Immunoblot analysis identified proteins which are known to bind to CSP, such as VAMP2 and HSC70; however, SNAP25 was also identified as a possible binding partner of CSP1 reciprocal. Pull down assays with immobilised SNAP25 confirmed that CSP, as well as HSC70 and VAMP2 bind to SNAP25. Truncation mutants of CSP (CSP(1-82), CSP(1-110), CSP(1-167), CSP(110-198) and CSP(138-198)) and CSP(SSP), which incorporates 12 serines instead of cysteines, were generated to address which domain(s) is/are implicated for binding to SNAP25. The linker domain was found to be crucial for the interaction between SNAP25 and CSP, as CSP(1-82) failed to interact with SNAP25, whereas CSP(1-

110) bound efficiently. Nevertheless, direct binding of CSP1 to SNAP25 (i.e. with recombinant CSP and SNAP25) was not detected.

1.5.4.6 Synaptotagmin

To identify additional interacting partners of CSP, pull-down assays from solubilised rat brain were performed using immobilised recombinant His_6-CSP (Evans and Morgan, 2002). This approach identified synaptotagmin as a CSP binding partner. Synaptotagmin is a vesicle associated protein and acts as a Ca^{2+} sensor in synchronous neurotransmitter release. It mediates calcium-dependent interactions with SNAREs, such as SNAP-25 (Schiavo *et al.*, 1997; Gerona *et al.*, 2000) and syntaxin 1A (Bennett *et al.*, 1992; de Wit *et al.*, 2009).

It has been recently shown that CSP interacts with the SNARE protein SNAP25 (Boal *et al.*, 2011; Sharma *et al.*, 2011). As Boal and colleagues (2011) showed that CSP/SNAP25 interaction was indirect (see 1.5.4.5), it was examined if CSP might bind indirectly to SNAP25 via a further protein expressed in pancreatic beta cells. Since SNAP25 has shown to bind directly to synaptotagmin 1 in neurons (Schiavo *et al.*, 1997; Gerona *et al.*, 2000), an interaction with synaptotagmin 9 (which regulates secretion in beta cells) was examined. Pull down assays with recombinant synaptotagmin 9 and immobilised CSP or SNAP25, showed that synaptotagmin 9 was able to bind to either of the immobilised proteins. Immunoprecipitation using an anti-CSP antibody, demonstrated that CSP bound with a higher affinity to synaptotagmin 9 than to synaptotagmin1 (Evans *et al.*, 2001) and synaptotagmin 5-7. A point mutation in the linker domain (CSP(E93V)) abolished the binding between CSP1 and synaptotagmin 9, in addition *in silico* analysis hypothesised that CSP(E93) generated a hydrophilic area, which might support the interaction to synaptotagmin 9 via positively charged ions, such as calcium (Boal *et al.*, 2011). To further investigate which domain of synaptotagmin 9 is important for CSP binding, FRET/FLIM in clonal MIN6 β cells analysis was undertaken, revealing that the calcium binding C_2A domain of synaptotagmin 9 is required and sufficient to mediate binding to CSP. Since the calcium binding C_2A domain of synaptotagmin 9 was involved in the interaction with CSP, it was investigated whether this interaction

could be modulated by calcium. Binding efficiency of His_6-CSPα(1-110) to GST-synaptotagmin 9(C_2A domain) was raised 10-fold in the presence of 1 μM – 10 μM calcium, which was interesting since these values are consistent with the Ca^{2+}-concentration range that is required for insulin exocytosis from pancreatic β cells.

1.5.4.7 Homomeric interactions of CSP

It has long been recognised that CSP forms dimers and higher molecular weight aggregates on SDS-PAGE gels. Analysis of CSP truncation mutants suggested that the linker and cysteine string domain are involved in homomeric interactions of CSP and that chaperone function at the synapse may involve CSP self-association (Swayne *et al.*, 2003). Further work using chemical cross-linking showed that CSP1 and CSP2 differed in homodimerisation, suggesting that the C-terminus influences oligomerisation of CSP (Boal *et al.*, 2004). However, to date it has not been demonstrated that oligomerisation of CSP is physiologically relevant, although Boal *et al* (2004) reported that CSP dimer formation was increased during stimulation of exocytosis in HIT-T15 pancreatic beta cells.

1.5.5 Phospho-regulation of CSP

Protein kinase A (PKA) and protein kinase C (PKC) modulate calcium-triggered exocytosis in many cell types (Morgan and Burgoyne, 1992; Morgan *et al.*, 1993; McFerran and Guild, 1996; Scott *et al.*, 1998; Murphy *et al.*, 1999). CSP was identified as a novel PKA and PKC substrate in vitro and in vivo, together with proteins such as α-SNAP and Rab3a (Evans *et al.*, 2001). Identification of the PKA phosphorylation site of CSP was determined by analysis of preparative quantities of recombinant CSP phosphorylated in vitro by PKA. Phosphorylated CSP proteins were digested with trypsin and tryptic fragments separated by reversed phase high-performance liquid chromatography (RP-HPLC). The results demonstrated that CSP was phosphorylated by PKA on serine at amino acid position 10 (Ser^{10}) in the N-terminal domain.

PKA phosphorylation of Ser^{10} of CSP has been demonstrated to affect exocytosis in adrenal chromaffin cells. Wild type CSP and a CSP(S10A) mutant were transfected into chromaffin cells, which were then permeabilised with digitonin and Ca^{2+} stimulated exocytosis measured through amperometric recordings. Over-expression of wild type CSP resulted in a reduction of evoked exocytotic spikes (Graham and Burgoyne, 2000). This reduction in spike number was also observed with the serine 10 mutant CSP(S10A). However, analysis of spike kinetics found that the expression of CSP(S10A) had no effect on the rise time and half-width of spikes relative to control, whereas spike kinetics were altered in cells over-expressing wild type CSP (Evans *et al.*, 2001). These observations provide clear evidence that Ser^{10} is important for the effect of CSP on amperometric spike parameters and highlight a likely role for PKA/PKC in modulating CSP regulation of exocytosis.

Phosphorylation of CSP is likely to affect exocytosis by modulating protein-protein interactions. Interestingly phosphorylated CSP (P-Ser^{10}) bound less efficiently to synaptotagmin *in vitro* via pull down assays, suggesting that synaptotagmin binding is refractive to CSP phosphorylation. CSP-synaptotagmin binding likely requires Ser^{10} as serine to alanine mutation disrupted this interaction (Evans and Morgan, 2002). Furthermore it was also revealed that mutation at the phosphorylation site of CSP (CSP(S10D)) significantly reduced binding to synaptotagmin 9 in pancreatic beta cells, indicating the importance of phosphorylated CSP for binding topology. CSP-syntaxin 1A binding was also decreased when CSP was phosphorylated by PKA (Evans *et al.*, 2001), suggesting that PKA might modulate CSP function by disrupting several interactions important for exocytosis.

1.5.6 CSP domains important for regulated exocytosis

As discussed earlier, there is strong *in vivo* evidence that interaction with HSC70 plays an important role in CSP functions. The rescue of CSP over-expression phenotypes in *Drosophila* by syntaxin over-expression also provides evidence that the CSP-syntaxin interaction is important *in vivo*. However, at present there is a lack of compelling evidence that CSP interactions with VAMP and synaptotagmin are important *in vivo*. Domains outside the J-domain are important for CSP function

although the effects of mutations in these regions of CSP have not been linked to a loss of interaction with a specific protein(s). The role of the highly conserved linker domain of CSP was analysed at nerve terminals of CSP null *Drosophila* neuromuscular junctions (Bronk *et al.*, 2005), by generating a ΔL-CSP (deletion of the linker domain) mutant. ΔL-CSP did not rescue the temperature sensitive lethality of CSP null *Drosophila*, although it did reverse the loss of synaptic boutons in NMJs from CSP null mutants. Indeed, the number of synaptic boutons in cells expressing ΔL-CSP was even higher than control. Rescue experiments with ΔL-CSP also demonstrated that the L-domain of CSP is not required for maintaining normal evoked release, which is in agreement with the findings of Arnold *et al.* (2004), who observed that deletion of the linker domain of CSP rescued the temperature-sensitive paralysis of *Drosophila* CSP null mutants (Arnold *et al.*, 2004).

Studies in Drosophila and pancreatic beta cell lines by the Lang group have examined the importance of distinct domains of CSP for regulated exocytosis in mammalian cells. This group have employed over-expression of point and truncated mutants of CSP1 and CSP2. These studies are complicated somewhat by the fact that over-expression of wild type CSP1 or CSP2 promotes a large inhibition of regulated exocytosis, and functional importance is placed on residues or domains that lessen this inhibitory effect when mutated. Exocytosis was measured from HIT-T15 cells co-transfected with human preproinsulin (phINS) and CSP (Zhang *et al.*, 1999; Boal *et al.*, 2004). A point mutation, CSP1(E93V), in the highly conserved linker region (amino acids 83-112) of CSP inhibited insulin secretion to the same extent as seen with over-expression of wild type CSP (Zhang *et al.*, 1999). Point mutations in the linker (E93V) and J-domain (H43Q) in CSP2 (CSP2(H43Q/E93V)), which has a shorter C-terminus than CSP1 (Chamberlain and Burgoyne, 1996), abolished the inhibitory effect on secretion compared to full-length CSP2 over-expression. As the corresponding mutations in CSP1 did not prevent the inhibitory effect of exocytosis, this suggested that there might be a functional interaction between the C-terminus and J-domain in the regulation of exocytosis. These results suggested that the C-terminal domain of CSP has an important function in regulated exocytosis (Zhang *et al.*, 1999). The effect of CSP mutations on exocytosis is summarised in Table 1.2.

Table 1.2: Effects of CSP mutations on exocytosis in relation to over-expression of wild type CSP, which has an inhibitory effect on exocytosis.

Organism/Cell Type	Mutant	Method of Analysis	Effect	Reference
Drosophila neuromuscular junction	ΔL-CSP	Electrophysiology	Relieve inhibitory effect	(Bronk *et al.*, 2005)
HIT-T15 cells	CSP1(E93V)	Insulin ELISA	Inhibition of exocytosis	Zhang *et al.*, 1999
HIT-T15 cells	CSP1(H43Q)	Insulin ELISA	Inhibition of exocytosis	Zhang *et al.*, 1999
HIT-T15 cells	CSP2(E93Q)	Insulin ELISA	Reduced inhibitory effect by 33 %	Zhang *et al.*, 1999
HIT-T15 cells	CSP2(H43Q)	Insulin ELISA	Reduced inhibitory effect by 50 %	Zhang *et al.*, 1999
HIT-T15 cells	CSP2(H43Q/E93V)	Insulin ELISA	Abolished inhibitory effect	Zhang *et al.*, 1999

1.5.7 Additional functions of CSP

As CSP has been functionally implicated in regulated exocytosis (discussed in 1.5.3), it was assessed whether CSP might function in other membrane trafficking steps, including plasma membrane delivery of cystic fibrosis transmembrane conductance regulator (CFTR) (Zhang *et al.*, 2002a). CFTR is responsible for the cAMP-activated chloride conductance of epithelial cell membranes and mutations of CFTR, such as CFTRΔF508 (Kerem *et al.*, 1990), cause cystic fibrosis. To examine subcellular distribution of CSP in airway epithelial cells, immunofluorescent staining was performed and analysed by confocal imaging. CSP showed a punctate and vesicular distribution pattern and colocalised partially with the endoplasmic reticulum and also with CFTR at the apical plasma membrane. Coimmunoprecipitation experiments using CSP antibody revealed that CSP associates with the immature (core-glycosylated) form of CFTR present at the ER and with the mature (fully-glycosylated) CFTR, which resides at the apical membrane domain. The effect of CSP on CFTR-dependent membrane current (ΔI_m) and membrane capacitance (ΔC_m) changes during cAMP stimulation were also studied. Co-expression of CSP with CFTR decreased the ΔI_m and ΔC_m responses that resulted from CFTR stimulation. Immunoblotting analysis revealed that CSP co-expression eliminated the mature glycosylated form of CFTR and led to an accumulation of immature CFTR, suggesting that CSP might be a CFTR co-chaperone that stabilises intermediate forms of CFTR to promote its folding and maturation. Furthermore it was suggested that CSP is implicated in the production of immature CFTR and subsequently assists the progression of CFTR to the Golgi (Zhang *et al.*, 2006). CSP knock down experiments augmented the expression of mature CFTR, whereas increased levels of CSP led to a block in progression of CFTR to the mature form. The J-domain of CSP was central to the effects on CFTR maturation, because another J protein (Hdj-2) also increased the levels of immature CFTR, and the CSP(H43Q) mutant rescued CFTR maturation. CSP might regulate the trafficking of CFTR from the endoplasmic reticulum, and co-expression of CSP resulted in CFTR accumulation in a perinuclear compartment that colocalised with the ER protein calnexin. CSP over-expression also increased the amount of HSC70 which co-immunoprecipitated with CFTR (see Table 1.1) (Schmidt *et al.*, 2009). Furthermore, the increased association of HSC70

with CFTR was mirrored by an increase in CHIP co-precipitation (C terminus of HSC70 interacting protein) with CFTR. CHIP has been shown to target CFTR for proteasomal degradation and it was therefore suggested that CSP might promote proteasome-mediated degradation of CFTR by increasing the interaction of CFTR with CHIP.

CSP may also function in constitutive fusion events at the plasma membrane. Indeed CSP is expressed in IM-2 mammary epithelial cells at approximately 10-fold lower levels than in brain (Gleave *et al.*, 2001). Sucrose gradient fraction of KIM-2 cells, together with immunoisolations from post-nuclear supernatants and immunofluorescence analyses illustrated that CSP is localised on vesicles in this cell type. The role of CSP in constitutive exocytosis was detected via the secretion of growth hormone, which was transiently transfected into KIM-2 cells. The results revealed that CSP over-expression had no effect on constitutive exocytosis in KIM-2 cells (see Table 1.1).

1.5.8 Palmitoylation and membrane-association of CSP

The defining motif of CSP, the cysteine string domain, is extensively palmitoylated (Gundersen *et al.*, 1994; Mastrogiacomo *et al.*, 1994a). Palmitoylation is a common post-translational modification most often involving the attachment of palmitate groups onto cysteine residues via thioester linkage. Many cellular proteins undergo rapid dynamic cycles of palmitoylation and depalmitoylation, which can have a major effect on protein function (Salaun *et al.*, 2010). Palmitoylation is now known to regulate modified proteins in many ways, including regulating protein sorting, membrane microlocalisation, protein-protein interactions and protein function. Other than mediating membrane binding, there has been interest in the dynamics of CSP palmitoylation, and how this modification might affect CSP function.

It was examined if synaptic vesicle cycling correlated with changes in the palmitoylation status of *Drosophila* CSP (van de Goor *et al.*, 1995). These experiments were performed in temperature sensitive *Drosophila* dynamin mutants

(shibire^{ts1})(Poodry and Edgar, 1979). At restrictive temperatures synaptic vesicle recycling in shibire^{ts1} flies is blocked at an early stage of endocytotic retrieval of vesicles from the plasma membrane, and synaptic vesicle proteins become localised to the plasma mebrane. No obvious difference in CSP palmitoylation, judged by migration on SDS-PAGE, was observed in fractionated post-nuclear supernatants of shibire^{ts1} flies incubated at permissive and restrictive temperatures. This suggested that CSP does not undergo marked changes in palmitoylation during vesicle cycling in *Drosophila*. The question of whether CSP undergoes cycles of palmitoylation and depalmitoylation and whether dynamic palmitoylation has any role in neurotransmitter release, was also addressed by Gundersen's group (Gundersen *et al.*, 1996). Here, a larval neuromuscular preparation of Drosophila was treated with tunicamycin to block palmitoylation. Electrophysiological recordings of nerve-evoked responses showed no obvious change in tunicamycin treated cells, even at sustained high level transmitter release, and no depalmitoylation of CSP was observed. Thus, it was suggested that CSP does not undergo cycles of palmitoylation/depalmitoylation. However, it should be mentioned that this work showed no control to demonstrate that tunicamycin actually blocks palmitoylation and indeed tunicamycin is not commonly used as a palmitoylation inhibitor (Resh, 2006).

More recent studies have investigated the enzymes that palmitoylate CSP. A family of 'DHHC' proteins that catalyse cellular palmitoylation reactions was recently characterised (Fukata *et al.*, 2004); about 20 of these proteins are expressed in *Drosophila* (Bannan *et al.*, 2008). The Huntingtin-interacting protein 14 (Hip14), which is a homologue to mammalian DHHC17, was found to be a candidate palmitoyl-tranferase for CSP in *Drosophila* (Ohyama *et al.*, 2007). A genetic screen was used to identify mutations that affect neurotransmitter release; hereby Hip14 was identified. Hip14 was shown to be expressed throughout the nervous system, but was also present in other tissues. Interestingly, Hip14 mutants exhibited mislocalisation of both CSP and SNAP25 in larval ventral cord neurons (VCN). Furthermore, the level of CSP at neuromuscular junctions (NMJ) was reduced, and the molecular mass of the protein was 6-7 kDa lower than in control flies. Moreover Hip14 mutants exhibited temperature sensitive exocytotic defects, similar to those observed in CSP

null mutant *Drosophila* (Zinsmaier *et al.*, 1994). These results led to the suggestion that Hip14 palmitoylates CSP and that the defects in evoked release observed in Hip14 mutants are caused by a failure of palmitoylation and therefore mislocalisation of CSP. This idea was confirmed by an elegant experiment in which the defect in evoked release in Hip14 mutants was overcome by expressing a chimeric form of CSP fused to the transmembrane domain (TMD) of VAMP. The VAMP TMD facilitated the targeting of CSP to synapses in the absence of palmitoylation. The fact that the unpalmitoylated CSP-VAMP TMD chimera rescued exocytosis suggests that palmitoylation of the cysteine-string domain might only be required as a membrane binding and targeting module, and does not have other important functions for CSP, although this clearly merits further investigation.

24 DHHC proteins have been identified in mammalian cells and many of these proteins have been shown to palmitoylate specific substrates (Fukata *et al.*, 2004). Greaves *et al.*, 2008 showed that DHHC3, DHHC7, DHHC15 and DHHC17 were able to palmitoylate CSP in co-expression studies in HEK293 cells; it was also shown that these DHHC proteins are localised to the Golgi. By analysing membrane binding and palmitoylation of a large panel of CSP mutants (Greaves and Chamberlain, 2006; Greaves *et al.*, 2008) it was proposed that CSP has a weak membrane affinity that mediates membrane interaction and proximity to Golgi-localised DHHC proteins. Subsequent palmitoylation mediates tight membrane association, facilitating targeting of CSP to secretory vesicles and plasma membrane.

1.5.9 Phenotype of CSP null mice

Analysis of null mutants clearly highlighted an important role for CSP in evoked neurotransmitter release in *Drosophila* (Zinsmaier *et al.*, 1994). Subsequent work from several groups also provided strong evidence that CSP functions in regulated exocytosis pathways in mammalian cells (see 1.5.3).

CSPα knock out mice were generated by isolating genomic CSPα clones and constructing a targeting vector that deleted the first exon encoding residues 1-36 of

mouse CSPα. Thereafter a targeting vector was electroporated into embryonic stem cells and homologous recombinants were selected and used to breed CSPα KO mice. Genotyping and immunoblotting indicated if the mice were hetero- or homozygote, and clearly showed that CSPα was not detectable in the homozygote KO mice. Immunoblotting of brain samples also demonstrated that expression of proteins including VAMP2, SCAMP1 and complexins were not affected by the ablation of CSPα. At birth CSPα$^{-/-}$, CSPα$^{+/-}$ and CSPα$^{+/+}$ mice were similar, based on weight and survival. Interestingly however, around two to three weeks after birth CSPα$^{-/-}$ mice suffered from progressive weakness and stopped gaining weight. Furthermore the CSPα$^{-/-}$ mice lost spontaneous physical activity, which could also be observed to a lesser extent in CSPα$^{+/-}$ mice. At this time, the CSPα$^{-/-}$ mice also showed muscle weakness, revealed by their tendency to clasp hindlimbs when suspended by the tail and the lack of gripping strength on fore- and hindlimbs. By P30, CSPα$^{-/-}$ mice were only able to eat when stimulated to do so. CSPα$^{-/-}$ mice died from P21 onwards and none survived beyond three months of age. Internal examination revealed no major abnormalities, except bilateral intraabdominal cryptorchidism, a failure of testicular descent. When P15 KO mice were placed on their left or right side, they had difficulties in getting up. CSPα$^{-/-}$ mice also displayed a poor acoustic startle response. These conditions became more severe at P25 and indicated that synaptic transmission at the neuromuscular junction (NMJ) may be perturbed.

Electromyography is a technique for evaluating and recording the electrical activity produced by skeletal muscles. This technique was used to study skeletal muscle responses in wild type and CSPα$^{-/-}$ mice at P15, P23 and P45. Wild type mice had a small mean amplitude of compound muscle action potentials (CMAPs) at P15, but this increased ~2 fold at P23 and P45. The CSPα$^{-/-}$ mice exhibited reduced (relative to wild type) CMAPs at P15 and this was more profound at P23 and P45. These findings indicate that older CSPα$^{-/-}$ mice exhibit a limited functional impairment of the NMJ. Further analysis using light- and electron microscopy revealed that wild type mice showed ramified NMJs by ~P21 and each receptor rich branch of the postsynaptic apparatus was directly apposed by a presynaptic nerve terminal. In contrast the postsynaptic apparatus of CSPα$^{-/-}$ mice was less mature and had a

perforated appearance with some branches appearing thinner than in wild type animals. Since the pre- and postsynaptic apparatus develop in parallel, these observations suggest that nerve terminals initially formed normally, but then began to degenerate. Further electromicroscopic analyses of the synaptic ultrastructure of sternocleidomastoid muscles revealed a normal appearance in mutants, related to the number of presynaptic active zones. However, 42 % of the terminals contained vacuoles and/or multilamellar bodies, which is symptomatic of a degenerative process, and 45 % of nerve terminals were invaginated at the surface.

Previous work had hypothesised that CSPα functions as a molecular chaperone, is involved in calcium channel activity or plays a role in Ca^{2+}-triggered exocytosis (see 1.5.5). These models for CSPα function were tested through further analysis of CSPα$^{-/-}$ mice. Thus, synaptic transmission and calcium channel function were examined at the Calyx of Held synapse. The analysis suggested that calcium channel function was normal in CSPα$^{-/-}$ mice, as similar activation time course and voltage dependence of Ca^{2+} currents was observed. Aga-IVa toxin, which inhibits Ca^{2+} current at the Calyx synapse mediated by Aga-IV-sensitive P/Q-type VGCCs, inhibited the majority of Ca^{2+} currents in both wild type and CSPα$^{-/-}$ synapses. This demonstrated that there was not a loss of P/Q-channel function in the mutants which was being masked by compensation by other channel subtypes. Presynaptic N-type calcium currents were analysed after adding the specific antagonist ω-conotoxin and applying voltage steps every 15 seconds; no significant difference between wild type and CSPα$^{-/-}$ mice was evident. Together, this data provides good evidence that CSPα is not essential for presynaptic Ca^{2+} channel function. The coupling of G protein-coupled receptors to voltage-gated calcium channels was also analysed in CSPα$^{-/-}$ mice. The G protein-mediated coupling of $GABA_B$ receptors to P/Q-type channels was also unchanged in CSPα$^{-/-}$ mice.

To examine the importance of CSP for synaptic exocytosis, synaptic transmission was studied at the Calyx of Held synapse from P9-P11 mice using afferent fiber stimulation in brainstem slices and recording AMPA receptor-mediated excitatory postsynaptic currents (EPSCs). Shapes and amplitudes, as well as rise and decay times of EPSCs were indistinguishable between wild type and CSPα$^{-/-}$ mutants.

Furthermore CSPα deletion did not alter synaptic responses during stimulus trains or spontaneously occurring miniature EPSCs in the recording intervals between evoked EPSCs. Nevertheless synaptic responses were more heterogeneous in the CSPα mutants than in wild type mice. To study exocytosis more accurately, the kinetics of the slow and fast components of transmitter release were recorded using pre- and postsynaptic voltage-clamp recordings, and the kinetics of these were analysed, however no differences were detected. This led to the suggestion that coupling of Ca^{2+} channels to vesicle fusion and the Ca^{2+} sensitivity of vesicle fusion were not significantly altered in CSPα$^{-/-}$ mice (Fernandez-Chacon *et al.*, 2004).

It is possible that CSPα inactivation leads to more pronounced defects at the Calyx of Held at later stages of development, as seen in NMJs (see above). Therefore synaptic transmission in Calyx synapses was also tested in P20-P23 mice using afferent fiber stimulation. At this developmental stage significant changes were detected for the CSPα$^{-/-}$ mice. The average initial EPSC amplitude was smaller at P20-P23 than at P9-P11 in the CSPα$^{-/-}$ mice and ~2 fold lower than in wild type animals of similar age. In addition transmitter release was more asynchronous in the CSPα$^{-/-}$ mice than in wild type animals, as shown by the decreased ESPC rise time and decay. Morphological examination of Calyx terminals in CSPα mutants at P25 revealed severe synapse structural changes. Neurons were surrounded by distinct wide electron-lucent areas, containing black, electron dense particles, which were identified as degenerated mitochondria. Some electron-lucent areas also contained aggregates of agglutinated presynaptic vesicles. The postsynaptic cells of the CSPα$^{-/-}$ mice were smaller than wild type, but overall had a normal appearance.

As a whole, the work of Fernandez-Chacon *et al.*, 2004 showed that deletion of CSPα caused progressive dysfunction of synapses that eventually killed the mice. This lethality seemed to be caused by the loss of nerve terminal integrity, instead of changes in transmission as hypothesised previously.

Later work which focused more on photoreceptor synapses of the retina in CSPα$^{-/-}$ mice indicated that these mutants initially have some visual function but suffer from complete blindness after 4 weeks (Schmitz *et al.*, 2006). Changes were detected in

the ultrastructual appearance of the photoreceptor ribbon synapses in mutant mice and photoreceptor terminals tended to be smaller than in wild type and terminals showed an increase in synaptic vesicle density.

It is known that over-expression of α-synuclein causes late onset neurodegeneration (Fernagut and Chesselet, 2004). The relationship between transgenic α-synuclein effects and the CSPα function was studied by generating mice homozygous for CSPα deletion and hemizygous for transgenic α-synuclein over-expression. Intriguingly the transgenic expression of human and mouse α-synuclein prevented the weight loss, neuronal cell death and completely abolished the lethality associated with the CSPα$^{-/-}$ genotype.

A quantitative assessment of motor behaviour of wild type, CSPα$^{-/-}$ and CSPα$^{-/-}$ mice over-expressing transgenic α-synuclein (CSP$^{-/-}$ Syn^{htg}) was undertaken (Chandra *et al.*, 2005). This analysis revealed that CSPα$^{-/-}$ mice had restricted exploratory behaviour and showed 'jagged and jerky' movements and sudden falls, reflecting ataxic behaviour. The co-expression of α-synuclein in CSPα$^{-/-}$ mice reversed this ataxic behaviour. As over-expression of α-synuclein rescues the CSPα$^{-/-}$ phenotype, it was examined whether endogenous α-synuclein dampens the progression of the CSPα$^{-/-}$ phenotype. For this, CSPα$^{-/-}$ mice were crossed with α/β-synuclein double knock out mice, which do not exhibit a major phenotype. The 'triple' knock out mice weighed less at P8 than control and at P20 they were half the size compared to wild type mice. They eventually died a few days after weaning (generally no survival after P30). In contrast, the CSPα$^{-/-}$ mice stopped gaining weight after ~ P21 and survived as far as three months. These results showed that the loss of endogenous synuclein accelerated the CSPα$^{-/-}$ phenotype, highlighting that endogenous synuclein dampens the effect of CSPα$^{-/-}$ phenotype, as suspected.

The observed rescue of the CSPα$^{-/-}$ phenotype by synuclein over-expression suggested that α-synuclein might act as a co-chaperone with CSPα or function downstream of CSPα. To address this idea, it was examined whether α-synuclein interacts with CSPα, HSC70 and SGT, and if α-synuclein can replace CSPα in

stimulating HSC70 ATPase activity. This analysis found that α-synuclein did not show binding to any of these proteins and did not activate the HSC70 ATPase activity. The possibility of α-synuclein acting as a general chaperone was explored by crossing the transgenic α-synuclein mice with transgenic mice, which expressed mutant superoxide dismutase (SOD), causing spinal cord neurodegeneration. Transgenic α-synuclein did not improve neurodegeneration which was caused by SOD over-expression, suggesting that α-synuclein does not act as a general chaperone, and therefore that its effects are more specific for CSPα (Chandra *et al.*, 2005).

Interestingly it was found that the levels of the SNARE-protein SNAP25 were decreased by 30 %- 40 % at all ages (P5, P10 and P40) in CSPα$^{-/-}$ mice and smaller decreases (~ 20 %) in HSC/HSP70 and α-synuclein levels were also detected. Other synaptic proteins, such as VAMP2, syntaxin and complexin did not exhibit altered expression levels in CSPα$^{-/-}$ mice. Reduced SNAP25 levels were specifically related to the loss of CSPα, since over-expression of α-synuclein did not rescue SNAP25 expression throughout development, whereas it did rescue the decrease of HSC/HSP70 levels. This suggested that α-synuclein and CSPα might both alter SNARE function but possibly via different mechanisms. Immunoprecipitation of assembled ternary SNARE complexes from CSPα$^{-/-}$ mice revealed that SNARE complex levels were also significantly decreased in the knock out mice, which was reversed by transgenic wild type α-synuclein.

Another group looked at synaptic function of CSPα using the CSPα$^{-/-}$ mice generated by Fernandez-Chacon (Fernandez-Chacon *et al.*, 2004; Ruiz *et al.*, 2008). Here it was suggested that CSPα is essential for normal Ca^{2+} sensitivity of regulated exocytosis in mature synapses, as calcium sensitivity was decreased in CSPα$^{-/-}$ terminals, but the amplitudes of the postsynaptic responses were rescued with high Ca^{2+} concentrations.

The function of CSPα at small central synapses was explored in CSPα$^{-/-}$ mice, by studying long-term hippocampal cultures (Garcia-Junco-Clemente *et al.*, 2010). Neurons that lacked CSPα failed to maintain a high number of synapses compared to

control, observed after 30 days of culturing the neurons. Interestingly, further analyses demonstrated that the loss of synapses was restricted to GABAergic synapses in culture. However, it should be noted that such a difference was not readily apparent in brain slices. In contrast, the number of glutmatergic terminals was similar between mutant and wild type cultures. It was also found that GABAergic terminals expressing synaptotagmin-2 were more imperilled, since KO cultures did not show any expression of synaptotagmin-2 after 30 divisions, whereas wild type cultures exhibited colocalisation of synaptotagmin-2 and the GABA transporter VGAT. Synaptotagmin-2 is a member of hippocampal basket cell terminals, which are a subpopulation of GABAergic cells, and electron microscopy analyses indicated degeneration of these basket cell terminals. Further analysis revealed that spontaneous release, measured by the miniature inhibitory postsynaptic current (mIPSC), was also impaired in mutant cultures. Generally CSPα appears to be an important component of an unknown physiological mechanism that maintains presynaptic function, especially of synaptotagmin-2 expressing GABAergic synapses, which fire action potentials at high frequencies.

As discussed previously, transgenic α-synuclein expression, which was able to rescue the CSPα KO phenotype and SNARE complex levels, did not reverse the decrease of SNAP25 levels present in CSPα$^{-/-}$ mice. Recent work has revealed that SNAP25 mRNA levels are normal in CSPα$^{-/-}$ mice (Sharma *et al.*, 2011) and SNAP25 degradation is a temperature-sensitive phenotype in CSPα$^{-/-}$ neuronal cultures. No temperature-sensitive changes were observed with the closely related SNAP23 protein or with SGT and syntaxin. In addition CSPα depletion resulted in a 40 % increase in ubiquitination of SNAP25, as well as HSC70. In order to examine if SNAP25 degradation is dependent on synaptic activity in mutants, cycles of assembly and disassembly of SNARE-complexes were analysed. Synaptic activity was silenced using tetrodotoxin (TTX) or enhanced with increased K^+ or Ca^{2+} concentrations. Examination of steady-state levels in CSPα$^{-/-}$ cultures revealed that synaptic silencing induced a 70 % increase in SNAP25 levels, whereas synaptic activation caused a 30 % decrease, compared to syntaxin 1 and VAMP2 levels, which were unchanged. This revealed that SNAP25 levels were controlled by

synaptic activity in the absence of CSPα. Interestingly, HSC70 and SGT levels were significantly increased upon enhancement of synaptic activity in both genotypes (wild type and CSPα$^{-/-}$), suggesting that their increase during high activity may serve to protect SNAP25 from activity-dependent degradation.

1.5.10 Mammalian CSP isoforms

Two distinct CSP cDNA species were identified through PCR amplification of bovine chromaffin cell cDNA and termed CSP1 and CSP2 (Chamberlain and Burgoyne, 1996). The primers used to amplify these cDNAs corresponded to the 5' and 3' ends of the previously identified rat CSP coding sequence. Both DNA bands were detected in every rat tissue examined (e.g. kidney, liver, pancreas, spleen, lung and adrenal), except in brain, where only one DNA band (CSP1) was detected. Sequencing of the DNA bands revealed that CSP1 had 88 % nucleotide identity and 95 % amino acid identity with rat CSP. CSP2 was shown to be a novel splice variant of CSP1; CSP2 is identical to CSP1, but has a 72-base pair insert, which incorporates two stop codons into the C-terminus of the encoded protein, resulting in a truncated isoform. Subsequent work confirmed that CSP2 mRNA is also expressed in humans (Coppola and Gundersen, 1996). Expression of CSP2 protein has not been reliably established to date.

Two additional novel mammalian CSP isoforms were identified in human testis, and called CSPβ and CSPγ (Tobaben and Stahl, 2001; sequences to be found in GenBank, CSPβ: AF368276, CSPγ: AF368277; unpublished; Figure 1.3 and Figure 1.4). Both of these isoforms were also identified in mouse testis (Fernandez-Chacon *et al.*, 2004). CSPα, CSPβ and CSPγ are present on separate chromosomes (Evans *et al.*, 2003); the overall amino acid homology between CSPα and CSPβ is 69 %, CSPα and CSPγ 55 %, and CSPβ and CSPγ 52 %. Comparing the defining motifs of the CSP isoforms, reveals that the cysteine-string domain of CSPα and CSPβ share a 76 % similarity, whereas CSPα and CSPγ, as well as CSPβ and CSPγ, share 56 % congruency. The J-domain of CSPβ is 83 % identical to CSPα, the CSPγ J-domain

Figure 1.3: Alignment of rat CSP isoforms. Alignment of the sequences of rat CSPα, -β and -γ. Conserved amino acids present in all 3 isoforms are coloured green, conserved residues present within 2 isoforms are coloured yellow. The blue box highlights the highly conserved J-domain and the red box the highly conserved cysteine string domain.

shares 74 % identity with the J-domain with CSPα and the J-domains of CSPβ and CSPγ are 69 % identical.

Although CSPβ and CSPγ were reported to be largely testis-specific, quantitative PCR revealed that CSPβ is expressed in inner hair cells (Schmitz *et al.*, 2006).

Pull down experiments with homogenates from insulin-secreting MIN6 cells on immobilised recombinant CSPβ or CSPα showed that recombinant CSPβ bound to HSC70/SGT complex to a similar extent as CSPα (Boal *et al.*, 2007). To further characterise the biochemical properties of CSPβ, this isoform was over-expressed in HIT-T15 pancreatic beta cells, which were then fractionated into cytosol and membrane fractions. CSPβ was mainly present in the membrane fraction and this association was only disrupted after Triton X-100 treatment, demonstrating that membrane attachment is tight. Immunoblot analysis showed that over-expressed myc-tagged CSPβ was detected in three different sizes, with the major band at 30 kDa, a minor band and at 33 kDa and a band observed at 65 kDa, which probably corresponded to a dimeric form of myc-CSPβ. The myc-CSPβ bands detected at 30 kDa and 33 kDa indicate a non-palmitoylated (30 kDa) and palmitoylated form of CSPβ. As the major CSPβ band (30 kDa) was refractive to hydroxylamine treatment

A

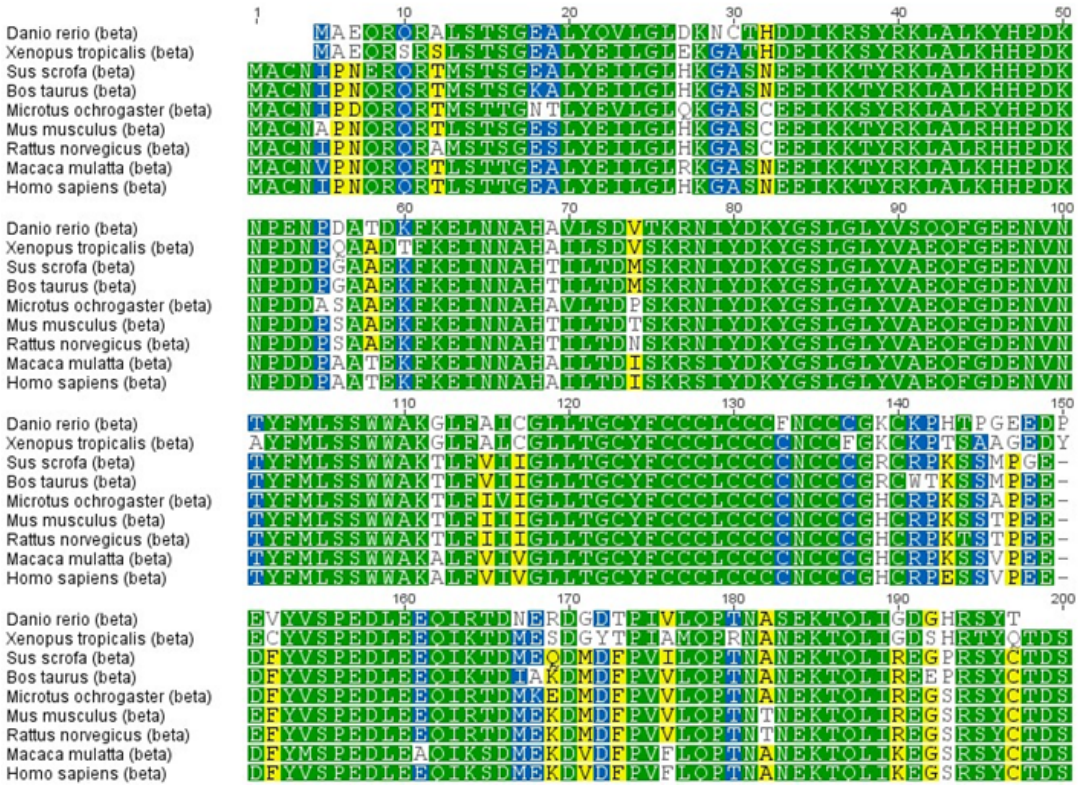
Danio rerio (beta)
Xenopus tropicalis (beta)
Sus scrofa (beta)
Bos taurus (beta)
Microtus ochrogaster (beta)
Mus musculus (beta)
Rattus norvegicus (beta)
Macaca mulatta (beta)
Homo sapiens (beta)

B

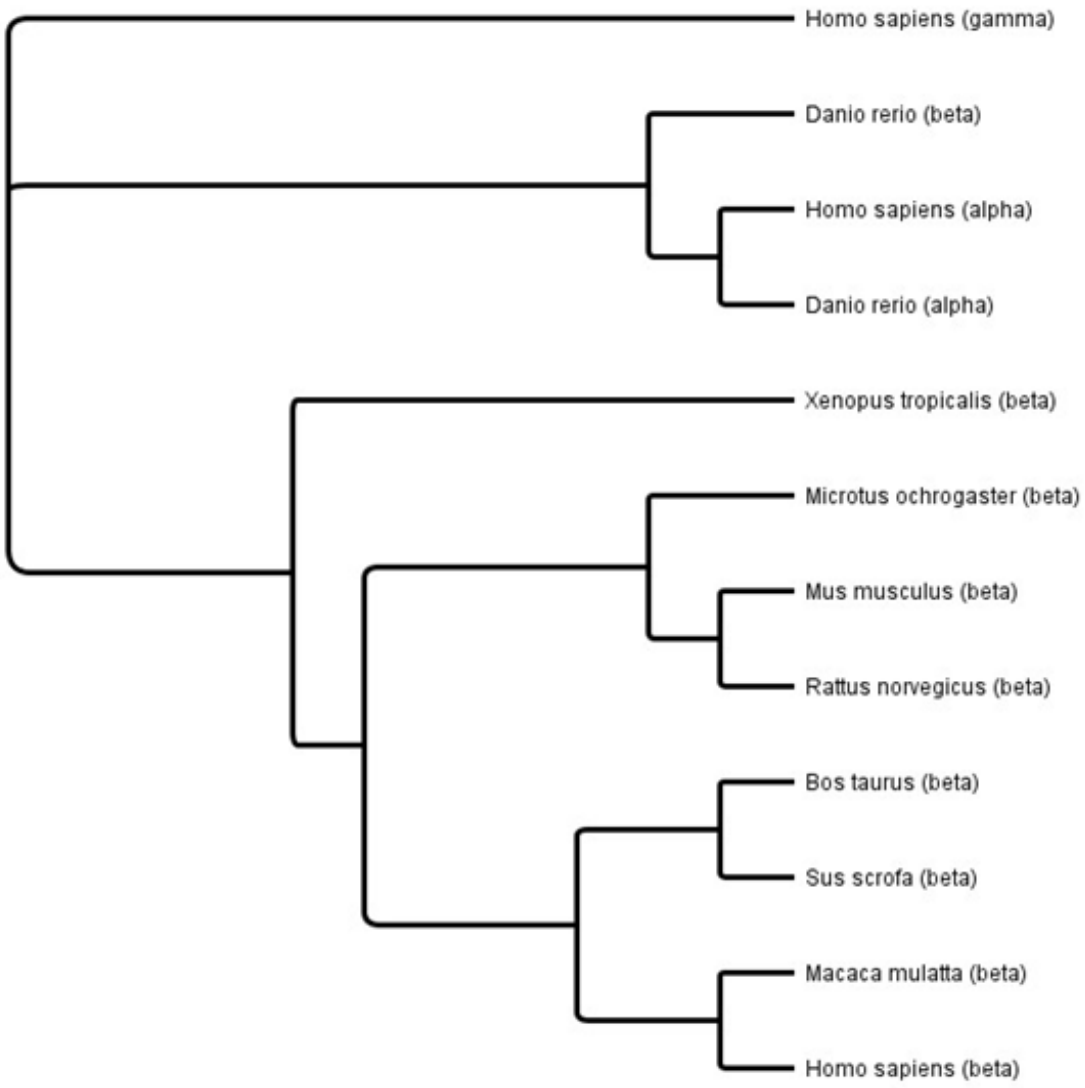

Figure 1.4: Alignment and phylogenetic tree of CSPβ in a section of vertebrates. *A*. Amino acid sequences of CSPβ (beta) from several species (as noted in the figure) were aligned. Conserved amino acids present in all species are highlighted green, conserved residues present in 80 % of the species are coloured blue and conserved residues present in 60 % of the species are coloured yellow. *B*. Amino acid sequences of CSPα (*alpha)* from *Danio rerio* and *Homo sapiens*, CSPβ (*beta*) from several species (as noted in the figure) and CSPγ (*gamma*) from *Homo sapiens* were used to construct a phylogenetic tree. The tree depicts the branching history of the CSP isoforms, in particular the relationship of CSPβ in vertebrates. CSPβ from *Xenopus tropicalis* to *Homo sapiens* show close evolutionary relation, compared to *Homo sapiens* and *Danio rerio* CSPα and *Homo sapiens* CSPγ, which are more distantly related on the tree. However, the tree indicates that *Danio rerio* CSPβ is closely related to *Danio rerio* and *Homo sapiens* CSPα. (Geneious v5.4, available from http://www.geneious.com/).

and did not incorporate [^{3}H]-palmitic acid, this suggests that CSPβ is predominantly non-palmitoylated. The subcellular distribution of CSPβ in HIT-T15 cells was examined by immunofluorescence in cells expressing HA-tagged CSPβ. This tagged-CSPβ did not colocalise with insulin containing granules like CSPα, but instead was detected on the trans Golgi network (TGN), colocalising with the TGN marker Vti1b.

Mutations in the cysteine string domain of CSPβ, to make it more similar to CSPα did not result in colocalisation of CSPβ with insulin granules, suggesting that the cysteine-string domain is not the predominant factor determined for the different localisation of CSPα and CSPβ. Recently a CSPβ antibody was generated against the C-terminal amino acid sequence QPTNTNEKTQLIREGSRSY (Gundersen *et al.*, 2010). This antibody was specific for recombinant CSPβ; however it only detected a protein band at 100 kDa in testis. The authors suggested that this band represents a homotetramer of CSPβ or a complex consisting of other proteins. Interestingly this 'CSPβ' band was also detected at 100 kDa in mouse brain, contrasting to the work of Fernandez-Chacon *et al.*, 2004, who claimed that CSPβ was testis specific, revealed through northern blot analysis. In the work of Gundersen *et al.*, 2010 it was demonstrated that CSPβ RNA could only be detected in brain samples by northern blotting when more than 10 μg of RNA was used. The 'CSPβ' protein band was detected throughout the CNS and subcellular fractionation also revealed that CSPβ is mainly found within synaptosomes and synaptic vesicle fractions. Over-expression of CSPβ in frog oocytes led to a block of cortical granule exocytosis, suggesting that CSPβ might be involved in regulated exocytosis similar to CSPα (see Table 1.1). However, the exact localisation, palmitoylation and function of CSPβ requires further investigation.

1.6 Aims and hypothesis

Depletion of CSPα in *Drosophila* is embryonic lethal and in embryos synaptic vesicle exocytosis was decreased by approximately 50 % at 22°C and abolished at

higher temperatures. These results provided strong evidence that CSPα has an important role in presynaptic neurotransmission. However, more recent work on CSPα null mice uncovered an important neuroprotective function for CSPα in brain, but also challenged the proposed function of CSPα in neuronal exocytosis, as no defect in this pathway was evident, at least in young animals. The only reported developmental abnormality of CSPα null mice was bilateral cryptorchidism, a failure of testicular descent during development. Interestingly, two additional CSP isoforms were recently identified in mouse and human testis, CSPβ and CSPγ. One consequence of the identification of CSPβ and CSPγ is that they may complicate analysis of CSPα knockout mice.

Our hypothesis is that CSPα performs an important function in exocytosis pathways throughout the body. With this in mind, the aims of this thesis are: (i) to deplete CSPα expression using siRNA and examine the effect of this on regulated and constitutive exocytosis; (ii) to examine how the expression of CSPα and interacting partners changes in defined neurological disorders; (iii) to define the localisation and function of CSPα in testis and investigate possible co-distribution with INSL3, since depletion of INSL3 also leads to cryptorchidism; (iv) to delineate the expression profiles of the CSP isoforms CSPβ and CSPγ, by generating and using CSPβ and CSPγ antibodies; and (v) to analyse the features of CSPα that contribute to intracellular targeting.

CHAPTER TWO: MATERIAL AND METHODS

2.1 Material and suppliers

2.1.1 Chemicals

If not stated otherwise, all chemicals used were supplied by Sigma-Aldrich Company (Dorset, U.K.) and Invitrogen Ltd. (Paisley, U.K.), and were of the purest grade available.

2.1.2 Molecular biology reagents

XL10-Gold® Ultracompetent bacterial cells (genotype TetrD(*mcrA*)*183* D(*mcrCB-hsdSMR-mrr*)*173 endA1 supE44 thi-1 recA1 gyrA96 relA1 lac* Hte [F′ *proAB lacI*qZD*M15* Tn*10* (Tetr) Amy Camr]) were purchased from Stratagene (La Jolla, U.S.A). TOP 10 Chemically Competent Cells (strain F- *mcr*A Δ(*mrr-hsd*RMS-*mcr*BC) Φ80*lac*ZΔM15 Δ*lac*X74 *rec*A1 *ara*D139 Δ(*araleu*) 7697 *gal*U *gal*K *rps*L (StrR) *end*A1 *nup*G), PureLink™ Quick Plasmid Miniprep Kit, PureLink™ HiPure Plasmid Filter Purification Kit, SYBR® Safe DNA gel stain and DNA ladder (1 kb) were obtained from Invitrogen Ltd. (Paisley, U.K.). RNeasy® Mini Kit and *E. coli* M15 [pREP4] cells were purchased from Qiagen (Crawley, U.K.); the M15 cells are derived from *E. coli* K12 and harbour the *lacIq* mutation. GoTaq®DNA polymerase, *pfu* polymerase, Oligo $(dT)_{15}$ Primer, M-MLV Reverse Transcriptase, Recombinant RNasin® Ribonuclease Inhibitor, dNTPs (dATP, dCTP, dGTP, dTTP) and T4 DNA Ligase were purchased from Promega (Southampton, U.K.). Oligonucleotide Primers were synthesised by Sigma-Proligo (Sigma-Aldrich®, Dorset, U.K.). Dharmafect transfection reagent and small interference RNA (siRNA) were obtained from Dharmacon (Epson, U.K.).

2.1.3 Small interference RNA

Table 2.1: Small interference RNA oligonucleotides (5'>3') for rat CSPα in rat

siRNA Name	Target Sequences
CSP #1	AGACAGAAUUCUACGUAUCUU
CSP #2	AGACACACCGAUCGUCAUAUU
CSP #3	UUAACAACGCCCACGCAAUUU
CSP #4	CUUGAUACAUGAAGUGCGUUU

Table 2.2: Small interference RNA oligonucleotides (5'>3') for human CSPα

siRNA Name	Target Sequences
hCSP #1	GGGUUGGACAAGAACGCAA
hCSP #2	GGAUACAUCUGGACGUGCU
hCSP #3	ACUAAAAUGAUCACGAAGA

2.1.4 Primers

2.1.4.1 PCR primers

Table 2.3: Oligonucleotide primers (5'>3') for DNA amplification of CSP isoforms from mammalian tissues

Primer Name	Forward Sequences	Reverse Sequences
CSPα (594 bp)	ATGGCTGACCAGAGGCAGCGCTC	GTTGAACCCGTCGGTGTGATAGCTG
CSPβ (539 bp)	TATGAAATCCTTGGTCTGCATAAGGGAG	CAAGAGTCTGTGCAGTAACTTCGAGATCC
CSPγ (361 bp)	ATGCCTCGTGCGTATGAAGC	CCGGTCAGCAGGCAACAAA

Table 2.4: Oligonucleotide primers (5'>3') for CSPβ and CSPγ. having HindIII (AAGCTT) and BamHI (GGATCC), and INSL3 having HindIII (AAGCTT) and Sal1 (GTCGAC) restriction sites incorporated, which allowed the amplified DNA to be inserted into pQE30 and/or pEGFP-C2 vectors

Primer Name	Forward Sequences	Reverse Sequences
pQE30-CSPβ	TGCA**GGATCC**GCATGTAA CATACCTAATC	TGCA**AAGCTT**TCAAGAGT CTGTGCAGTAACTTCG
pQE30-CSPγ	TGCA**GGATCC**CCTCGTGCG TATGAAGCAAC	CGCG**AAGCTT**TTAATCCTC TTCTTCAATG
eGFP-CSPβ	TGCA**AAGCTT**CGCATGTAA CATACCTAATC	TGCA**GGATCC**TCAAGAGT CTGTGCAGTAACTTCG
eGFP-CSPγ	TGCA**AAGCTT**CCCTCGTGC GTATGAAGCAAC	TGCA**GGATCC**TTAATCCTC TTCTTCAATG
eGFP-INSL3	GTAC**AAGCTT**ATGCACGCA CTGCTGCTACTGCTGCTC	GTAC**GTCGAC**GCGTGGGG ACACAGACCCAA AAGGTCTTGC

Table 2.5: Oligonucleotide primers (5'>3') used to generate CSPα N-terminal truncation mutants incorporating HindIII (AAGCTT) and BamHI (GGATCC) restriction sites, which allowed the amplified DNA to be inserted into the pEGFP-C2 vector

Primer Name	Forward Sequences	Reverse Sequences
CSP17-198	GCAT**AAGCTT**ATACCATG TTCTTGGACTG	GCAT**GGATCC**TTAGTTGA ACCCGTCGGTG
CSP70-198	GCAT**AAGCTT**CGCCACGA AAAGAAACATTTATG	GCAT**GGATCC**TTAGTTGA ACCCGTCGGTG
CSP84-198	GCAT**AAGCTT**GCTCTATG TGGCTGAGC	GCAT**GGATCC**TTAGTTGA ACCCGTCGGTG
CSP98-198	GCAT**AAGCTT**CTACTTCG TACTCTCCAG	GCAT**GGATCC**TTAGTTGA ACCCGTCGGTG

Table 2.6: Oligonucleotide primers (5'>3') to generate CSPα– and CSPβ–chimeras incorporating or deleting EcoRI (GAATTC) restriction sites through site-directed mutagenesis

Primer Name	Forward Sequences	Reverse Sequences
CSPα ECORI	CAAGGCCCTGTTCATCTTC **GAATTC**TGTGGGCTCCTC ACCTGC	GCAGGTGAGGAGCCCACA **GAATTC**GAAGATGAACAG GGCCTTG
CSPβ ECORI	CATTGGCCTCTTGACCGG C**GAATTC**TGCTATTTTTG CTGCTGC	GCAGCAGCAAAAATAGCA **GAATTC**GCCGGTCAAGAG GCCAATG
CSPα–Nterm β ΔECORI	CATTGGCCTCTTGACCGG CTGTGGGCTCCTCACCTG CTGC	GCAGCAGGTGAGGAGCCC ACAGCCGGTCAAGAGGCC AATG
CSPβ–Nterm α ΔECORI	GCCAAGGCCCTGTTCATC TTCTGCTATTTTTGCTGCT GCCTATG	CATAGGCAGCAGCAAAAA TAGCAGAAGATGAACAGG GCCTTGGC

Table 2.7: Oligonucleotide primers (5'>3') used for quantitative real-time PCR in rat testicular cells samples

Primer Name	Forward Sequences	Reverse Sequences
CSPα	CTGACAGACGCCACGAAA AGAAACA	CAGTAGCAGCAGGTGAGG AGGCC
CSPβ	CGTGGCCGAGCAATTTGG AG	TGGGCCGACAATGTCCACA AC
CSPγ	CGTGCGTATGAAGCAACC CAGC	GCCGCTTGAGAGTTCCCTG GA

Table 2.8: Oligonucleotide primers (5'>3') used for quantitative real-time PCR in mouse testicular cells

Primer Name	Forward Sequences	Reverse Sequences
CSPα	TGGACTGGACAAGAATGCAACCTCA	TTCTTTTCGTGGCGTCTGTCAGG
CSPβ	GTTCTATGTGTCACCAGAGGACCTTGAGG	CGGGCCAACATTAAGAGTCTGTGC
CSPγ	TGGGAAAAGCCTCTATGCAGTGCT	TGGCATGGGCTGTGTTGATCTC

2.1.5 Plasmids

The plasmid vector pEGFP-C2 was purchased from Clontech Laboratories Inc. (Mountain View, California, U.S.A), which encodes a red-shifted variant of wild-type GFP (excitation maximum: 488 nm, emission maximum: 507 nm) and expresses kanamycin resistance in *E.coli*. The pQE-30 plasmid vector was obtained by Qiagen (Crawley, U.K.). mCherry plasmid, which has an maximum excitation at 587 nm and maximum emission at 610 nm, was synthesised by Colin Rickman (Rickman *et al.*, 2010) and contains mCherry in the pEGFP-C2 backbone and expresses kanamycin resistance in *E.coli*. pGH-CSPalpha-beta and pGH-CSPbeta-alpha plasmid vectors were designed to include flanking HindIII and BamHI restriction site, and were synthesised by Biomatik (Wilmington, U.S.A). Both plasmids expressed an ampicilin resistance in *E.coli*. pEGFP-C2-CSPα was constructed by Dr Luke Chamberlain (Greaves and Chamberlain, 2006).

2.1.6 Cell culture plastics and media

All cell culture plasticware was obtained from Greiner Bio-One (Kremsmünster, Austria). 30 mm coverslips were purchased from VWR International (Lutterwoth, Leicestershire, U.K.). 12 mm pre-coated poly-D-lysine coverslips were obtained

from BD Biosciences (Oxford, U.K.). The 30 mm coverslips were coated with 1.5 ml Poly-D Lysine (100 ng/ml, in sterile distilled H_2O; Sigma-Aldrich) for at least 1 hour at room temperature, washed, dried and sterilised under ultra violet (UV) light. Each 75 cm² flask for growth of PC12 cells was coated with 200 µl collagen (extracted from rat tail, see 2.2.2), dried and sterilised under UV-light for at least 16 hours and stored at 4°C until required. Advanced RPMI 1640 Media, Dulbecco's Modifies Eagle Media (D-MEM; with and without Pyruvate), D-MEM/F-12 (1:1) Media, F-12 Media (Nutrient Mixture), Hanks' Balanced Salt Solution (HBSS) (without $CaCl_2$ and $MgCl_2$), GlutaMAXT-I, Versene, Foetal Calf Serum, Lipofectamine™ 2000, and Trypsin-EDTA were all purchased from Invitrogen Corporation (Paisley, U.K.). Equine Serum Defined Donor Hyclone and Defined Foetal Bovine Serum Hyclone were purchased from Hyclone (Logan, Utah, USA).

2.1.7 Antibodies

2.1.7.1 Primary antibodies

A polyclonal CSPα antibody and an Hsc70 polyclonal antibody were obtained from Stressgen® Biotechnologies Corporation (Victoria, British Columbia, Canada). The immunoaffinity purified CSPα antibody, which was raised in rabbit, was derived from a synthetic peptide sequence from the carboxy-terminus of rat CSPα. Hsc70 was protein A affinity purified, and was derived from rabbits inoculated with a synthetic peptide from the sequence of human Hsc70. This sequence is identical to cow, hamster, mouse and rat. For immunoblotting, the antibodies were used at a dilution of 1:1,000. The CSPα antibody was further used at a dilution of 1:50 for immunofluorescence or 1:100 for immunohistochemistry.

SNAP25 (SMI 81) monoclonal antibody raised in mice immunized with full-length SNAP25, was purchased from Covance Inc. (Princeton, New Jersey, U.S.A). The

specific epitope lies at the N-terminus of the SNAP25 protein (Connell *et al.*, 2009). The dilution factor for use in immunoblotting was 1:10,000.

The anti-HA monoclonal antibody raised in rat was purchased from Roche Diagnostics Ltd. (Burgess Hill, U.K.). This antibody recognises the HA peptide sequence YPYDVPDY derived from the human influenza virus hemagglutinin protein (amino acids 98-106) and its dilution factor for immunoblotting was 1:1,000.

Living Colors® A.v. Monoclonal GFP Antibody (JL-8) was obtained from Clontech Laboratories Inc. (Mountain View, California, U.S.A). The affinity purified monoclonal antibody was produced by hybridoma cells against full-length *Aequorea victoria* green fluorescent protein (GFP). The antibody was used at a dilution ratio of 1:3,000 for immunoblotting.

Synaptic Systems GmbH (Göttingen, Germany) provided the monoclonal synaptobrevin 2/VAMP2 antibody, Synaptotagmin I and polyclonal SNAP23. VAMP2 antibody was produced in mice against the synthetic peptide SATAATVPPAAPAGEG (amino acids 2-17 in rat synaptobrevin 2). The SNAP23 antibody was derived in rabbit against the synthetic peptide DRIDIANARAKKLIDS (amino acids 196-211 in human). The Synaptotagmin I antibody was derived from mouse against amino acids 80 - 421. The dilution ratio of VAMP2 antibody for immunoblotting was 1:10,000, whereas SNAP23 and Synaptotagmin I antibodies were used at 1:1,000.

Monoclonal antibodies recognising Syntaxin 1 (HPC-1), HSP70 and α-Tubulin (DM1A) all produced in mice, were purchased from Sigma-Aldrich Company Ltd. (Dorset, U.K.). Syntaxin antibody was derived from a synaptosomal plasma membrane fraction from adult rat hippocampus. The immunogen for the HSP70 antibody was full-length HSP70 isolated from bovine brain. The α-Tubulin antibody was derived from rat brain. Syntaxin 1 and HSP70 antibodies were used at a dilution of 1:5,000 for immunoblotting. The α-tubulin antibody was used for

immunofluorescence or immunohistochemistry at a dilution of 1:50 or 1:100 respectively.

Abcam plc (Cambridge, U.K.) supplied the primary monoclonal actin antibody, which was raised in mouse and protein G purified. The affinity purified rabbit polyclonal Cyclophilin B antibody was raised against a C-terminal peptide of human Cyclophilin B. α-Synuclein antibody, which was an affinity purified polyclonal antibody, and was derived from a peptide from human α-Synuclein around the phosphorylation site of tyrosine 133 and raised in rabbit. The protein A purified GAPDH antibody was raised in rabbits against the human protein. The dilution factor used in immunoblotting for the actin antibody was 1:5,000, 1:2000 for GAPDH and 1:1,000 for both Cyclophilin B and α-Synuclein.

Monoclonal antibodies recognising Trans Golgi network 38 (TGN38) and GM130 were raised against the rat proteins and purified from tissue culture supernatant or ascites by affinity chromatography. Both antibodies were used for immunofluorescence at a dilution of 1:50. The GM130 antibody was also used for immunohistochemistry at a dilution of 1:100.

Cell Signaling Technology® (Hitchin, Hertfordshire, U.K.) provided the polyclonal antibodies against Heat Shock Protein 60 (HSP60) and Heat Shock Protein 90 (HSP90). Both antibodies were produced by immunising rabbits with synthetic peptides corresponding to human HSP60 and human HSP90 respectively. The antibodies were purified by protein A and peptide affinity chromatography.

2.1.7.2 Secondary antibodies

Amersham ECL (Little Chalfont, Buckinghamshire, U.K.) provided sheep anti-mouse IgG, donkey anti-rabbit IgG and goat anti-rat IgG, which were all HRP-conjugated and used at a dilution ratio of 1:2,000 for immunoblotting.

The AlexaFluor® 647 goat anti-mouse, AlexaFluor® 546 donkey anti-mouse and AlexaFluor® 488 goat anti-rabbit, which are labelled with a tandem dye construct and are prepared from affinity-purified antibodies, were purchased from Invitrogen Ltd.

2.1.8 Radioactive materials

[7, 8, ^{3}H] Dopamine was purchased from Amersham ECL (Little Chalfont, Buckinghamshire, U.K.).

2.1.9 Animal tissues

The *Sprague Dawley* albino laboratory rat breed (species *rattus norvegicus*) was sacrificed to collect various organs for analysis (University of Edinburgh, Hugh Robson Building, U.K.).

2.1.10 Mammalian cell lines

HeLa-C1 cells were kindly provided Dr Andrew Peden (Department of Clinical Biochemistry, University of Cambridge, Cambridge Institute for Medical Research). William Walker provided the Sertoli cells 15P-1 (derived from rat) and MSC-1 (derived from mouse) (Department of Cell Biology and Physiology, Magee Women's Research Institute, University of Pittsburgh, 204 Craft Avenue, Room B305, Pittsburgh, PA 15261, USA). The Leydig cells (R2C) were obtained from Douglas

Stocco (Department of Cell Biology and Biochemistry, Texas Tech University Health Sciences Centre).

2.2 Animal dissection

Sprague Dawley rats (see 2.1.9), which were sacrificed, were dissected to collect organs for research analysis.

2.2.1 Sperm isolation

For sperm isolation mature male rats (> 3 months old) were used (see 2.1.9). The male rat was disinfected with 70 % ethanol to avoid any contamination and the testis with the attached *vas deferens* was dissected out of the animal and kept in PBS [137 mM NaCl, 25.36 mM Na_2HPO_4, 4.41 mM KH_2PO_4, 2.7 mM KCl, pH 7.4]. Under a light microscope the testis was carefully detached from the *vas deferens* and the fat. Thereafter the vas deferens with the *epididymis* was unfolded in a small sterile petri dish. Finally the spermatozoa were squeezed out of the *vas deferens* and *epididymis* into 500 µl homogenisation buffer [20 mM HEPES, 1 mM $MgCl_2$, 250 mM sucrose, 2 mM EDTA, 1 % (v/v) nonyl phenoxylpolyethoxylethanol (NP-40), 1 mM DTT, protease inhibitor cocktail (Roche), pH 8.0] and collected in a fresh and sterile 1.5 ml tube. For further procedures see 2.6.5.

2.2.2 Collection of rat-tail collagen

Collagen, collected from mature rat tails, was used to coat flasks to facilitate PC12 cells adherence (see 2.1.6). Rat tails were immediately frozen down after collection from the donor. When required, the tails were removed from the freezer and placed in a sterile 50 ml tube filled with 70 % alcohol and allowed to thaw (approximately 15-20 minutes). The tip of the tails was then pinched with a pair of sterile pliers and

the skin pulled back until the tendons were visible. The tendons were gently dissected from the tail and placed in a sterile petri dish containing 10 ml of dH_2O for 20 minutes to hydrate them. A sterile conical flask was filled with 500 ml of sterile dH_20 and filled with tendons (1 g/100 ml). Glacial acetic acid was added to a final concentration of 1 % (v/v). The tendons were left to soak for 48 hours at 4°C with gentle mixing at 50 rpm. Thereafter the soaked tendons were centrifuged at 35,000 x g for 1 hour and the supernatant was collected and aliquoted in 5 ml volumes. The collagen was made and provided by Colin Rickman.

2.3 Molecular biology

2.3.1 Standard molecular biology protocols

All overnight cultures were grown in Luria-Bertani broth (LB) media [10 g/L NaCl, 10 g/L tryptone (Merck), 5 g/L yeast extract (Bacto™ Yeast Extract, BD)], which was autoclaved prior to use. The LB agar solutions contained LB media and 20 g/L agar (Invitrogen). LB media was supplemented with the appropriate antibiotics (100 µg/ml ampicillin, 30 µg/ml kanamycin).

Diethylpyrocarbonate (DEPC)-water was made by adding 0.1 % DEPC to ultra pure water, incubating over night and autoclaving to inactivate traces of DEPC.

2.3.2 DNA amplification by polymerase chain reaction (PCR)

Polymerase chain reaction (PCR) is used to amplify specific DNA sequences and is also a method to introduce mutations into DNA.

PCR reaction mixes contained 50 ng of DNA template (either cDNA or plasmid DNA) and 125 ng each of sense and antisense oligonucleotide primers, which were

synthesised by Sigma-Proligo. The sequences of all primers used in this thesis are shown in section 2.1.4. Also added to the PCR-mix was 5 µl 10 x *Pfu* reaction buffer (Promega), 1 µl of 40 mM dNTP (10mM of each dATP, dTTP, dGTP and dCTP), 1 µl *Pfu* DNA polymerase (Promega) and DEPC-treated dH_2O to a final volume of 50 µl. The PCR reaction consisted of an initial denaturation step for 1 minute at 94°C to melt the DNA. Following this, 30 cycles were performed consisting of a denaturing step at 94°C for 30 seconds, an annealing step at 50°C for 30 seconds and an extension step at 72°C for 3 minutes. PCR products were stored at 4 °C until required. This protocol was used for amplification of coding regions and specific truncation mutants for cloning purposes, and also for analysis of CSP expression patterns in rat tissues.

2.3.3 Amplification of CSPβ and CSPγ and INSL3 from rat testis

2.3.3.1 RNA purification

Total RNA was purified from ~ 30 mg of tissue using an RNeasy Mini Kit (Qiagen Ltd.) according to the manufacturer's protocol. The tissue was homogenized, until it was uniformly homogenous, with a rotor-stator homogenizer in 600 µl RLT buffer (composition proprietary), containing 10 % (v/v) β-Mercaptoethanol (β-ME). Following this, 600 µl of 70 % ethanol was added to the homogenised lysate and mixed through pipetting and then applied to an RNeasy mini column contained within a 2 ml collection tube. The solution was passed through the column by centrifugation for 15 seconds at 10,000 rpm and the column was then washed by adding 700 µl of RW1 (composition proprietary) and centrifuging at 10,000 rpm for 15 seconds. Thereafter 500 µl of RPE buffer (composition proprietary) was added and the column centrifuged at 10,000 rpm for 15 seconds. To dry the spin column membrane, which avoids ethanol carry over during RNA elution, the column was centrifuged at 10,000 rpm for 2 minutes. After centrifugation the column was placed

in a fresh collection tube and 40 µl of RNase-free water (DEPC treated dH_2O) added directly to the column and centrifuged at 10,000 rpm for 1 minute to eluate RNA.

2.3.3.2 Reverse transcription (RT) PCR of CSPβ,CSP γ and INSL3

Purified RNA was translated into cDNA by RT-PCR (Transcriptor High Fidelity cDNA Synthesis Sample Kit (Roche)) according to the manufacturer's protocol.

For RT-PCR, 0.5 µg of purified RNA was added to 0.5 µg oligo $(dT)_{18}$ primer. DEPC water was added to a final volume of 11.4 µl. To ensure denaturation of RNA secondary structure the template–primer mixture was heated in a thermal block for 10 minutes at 65°C. Thereafter 4 µl of 5 x reaction buffer, 0.5 µl protector RNase inhibitor (40 U/µl), 2µl deoxynucleotide mix (10 mM each dATP, dTTP, dGTP, dCTP), 1µl dithiothreitol (DTT) and 1.1 µl reverse transcriptase (20 U/µl) was added to the denatured template-primer mix and carefully mixed by pipetting. The reaction was then incubated at 50°C for 30 minutes, following which the sample was heated to 85°C for 5 minutes, to inactivate the RT enzyme. The cDNA was either directly used for PCR amplification or stored at -20°C for later use.

2.3.3.3 Cloning of CSPβ, CSPγ and INSL3 into pQE30 and eGFP-C2 vectors

Cloning CSPβ and CSPγ into pQE30 and eGFP-C2 produces the CSP isoform proteins with an N-terminal His_6-tag or GFP-tag, however, INSL3 is only cloned into the eGFP-C2 vector. The His_6-tag is important for protein purification (see 2.5), whereas the GFP-tag allows proteins to be visualised by confocal imaging (see 2.9).

The CSP isoforms and INSL3 were amplified through PCR using primers with the required restriction sites (BamHI and HindIII, see table 2.3). To clone the CSP isoforms into pQE30 vector the BamHI restriction site is on the N-terminus and

HindIII on the C-terminal site, in contrast to cloning into eGFP-C2 vector, where the restriction sites are on the opposite sites. To create "sticky ends" the amplified CSP isoforms and INSL3 as well as the vectors underwent an approximately one hour digest procedure (see 2.3.9) and were subsequently run on 1 % agarose gel (see 2.3.7). The target DNA samples were purified from the agarose gel (see 2.3.8), and were cloned using ligation and subsequent transformation (see 2.3.11).

2.3.4 RT-PCR analysis of CSP isoforms mRNA expression in mammalian tissues

Note that the RT-PCR protocol used to analyse mRNA expression was different to that used in the previous section for cloning of CSPβ and CSPγ.

After RNA purification as described in section 2.3.3.1, 2 µg of the extracted RNA was combined with 0.5 µg of Oligo $(dT)_{15}$ Primer (Promega) and made to a final volume of 15 µl, by adding RNase free dH_2O (DEPC-dH_2O). The mix was then incubated at 70°C for 5 minutes prior to the addition 5 µl dNTPs, 0.625 µl Recombinant RNasin® Ribonuclease Inhibitor, 1 µl murine retroviral reverse transcriptase (M-MLV RT), 10 µl of 5 x reaction buffer and nuclease-free water (DEPC-treated H_2O) to a final volume of 50 µl. This reaction-mix is incubated for 60 minutes at 42°C.

To probe for CSP isoform expression, specific primers for each of the three isoforms were designed. The sequence of these primers is shown in table 2.3 of section 2.1.4. 250 ng of forward and reverse primers were added to 5 µl of the RT-PCR reaction mix (see above) in a sterile 0.2 ml PCR-grade tube, followed by 10 µl of 5 x Green GoTaq® Reaction Buffer, 1 µl of 10 mM dNTPs, 0.25 µl GoTaq® DNA Polymerase and DEPC-treated dH_2O to 50 µl. The PCR amplification was performed as described in 2.3.2.

2.3.5 Site-directed mutagenesis

Site-directed mutagenesis allows specific mutations to be created at defined sites in a cloned DNA molecule.

Primers encoding for the desired mutations were designed for plasmid amplification. The mutagenesis mixture consisted of 50 ng of plasmid DNA, 125 ng of each forward and reverse primer, 5 µl of 10 x *Pfu* buffer, 1 µl of 10 mM dNTPs and 1 µl *Pfu* polymerase. The mixture was made to a final volume of 50 µl by adding DEPC-treated dH_2O. The mutagenesis-mix was heated to 95°C for 1 minute to denature the DNA-template. This was followed by 18 cycles consisting of a DNA denaturation step at 95°C for 30 seconds, an annealing step for 1 minute at 50°C and a DNA extension step at 68°C for 13 minutes (2 minute per kb, plasmid is approximately 6kb).

Following PCR amplification the template DNA was removed by enzymatic digestion with *Dpn I* for 2 hours at 37°C. An aliquot of the PCR mixture was visualised on a 1 % (w/v) agarose gel (see 2.3.7) against the DNA-template to confirm that PCR was successful. If successful, 2 µl of the *Dpn I* treated PCR mixture was used for transformation (see 2.3.11) of XL10® gold supercompetent cells (Stratagene). Colonies that formed on antibiotic selection plates were grown overnight in 5 ml Luria-Bertani broth (LB) medium (see 2.3.1) and the plasmid was isolated using a small-scale plasmid preparation (see 2.3.12), followed by DNA sequencing to ensure that the DNA contained the desired mutation. Sequencing was performed by the University of Dundee DNA sequencing service (see 2.3.16).

2.3.6 Quantitative real-time PCR

Primers designed for DNA amplification were obtained from MWG-Biotech (Ebersberg, Germany). The mutagenesis mixture consisted of 50 ng of testis DNA, 100 pmol of each forward and reverse primer and 125 µl of Brilliant® Sybr Green QPCR Master Mix (Stratagene). The qRT-PCR-mix was heated to 95°C for 7.5 minutes to denature the DNA template. This was followed by 45 cycles consisting of

a DNA denaturation step at 95°C for 25 seconds, an annealing step for 25 seconds at 63°C and a DNA extension step at 72°C for 25 seconds. Finally the dissociation stage, where the double-stranded DNA product is melted into single-stranded DNA, was initiated by 1 cycle consisting of 1 minute at 95°C, 30 seconds at 63°C and 95°C for 30 seconds. The dissociation curve is used to ensure that only a specific PCR product was generated with the specific set of primers. The external control luciferase and internal control succinate dehydrogenase (SDH) were amplified under the same conditions.

2.3.7 Agarose gel electrophoresis

For visualisation or purification of DNA fragments amplified by PCR or following restriction endonuclease digestion (see 2.3.9), the sample was electrophoretically separated in a 1 % (w/v) agarose gel in TBE buffer [44.5 mM Tris Base, 44.5 mM boric acid, 1.59 mM EDTA, pH 8.3] supplemented with Sybr Safe® (1: 10,000, Invitrogen). DNA was visualised after electrophoresis under an ultraviolet lamp.

2.3.8 DNA purification from agarose gels

DNA bands were excised from agarose gels in a minimal volume of agarose and transferred to a 1.5 ml tube. DNA purification was performed with a QIAquick® Gel Extraction Kit (Qiagen Ltd) according to the manufacturer's protocol. First the weight of the DNA gel slice was determined. Thereafter 3 volumes of QG Buffer was added to the gel slice (*i.e.* 100 mg gel slice = 300 µl QG buffer) and subsequently heated at 50°C for 10 minutes with occasional vortexing to melt the gel slice containing the DNA. When the DNA gel slice was completely solubilised, 1 gel volume of isopropanol was added to the mixture and gently mixed by pipetting. The mixture was then transferred to a QIAquick® Spin Column and centrifuged for 1 minute at 13,000 rpm and the flow-through was discarded. The column was then

washed with 500µl QG Buffer to remove any residual agarose and subsequently washed with 750 µl PE Buffer by centrifuging the column for 1 minute at 13,000 rpm. The flow-through was again discarded and the column was centrifuged for a further 1 minute to remove any residual buffer. The column was then transferred to a fresh 1.5 ml collection tube, and the DNA eluted by adding 30 µl of DEPC-treated dH_2O to the column, followed by centrifuging for 1 minute at 13,000 rpm. One tenth (v/v) of the eluted DNA was resolved on a 1 % (w/v) agarose gel against a 100 bp or 1 kB DNA ladder to determine whether the DNA purification was successful (see 2.3.7).

2.3.9 Restriction endonuclease digestion of DNA

DNA restriction digestion reactions contained 1-2 µg vector DNA, 1µl of each FastDigest® restriction enzymes (Fermentas Life Sciences), 2µl of 10 x FastDigest® Buffer and DEPC-treated water added to a volume of 20 µl. The mixture was incubated for 1 hour at 37°C. Agarose gel electrophoresis was performed to determine if the digestion was successful (see 2.3.7).

2.3.10 Ligation of insert DNA with plasmid vector

To ensure high ligation efficiency it is important to use a higher concentration of the insert than the plasmid vector following restriction digestion. An estimate of vector and insert concentration was achieved by comparison of the band intensities with molecular standards of known concentration on an agarose gel (see 2.3.7). The molar mass ratio for DNA molecules was estimated using the following formula:

[(ng vector * insert size (kb)) / vector size (kb)] x molar ratio of insert = ng of insert required.

The ligation reaction mixes consisted of the calculated vector:insert ratio, 1 µl T4 DNA ligase (Promega) and 10 µl 2 x LigaFast™ DNA ligation buffer (Promega). The final volume of the ligation mix was made to 20 µl with DEPC-treated dH_2O. The ligation reaction was allowed to proceed at room temperature for at least 5 minutes.

2.3.11 Transformation of competent bacterial cells

To amplify recombinant plasmid DNA, transformations were performed into ultracompetent XL10 gold (Stratagene) (or supercompetent TOP10 cells (Invitrogen)). The competent cells, stored at -80°C, were defrosted on ice and 30 µl transferred into a fresh 15 ml tube per transformation. Subsequently 1 µl of ligation mix or 10 ng of purified plasmid DNA was added to the cells and incubated on ice for 20 minutes. The cells were then heat shocked for exactly 30 seconds at 42°C and immediately put back on ice for 5 minutes to allow the cells to recover. Thereafter 200µl of LB medium was added to the cells and incubated at 37°C for 30-60 minutes on an orbital shaker at 200 rpm. The entire transformation mixture was then plated on prewarmed agar plates (see 2.3.1) which contained the appropriate antibiotic (100 µg/ml ampicillin and/or 30µg/ml kanamycin). The plates were incubated over night at 37°C.

2.3.12 Small-scale (miniprep) plasmid purification

Miniprep plasmid preparations were used to screen bacterial colonies for the presence of the appropriate plasmid DNA. Subsequent restriction digestion (see 2.3.9) and agarose gel electrophoresis (see 2.3.7) then confirmed if the ligation of the insert and vector was successful (see 2.3.10). This Miniprep purification typically yields ~ 5 µg of plasmid DNA. A colony was picked from the agar plate and grown in 5 ml of LB media, containing the appropriate antibiotic at 37°C and 200 rpm for approximately 16 hours. After growing the bacteria overnight, 1.5 ml of the culture

was transferred to a fresh 1.5 ml tube and centrifuged at 12,000 x g to pellet the bacteria. The remaining 3.5 ml were kept at 4°C until required. The rapid small-scale plasmid preparation, also known as “miniprep”, is based on the alkaline lysis method (Birnboim and Doly, 1979). Here, the PureLink™ Quick Plasmid Miniprep Kit from Invitrogen was used to isolate the recombinant plasmid DNA. The bacteria pellet was completely resuspended by thoroughly pipetting in 250 µl Resuspension Buffer [50 mM Tris-HCl, pH 8.0; 10 mM EDTA], followed by the addition of 250 µl of Lysis Buffer [200 mM NaOH, 1 % (w/v) SDS]. The suspension was gently mixed by inverting the tube several times and the mixture was incubated for 5 minutes at room temperature. Subsequently, 350 µl of Precipitation Buffer [3.1 M potassium acetate, pH 5.5] was added and mixed by inverting the tube several times until the mixture was homogenous. To separate the plasmid lysate from cell debris, the mixture was centrifuged at 12,000 x g for 10 minutes. The recovered lysate was then loaded onto a spin column contained within a 2 ml collection tube. Thereafter, the spin column was centrifuged at 12,000 x g for 1 minute and the flow-through was discarded. Afterwards 500 µl of Wash Buffer was added to the column, incubated for 1 minute at room temperature, then centrifuged at 12,000 x g for 1 minute and the flow-through discarded. This wash step was repeated once. To remove any residual solution remaining on the column, a final centrifugation step (12,000 x g for 1 minute) was performed. The spin column was then placed into a fresh 1.5 ml tube and the recombinant DNA was eluted by adding 50 µl of DEPC-treated dH_2O to the spin column and centrifuging at 12,000 x g for 2 minutes. The eluate contained purified plasmid DNA which was then analysed by endonuclease digestion (see 2.3.9) for 1-2 hours and agarose gel electrophoresis beside 100 bp or 1 kb DNA ladder standards to determine the size of the DNA.

2.3.13 Large-scale (maxiprep) plasmid purification

Maxiprep plasmid preparations were used to obtain high yields and purity of DNA (~ 200-500 µg) for sequence analysis and transfection of mammalian cell lines. As with the Miniprep purifications, the principle is based on the alkaline lysis method.

PureLink™ HiPure Plasmid Filter Purification Kits (Invitrogen) were used for maxiprep purification of plasmid DNA. When analysis of miniprep DNA had shown that cloning was successful, the remaining 3.5 ml of the miniprep overnight culture (see 2.3.12) was added to 100 ml LB media containing the appropriate antibiotic. The culture was grown for approximately 16 hours at 37°C on a shaker (200 rpm). Following this growth phase, the culture was centrifuged at 4,000 x g for 20 minutes to pellet bacteria. The bacteria pellet was then completely resuspended by pipetting in 10 ml Resuspension Buffer [50 mM Tris-HCl, pH 8.0; 10 mM EDTA, 20 mg/ml RNase]. Thereafter 10 ml of Lysis Buffer [0.2 M NaOH, 1 % (w/v) SDS] was added, mixed by inverting the capped 50 ml tube until homogenous and then incubated at room temperature for 5 minutes. Following this, 10 ml Precipitation Buffer [3.1 M potassium acetate, pH 5.5] was added and immediately mixed by inverting the tube several times until the solution was homogenous. The precipitated lysate was transferred to a HiPure Filter Maxi Column, which was pre-equilibrated with 25 ml Equilibration Buffer [0.1 M sodium acetate, pH 5.5; 0.6 M NaCl, 0.15 % (v/v) Triton® X-100], and the lysate run through the filter via gravity flow. The filter maxi column contains a filter insert inside the DNA-binding column; the filter insert removes cells debris, allowing the purified lysate onto the DNA-binding matrix. To increase the final DNA yield, the filter column was washed with 10 ml Wash Buffer [0.1 M sodium acetate, pH 5.0; 825 mM NaCl] before discarding. The Maxi DNA-binding column was then washed with 50 ml of wash buffer, followed by elution of the DNA with 15 ml Elution Buffer [100 mM Tris-HCl, pH 8.5; 1.25 M NaCl] into a fresh 50 ml tube. Isopropanol (10.5 ml) was added to the eluted DNA, mixed by inversion, and the DNA-propanol mixture centrifuged at 15,000 x g for 30 minutes at 4°C. The supernatant was discarded and 5 ml of 70 % ethanol was added onto the remaining pellet without resuspension. Following centrifugation for 5 minutes at 15,000 x g, the supernatant was carefully removed and the remaining DNA pellet air-dried for 2-4 hours at room temperature. The dry DNA pellet was resuspended in 100 µl DEPC-treated dH_2O and the concentration was quantified via spectrophotometery (see 2.3.15), and additional DEPC-water added to give a final concentration of 1 mg/ml.

2.3.14 Glycerol stocks

For prolonged storage of bacteria transformed with recombinant plasmid DNA, 500 µl bacteria suspension was added to 500 µl sterile glycerol. The suspension was mixed by vortexing and stored in a -80°C freezer. When fresh plasmid DNA was required, a scraping from the frozen glycerol stock was placed into 50-250 ml LB media. The DNA was purified as described in section 2.3.13.

2.3.15 Spectrophotometric quantification of DNA and RNA

Analysis of UV absorption by purified RNA or DNA was used to determine concentration. Purines and pyrmidines in nucleic acid show absorption maxima around 260 nm (*e.g.*, dATP: 259 nm; dCTP: 272 nm; dTTP: 247 nm) if the DNA sample is pure without significant contamination from proteins or organic solvents (proteins have a peak absorption at approximately 280 nm). The ratio of OD_{260}/OD_{280} was therefore determined to assess the purity of the sample. A ratio of 1.8-2.0 showed that the absorption in the UV range was due to nucleic acid. The amount of DNA/RNA was quantified using the following formula:

Absorbance (OD) * dilution factor * 50 = DNA concentration (µg/ml)

Absorbance (OD) * dilution factor * 40 = RNA concentration (µg/ml)

2.3.16 DNA sequencing

The DNA which was generated by standard or mutagenesis PCR was sequenced on both strands by The University of Dundee DNA Sequencing Service™ (Dundee, U.K.).

2.4 Mammalian cell culture

2.4.1 Storage and reuse of mammalian cells

For long-term storage of mammalian cells 1 ml of growth media containing approximately 10^6 cells, was made to 10 % (v/v) dimethyl sulfoxide (DMSO) in 1.5 ml cyrotubes (Nunc™). The cell suspension was then frozen down in a controlled manner by using isopropanol on dried ice, followed by storage at -80°C.

For use, frozen cells were thawed quickly at 37°C and added to a 25 cm² flask which contained 10 ml pre-warmed (37°C) cell specific media. The cells were incubated at 37°C and 5/7.5 % CO_2 overnight. Thereafter the media was taken off, to remove DMSO supplement, and replaced with fresh and pre-warmed media.

2.4.2 Culturing mammalian cells

Rat pheochromocytoma-12 (PC12) cells were grown in collagen-coated 75 cm² flasks under controlled conditions, in Complete Media [Advanced RPMI-1640 containing 10 % (v/v) horse serum, 5 % (v/v) foetal bovine serum, 1 % (v/v) glutamax and 0.1 % (v/v) gentamycin, (Invitrogen Ltd.)]. The cells were maintained at an appropriate temperature and gas mixture of 37°C and 7.5 % CO_2 in a cell incubator.

PC12 cells were subcultured at least once a week, depending on their density. For this the complete media was removed and 2 ml of Versene gently added to the cells to remove dead cells and residual media. Afterwards, 5 ml Versene was added and the cells were detached from the surface of the flask by pipetting. The cells were then collected in a 50 ml tube containing 45 ml of antibiotic-free media [Advanced RPMI-1640 containing 10 % (v/v) horse serum, 5 % (v/v) foetal bovine serum and 1 % (v/v) glutamax, (Invitrogen Ltd.)]. The cell suspension was then centrifuged at 500 x g for 5 min, the supernatant discarded and the cell pellet resuspended in 10 ml media by pipetting. Cells were then reseeded at a dilution ratio of 1:3 in 75 cm² flasks or 6/24-well plates as appropriate for microscopy and assay purposes.

Human Embryonic Kidney (HEK)-293 cells and Henrietta Lacks (HeLa) cells were cultured in 75 cm² flasks in D-MEM containing 5 % FBS (Invitrogen Ltd) at 37°C and 5 % CO_2. HeLa-C1 cells were cultured in D-MEM containing 10% (v/v) FBS, 50 IU/ml penicillin, 50 µg/ml streptomycin (Sigma-Aldrich). Sertoli cells (15P-1 (rat) and MSC-1 (mouse)) were cultured in 75 cm² flasks in DMEM (containing pyruvate) supplemented with 5 % (v/v) FBS (Invitrogen Ltd), 50 IU/mL penicillin and 50 µg/mL streptomycin at 32°C and 5 % CO_2. Leydig (R2C) cells were cultured in F-12 solution containing 15 % (v/v) HS, 2.5 % (v/v) FBS and 0.4 % (v/v) gentamycin (Invitrogen Ltd). To subculture the cells, they were washed briefly in 5 ml of Trypsin-EDTA [0.05 % trypsin, 0.53 mM EDTA*4Na; (Invitrogen Ltd)] and then incubated at 37°C or 32°C for 2 minutes in 3 ml Trypsin-EDTA. The cells were then detached from the surface of the flask by gentle tapping. Cells were subcultured at a dilution ratio of 1:3 (Leydig cells (R2C) and Sertoli cells (MSC-1)), 1:10 (HEK293 and HeLa cells), 1:20 (Sertoli cells (15P-1)) and (HeLa-C1 cells).To subculture the cells onto 6/24-well plates or coverslips for further analysis, the cells were diluted with their appropriate media without antibiotics.

2.4.3 Small interference RNA transfection into mammalian cells

RNA interference (RNAi) is a specific gene-silencing technique, where a double-stranded (ds) RNA binds to a specific target mRNA sequence and brings about its cleavage. Small interference RNAs (siRNA) can also be introduced exogenously into cells. Double stranded siRNAs are designed that have sequences which are complementary to a specific target mRNA. siRNAs assemble into an RNA-induced silencing complex (RISC) to form an RNA-protein complex (known as siRISC); siRISC binds to the target mRNA and silences gene expression.

To introduce siRNA into cells the lipid transfection reagents DharmaFECT® 1 (for animal cell lines) and DharmaFECT® 2 (for human cell lines) (Dharmacon; Thermo Scientific) were used, which are functionally verified to produce at least 75 % transfection efficiency. 0.25 x 10^6/ml cells were seeded on a 24-well plate to achieve a successful knock down efficiency and grown for 24 hours. siRNA (600 nM) was

made in 35 µl serum free media [Advanced RPMI-1640 supplemented with 1 % (v/v) glutamax]. In a separate tube 1 µl DharmaFECT® siRNA transfection reagent was added to 49 µl serum free media. After 5 minutes incubation time at room temperature, the siRNA solution and the Dharmafect solution were combined and incubated for 20 minutes at room temperature. Following this, 200 µl antibiotic-free media was added the siRNA-Dharmafect solution. The media from the cells was then removed and the entire 300 µl reaction mix was added to the cells (final siRNA concentration of 100 nM). The 24 well-plate was then returned to the 37°C incubator for 72 hours.

2.4.4 Plasmid DNA transfection into mammalian cells

Plasmid DNA was introduced into PC12, HEK 293, HeLa, HeLa-C1, Sertoli (15P-1 and MSC-1) and R2C Leydig cells using Lipofectamine™ 2000 reagent (Invitrogen Ltd).

The required quantity of plasmid DNA was added to 50 µl of serum free media in a sterile 1.5 ml tube and mixed by pipetting. Lipofectamine™ 2000 was was added into 50 µl of serum free media; Lipofectamine™ 2000 was used at a ratio of 2 µl/µg DNA. The plasmid and lipofectamine were incubated for 5 minutes at room temperature, then combined and incubated for a further 20 minutes. Subsequently, the plasmid-lipofectamine mixture was added to the cells, which were then returned to the incubator for 24 hours for all cell lines except PC12 cells, which were transfected for 48 hours.

2.5 Purification of recombinant CSP proteins

CSPβ and CSPγ were cloned into pQE30 as described in section 2.3.3.3. CSPα inserted between BamHI and HindIII sites in pQE30 was previously described (Chamberlain and Burgoyne, 1996). The pQE-30 vector encodes 6 histidine residues

(His_6 tag) upstream of the cloned DNA, which has an affinity to metal ions like nickel (Ni^{2+}). PQE30-CSPα, pQE30-CSPβ and pQE30-CSPγ were transformed into competent *E. coli* M15 [pREP4] cells and transformed bacteria selected by growth on kanamycin and ampicilin agar plates (pREP4 encodes Kan^r, pQE30 encodes Amp^r) (see 2.3.11). Bacterial colonies were picked and grown in 5 ml LB media with the appropriate antibiotics for approximately 5 hours and then transferred into 500 ml supermedia [150mM NaCl, 1.5 % (w/v) tryptone, 2.5 % (w/v) yeast extract] with the appropriate antibiotics (see 2.3.1) and grown overnight on an orbital shaker at 250 rpm and 37°C. The following day another 500 ml of supermedia was added to the overnight culture, which was also supplemented with Isopropyl β-$_D$-1-thiogalactopyranoside (IPTG; Calbiochem) to a final concentration of 1 mM, and incubated for a further 5 hours at 37°C and 250 rpm. The culture was then centrifuged at 4000 x g for 20 minutes and the cell pellet was resuspended in 200 ml breaking buffer [100 mM Hepes, 2 mM MgCl2, 500 mM KCl, 2 mM 2-mercaptoethanol, pH 7.0]. The bacterial cells were then centrifuged again at 4,000 x g for 20 minutes and the pellet resuspended in 20 ml breaking buffer containing a protease inhibitor cocktail (Roche). The suspension was then subjected to a freeze-thaw cycle at – 80°C, lysozyme added to 1 mg/ml and incubated on ice for 30 minutes. Subsequently the suspension was subjected to four sonication cycles (Sanyo Soniprep 150) at an amplitude of 10 μm for 15 seconds. Finally the suspension was centrifuged at 50,000 x g for 30 minutes and the supernatant (containing soluble proteins) collected.

The purification resin used for His_6-tagged proteins is Ni^{2+}-Nitrilo Triacetic Acid (NTA)-coupled agarose beads (Qiagen). The purified bacterial supernatant was incubated with 3 ml of Ni^{2+}-NTA beads in a 50 ml tube for 1 hour at 4°C with end over-end rotation. The beads were then collected by centrifugation at 2,000 x g for 5 minutes, followed by 3 washes in 40 ml imidazole buffer [50 mM imidazole, 20 mM HEPES, 200 mM KCl, 2 mM β-Mercaptoethanol, 2 mM $MgCl_2$, 10 % (v/v) glycerol, pH 7.5] for 30 minutes each, imidazole competes with histidine for binding to Ni^{2+}. Imidazole at 50 mM is not sufficient to elute His_6-tagged proteins but removes proteins that are weakly bound to the resin. Elution of His_6-tagged CSPs was achieved by adding successively 1 ml imidazole buffer containing 100, 150, 200, 250

or 500 mM imidazole. All elution steps were performed on ice with an incubation time of 5 minutes and subsequent centrifugation at 2,000 x g for 5 minutes. Each fraction was collected and an aliquot run on an SDS-PAGE gel (see 2.6.1 and 2.6.2) which was stained with Coomassie Blue to identify the peak fractions that contained the target protein. The fractions which containing the highest concentration of protein were combined and dialysed (Slide-A-Lyzer G2 Dialysis Cassettes, 10 K molecular weight cut off (MWCO), Thermo Fisher Scientific Inc.) against 5 litres of PBS at 4°C for 2 hours and then a fresh 5 litres of PBS overnight. The following day the protein solution was centrifuged at 14,000 x g for 10 minutes to remove any aggregated protein and the concentration measured through a BCA assay (see 2.6.6)

2.6 Protein biochemistry

2.6.1 Sodium dodecyl sulphate polyacrylamide gel electrophoresis (SDS-PAGE)

SDS-PAGE is a technique used to fractionate proteins according to their weight (Laemmli, 1970).

The gel was made by pouring polyacrylamide solutions between glass plates assembled in a casting stand (BIO RAD Mini–PROTEAN Tetra Electrophoresis System). The final gel consists of two different gels. The main gel is the so-called resolving gel, which is responsible for protein seperation. The pore size can be varied according to the size of the target protein of interest, and is determined by the final concentration of acrylamide/bis-acrylamide. Unless specifically mentioned, all gels used were 12 %, made by mixing 5 ml of 2 x resolving buffer (0.2 % (w/v) SDS, 4 mM EDTA, 750 mM Tris Base, pH 8.9), 4 ml 30 % acrylamide/bis-acrylamide, 1 ml dH_2O, 8 µl N,N,N',N'-tetramethyl-ethane-1,2-diamine (TEMED), and 20 mg of ammonium persulfate (APS). TEMED is used for the chemical polymerisation of the polyacrylamide gel and the reaction is started by the addition of APS. The stacking gel is polymerised above the resolving gel and has a large pore size and a low

concentration of acrylamide. This stacking gel was prepared by mixing 4 ml stacking buffer (0.2 % (w/v) SDS, 4 mM EDTA, 250 mM Tris Base, pH 6.8), 1.2 ml acrylamide/bis-acrylamide, 2.8 ml dH_2O, 10 µl TEMED, and 10 mg of APS. The purpose of the stacking gel is to concentrate proteins into a thin layer at the top of the resolving gel, thus improving resolution. A comb is placed into the unpolymerised stacking gel to create wells to load the protein samples.

Prior to loading, the protein samples were made up in SDS sample buffer [50 mM Tris Base (pH 6.8), 0.1 % (w/v) bromophenol blue, 10 % (v/v) glycerol, 2 % (w/v) SDS, 25 mM Dithuothreitol (DTT)] and denatured at 100°C for 5 minutes.

Protein samples were then loaded into the gel wells in a gel tank filled with running buffer [25 mM Tris Base, 250 mM glycine, 1 % (w/v) SDS]. The denatured proteins are concentrated at 80 V in the stacking gel and separated at 150 V through the resolving gel.

2.6.2 Coomassie blue staining

Polyacrylamide gels were incubated in Coomassie staining solution [0.3 % (w/v) Coomassie Brilliant Blue R250 (Merck), 54.2 % (v/v) methanol, 9 % (v/v) glacial acetic acid] for 30 minutes at room temperature on an orbital shaker. Subsequently, the gels were destained [14 % (v/v) glacial acetic acid, 7 % (v/v) methanol] overnight.

2.6.3 Immunoblotting

After SDS-PAGE (see 2.6.1), proteins in the gel were transferred onto a nitrocellulose membrane (Protran® nitrocellulose membrane, 0.45 um pore size; Whatman plc, Brentford, Middlesex, U.K.). For this the nitrocellulose membrane was placed on top of the gel and between two pieces of Whatman paper (Thermo Fischer). All items were previously soaked in transfer buffer [48 mM Tris Base, 39 mM glycine, 1.3 mM SDS, 20 % methanol] and great care was taken to remove any

air pockets. The gel and membrane sandwich was held within a gel holder cassette and submerged entirely in transfer buffer in the BIO RAD Trans-Blot cell (16 x 20 cm blotting area) tank transfer system. The gel was positioned towards the cathode, allowing proteins to move from the gel to the membrane when a constant current of 70 mA is applied for 16 hours.

To confirm protein transfer, the nitrocellulose membrane was stained with Ponceau S dye (Invitrogen Ltd.) for approximately 60 seconds.

The nitrocellulose membrane was then washed in PBS-T [137 mM NaCl, 10 mM Phosphate, 2.7 mM KCl, 0.02 % (v/v) Tween® 20, pH 7.4] and incubated in 5 % (w/v) non-fat milk (Marvel) in PBS-T for approximately 45 minutes at room temperature to block non-specific binding of the antibodies. The membrane was then probed with primary antibody (diluted in PBS-T) against the protein of interest. The dilution factors for specific antibodies are given in section 2.1.7. The primary antibody solution was left on the blot for 45 minutes at room temperature or over night at 4°C with gentle shaking. The membrane was then washed five times in PBS-T (10 minutes per wash). The secondary antibody (Amersham ECL™; GE Healthcare) is species-specific to the primary antibody and is linked to horseradish peroxidase (HRP); the appropriate secondary antibody was diluted (1:2,000) in 1 % (w/v) non-fat milk and added to the nitrocellulose membrane for 45 minutes at room temperature with shaking. This was followed by washing the membrane 5 x 10 minutes in PBS-T. Binding of HRP-coupled antibodies was visualised by enhanced chemiluminescence (ECL). For this a working solution of ECL was prepared by mixing equal volumes of ECL Solution 1 (100 mM Tris Base (pH 8.5), 2.45 µM Luminol, 0.9 µM Coumaric acid) and ECL Solution 2 (100 mM TrisBase (pH 8.5), 0.061 % (v/v) H_2O_2). The ECL solution was added to the nitrocellulose membrane for 1 minute and the reaction product (luminescence) detected on light sensitive photographic film (Kodak) using an X-OMAT developer (Konica SRX-101A, Medical Film processor, Konica Corporation, Tokyo, Japan).

2.6.4 Protein cross-linking

Amine specific chemical cross-linkers with different length spacer arms were employed to investigate protein interactions of CSPα. PC12 cells (10^6 cells/well of a 24-well plate) were plated 24 hours prior to the experiment. The cells were washed twice with 300 µl Ca^{2+}-Krebs buffer [154 mM NaCl, 5 mM KCl, 1.3 mM $MgCl_2$, 1.2 mM NaH_2PO_4, 10 mM Glucose, 20 mM HEPES, 3 mM $CaCl_2$, pH 7.4], and then incubated with Ca^{2+}-Krebs buffer either with or without 4 µM ionomycin at 37°C. After 5 minutes of incubation, the various cross-linkers (Thermo Scientific; dissolved in dry DMSO) were added to a final concentration of 2 mM for 10 minutes at 37°C. The cells were then put on ice for 30 minutes, followed by quenching of the cross-linkers for 15 minutes with 50 mM Tris, pH 7.5. Finally the cells were lysed with 200 µl sample buffer, boiled and resolved by SDS-PAGE and transferred to nitrocellulose for immunoblotting analysis (see 2.6.1 and 2.6.3).

2.6.5 Lysis of mammalian tissues

Mammalian tissues were homogenized in a dounce homogenizer in 500 µl of ice-cold lysis buffer [20 mM HEPES, 1 mM $MgCl_2$, 250 mM sucrose, 2 mM EDTA, 1 % (v/v) NP-40, 1 ml protease inhibitor cocktail (Roche), pH 7.4]. The lysate was then centrifuged at 14,000 x g for 3 minutes to remove insoluble material. The supernatant was collected in a fresh 1.5 ml tube and the pellet re-homogenised in a further 500 µl of lysis buffer, which was then centrifuged at 14,000 x g for 3 minutes. The two collected lysate samples were then pooled and protein concentration determined by a BCA assay (see 2.6.6).

2.6.6 Bicinchoninic acid (BCA) assay

The Bicinchoninic Acid (BCA) assay is a technique to detect the total protein concentration in a solution. The assay is based on the reduction of Cu^{2+} to Cu^{+} by the

presence of protein in the solution. Bicinchoninic acid reacts with Cu^{+} to form a purple colour end product, with a peak absorbance at 562 nm which is measured in a spectrophotometer. A BCA Protein Assay Kit (Thermo Scientific) was used to determine protein concentrations. Standards were prepared with bovine serum albumin (BSA) of known concentrations in a range between 0 µg and 20 µg in 50 µl. The samples were diluted 1:50 in dH_2O. The samples and standards were then supplemented with the BCA working reagent, which consists of reagents A and B in a ratio of 50:1 according to the manufacturer's protocol. Finally the samples were incubated for 30 minutes at 37°C, followed by reading the absorbance at 560 nm on a spectrophotometer.

The protein concentration of the samples was determined by comparing the absorbance with the absorbance of the BSA standards.

2.6.7 Fractionation

Mammalian tissues and cell lines were routinely fractionated into cytosol and membrane fractions for analysis of protein localisation. All steps were carried out at 4°C.

Detection of the proteins in purified cytosol and membrane fractions was performed by resolving cell equivalents of the purified fractions by SDS-PAGE (see 2.6.1), followed by transferring the proteins onto nitrocellulose membranes (see 2.6.3).

2.6.7.1 Fractionation of mammalian tissues

A small amount of rat tissue (~ 100 mg) was homogenised in 1 ml fractionation buffer using a dounce homogenizer [20 mM TrisBase, 100 mM KCl, 250 mM sucrose, 2 mM $MgCl_2$, 1 mM DTT, protease inhibitor cocktail, pH 8.0]. 800 µl of the homogenised tissue was then centrifuged at 55,000 rpm for 30 minutes at 4°C. The supernatant, which contained the cytosol fraction, was mixed with 280 µl 4 x SDS sample buffer. The membrane pellet was resuspended in 800 µl fractionation buffer

supplemented with 1 % (v/v) Triton-X 100, followed by homogenisation. The homogenised pellet was incubated on ice for 20 minutes and subsequently centrifuged at 55,000 rpm for another 30 minutes. The supernatant containing solubilised membrane proteins was mixed with 280 µl 4 x SDS sample buffer. Equal volumes of the cytosol and membrane fractions were then resolved by SDS-PAGE for immunoblotting and analysis.

2.6.7.2 Fractionation of mammalian cell lines

PC12 and HEK 293 cells were fractionated using a ProteoExtract® Subcellular Proteome Extraction Kit (Calbiochem). This Kit has 4 different buffers for isolation of specific cell fractions. Only Buffer I was used for cell fractionation. Buffer I contains digitonin and EDTA and permeabilises the membrane to release cytosolic proteins.

Approximately 10^6 cells were plated per well of a 24-well plate and transfected with a specific amount of plasmid DNA for 24 hours (HEK cells) or 48 hours (PC12 cells). The cells were then washed twice with 300 µl PBS, followed by adding 150 µl Buffer I supplemented with the Protease Inhibitor Cocktail (Roche) and incubated on ice for 10 minutes. Afterwards, the buffer containing released cytosolic proteins was removed from the cells, collected in a fresh 1.5 ml tube, centrifuged for 10 minutes at 3,000 x g to remove any detached cells and mixed with 50 µl 4 x SDS sample buffer. The cells remaining on the 24-well plate were then washed once with 300 µl PBS and lysed with 200 µl SDS sample buffer.

2.6.8 Isolation of Leydig, germ and Sertoli cells from rat testis

To examine the testicular cells in which CSPα and CSPβ are expressed in vivo, the cells had to be isolated from rat testes.

Two testes were removed from an adult male rat (> 3 months), gently decapsulated and placed in a 50 ml tube. The decapsulated testes were then washed twice in 40 ml

1 x HBSS media (adjusted with 7.5 % sodium bicarbonate to pH 7.4; Invitrogen Ltd.). Disintegration of the seminiferous tubules was achieved by incubating the tubules in a 25 ml collagenase solution (Sigma-Aldrich; 0.5 mg/ml in 1 x HBSS media) at 34°C and 80 oscillations/minute for 15 minutes and left to settle for a few minutes. To avoid poor yields and purity it was important that the seminiferous tubules were not fragmented during the collagenase incubation. The supernatant contained the Leydig cells, which were centrifuged at 1000 x g for 5 minutes followed by resuspending the cells in 2 ml D-MEM/F-12 (Invitrogen Ltd.). The remaining cells in the seminiferous tubules were washed three times with 40 ml 1 x HBSS media and then incubated for 10 min at 37°C in a trypsin solution (Sigma Aldrich; 0.5 mg/ml in 25 ml 1 x HBSS). Afterwards the tubules were washed three times, whereat the third wash contained a trypsin inhibitor (Sigma-Aldrich; 0.3 mg/ml in 20 ml HBSS media), and allowed to settle for 2 minutes. To separate sertoli cells from germ cells, the tubules were incubated for 40 minutes at 34°C at 80 oscillations/minute in a solution (25 ml) containing 0.1 % collagenase, 0.2 % hyaluronidase, 0.04 % Dnase I and 0.03 % trypsin inhibitor (Sigma-Aldrich). Thereafter the tubules were centrifuged at 1000 x g for 4 minutes to pellet the sertoli cells and subsequently washed three times. The supernatant, which contained germ cells, was collected and centrifuged at 1000 x g for 5 minutes to pellet the cells, which were then resupended gently in 2 ml D-MEM/F-12. At this stage the Sertoli cells were 40 % pure and the majority were single cells; any cell clumps would be lost in the steps that followed. In the next step the pelleted sertoli cells underwent a hypotonic shock to increase their purity. This was achieved by resuspending the pellet in 10 ml of HBSS media and then adding 25 ml of HBSS media which had been diluted 1:10 with deionised water. The tube was gently inverted for at least three times to disperse the cells. Thereafter the Sertoli cells were centrifuged at 500 x g for 4 minutes and the supernatant decanted. The Sertoli cells were then gently resuspended in a total volume of 2 ml D-MEM/F-12 (Anway *et al.*, 2003).

2.6.9 Chemical depalmitoylation of palmitoylated proteins

Neutral hydroxylamine is commonly used to depalmitoylate proteins in vitro. 200 µl of 1 M HA (pH 7) or 1 M Tris (pH 7, control) were added to 200 µl of a purified membrane fraction (see 2.6.7.1), and incubated overnight at room temperature in the presence of protease inhibitors. The treated membrane fractions were then mixed with 140 µl 4 x SDS sample buffer containing 100 mM DTT. Tris and HA-treated membrane samples were loaded on SDS gels alongside untreated membranes and protein depalmitoylation (indicated by a shift in molecular mass) was characterised by immunoblotting.

2.6.10 Constitutive exocytosis assay

The HeLa-C1 cell line stabley expresse the pQCXIP-S1-eGFP-FM4-FCS-hGH construct. This construct was virally transfected into HeLa-M cells and then autocloned using a MoFlow Flow cytometer based on GFP fluorescence. The clonal cell lines were then screened for their ability to efficiently secrete the reporter construct (Gordon *et al.*, 2010). The construct (pQCXIP-S1-eGFP-FM4-FCS-hGH) forms ligand reversible aggregates that get trapped during trafficking in the endoplasmic reticulum (ER). When the cells are incubated with rapamycin the aggregates are solubilised and efficiently secreted from the cells.

HeLa-C1 cells were seeded onto 24-well plates 24 hours prior to siRNA or plasmid transfection (see 2.4.3 and 2.4.4). The transfection media was removed from the cells and 200 µl of pre-warmed D-MEM supplemented with or without 1 µM rapamycin was added to the cells followed by returning the 24-well plates back into the incubator at 37°C and 5 % CO_2 for 1 or 2 hours. To stop secretion, the cells were immediately placed on ice. The cell media was then added into 1.5 ml tube containing 70 µl 4 x SDS sample buffer and the remaining cells on the 24-well plates were lysed with 270 µl 1 x SDS sample buffer. The media samples (containing secreted proteins) were loaded beside cell lysates on SDS gels and the amount of secretion was characterised by quantification of GFP signal on immunoblots.

Secretion was expressed as a percentage of the total cell content of the GFP-labelled construct.

For live cell imaging, the cells were seeded onto 30 mm coverlips (see 2.4.2) 24 hours prior to imaging. The cells were imaged for 1 minute, followed by adding 1 µM rapamycin and continuing imaging for another 2 hours.

2.6.11 Exocytosis assay

PC12 cells were seeded onto 24-well plates 24 hours prior to siRNA or plasmid transfection (see 2.4.3 and 2.4.4). The cells were then washed twice with 300 µl Ca^{2+}-Krebs buffer, followed by adding 300 µl of Ca^{2+}-Krebs buffer with or without 300 µM ATP to stimulate regulated exocytosis. After 15 minutes stimulation, supernatants were added to fresh 1.5 ml tubes containing 10 µl protease inhibitor cocktail. The cells on the 24-well plate were then lysed with 200 µl lysis buffer [PBS, 0.5 % (v/v) Triton-X 100, protease inhibitor cocktail (Roche)] for 20 minutes. A small fraction of the solubilised cells can be supplemented with 4 x SDS sample buffer for detection of protein expression by SDS-PAGE and immunoblotting (see 2.6.1 and 2.6.3).

2.6.12 [^{3}H]-dopamine assay

PC12 cells (0.25 x 10^6) were seeded onto a 24-well plate 24 hours prior to siRNA transfection. Following addition of siRNA, cells were incubated for a further 72 hours. Each well of cells was incubated in 300 µl RPMI 1640 media with 0.0088 mg/ml ascorbic acid and 0.0185 MBq/ml [7, 8, ^{3}H] dopamine at 37°C for 90 minutes. Thereafter the exocytosis assay is performed on the cells (see 2.6.11). Stimulation was performed for 15 minutes at room temperature, following which the supernatant was removed and added to ice-cold 1.5 ml tubes and centrifuged at 15, 000 x g for 2 minutes to pellet any detached cells (see 2.6.11). The supernatant from this spin was

transferred into fresh tubes. The cells on the 24-well plate were lysed in 300 µl 0.5 % (v/v) Triton-X 100 in H_2O with protease inhibitors for 20 minutes at room temperature, and mixed with detached cells (see 2.6.11).

100 µl of supernatant and 100 µl of cell lysate were added to 4 ml scintillation fluid and [^{3}H]-dopamine detected by scintillation counting (Tri-Carb 2500 TR Liquid Scintillation Analyzer, Packard Biocsciences, U.S.A). Secretion of [^{3}H]-Dopamine was expressed as a percentage of total cell content (i.e. ([^{3}H]-supernatant/([^{3}H]-supernatant + [^{3}H]-cells) * 100).

2.6.13 Human growth hormone (hGH) assay

Plasmid transfection of PC12 cells has a low efficiency (~ 20 %). Therefore the [^{3}H]-dopamine assay which monitors release from the whole cell population is not useful to determine the effects of transient plasmid transfection on exocytosis efficiency (as only ~ 20 % of the signal would be from transfected cells). Therefore a co-transfection with a plasmid of interest and a plasmid encoding human growth hormone (hGH) is performed. Co-transfection efficiency of PC12 cells is ~ 90-95 % (Graham *et al.*, 1997). Human growth hormone release is monitored by an enzyme-linked immunosorbent assay (ELISA) (Roche). 10^6 PC12 cells were seeded per well of a 24-well plate, transfected (1 µg DNA plasmid or 100 nM siRNA) and 0.5 µg hGH plasmid. The assay was performed 48 hours after transfection, starting with the exocytosis assay as described in section 2.6.11.

In the ELISA assay, hGH antibody is bound to the surface of a microtiter plate. Human growth hormone standards are set up with hGH concentration between 0 and 400 pg/ml. 200 µl of each standard were added in duplicate to the microtiter plate. The supernatant and cell lysate samples from the exocytosis assay were initially centrifuged at 14,000 x g for 3 minutes, before adding 200 µl of the supernatant and 15 µl of cell lysate solutions (added up to 200 µl with sample buffer; provided in the kit) to the plate. The microtiter plate was then covered with a foil and incubated for 1 hour at 37°C. Afterwards the solution was removed from the plate and the plate

washed 5 x with 250 µl washing buffer (supplied in the kit). Anti-hGH-digoxigenin (anti-hGH-DIG); 200 µl of 1 µg/ml was then added to the microtiter plate which was incubated at 37°C for an hour. Thereafter the solution was discarded and washed 5 x with washing buffer to remove unbound anti-hGH-DIG. Subsequently, 200 µl of 200 mU/ml anti-DIG-peroxidase (anti-DIG-POD) was added to each well of the microtiter plate and incubated for an hour at 37°C. After the incubation time, the anti-DIG-POD solution on the plate was discarded and each well washed again with 5 x washing buffer. Finally 200 µl of POD substrate was added to the wells and incubated at room temperature until a colour change occurred. The optical density (OD) of the samples was measured at 405 nm with a reference wavelength at 490 nm, using a microtiter plate reader. Remaining cell lysate sample from the exocytosis assay was diluted in SDS sample buffer, resolved by SDS-PAGE and transferred onto a nitrocellulose membrane, to analyse either protein over-expression or knock-down as appropriate.

The data from the hGH assays was analysed in Excel (Microsoft® Office Package). The hGH concentration of experimental samples was determined by comparison with the value of the known standards.

2.7 Indirect immunofluorescence

Approximately 10^6 PC12 cells were added per well of a 6-well plate containing sterile poly-D-lysine coated coverslips (VWR). The following day, the cells were transfected for 48 hours. The amount of transfected DNA varied and is indicated in the figure legends of result chapters. The cells were washed twice with 2 ml of ice-cold PBS, followed by fixation in 1 ml of 4 % (v/v) formaldehyde for 30 minutes at room temperature. Afterwards, the fixed cells were washed twice with 2 ml PBS and permeabilised in PBS containing 0.3 % (w/v) BSA and 0.1 % (v/v) Triton® X-100 for 6 minutes at room temperature. After removing the permebilisation solution the coverslips were washed three times with 2 ml PBS containing 0.3 % (w/v) BSA. The permebialised cells were incubated in 30 µl primary antibody at its appropriate

dilution (see 2.1.7.1) by inverting the coverslips upside down in the antibody solution placed on parafilm for 60 minutes. The coverslsips were then returned to the 6-well plate with the cells facing up and washed three times with 2 ml of PBS containing 0.3 % (w/v) BSA to remove unbound primary antibody. The coverslips were subsequently incubated (cell slide down) with secondary antibody at its appropriate dilution (see 2.1.7.2) on a strip of parafilm for 60 minutes, covered in a box impervious to light. The secondary antibodies used were specific to the host IgG in which the primary antibody was raised and were conjugated to an appropriate Alexa Fluor dye (488, 543 or 647, Invitrogen Ltd.). To remove excess secondary antibody the coverslips were washed three times with 2 ml of PBS (0.3 % (w/v) BSA, rapidly submerged in dH_2O and allowed to air dry at room temperature. The coverslips were then mounted cell side down on slides using mowiol (10.5 % (w/v) Mowiol 4-88 (Calbiochem), 21 % (v/v) Glycerol, 2.5 % (w/v) 1,4-diazabicyclo[2.2.2]octane (DABCO, Sigma-Aldrich), 0.2 M Tris pH 8.5), left to dry over night and stored in a box impervious to light.

2.8 Immunohistochemistry

Immunohistochemistry is a technique to localize proteins in tissue sections by the use of antibodies. The antigen-antibody interaction are here visualised through fluorescence.

2.8.1 Fixation, paraffin embedding and sectioning of testis

The fixation of tissues is essential to ensure the preservation of the cell morphology and tissue architecture. Testis, of adult male rats, were directly fixed in 4 % (v/v) formaldehyde for 24 hours. Afterwards the tissues were kept in 70 % (v/v) ethanol until required.

Testis was embedded in paraffin through an overnight programme. Firstly the testis was incubated in 70 % (v/v) ethanol for 45 minutes, followed by 90 minutes in 80 %

(v/v) ethanol and a 2 hour incubation in 95 % (v/v) ethanol. Thereafter the tissues were incubated for 6 hours in 99 % ethanol and finally in 100 % ethanol to ensure that no water was left in the tissue. To clear the tissue, it was incubated in xylene for 5 hours and 30 minutes. The final step was the actual paraffin wax embedding; the tissue was incubated in paraffin wax for 8 hours at 60 °C. Afterwards the paraffin embedded testis was set in a block of paraffin wax for sectioning.

To section testis in 10 µm thick slices, a rotary microtome (Jung RM 2035, Leica Microsystems (U.K.) Ltd, Milton Keynes, U.K.) was used. The sections were then placed in 30°C warm water to ensure that the sections flatten out fully, and then carefully placed on special adhesion slides (SuperFrost® Plus Microscope Slides, VWR International), which are permanent positive charged to bind the sections. The slides were dried for 24 hours in a 37 °C incubator and kept in a slide box until required.

2.8.2 Immunolabelling of testis sections

The testis sections were initially dewaxed for approximately 30 minutes in xylene, followed by 5 minutes washes in 100 %, 95 %, 90 % and 70 % ethanol respectively. Afterwards the slices were rehydrated in distilled water for at least 5 minutes, followed by equilibration in 10 mM Citrate buffer (10 mM Citric acid, 0.05 % Tween 20, pH 6) for 10 minutes to facilitate optimal binding of primary antibodies. The sections were then microwaved four times for 5 minutes; to keep the slices covered in solution they were replenished with dH_2O after each 5 minutes and left to cool off for at least 20 minutes. To reduce background fluorescence, the slices were covered in methanol supplemented with 3 % H_2O_2 (Sigma-Aldrich) and incubated for 30 minutes. Thereafter the testis sections were washed three times for 5 minutes with PBS. The slides were then dried around the sections, the edges of the slide were sealed with a Dako Pen (Dako Denmark A/S, Glostrup, Denmark), and blocked with 300 µl goat serum [20 % goat serum (Sigma-Aldrich), 5 % BSA in PBS] for 30 minutes. Afterwards the sections were incubated overnight at 4 °C with 300 µl primary antibody (see 2.1.7.1) diluted in goat serum.

The following day the slides were washed three times in PBS for 5 minutes per wash. Thereafter the sections were incubated for 60 minutes at room temperature with the appropriate AlexaFluor® secondary antibody (see 2.1.7.2), followed by three 5 minutes washes with PBS. The sections were then dried and a coverslip (22*64 mm, VWR International) was mounted on the sections with ProLong® Gold antifade reagent with DAPI (Invitrogen Ltd.), which stains double stranded DNA. The slides were dried overnight and stored in a box impervious to light.

2.9 Optical microscopy

2.9.1 Widefield microscopy

For live cell imaging, the fluorescence-based wide-field microscopy was used because it illuminates full samples. Here the Olympus IX-81 microscope equipped with Olympus Cell^R acquisition software (Olympus, Essex, U.K.) and an Image EM EM-CCD 512x512 camera (Hamamatsu UK) were used. The images were taken with 63 x oil Plain Apochromat objective, and were acquired every 10 seconds. EGFP fluorescence was visualised by using 488nm laser excitation and monitoring fluorescence at 500-555nm.

2.9.2 Confocal microscopy

In this work, confocal microscopy was used to analyse fixed cells. The principal of a confocal microscopy is that it uses a point illumination and a pinhole in an optical plane in front of a detector to filter out of focus light information. This means that only the light from the fluorescence object is viewed.

Here the Zeiss LSM510 confocal system (Carl Zeiss, Oberkochen, Germany) or the Leica SP5 C system (Leica Microsystems GmbH, Wetzlar, Germany) were used for confocal laser scanning microscopy (CLSM). Different fluorophores were detected

with a dichroic beam splitter, which seperates the excitation and the emission light. Sample excitation was achieved using the appropriate laser line (488, 543 or 633 nm). Fluorescence emission was monitored using a 500-550 nm band-pass filter (488 nm excitation), a 560 nm long-pass filter (543 nm excitation), or a 650 nm long-pass filter (633 nm excitation). To detect Dapi stain a Multiphoton laser was used and set 770 nm. Image stacks were collected in 130 nm steps with pinhole set to 1 Airy unit. Afterwards, images stacks were deconvolved with Huygens Scientific Volume Imaging (SVI). The images were taken with 63 x/1.40 oil Plan Apochromat objective.

2.10 Data analysis

Immunoblots were scanned and protein band intensity was quantified using ImageJ software (Image Processing and Analysis in Java). Great care was taken to ensure that band intensities were not saturated and likely to be in the linear range. Relative protein expression levels were calculated using Excel software (Microsoft® Office system). The values measured were presented as the standard error of the mean (SEM). The statistical significance was ascertained through the unpaired two samples Student's *t*-test or one-way analysis of variance (ANOVA) test, useful for comparing three or more means (GraphPad Prism® software).

CHAPTER THREE:

ANALYSIS OF CSPα FUNCTION IN EXOCYTOSIS BY SIRNA-MEDIATED KNOCKDOWN

3.1 Introduction

Exocytosis, the fusion of intracellular vesicles with the plasma membrane, is fundamental to intercellular communication in multicellular organisms. This pathway facilitates the release or secretion of molecules from the cell. In addition, exocytosis is essential for delivery of resident proteins to the plasma membrane. There are two different pathways of exocytosis, constitutive and regulated exocytosis. Constitutive exocytosis occurs without regulation, e.g. pathways regulating the delivery of lipids and 'house-keeping' proteins to the plasma membrane or the secretion of antibodies and extracellular matrix components from the cell. In contrast, regulated exocytosis facilitates the controlled release of extracellular molecules or insertion of membrane components in response to a physiological signal. The most common signal for regulated exocytosis is an increase in intracellular Ca^{2+} concentration (Burgoyne and Morgan, 2003).

Regulated exocytosis occurs in specialized secretory cells, such as mast cells, chromaffin cells and pancreatic β cells, controlling the release of histamine, catecholamines and insulin, respectively (Burgoyne and Morgan, 2003). Several proteins function in exocytosis, and the membrane fusion step is widely believed to result from an interaction between SNARE (SNAP receptor) proteins on the vesicle membrane and plasma membrane. In neuroendocrine cells, these SNARE proteins are VAMP2, which is bound to vesicle membranes and syntaxin1A and SNAP25, which are associated with the plasma membrane (Hong, 2005).

Several proteins have been implicated as SNARE regulators. NSF (N-ethylmaleimide sensitive factor) and its cofactor α-SNAP (α-soluble NSF attachment protein), function to disassemble SNARE complexes following fusion (Hong, 2005). Munc18 is thought to function by regulating the formation of functional SNARE complexes (Shen *et al.*, 2007). Synaptotagmin is a calcium-binding protein that is proposed to facilitate calcium-dependent SNARE-mediated membrane fusion via interactions with the SNARE proteins and negatively charged phospholipids (Chapman, 2008). Another possible SNARE regulator is cysteine string protein (CSP) (Evans *et al.*, 2003).

CSP was first identified in *Drosophila melanogaster (*Zinsmaier *et al., 1990)* and was later identified in *Torpedo* as a possible Ca^{2+}-channel regulator (Gundersen and

Umbach, 1992). Inactivation of the CSP gene in *Drosophila* is lethal at an embryonic stage, with only 4% of the mutant flies surviving into adulthood (Zinsmaier *et al.*, 1994). Analysis of the surviving flies showed that they displayed uncoordinated, sluggish movements and exhibited intense shaking. Furthermore, the surviving adult mutant flies were temperature sensitive and died within 4-5 days at 22°C or within an hour if the temperature was raised to 30°C. It was subsequently shown that neurotransmitter exocytosis was decreased by ~50 % at 22°C in the mutant embryos and abolished at higher temperatures (Umbach *et al.*, 1994). These results indicate that CSP has an important role in presynaptic neurotransmission (Chamberlain and Burgoyne, 1998, 2000). One of the important regulatory domains of CSP is the cysteine string domain (Chamberlain and Burgoyne, 2000; Evans *et al.*, 2003). The cysteine string is a 24 amino acid motif, containing 14 cysteine residues, the majority of which are thought to be palmitoylated (Gundersen *et al.*, 1994), and this domain is responsible for the localization of CSP to the membranes of organelles and secretory vesicles (Greaves *et al.*, 2008). Another important domain is the J-domain, which is the defining motif of the DnaJ family of co-chaperones, and this region mediates CSP binding and activation of the chaperone Hsc70 (heat shock protein 70 kDa) (Braun *et al.*, 1996; Chamberlain and Burgoyne, 1997a).

The function of CSP in exocytosis is not clear, but may involve the regulation of protein folding. It has been suggested that a CSP-HSC70 chaperone complex, together with SGT (small glutamine rich tetratricopeptide repeat protein), regulates the folding of exocytotic proteins including SNAREs (Tobaben *et al.*, 2001; Tobaben *et al.*, 2003), indeed CSP has been shown to interact with both VAMP and syntaxin (Nie *et al.*, 1999; Chamberlain and Burgoyne, 2000; Evans *et al.*, 2003).

In addition to the role of CSPα in neurotransmission in *Drosophila*, several subsequent studies suggested that this protein also functions in regulated exocytosis in a range of mammalian cell types including: adrenal medullary chromaffin cells (Graham and Burgoyne, 2000), pancreatic beta cells (Brown *et al.*, 1998; Zhang *et al.*, 1998) and PC12 cells (Chamberlain and Burgoyne, 1998). However, recent work found no obvious exocytosis defect in CSP null mice (Fernandez-Chacon *et al.*, 2004), raising a number of questions about the proposed role of CSP in exocytosis.

Since the function of CSP is not clear, the aim in this chapter is to bring more clarity to this topic. Most studies that have investigated CSP function in mammalian cells have used over-expression of wild-type or mutant CSPs. However, results from over-expression can be complicated to interpret and therefore we aimed to examine effects of CSP depletion. By knocking down CSP expression using siRNA, the role of CSP in exocytosis can be studied.

3.2 Results

3.2.1 Successful knock down of CSPα in PC12 cells

Phaeochromocytoma-12 (PC12) cells, which are a tumour cell derivative of rat neuroendocrine adrenal medullary chromaffin cells, express endogenous CSPα and neuronal SNARE proteins and are specialised in regulated exocytosis (Greene and Rein, 1977; Schubert and Klier, 1977; Rebois *et al.*, 1980). To date, CSPα knockdown had been successfully achieved in 3T3 cells (Zhang *et al.*, 2006), but not in PC12 cells. Indeed there are only a few reports of successful knockdown of proteins in PC12 cells using siRNA (Thonberg *et al.*, 2004; Noordman *et al.*, 2006; Podszywalow-Bartnicka *et al.*, 2010). Four different siRNAs were tested for their ability to deplete CSPα expression. Three siRNAs correspond to the open reading frame of CSPα and one to the non-coding region. Initially it was determined what cell density is optimal for successful knock down. PC12 cells were plated at different densities 24 hours prior to the transfection (2, 1, 0.5 and 0.25 x 10^6 cells/well) and transfected with 100 nM of either CSPα siRNA, cyclophilin b siRNA or no siRNA (as control) (see 2.4.3) for 72 hours. The cells were lysed, resolved by SDS-PAGE and transferred to nitrocellulose membrane for immunoblotting analysis using anti-CSPα antibody. Figure 3.1*A* indicates that a cell density of 0.25 x 10^6 cells achieved an effective depletion of CSPα.

To investigate the optimal transfection time to achieve the highest CSPα knock down efficiency at a cell density of 0.25 x 10^6 cells, cells were transfected for 3 days, 5

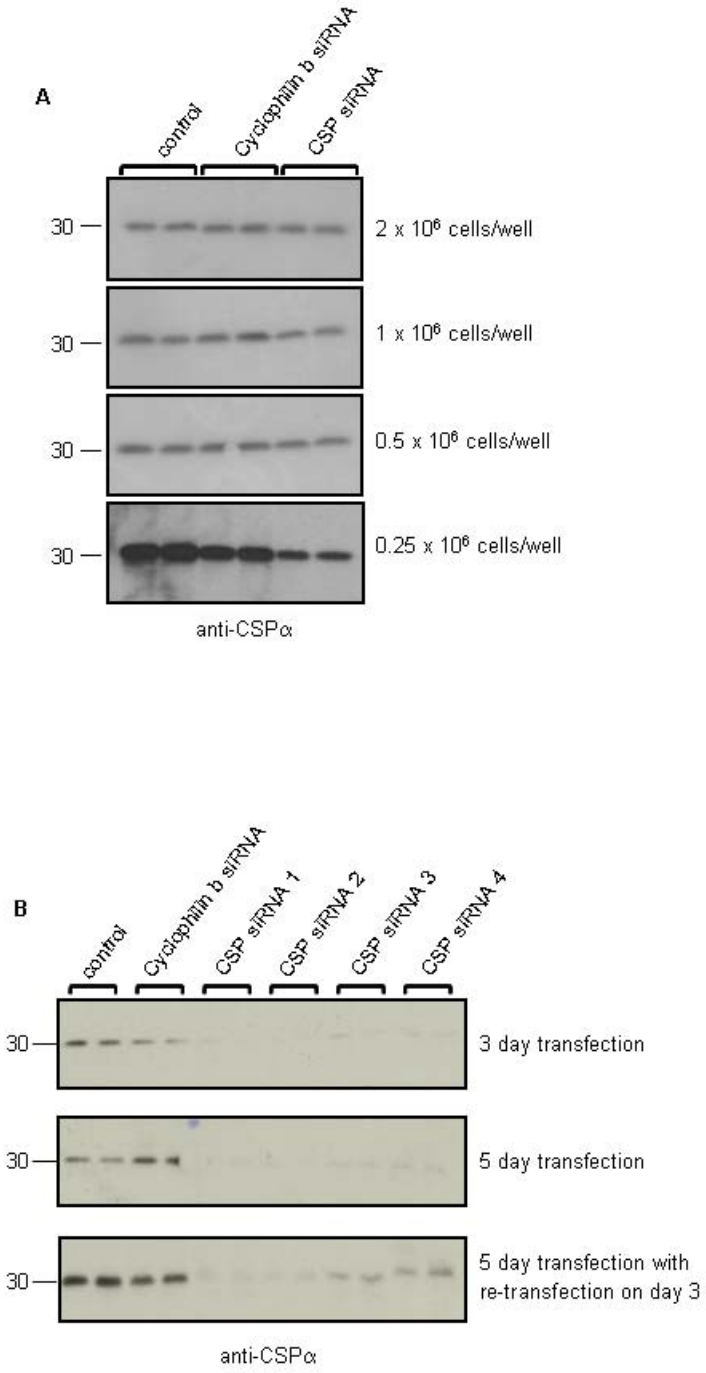

Figure 3.1: siRNA-mediated depletion of CSPα in PC12 cells. *A*. PC12 cells growing on 24-well plates and seeded at the indicated densities were incubated with 100 nM of siRNA molecules directed against CSPα or with siRNA against cyclophilin B for 3 days. The cells were lysed, samples resolved by SDS-PAGE and protein levels examined by immunoblotting with a polyclonal CSPα antibody (Stressgen). *B*. CSPα siRNA transfection was carried out with four different siRNA for different time periods as indicated. Cells were plated at 0.25 x 10^6/well. CSPα expression levels were detected by immunoblotting. Position of molecular weight standards are shown on the left of all panels.

days or 5 days with a re-transfection after 72 hours. The results (Figure 3.1*B*) demonstrate that CSPα depletion was not further enhanced by either a longer incubation period or a double transfection.

Thus, all subsequent CSPα knock down experiments in PC12 cells were carried out at a cell density of 0.25 x 10^6 cells/well and an incubation time of 72 hours. This treatment protocol promoted a significant knock down of CSPα expression by ~80 % (Figure 3.2*A* and 3.2*B*). Furthermore all four siRNAs were effective at depleting CSPα expression levels.

It has been suggested that a CSPα-HSC70 chaperone complex regulates the folding of exocytotic proteins including SNAREs. Indeed, CSPα has been shown to interact with both VAMP2 and syntaxin 1A (Nie *et al.*, 1999; Chamberlain and Burgoyne, 2000; Evans and Morgan, 2003) and SNAP25 levels are reduced in CSPα null mice (Chandra *et al.*, 2005). To examine whether CSPα knock down has any effect on the expression levels of exocytotic SNARE proteins, levels of SNAP25, VAMP2 and syntaxin 1A were analysed by immunoblotting. Figure 3.3 shows that the CSPα knock down had no effect on the expression levels of these SNARE proteins. This result also demonstrates that CSPα siRNAs have a high specificity towards CSPα.

Together these results show that CSPα can be successfully depleted in PC12 using siRNA and that this knockdown has no effect on expression of SNARE proteins. The siRNA approach was therefore used for further experiments to investigate if CSPα plays a role in regulated exocytosis in PC12 cells.

3.2.2 CSPα depletion results in a decreased secretion of ^{3}H-dopamine and human growth hormone from PC12 cells

Previous studies have implicated CSPα in exocytosis by examining effects of over-expression (Chamberlain and Burgoyne, 1998; Zhang *et al.*, 1999; Graham and Burgoyne, 2000). However, recent work found no obvious exocytosis defect in neuronal cells of CSPα null mice (Fernandez-Chacon et al., 2004), raising a number of questions about the proposed role of CSPα in exocytosis. Thus, CSPα knockdown

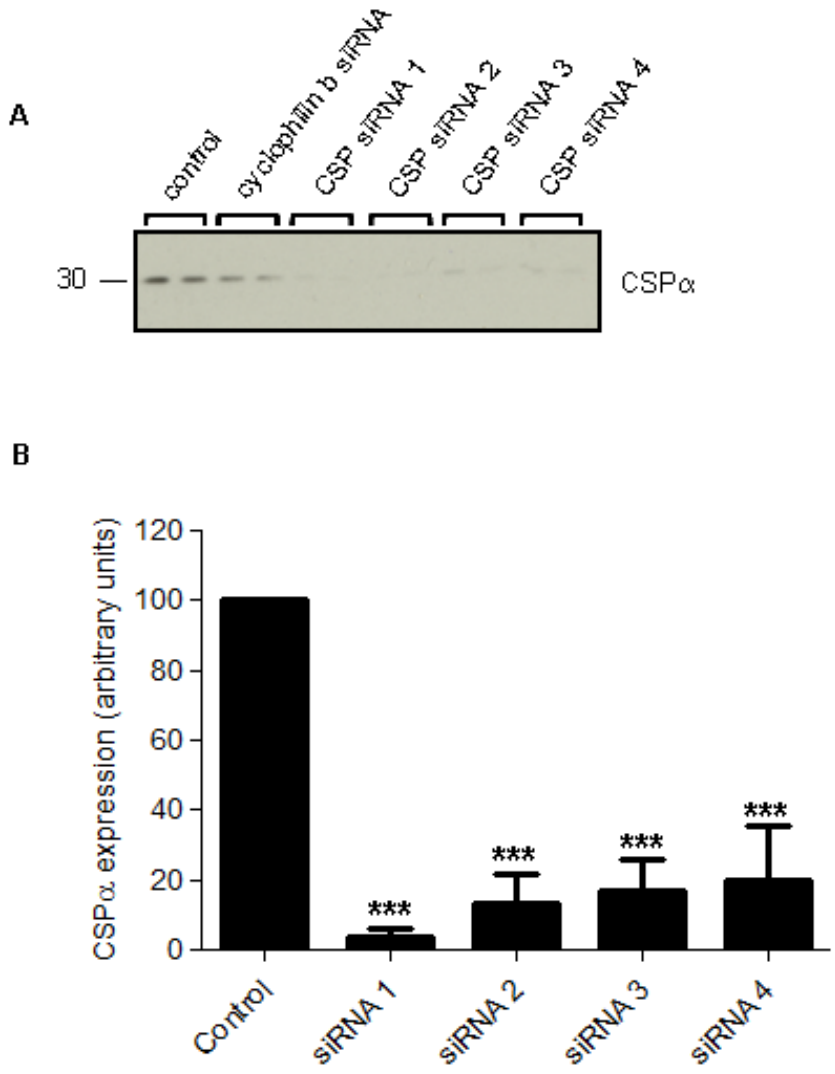

Figure 3.2: CSPα depletion with siRNA and quantification of knock down efficiency. PC12 cells were transfected with 100 nM of 4 different CSPα siRNAs, a cyclophilin B siRNA or no siRNA (control), and incubated for 72 hours. The cells were subsequently lysed, resolved by SDS-PAGE and transferred to a nitrocellulose membrane. Protein levels were examined by immunoblotting with a polyclonal CSPα antibody (Stressgen). *A*. Shows a representative immunoblot. Position of molecular weight standard is shown on the left. *B*. CSPα levels were quantified in control and siRNA treated cells (n=4) by densitometry. Expression in control cells was arbitrary set to 100 and expression in siRNA-transfected cells are shown relative to this. *** indicates a significant decrease ($p<0.0001$) in CSPα expression compared to control cells using a one-way ANOVA test.

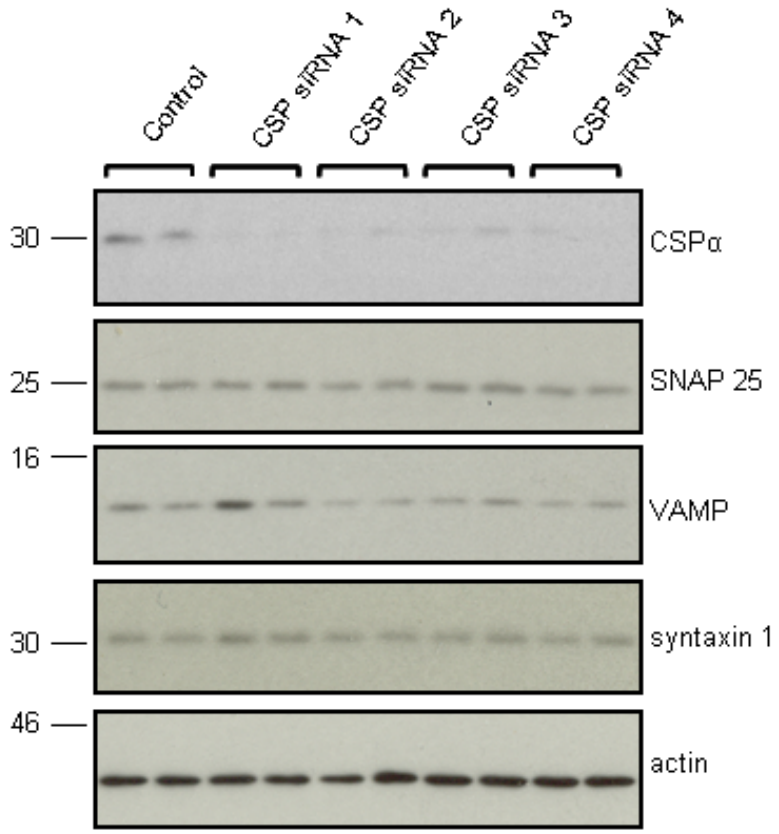

Figure 3.3: SNARE protein levels in CSPα-depleted cells. CSPα siRNAs, at a concentration of 100 nM, were transfected into PC12 cells for 3 days. Cells were then lysed, the samples resolved by SDS-PAGE and transferred to nitrocellulose membranes, which were then probed with specific SNAP25 (Synaptic Systems), VAMP (Synaptic Systems) and syntaxin (HPC-1, Sigma) antibodies; actin (monoclonal, Abcam) served as a control. Position of molecular weight standards are shown on the left of panels.

in a model system may provide further insight into CSPα function in regulated exocytosis.

PC12 cells are specialised in regulated exocytosis releasing catecholamines, such as dopamine, and are therefore widely used as a secretory cell model (Schubert *et al.*, 1974). PC12 cells are known to synthesise, store and release dopamine (Greene and Tischler, 1976).

To analyse CSPα function in regulated exocytosis in PC12 cells, a radio-labelled [^{3}H]-dopamine assay was performed that reliably reports exocytotic responses (Chamberlain and Burgoyne, 1998). PC12 cells (0.25 x 10^6 cells/well) on 24-well plates were transfected with siRNA for 72 hours. CSPα siRNA#1 and #2 were selected for analysis, because they showed the highest CSPα knock down (Figure 3.2*B*) and CSPα siRNA 4 was chosen, as it targets the non-reading frame. Following a 3 day incubation, cells were incubated with [^{3}H]-Dopamine in RPMI 1640 media for 90 minutes at 37°C (see 2.6.12). Thereafter the cells were washed and incubated in Krebs buffer with or without 300 μM ATP. ATP activates regulated exocytosis by promoting Ca^{2+} entry through ligand-gated P2X receptors (Burnstock and Kennedy, 1985; Surprenant *et al.*, 1995). After 15 minutes the buffer was removed and the cells were lysed in 0.5 % Triton X-100. The ^{3}H content in the buffer and the cell lysate was calculated by scintillation counting. The results in Figure 3.4*A* demonstrate that basal release of dopamine was unaffected by CSPα siRNAs. However, dopamine release from ATP-stimulated PC12 cells was significantly decreased by all three CSP siRNAs (Figure 3.4*A* and 3.4*B*).

In these dopamine release assays 'non-targeting' siRNA was used as a control. It was important to ensure that the non-targeting siRNA had no effect on exocytosis. Thus, [^{3}H]-Dopamine assays were performed comparing 'non-targeting' siRNA with no siRNA (transfection reagent alone). Figure 3.4*C* reveals that these two treatments show no significant difference in dopamine release and explicitly shows that the 'non-targeting' siRNA has no effect on regulated exocytosis.

Previous work has suggested that CSPα may regulate uptake of vesicle content (Jin *et al.*, 2003).

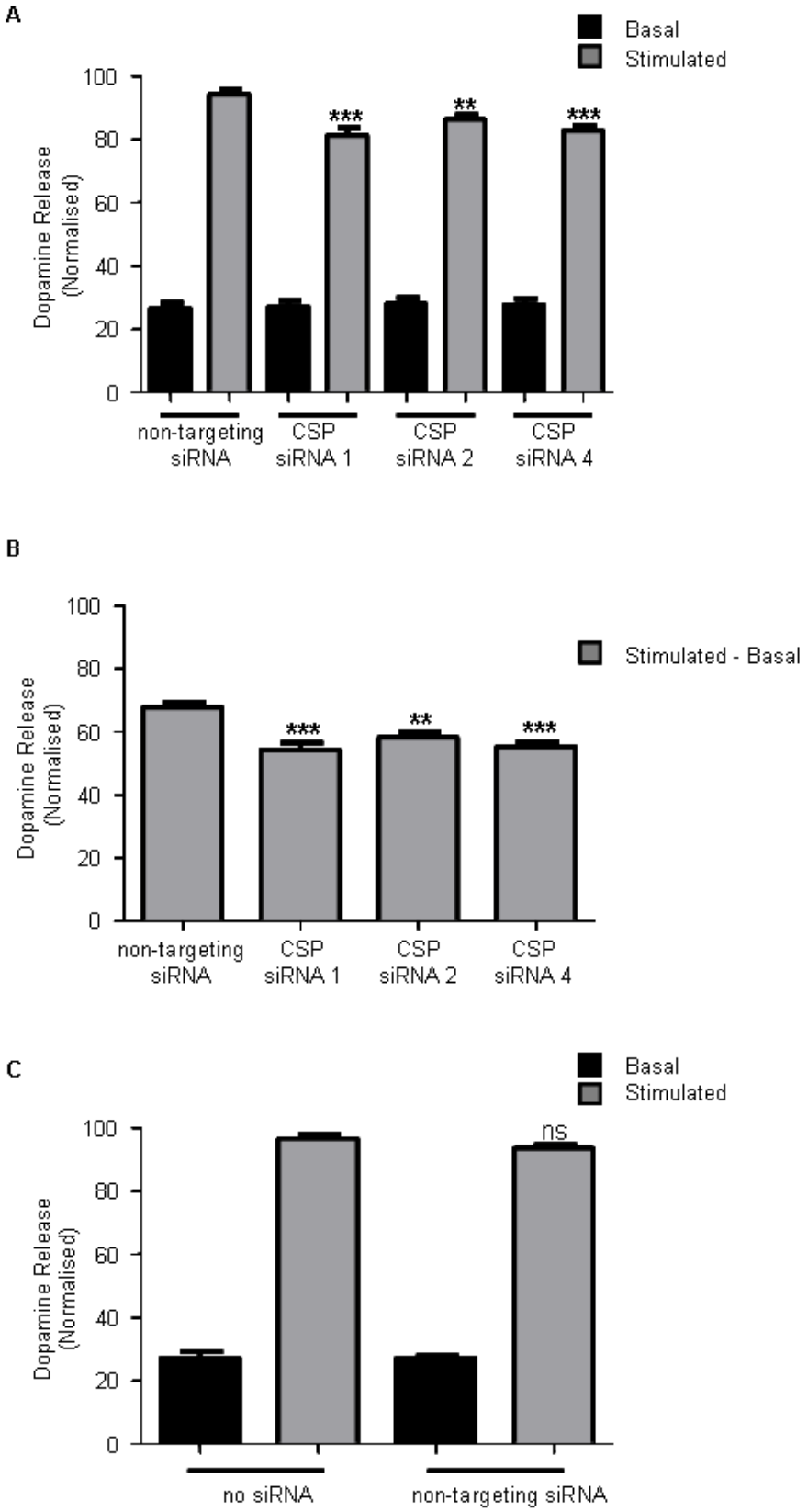

Figure 3.4: Reduced CSPα expression levels correlates with a decreased level of Ca^{2+}-stimulated exocytosis in PC12 cells.

Figure 3.4: Reduced CSPα expression levels correlates with a decreased level of Ca^{2+}-stimulated exocytosis in PC12 cells.PC12 cells transfected with 100 nm of the indicated siRNA for 3 days were washed and loaded with [^{3}H] dopamine for 90 minutes at 37°C. Cells were then incubated in the presence or absence of 300 μM ATP for 15 minutes at room temperature. Secreted and cell-associated [^{3}H] dopamine was assayed by scintillation counting and secreted dopamine expressed as a percentage of the total cell content. *A*. Comparison of [^{3}H] dopamine release from PC12 cells treated with CSPα siRNAs or a non-targeting siRNA. The data presented show normalised mean values +/- SEM (n=18 from 6 independent experiments). Statistical significance was determined using a one-way ANOVA test. ** denotes a p value of <0.001 and *** indicates a p value of <0.0001 for ATP-stimulated secretion compared with cells treated with non-targeting siRNA. There were no significant differences between the values for basal secretion. *B*. The level of ATP-stimulated release (secretion in presence of ATP minus basal secretion) was calculated for each condition. All three CSP siRNAs caused a significant decrease in this component of dopamine release (*** indicates a p value <0.0001 for the ATP dependent component of dopamine secretion compared with cells treated with non-targeting siRNA). *C*. Comparison of dopamine release in cells that were mock-transfected or transfected with non-targeting siRNA. A Student's t-test revealed no significant difference in dopamine secretion between the two sets of cells (p=0.385 for basal secretion and p=0.482 for ATP-stimulated release; n=6 from 2 separate experiments).

To investigate if CSPα has any role in dopamine uptake into vesicles, the total ^{3}H-dopamine content was quantified in cells transfected with non-targeting siRNA compared to cells treated with CSPα siRNA. The results (Figure 3.5) show that all CSPα siRNA reduced cellular dopamine levels although this was only significant for oligos #1 and #2. These findings indicate a potential role for CSPα in regulating dopamine uptake into vesicles and this may warrant further investigation in the future. Note however that as secretion of [^{3}H]-Dopamine (Figure 3.4) is expressed as a % of total cell content, any reduction in dopamine uptake by CSPα depletion should not impact on secretion assay results.

[^{3}H]-Dopamine assays suggest that CSPα is required to ensure maximum efficiency of Ca^{2+}-stimulated exocytosis in neuroendocrine PC12 cells. We next planned to perform "rescue" experiment with CSPα mutants for structure-function studies. Rescue experiments are achieved by transfecting siRNA-resistant CSPα-expression plasmids into PC12 cells treated with siRNA. However, as the dopamine release assay measures secretion from the entire cell population, and plasmid transfection efficiencies in PC12 cells are not higher than ~ 30 %, the dopamine release assay was not suited for such rescue experiments.

The human growth hormone (hGH) assay however allows regulated secretion to be examined only in cells transfected by plasmid (Gleave *et al.*, 2001). Thus, PC12 cells are transfected with hGH plasmid and hGH secretion used as a measure of exocytosis only from transfected cells. For these experiments, a single siRNA (siRNA#1) was used. Following transfection with hGH plasmid and siRNA#1 (see 2.4.3 and 2.4.4), hGH secretion was measured using an ELISA kit (see 2.6.13). The results (Figure 3.6) show that the basal secretion levels were significantly lower in cells treated with CSPα siRNA compared to the control treated with no siRNA. Human growth hormone secretion in response to ATP stimulation also showed a significant reduction in the cells treated with CSPα siRNA. However, because the effects of CSP siRNA on hGH secretion were small, it was decided that the "window" to perform rescue experiments was not sufficient, and this was not pursued further.

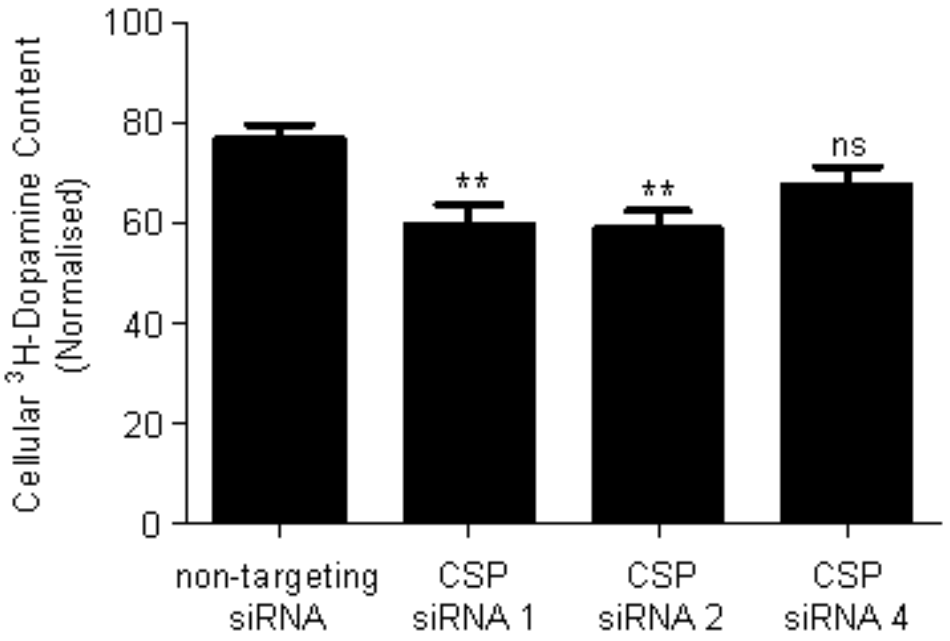

Figure 3.5 Effect of CSPα siRNAs on dopamine accumulation in PC12 cells. Cells were transfected with 100 nM CSPα siRNA or non-targeting siRNA (control) for 72 hours. Cells were then loaded with [^{3}H]-dopamine at 37°C for 90 minutes. The dopamine content of PC12 cells was determined by liquid scintillation counting. Error bars show the standard error of the mean (n=3). ** indicates a significant decrease ($p<0.001$) in dopamine content compared to cells treated with non-targeting siRNA using a one-way ANOVA test.

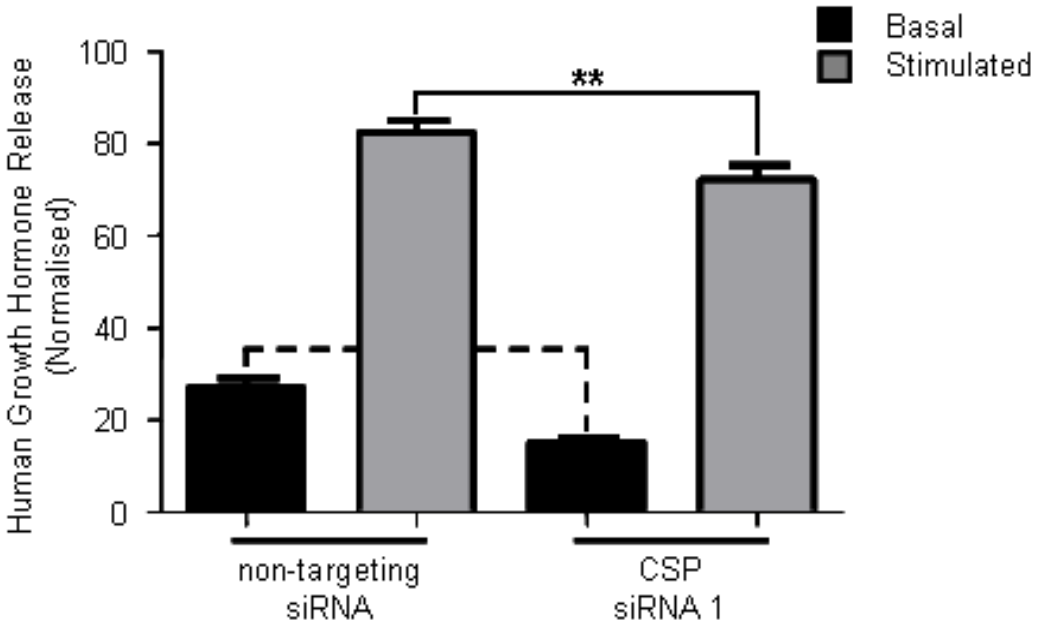

Figure 3.6: Growth Hormone secretion from PC12 cells treated with CSPα siRNA. PC12 cells were incubated for 3 days with 100 nM CSPα siRNA 1. The control had transfection reagent only. After 72 hours, cells were incubated for 15 minutes in either Krebs buffer or buffer containing 300 μM ATP at room temperature. Thereafter the cells were lysed and released and cell-associated hGH was assayed using an ELISA kit. Normalised results are expressed as a percentage of hGH release relative to the total cell hGH content. Error bars show the standard error of the mean (n=3). ** and *** indicate a significant decrease ($p<0.001$ and $p<0.0001$, respectively) in growth hormone release compared to control cells using a Student's t-test.

3.2.3 Chemical cross-linking experiments reveal that CSPα participates in distinct protein-protein interaction following elevation of $[Ca^{2+}]_i$

As previously mentioned, it was suggested that CSPα interacts with HSC70 (Braun *et al.*, 1996; Chamberlain and Burgoyne, 1997b), syntaxin (Nie *et al.*, 1999; Chamberlain *et al.*, 2001), VAMP (synaptobrevin) (Boal *et al.*, 2004; Weng *et al.*, 2009) and voltage gated Ca^{2+} channels (Leveque *et al.*, 1998; Magga *et al.*, 2000). It is also known that CSPα dimerizes, although the relevance of these interactions is not clear (Swayne *et al.*, 2003; Boal *et al.*, 2004). To further investigate whether CSPα function is linked to exocytosis, it was examined whether CSPα participates in distinct protein-protein interaction upon cell stimulation.

For this, chemical cross-linkers were used, which offer the potential to stabilise transient protein-protein interactions. To increase intracellular Ca^{2+} levels ionomycin was used, which causes a sustained Ca^{2+} influx, maximising chances of visualising protein-protein interactions.

Five different cross-linkers where used, which differ in reactive groups and size of the spacer arm (Figure 3.7*A*). Control cells were treated under the same conditions, but with no cross-linkers added. After 5 minutes of ionomycin-stimulation the cross-linkers were added, the cells were incubated for a further 10 minutes at 37°C and then incubated for 30 minutes on ice. Thereafter the cross-linkers were quenched for 15 minutes using 50 mM Tris on ice (2.6.4).

Cross-linked samples were resolved by SDS-PAGE and examined by immunoblotting. Figure 3.7*B* demonstrates that in addition to monomeric CSPα (~30 kDa) present in all lanes, distinct bands can be seen with some cross-linkers, which represent protein-protein interactions of CSPα. DFDNB cross-links a protein-complex at ~60 kDa (arrowhead in Figure 3.7*B*) in both basal and stimulated conditions. This appears to be a dimeric form of CSPα, which can also be detected in samples not exposed to cross-linker. In addition DSG and EGS treatment resulted in the appearance of a cross-linked species (asterisk) specifically in ionomycin-treated

A

Name	Size of Spacer
DSS (disuccinimidyl suberate)	11.4 Å
DSG (Dissucinimidyl glutarate)	7.72 Å
BSOCOES *Bis*[2-succinimidyloxycarbonyloxy ethyl]sulfone	13.0 Å
EGS [Ethylene glycolbis(succinimidylsuccinate)]	16.1 Å
DFDNB (1,5-difluoro-2,4-dinitrobenzene)	3.0 Å

B

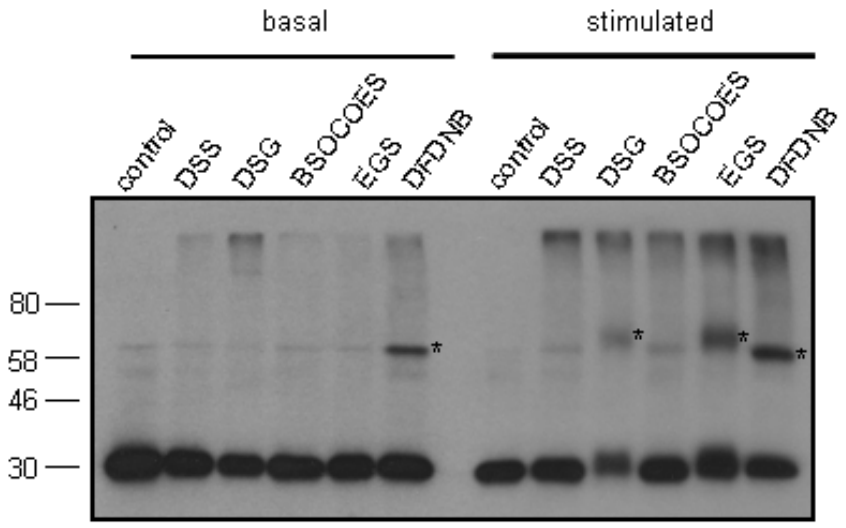

Figure 3.7: Chemical cross-linking of CSPα in PC12 cells. *A*. Table of the different chemical crosslinkers and their spacer arm lengths. *B*. Cells were incubated with or without 4 µM ionomycin at 37°C for 5 minutes. Afterwards 2 mM of the various crosslinkers were added, incubated for 10 minutes at 37°C and the cells were then incubated on ice for 30 minutes and quenched for 15 minutes with 50 mM Tris, pH 7.5. Cells were subsequently lysed, resolved by SDS-PAGE and transferred to a nitrocellulose membrane, which was probed for CSPα. Position of molecular weight standards are shown on the left of panel. This experiment was repeated 3 times with similar qualitative results.

cells. These protein complexes were detected in three separate experiments that were performed.

These findings show that CSPα participates in protein-protein interactions following stimulation which results in Ca^{2+} influx, promoting regulated secretion. To date, I have been unable to determine the composition of the protein complex cross-linked by DSG and EGS, and blotting with antibodies against SNAP25, syntaxin, synaptotagmin and VAMP did not suggest that any of these proteins were part of this complex.

3.2.4 Expression of CSPα in cell types that do not have defined regulated exocytosis pathways

CSPα was identified in *Drosophila melanogaster* (Zinsmaier et al., 1990) and surviving null mutants displayed impaired and sluggish movements (Umbach et al., 1994; Zinsmaier et al., 1994). Furthermore neurotransmitter release was decreased by ~50 % at 22°C in the mutant embryos and completely abolished at higher temperatures. These findings resulted in a more focused research on the role of CSPα in regulated exocytosis.

CSPα is known to be expressed in PC12 cells and in brain, which are specialised in regulated exocytosis. To establish if CSPα might also have a cellular function unrelated to regulated exocytosis, it was firstly investigated if CSPα is expressed in HEK293T and HeLa cells, which have not been reported to have regulated secretory pathways. Surprisingly CSPα was found to be expressed at high levels in both HEK293T and HeLa cells. Indeed, although CSPα is clearly enriched in brain, expression levels were similar in PC12 cells, which are highly specialised for regulated exocytosis, and HEK293T cells (Figure 3.8*A*). In contrast SNAP25, which functions in regulated exocytosis in neuronal and neuroendocrine cells, was only detected in PC12 cells and brain (Figure 3.8*A*). The constitutive SNARE protein SNAP23 was expressed in the four samples, but was clearly enriched in HEK293T and HeLa cells. Expression of CSPα in HeLa cells was confirmed by

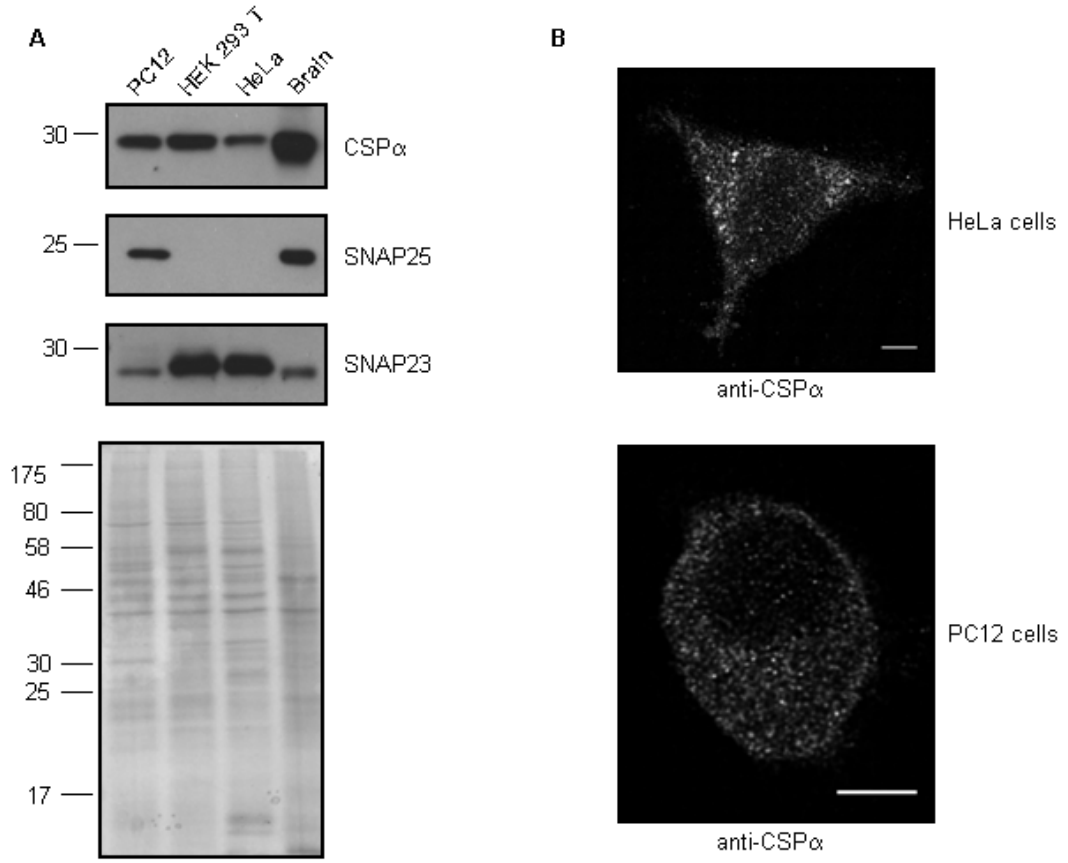

Figure 3.8: Expression of CSPα in mammalian cell lines. *A*. Equal amounts (7.5 µg) of lysate from PC12 cells, HEK 293T cells, HeLa cells and rat brain samples were resolved by SDS-PAGE. Thereafter the gels were either transferred to nitrocellulose membrane and probed with CSPα (Stressgen), SNAP25 (Synaptic Systems) or SNAP23 (Synaptic Systems) antibodies (top panel) or stained with coomassie blue (bottom panel). Position of molecular weight standards are shown on the left. *B*. HeLa cells and PC12 cells on glass coverslips were fixed with 4 % formaldehyde, and permeabilised in PBS containing 0.2 % Triton-X 100 and 0.3 % BSA for 6 minutes. Cells were then incubated in PBS/0.3 % BSA containing polyclonal CSPα antibody (Stressgen) at 1:50 dilution. Cells were then washed and stained with anti-rabbit-488 (1:400, PBS/BSA) for 1 hour. Cells were mounted on slides and imaged on Zeiss LSM510 laser scanning confocal microscope. Scale bars represent 5 µm.

immunofluorescence analysis (Figure 3.8*B*). Similar to PC12 cells (Figure 3.8, bottom panel), CSPa displayed a punctate, vesicular distribution in HeLa cells (Figure 3.8, top panel)

3.2.5 CSPα depletion in HeLa-C1 cells shows inconsistent results for constitutive exocytosis

Based on the finding that expression of CSPα is not restricted to cells with defined regulated exocytosis pathways (see 3.2.4), it was investigated if CSPα also plays a role in constitutive exocytosis. In constitutive exocytosis, proteins traffic from the endoplasmic reticulum (ER), to the Golgi complex and are then packed into vesicles that fuse directly with the plasma membrane (Kelly, 1985).

Constitutive exocytosis was examined in HeLa-C1 cells, which stably express a GFP-tagged ligand-reversible construct (pQCXIP-S1-eGFP-FM4-FCS-hGH), that is trapped in the ER, and upon incubation with rapamycin the aggregates solubilise and can get secreted through the secretory pathway (see 2.6.10) (Gordon *et al.*, 2010). HeLa-C1 cells were imaged 24 hours after subculturing on 30 mm coverslips. Live cell imaging was carried out on a wide-field Olympus IX-81 microscope. 1 µM rapamycin was added to start the solubilisation of the construct. Figure 3.9 indicates that the HeLa-C1 cells were able to secrete the GFP-tagged construct after adding rapamycin (t=0). It could be seen that over time the construct moved from the ER (dispersed localisation) to the Golgi complex and almost disappeared after 120 minutes, consistent with their secretion. A quantitative assay of GFP secretion was performed again over 240 minutes on 24-well plates to examine if the visual disappearance of the construct in Figure 3.9 was due to secretion. Constitutive secretion was detected via immunoblotting of cell lysates and the bathing buffer, which contained secreted molecules. Initial immunodetection of the GFP-tagged construct in the buffer could be visualised after 60 minute incubation with 1 µM rapamycin (Figure 3.10*A*). The control blot demonstrated no detection of the pQCXIP-S1-eGFP-FM4-FCS-hGH construct in all three supernatant fractions after 240 minute incubation without rapamycin. The graph in Figure 3.10*B* demonstrates

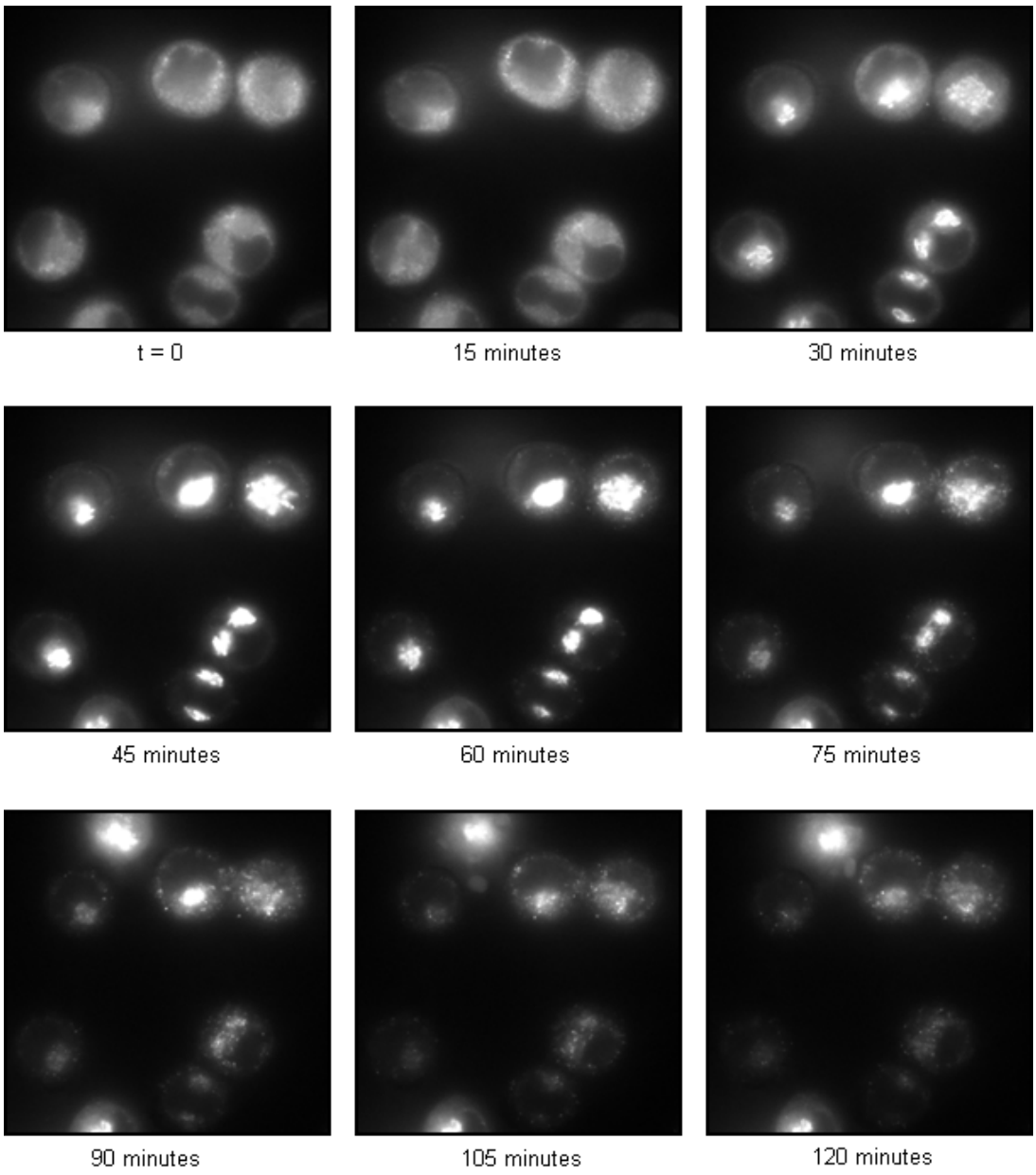

Figure 3.9: Visualisation of Constitutive Secretion in HeLa-C1 cells. The HeLa-C1 cell line is stably transfected with GFP-tagged pQCXIP-S1-eGFP-FM4-FCS-hGH. The encoded protein forms ligand-reversible dimers and is trapped in the endoplasmatic reticulum. These dimers are disassembled by rapamycin, which was added (1 µM) at t=0. Following addition of rapamycin, cells were imaged on a Olympus IX-81 microscope, 60 x magnification, over a period of 120 minutes, with images obtained every 10 seconds, using indentical microscope settings at 488 nm excitation. Shown are the images taken every 15 minutes. Rapamycin leads to a progressive movement from endoplasmic reticulum to Golgi and a loss of fluorescence at later time points, indicating secretion into the cell media.

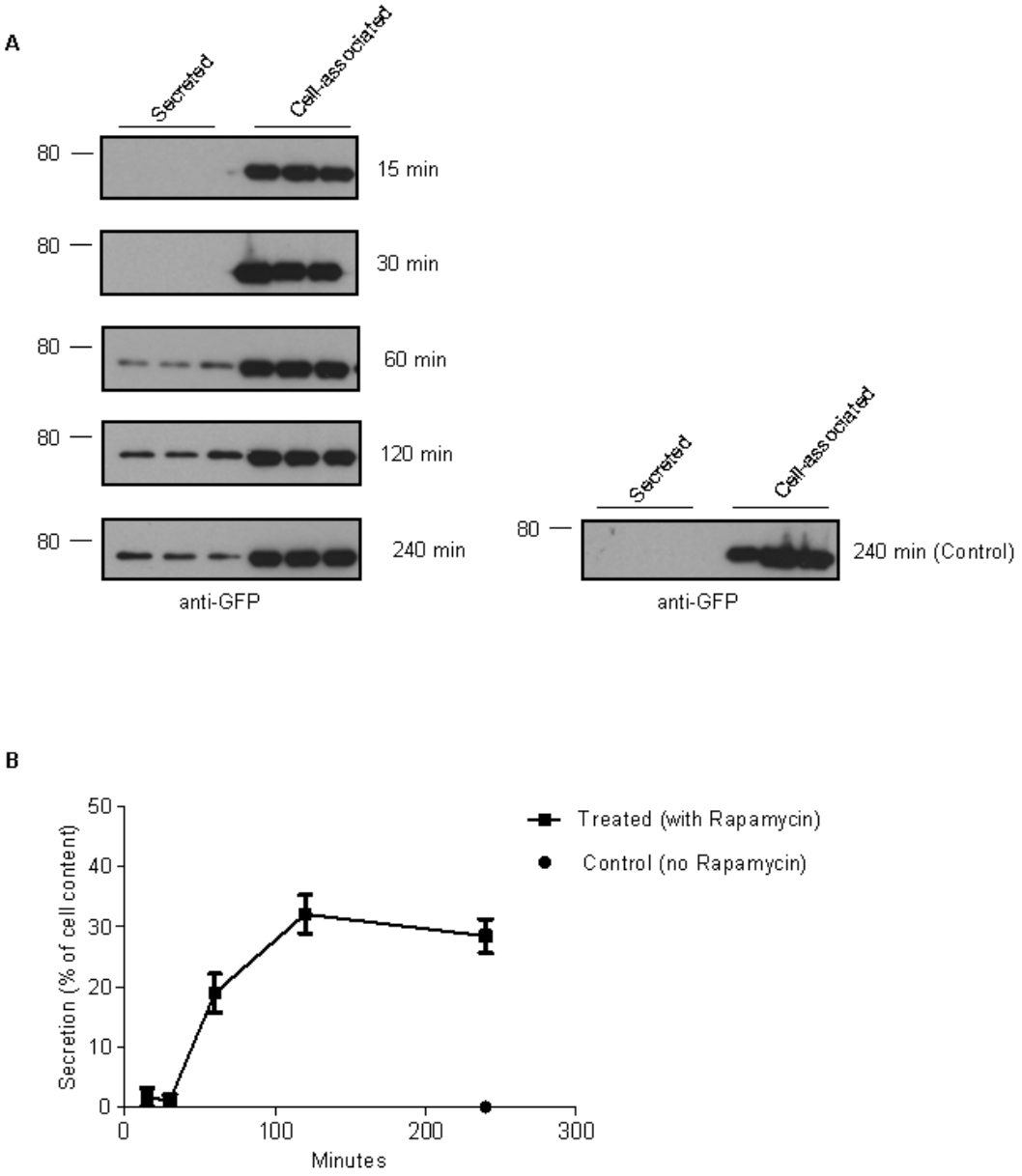

Figure 3.10: Quantitative measurement of constitutive secretion by immunoblotting. HeLa-C1 cells were incubated in the presence of 1 μM rapamycin for 15, 30, 60, 120 or 240 minutes. Control cells were incubated in the absence of 1 μM rapamycin for 240 minutes. Intracellular trafficking was stopped at the indicated time points by placing cells on ice. Media, containing secreted protein, was transferred into fresh 1.5 ml tubes and the remaining cells were lysed. *A*. secreted and cell-associated proteins were resolved by SDS-PAGE and transferred to nitrocellulose for immunoblotting analysis with a GFP antibody. *B*. Secreted GFP-tagged construct (supernatant) is expressed as a percentage of the total cell content (n=1 experiment in 3 replicates).

the quantified immunodetection of constitutive secretion, which is expressed as a percentage of the total cell content. Constitutive secretion increases for the first 2 hours and then remains static between 120 minutes and 240 minutes. The control indicates that no release can be detected when no rapamycin is added.

To examine the role of CSPα in constitutive secretion, an siRNA knockdown approach was used. Two different human CSPα siRNA's (hCSP siRNA) were purchased and their ability to knock down CSPα was examined. To verify which siRNA concentration leads to optimal knock down, three different concentrations were tested (10 nM, 50 nM and 100 nM). Seventy-two hours post transfection the cells were lysed and samples resolved by SDS-PAGE, transferred to nitrocellulose membrane and protein levels determined by immunoblotting. Visual comparisons of the control knock down with non-targeting siRNA and hCSP siRNA showed that all concentrations of the two oligos were able to knock down CSPα (Figure 3.11*A*). The SNAP 23 blot served here as a loading control. Quantitative analyses of CSPα knock down demonstrated that both oligos at all concentrations tested were able to deplete CSPα significantly compared to the control (~ 70 %; Figure 3.11*B*). However, the best knock down results were achieved with 100 nM siRNA with both oligos, where 80-85 % depletion could be achieved. Henceforward, all experiments involving knock down of CSPα in HeLa cells were done at a hCSP siRNA concentration of 100 nM.

The involvement of CSPα in constitutive exocytosis was examined in HeLa-C1 cells (see 2.6.10). Experiments were performed as described above, except that the rapamycin incubation was carried out for 60 and 120 minutes (120 minutes for the control (no rapamycin)). Initially, the effects of non-targeting siRNA on constitutive exocytosis were examined. The results showed (Figure 3.12*A*) that the non-targeting siRNA had no effect on the secretion compared to the mock-transfection. Figure 3.12*B* indicated that constitutive secretion in cells in which CSPα was depleted with hCSP siRNA 1 was lower after 60 minutes rapamycin incubation compared to the mock-transfection. However, after 120 minutes, secretion in CSPα depleted cells was similar to mock-transfected cells.

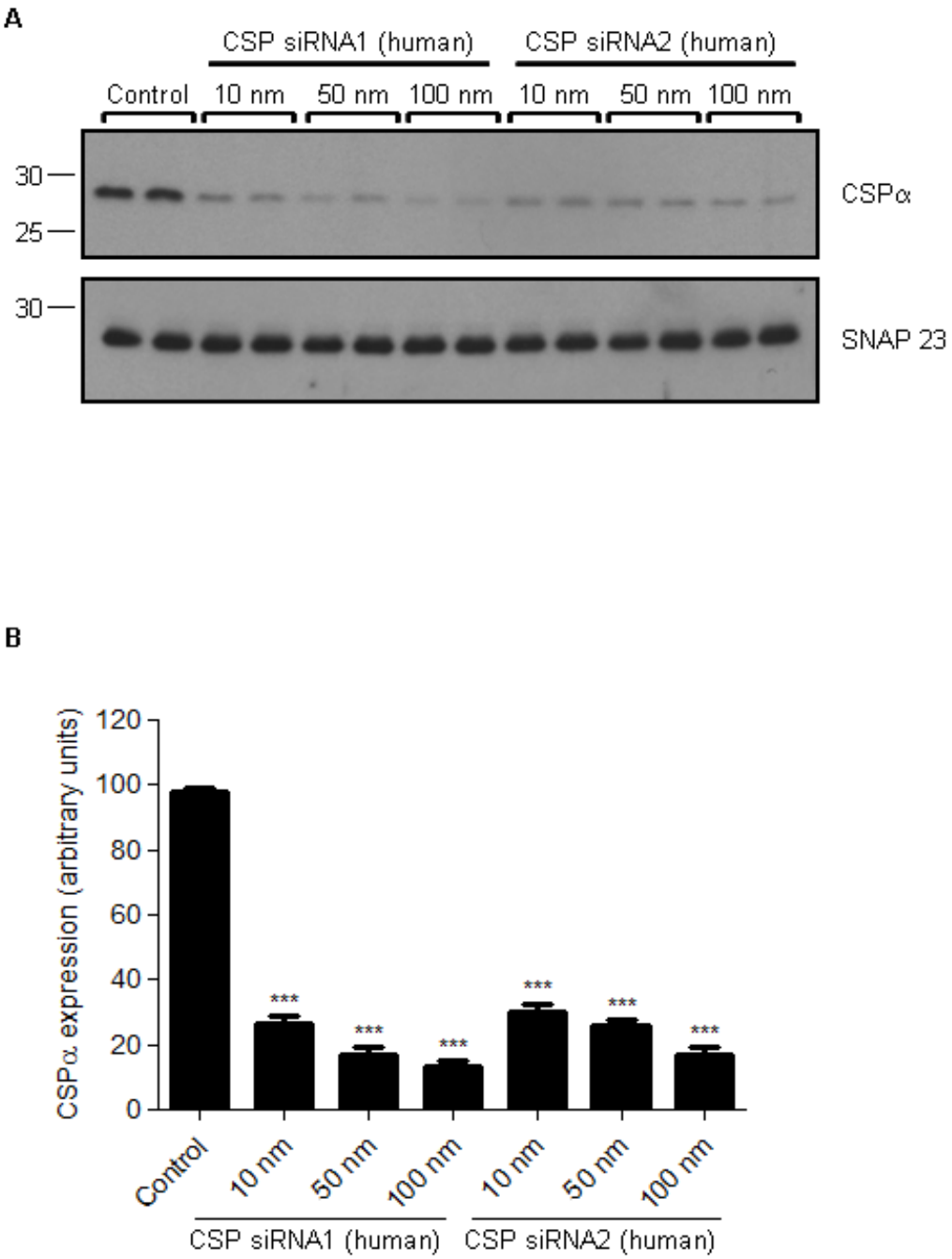

Figure 3.11: siRNA-mediated depletion of CSPα in HeLa cells. HeLa cells were incubated with 10 nM, 50 nM and 100 nM of two siRNA molecules directed against distinct regions of human CSPα (see table 2.2) or with non-targeting siRNA as control. 72 hours post transfection, the cells were lysed, resolved by SDS-PAGE and transferred to nitrocellulose for immunoblotting analysis with a CSPα antibody (Stressgen) or SNAP23 (Synaptic Systems) antibody as loading control. *A*. CSPα and SNAP23 levels in siRNA treated cells from a single experiment. *B*. CSPα levels were quantified in control and siRNA treated cells (n=4 from 2 independent experiments). *** indicates a significant decrease ($p<0.0001$) in CSPα expression compared to control cells using a one-way ANOVA test.

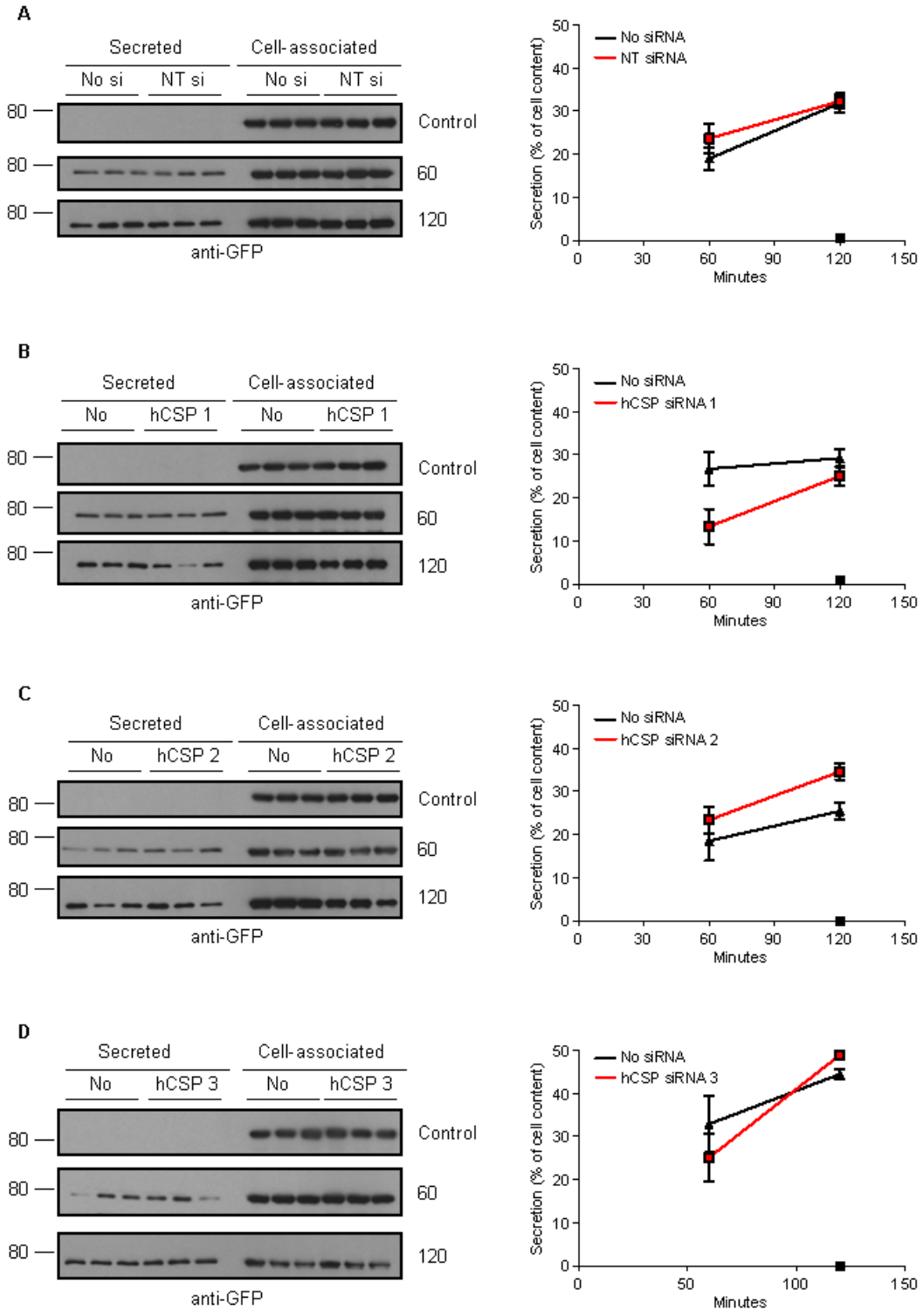

Figure 3.12: Quantitation of constitutive exocytosis in HeLa-C1 cells treated with CSPα siRNA.

Figure 3.12: Quantification of constitutive exocytosis in HeLa-C1 cells treated with CSPα siRNA. siRNA treated (hCSP 1,2 or 3), non-targeting siRNA (NT si) or mock-transfected (No si) cells were incubated without (control) or with 1 µM rapamycin for 60 or 120 minutes. Intracellular trafficking was stopped by placing the cells on ice and media containing cell proteins was removed into fresh 1.5 ml tubes and the remaining cells were lysed. Secreted and cell-associated proteins were resolved by SDS-PAGE and transferred to nitrocellulose for immunoblotting with a monoclonal GFP (JL8, Living Colours) antibody (left panels). Position of molecular weight markers are shown on the left. The graphs (right panels) show secretion expressed as a percentage of the total cell content in cells treated with CSPα siRNA compared to the mock-transfected cells. ● (No siRNA; no rapamycin), ■ (NT or hCSP siRNA 1, 2 or 3; no rapamycin), ▲ (No siRNA; treated with rapamycin), ▪ (NT or hCSP siRNA 1, 2 or 3; treated with rapamycin). Note ● (No siRNA; no rapamycin) cannot be seen as ■ (NT or hCSP siRNA 1, 2 or 3; no rapamycin) covers the symbol.

In cells were CSPα knock down occurred through hCSP siRNA 2 transfection, constitutive secretion was slightly greater than in the control cells after 60 minutes and 120 minutes (Figure 3.12*C*). As results obtained with oligos #1 and #2 were different, a third hCSP siRNA was obtained. Figure 3.12*D* shows that secretion in cells treated with hCSP siRNA 3 was initially lower than for the mock-transfected cells (60 minutes), but was slightly higher compared to the control cells at 120 minutes. Overall, the results found no consistent effect of CSPα depletion on constitutive secretion from HeLa C1 cells.

3.3 Discussion

Here it was shown that CSPα expression levels could be depleted by ~80 % in PC12 cells (Figure 3.2) and that all four commercial siRNAs were effective to a similar extent. Depletion of CSPα in this manner had no consistent effect on expression levels of the important SNARE proteins syntaxin, SNAP25 and synaptobrevin (VAMP). In the CSPα knock out mouse, no change in syntaxin and VAMP levels were noted but SNAP25 levels were reduced by ~50 % (Fernandez-Chacon *et al.*, 2004; Chandra *et al.*, 2005). The lack of effect of CSPα depletion on SNAP25 levels in PC12 cells (Figure 3.3) may be due to the fact that CSPα expression in the knock out mouse is completely abolished (Chandra *et al.*, 2005), whilst here there is still a residual amount of ~20 % of CSPα in PC12 cells; a complete abolishment of CSPα in PC12 cells might be needed to see any effect on SNAP25 expression. It is also possible that a longer time frame of CSPα reduction is required to see an effect on SNAP25 levels.

The lack of effect on neuronal exocytosis in the CSPα null mice is inconsistent with previous over-expression studies in non-neuronal cells, including PC12 cells, chromaffin cells and pancreatic beta cells (Chamberlain and Burgoyne, 1998; Zhang *et al.*, 1998; Graham and Burgoyne, 2000). Thus, we employed knockdown of CSPα to more directly examine the importance of this protein for regulated exocytosis in PC12 cells. CSPα depletion significantly reduced regulated secretion of ^{3}H

dopamine by about ~15-20 %. This supports the notion that CSPα plays a regulatory role in regulated exocytosis in PC12 cells (Chamberlain and Burgoyne, 1998). Although effects on exocytosis were modest, a higher reduction in CSPα expression levels (> 80 %) might be predicted to further inhibit exocytosis. To reach a more complete depletion of CSPα in PC12 cells small hairpin RNA (shRNA) could be used to generate stable cell lines. With the prolonged expression of shRNA it may be possible to get a more pronounced reduction in CSPα levels, which might also lead to a reduction in SNAP25 levels, like that seen in the CSPα knock out mouse (Chandra *et al.*, 2005). If a greater effect of CSPα knockdown on exocytosis could be achieved, it would be interesting to look at the fundamental role of domains of CSPα, such as the N- and C-termini, linker domain, J-domain and the cysteine string domain. By "rescuing" exocytosis with such mutants in cells depleted of endogenous CSPα, it will be possible to test the importance of these domains of CSPα in exocytosis and by inference which protein-protein interactions of CSPα might be functionally relevant (Bronk *et al.*, 2005).

It is possible that more pronounced effects of CSPα reduction on exocytosis may become apparent following repeated rounds of exocytosis/endocytosis. This may be particularly relevant if CSPα has a chaperone function in this pathway, regulating protein folding during vesicle dynamics. It may be possible to test this idea in future experiments by measuring exocytosis in CSP-depleted PC12 cells following multiple cell stimulation/recovery procedures.

It has been reported that around 3 copies of CSPα are on each vesicle (Takamori *et al.*, 2006), which suggest that the siRNA knock down, which achieved a depletion of ~80 %, was not efficient enough for a rigorous effect in regulated exocytosis and that one copy of CSP might be sufficient to compensate for the loss of the other copies and still be a functional factor for successful regulated secretion.

As a further way to assess whether CSPα might function in regulated exocytosis, it was examined if intracellular Ca^{2+} elevation (the trigger for regulated exocytosis) promoted interactions of CSPα with other cellular proteins. It was found that during ionomycin stimulation, CSPα was cross-linked to an unidentified protein by the cross-linkers DSG and EGS (Figure 3.7). Another cross-linker DFDNB, cross-linked

a band that was observed both before and after stimulation. In this case the band might be a CSPα-dimer. It is known that CSPα forms dimers in resting cells, but shows an increase in homodimerisation during stimulation (Boal *et al.*, 2004). It would be interesting to further investigate which proteins are cross-linked to CSPα during stimulation. This could be achieved by screening several proteins by immunoblotting. Another approach would be to excise the band out from the SDS-gel and identify the cross-linked proteins via mass spectroscopy.

As already mentioned, CSPα might function in other pathways in addition to regulated exocytosis. Figure 3.8 shows that CSPα is expressed in HEK293T and HeLa cells, suggesting again that CSPα function might not be restricted to regulated secretion. HeLa and HEK293T cells are not thought to have well-defined regulated secretory pathways. This is supported in Figure 3.8 showing that SNAP25 is not detected in these cells, which is a specific indicator for regulated exocytosis in neurons (Oyler *et al.*, 1989; Tao-Cheng *et al.*, 2000; Washbourne *et al.*, 2002). Moreover, SNAP23 is clearly enriched in HeLa and HEK293T cells, which regulates a wide variety of diverse membrane-membrane fusion events outside neuronal and neuroendocrine cells (Ravichandran *et al.*, 1996). As CSPα is expressed in HeLa and HEK293T cells at comparable levels to that in PC12 cells, it was possible that CSPα has an important function that is universal. Therefore the possible role of CSPα in constitutive exocytosis (which occurs in all cell types) was examined in HeLa cells through siRNA-mediated depletion of CSPα in HeLa-C1 cells (3.6). However, the results obtained were inconsistent, and depletion of CSPα showed an increase in constitutive secretion (Figure 3.12*C*), a decrease (Figure 3.12*B*) or no obvious change (Figure 3.12*D*) using three different siRNAs. Thus, the outcome of this experiment revealed no clear involvement of CSPα in constitutive exocytosis. It may be that the depletion of CSPα was not sufficient to have a major effect on constitutive exocytosis. Indeed, oligo 1, which achieved the highest knock down, showed a reduction in constitutive secretion and might indicate a role for CSPα in constitutive exocytosis (Figure 3.12 *B*). Therefore, to achieve a more reliable result for CSPα function in constitutive exocytosis, a stable cell line of HeLa-C1 cells, which expresses small hairpin RNA, could be used to silence the CSPα gene

expression continuously and more effectively (Siolas *et al.*, 2005). It is interesting to note that siRNA screens to identify R-SNARE proteins that regulate constitutive exocytosis in this cell type have also been unsuccessful (Gordon *et al.*, 2010). This may indicate the requirement for a complete knockout of certain proteins to perturb this pathway.

Although here we found no effect of CSPα in constitutive exocytosis in HeLa and HEK293T cells, future work could examine the effects of CSPα knock down in these cells on other trafficking pathways such as endocytosis, granule biogenesis or cytokinesis.

CHAPTER FOUR:

ANALYSIS OF EXPRESSION LEVELS OF CSPα AND INTERACTING PARTNERS IN POST-MORTEM BRAIN SAMPLES FROM PATIENTS WITH BIPOLAR DISORDER, MAJOR DEPRESSION AND SCHIZOPHRENIA

4.1 Introduction

Perturbations in neuronal pathways and chemical imbalances in the brain are thought to contribute to a wide range of mental illnesses and neuronal disorders. There is a major effort to identify genetic alterations associated with specific disorders to provide a molecular description of changes that lead to brain dysfunction. Mutations or single nucleotide polymorphisms in protein coding sequences of genes can lead to disruption of protein function. In addition, mutations occurring in non-coding regions can lead to changes in protein expression or gene splicing. On top of primary disease-associated genetic mutations, there are also likely to be numerous downstream compensatory changes that occur in the expression of other proteins. Thus, deciphering the precise changes that are associated with disease phenotype is a major challenge.

Changes in neuronal communication are likely at the heart of several brain disorders, and therefore there is merit in analysing changes in the expression of the neurotransmitter release machinery in different disease states. It has been previously shown that mutation or deletion of certain proteins present at the active zone and involved in neurotransmitter release resulted in mental disorder phenotypes in mice. One of these proteins is RIM1α, which is required for presynaptic long-term potentiation (LTP) in hippocampus and cerebellum. RIM$\alpha^{-/-}$ mice exhibit behavioural endophenotypes associated with schizophrenia and deficits in social behaviour (Powell *et al.*, 2004; Blundell *et al.*, 2010). In addition, recent studies have shown that alterations in the mRNA and protein expression levels of SNARE proteins and interacting partners are associated with mental disorders (Johnson *et al.*, 2008): single nucleotide polymorphisms of syntaxin, synaptotagmin and SNAP25 (‘blind-drunk’ mutant mice) have been linked to schizophrenia. Furthermore it could be shown that a transgenic schizophrenia mouse model, which expresses a C-terminal truncation of hDISC1 (human disrupted-in-schizophrenia 1), has significantly reduced SNAP25 expression levels (Jeans *et al.*, 2007; Pletnikov *et al.*, 2008). Another protein that is associated with the SNARE proteins and implicated in mental disorders is complexin-2 (Sawada *et al.*, 2002). Complexin-2 knock out mice display schizophrenia-like behavioral phenotypes, but only after an enviromental traumatic experience during puberty (e.g. mild parietal neurotrauma) (Radyushkin *et*

al., 2010). Interstingly a recent human genetic study has identified a single nucleotide polymorphism in complexin-2 of patients with schizophrenia (Begemann *et al.*, 2010). Together, these phenotypic abnormalities in mouse mutants of SNARE proteins and interacting partners suggest that defects in exocytosis might be a prevalent underlying cause of specific mental disorders.

Three brain disorders that are of particular interest are major depression, bipolar disorder and schizophrenia. In table 1 these neuropsychiatric disorders and their characteristics are summarised (Nikolaus *et al.*, 2009; Brennaman and Maness, 2010). Major depressive disorder is characterised by recurrent major depressive episodes, consisting of severely depressed mood persisting for at least for 2 weeks. These episodes may be isolated or recurrent and are categorised as mild, moderate, or severe (Kennedy, 2008). Various hypotheses have been put forward to account for the pathogenesis of major depressive disorder. One hypothesis suggests that interplay between genetics, psychological and social factors plays a role in the development of depression, but the precise causes may vary considerably dependent on individual circumstances. Other hypotheses propose that neuroendocrine function and/or neuroanatomy are changed (Manji *et al.*, 2001; Sierksma *et al.*, 2010). In general the prefrontal cortex, amygdala and medial thalamus are thought to be particularly important in the pathophysiology (Drevets and Raichle, 1992). Modulation of neuroendocrine function is thought to centre on changes in monoamines, in particular serotonin

Table 4.1: Summary of neuropsychiatric disorder characteristics.

Disorder	Age of onset	Neurotransmitter(s)	Affected Brain region(s)
Depression	Can occur at any age	Serotonin, norepinephrine	Hippocampus, Frontal cortex, Hypothalamus, Amygdala, Striatium
Schizophrenia	Late adolescence, early adulthood	Dopamine, GABA	Hippocampus, Prefrontal cortex, Ventricular enlargements
Bipolar	Late adolescence, early adulthood	Mania: dopamine, GABA Depression: serotonin, norepinephrine	Hippocampus, Prefrontal cortex, Ventricular enlargements

(5-hydroxytryptamine), norepinephrine (noradrenaline) and dopamine (Di Giovanni *et al.*, 2006; Nutt, 2006). Indeed, monoamine oxidase inhibitors which prolong functional half-life, and selective serotonin reuptake inhibitors (SSRIs), which promote increased levels of serotonin at synapses (Burke *et al.*, 1997; Amsterdam, 1998), are frequently administered as antidepressants.

Bipolar disorder (also referred to as bipolar depression or manic depression) is normally characterised by depressive phases alternating with periods of mania (persistent feelings of sadness, insomnia, euphoria and rage) (Kruger and Prager, 2007). Again, interplay between environmental and genetic factors seems to be the underlying trigger for bipolar disorder. Interestingly, genetic studies have implicated a variety of genes that regulate metabolism of transmitters including serotonin, glutamate and dopamine (Kato, 2007). There are a variety of pharmacological treatments used for bipolar disorder including antidepressants and mood stabilisers, such as lithium.

Schizophrenia is a chronic mental disorder with a global prevalence of 1-5 % (Young *et al.*, 2010) and is characterised by a variety of symptoms, which lead to severe social dysfunctions. To date there are five major subtypes of schizophrenia that are distinguished by their symptoms, which includes delusions and hallucinations, thought disorder, immobilisation and agitated movement (McGlashan and Fenton, 1991). In some cases there are also links to major depression, such as "post-schizophrenic depression", where patients have depressive episodes with low-level schizophrenic symptoms present after a phase of acute schizophrenia. Another condition is "schizoaffective disorder", which is characterised by both symptoms displayed at the same time, schizophrenia and manic depressive episodes (Malhi *et al.*, 2008). According to the present classification, symptoms in general must have been present for at least one month in a period of six months of disturbed functioning. To date, the pathogenesis of schizophrenia is not well understood. Evidence suggest that genetic, psychological and/or environmental factors may act together (Corcoran *et al.*, 2003; Harrison and Owen, 2003). Similar to major depression and bipolar disorder, the neurotransmitter dopamine has been implicated in the pathophysiology of schizophrenia. This link is based on the positive effects of

drugs that block dopamine function, as well as effects of amphetamines (which trigger the release of dopamine), which can lead to schizophrenic symptoms (Seeman and Lee, 1975; Toda and Abi-Dargham, 2007).

Given the link between neurotransmitter release and development of these mental disorders, several studies have investigated how components of the neurotransmitter release machinery are affected in these conditions, or how drug treatments affect protein expression. The mood stabiliser lithium, which has been used in the treatment of major depression and bipolar disorder (Schou, 1997), has been shown to promote a significant increase in regulated neurotransmitter release (e.g. dopamine and serotonin) (Hesketh *et al.*, 1978; Maggi and Enna, 1980; Treiser *et al.*, 1981; Staunton *et al.*, 1982; Ebstein *et al.*, 1983; Wang and Friedman, 1989). Indeed, lithium enhances CSPα gene expression in nerve growth factor (NGF) differentiated PC12 cells as well as in rat brain (Cordeiro *et al.*, 2000), together with a coordinated up-regulation of secretory granule proteins (Codeiro, 2000b).

Several reports have examined expression levels of secretory proteins in post-mortem brain samples from patients suffering from mental disorders. However, CSPα has not been analysed. Here, we were able to gain access to human post-mortem brain samples from patients suffering from major depression, bipolar disorder and schizophrenia. Following on from the work Cordeiro *et al.* (2000) it was analysed if there were any differences in CSPα expression in these patients compared with controls. In addition, expression of the CSPα-interacting partners α-synuclein, HSP70, syntaxin and synaptotagmin I were examined. As CSPα and HSP70 are important molecular chaperones, this analysis was extended to examine expression levels of the general heat shock chaperone proteins HSP60 and HSP90.

4.2 Results

4.2.1 Human post-mortem samples

Human post-mortem samples were obtained from the Edinburgh Brain Bank. Anonymised details of the source of the brain material, including age, gender, post-

Table 4.2: Anonymised details of the human post-mortem control patients. PMI stands for post mortem interval (hours).

Patients Category	Gender	Age	PMI (h)	Cause of Death	Neuropath Diagnosis
Control	Male	53	44	Combined effects of ischaemic heart disease and hypertensive heart disease	Small vessel disease consistent with chronic hypertension.
Control	Male	67	50	Ruptured abdominal aortic aneurysm and coronary artery thrombosis. Atherosclerosis. Ischaemic heart disease. COPD.	No significant abnormality.
Control	Male	45	39	Ischaemic heart disease. Coronary artery thrombosis.	No significant abnormality.
Control	Male	70	50	Pulmonary embolism. Deep vein thrombosis.	No significant abnormality.
Control	Male	25	79	Extensive internal haemorrhage. Multiple injuries. Road traffic collision (car driver).	No significant abnormality.
Control	Male	57	52	Ischaemic heart disease. Coronary artery thrombosis. Coronary artery atherosclerosis.	No significant abnormality.

Table 4.3: Anonymised details of the human post-mortem depression patients. PMI stands for post mortem interval (hours).

Patients Category	Gender	Age	PMI (h)	Cause of Death	Neuropath Diagnosis
Depression	Male	57	66	Multiple injuries. Fall from a height.	Recent hypoxia. Chronic BBB breakdown. No evidence of brain traumatic injury.
Depression	Female	53	87	Suspension by a ligature	Acute hypoxia.
Depression	Male	19	51	Fatal Amitriptyline poisoning	Acute hypoxia. Pallidal siderosis.
Depression	Female	53	69	Bronchopneumonia. Alcoholic liver disease.	Central pontine myelinolysis.
Depression	Male	53	43	Suspension by a ligature.	No significant abnormality.
Depression	Female	20	40	Suspension by a ligature.	No significant abnormality.

Table 4.4: Anonymised details of the human post-mortem schizophrenia patients. PMI stands for post mortem interval (hours).

Patients Category	Gender	Age	PMI (h)	Cause of Death	Neuropath Diagnosis
Paranoid Schizophrenia	Male	44	99	Hypertensive heart disease. Hypertension.	Minor small vessel disease. Reasonably normal.
Schizoaffective Disorder	Male	70	45	Ischaemic heart disease. Severe cornary artery disease. Atherosclerosis. COPD. MS	Focal ischaemic injury. Small vessel disease.
Paranoid Schizophrenia	Male	50	75	Acute combined morphine, methadone, diazepam and alcohol toxicity.	No significant abnormality.
Schizoaffective Disorder	Male	41	41	External asphyxia by inhalation of helium.	No significant abnormality.
Schizophrenia	Male	42	46	Suspension by a ligature.	No significant abnormality.
Schizophrenia	Female	40	73	Intra-cerebral haemorrhage. Ruptured intra-cerebral artery. Hypertension	Perivascular bleeding adjacent to haematoma.

Table 4.5: Anonymised details of the human post-mortem bipolar patients. PMI stands for post mortem interval (hours).

Patients Category	Gender	Age	PMI (h)	Cause of Death	Neuropath Diagnosis
Bipolar	Male	24	117	Acute pulmonary oedema	Acute cerebellar infarct. Old cerebellar haemorrhage (possible old injury). Periventricular gliosis.
Bipolar	Female	57	72	Combined effects of chronic alcoholism and lithium use	Insufficient sampling to determine diagnosis.
Bipolar	Female	42	103	Hypertensive heart disease	Cerebrovascular disease.
Bipolar	Male	48	72	Bronchopneumonia	Acute cerebral hypoxia. Occasional neurofibrillary tangles in locus coeruleus.
Bipolar	Female	41	67	Suspension by a ligature	Cerebral hypoxia.

Table 4.6: Average age, gender ratio and PMI (post mortem interval (hours)) of human post-mortem depression, schizophrenia and bipolar samples. Using a Student's t-test revealed that the PMI of bipolar patients was significantly higher (*, $p<0.05$) compared to control samples.

Disorder	Average Age	Male/Female Ratio	Average PMI
Control	52.83 (± 6.71)	6/0	52.33 (± 5.68)
Depression	42.5 (± 7.3)	3/3	59.33 (± 7.33)
Schizophrenia	47.83 (± 4.67)	5/1	63.17 (± 9.38)
Bipolar	42.4 (± 5.41)	2/3	86.2* (± 10.01)

mortem interval (PMI), cause of death and neuropathology diagnosis are given in tables 2-5. Table 6 shows the average age, PMI and gender ratio. A Student's t-test revealed that the mean post mortem interval (PMI) of bipolar patients was significantly increased compared to control patients ($p< 0.05$). No other significant differences in the patient samples were recorded.

4.2.2 Samples from patients with major depression displayed a significant reduction of syntaxin expression in cortex compared with controls

To examine expression of CSPα and other proteins in mental illnesses, equal amounts of post mortem brain region lysates were resolved by SDS-PAGE. Proteins were then transferred to a nitrocellulose membrane and analysed by immunoblotting. Relative expression levels were quantified by densitometry and the highest value was arbitrarily set to 100 %, with all other values expressed relative to this. To limit gel-to-gel variability, each set of samples was run three times and average values for relative expression were calculated. These values were used to calculate average protein expression for each disorder in four brain regions relative to control.

Figure 4.2 shows that syntaxin expression was significantly decreased from ~90 % (control) to ~60 % in cortex of patients with major depressive disorder (Student's T-test, $p<0.05$). A scatter plot showing syntaxin expression levels in the cortex of individual patients is presented in Figure 4.3*C*. In contrast, statistical analysis revealed no significant differences in the expression of any proteins in cerebellum (Figure 4.1), hippocampus (Figure 4.3) and thalamus (Figure 4.4) from patients with major depression.

4.2.3 Patients with schizophrenia showed no significant change in protein expression levels compared with controls

Figures to 4.5-4.8 show quantified expression levels relative to controls in brain regions from schizophrenic patients. No significant differences were detected for any of these samples.

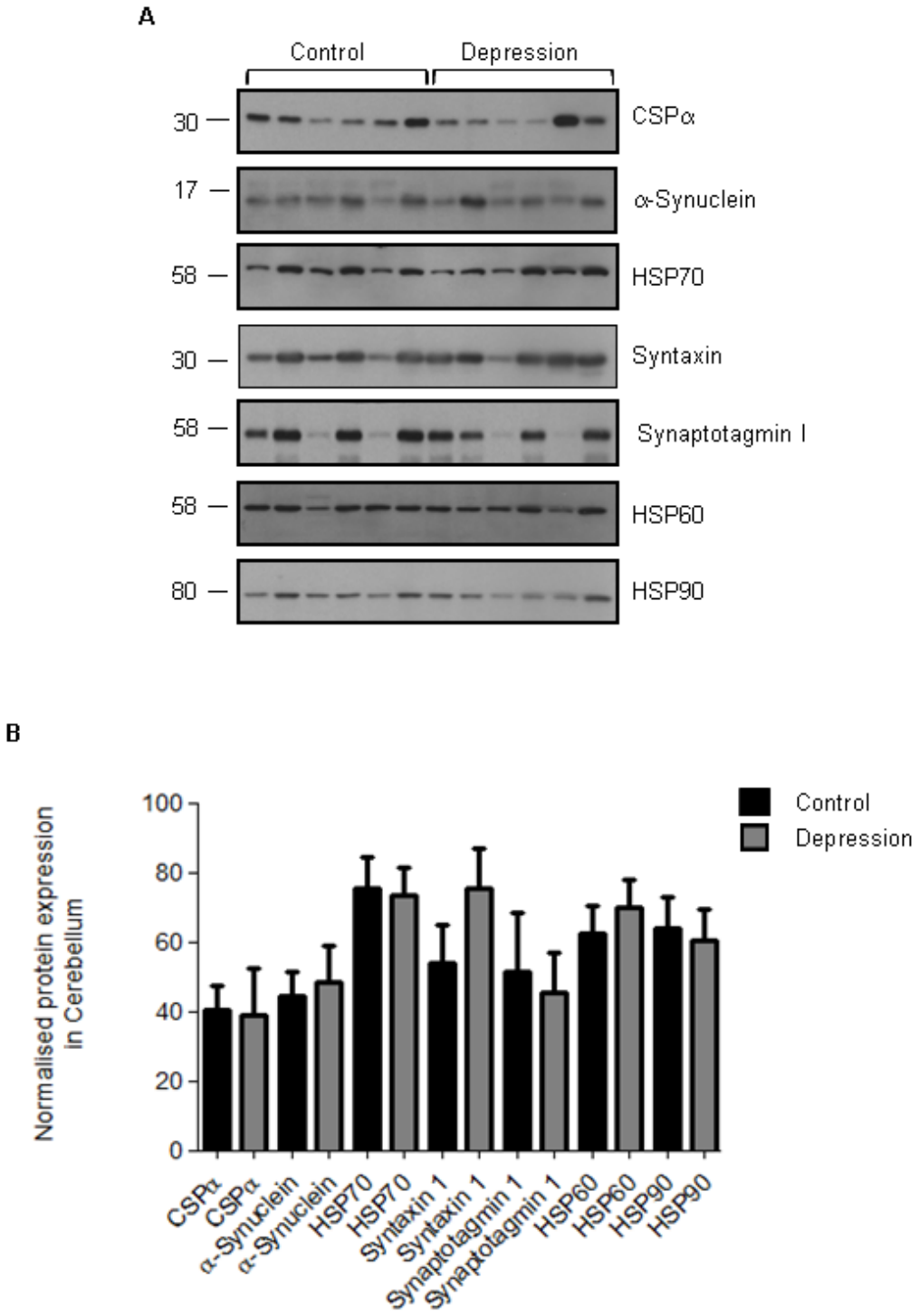

Figure 4.1: Protein expression in Cerebellum in depression disorder. Human brain samples were lysed, samples resolved by SDS-PAGE and transferred to nitrocellulose membranes, which were then probed with specific CSPα, α-Synuclein, HSP70, HSP60, HSP90, Synaptotagmin 1 and Syntaxin 1 antibodies. *A*. Shows representative immunoblots. Position of molecular weight standards are shown on the left of panels. *B*. Relative protein expression levels were quantified as described in section 4.2.2. Error bars show the standard error of the mean (n=3). Multiple Student's t-tests revealed no significant difference in the expression of any protein in depression compared to control patients.

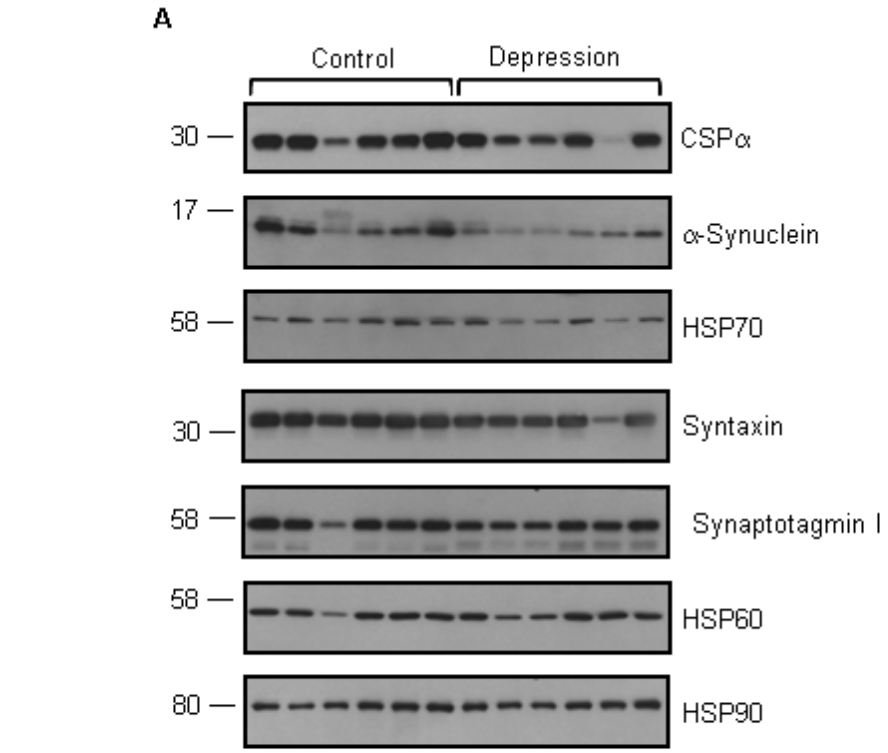
A
Control
Depression
30
CSPα
17
α-Synuclein
58
HSP70
30
Syntaxin
58
Synaptotagmin I
58
HSP60
80
HSP90

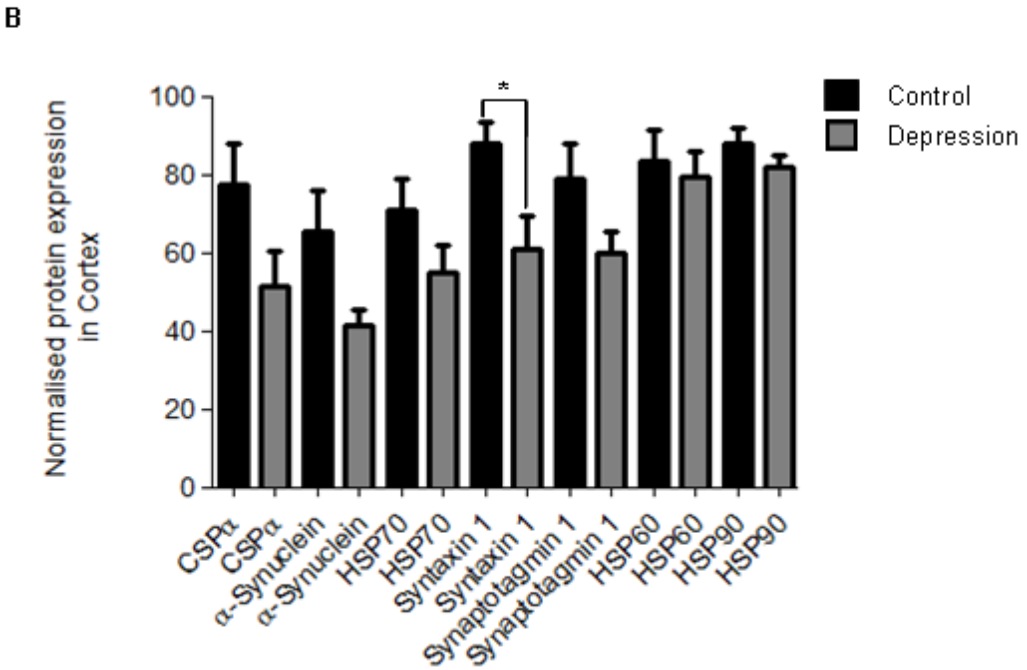
B
Normalised protein expression
In Cortex
100
80
60
40
20
0
*
Control
Depression
CSPα
CSPα
α-Synuclein
α-Synuclein
HSP70
HSP70
Syntaxin 1
Syntaxin 1
Synaptotagmin 1
Synaptotagmin 1
HSP60
HSP60
HSP90
HSP90

C

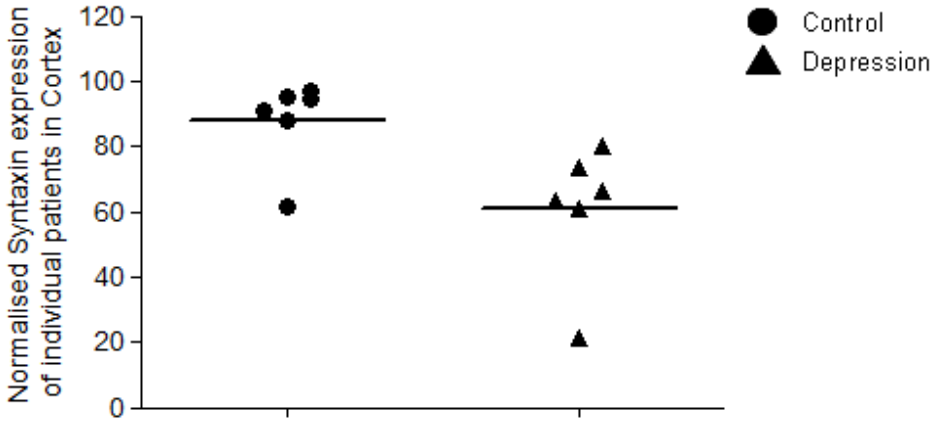

Figure 4.2: Protein expression in Cortex in depression disorder. Human brain samples were lysed, samples resolved by SDS-PAGE and transferred to nitrocellulose membranes, which were then probed with specific CSPα, α-Synuclein, HSP70, HSP60, HSP90, Synaptotagmin 1 and Syntaxin 1 antibodies. *A*. Shows representative immunoblots. Position of molecular weight standards are shown on the left of panels. *B*. Relative protein expression levels were quantified as described in section 4.2.2. Error bars show the standard error of the mean (n=3). * indicates a significant decrease ($p<0.05$) in syntaxin expression in depression which was compared to control samples using a Student's t-test. *C*. The scatter plot shows the normalised Syntaxin 1 expression levels in cortex of individual depression patients.

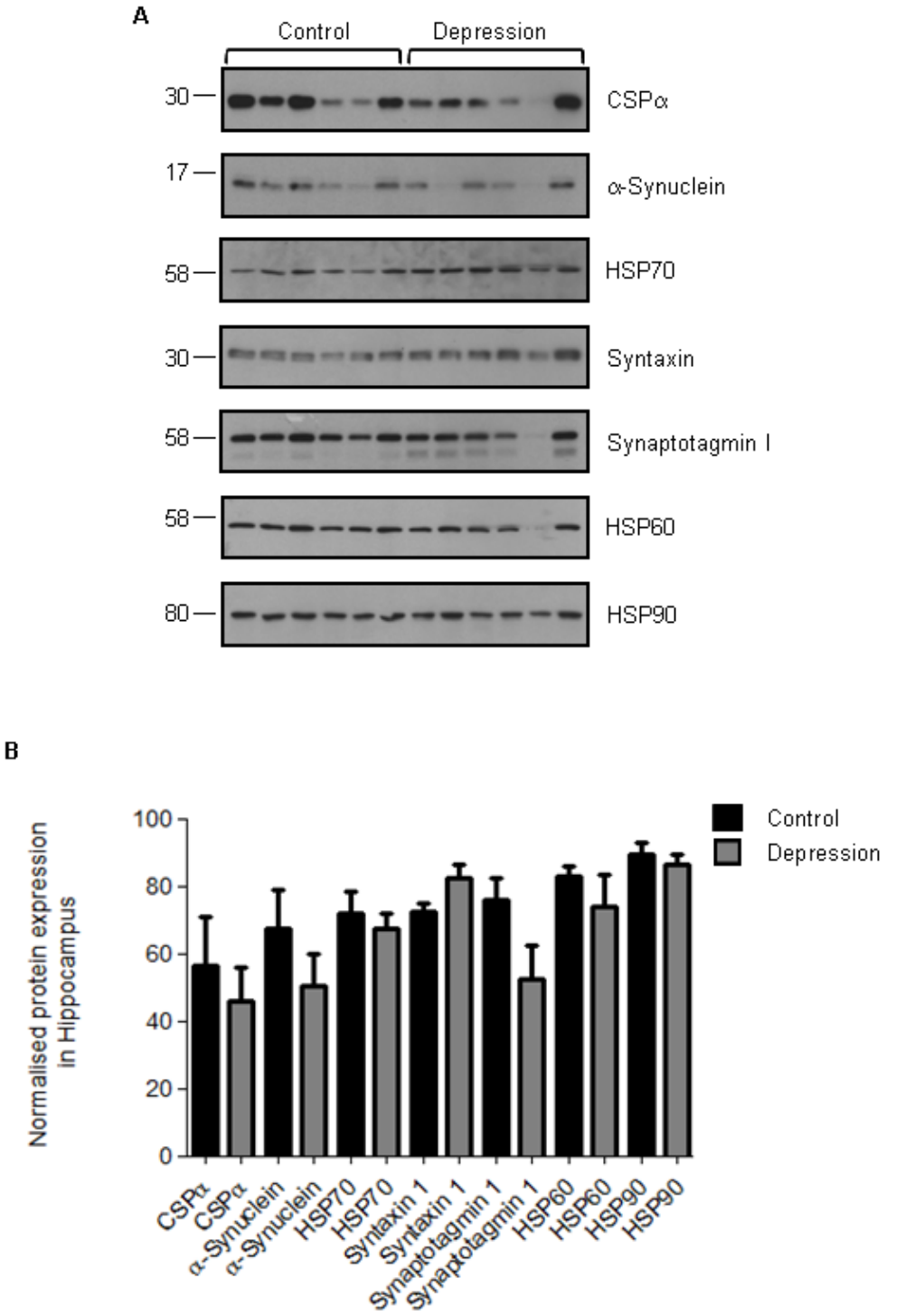

Figure 4.3: Protein expression in Hippocampus in depression disorder. Human brain samples were lysed, samples resolved by SDS-PAGE and transferred to nitrocellulose membranes, which were then probed with specific CSPα, α-Synuclein, HSP70, HSP60, HSP90, Synaptotagmin 1 and Syntaxin 1 antibodies. *A*. Shows representative immunoblots. Position of molecular weight standards are shown on the left of panels. *B*. Relative protein expression levels were quantified as described in section 4.2.2. Error bars show the standard error of the mean (n=3). Multiple Student's t-tests revealed no significant difference in the expression of any protein in depression compared to control patients.

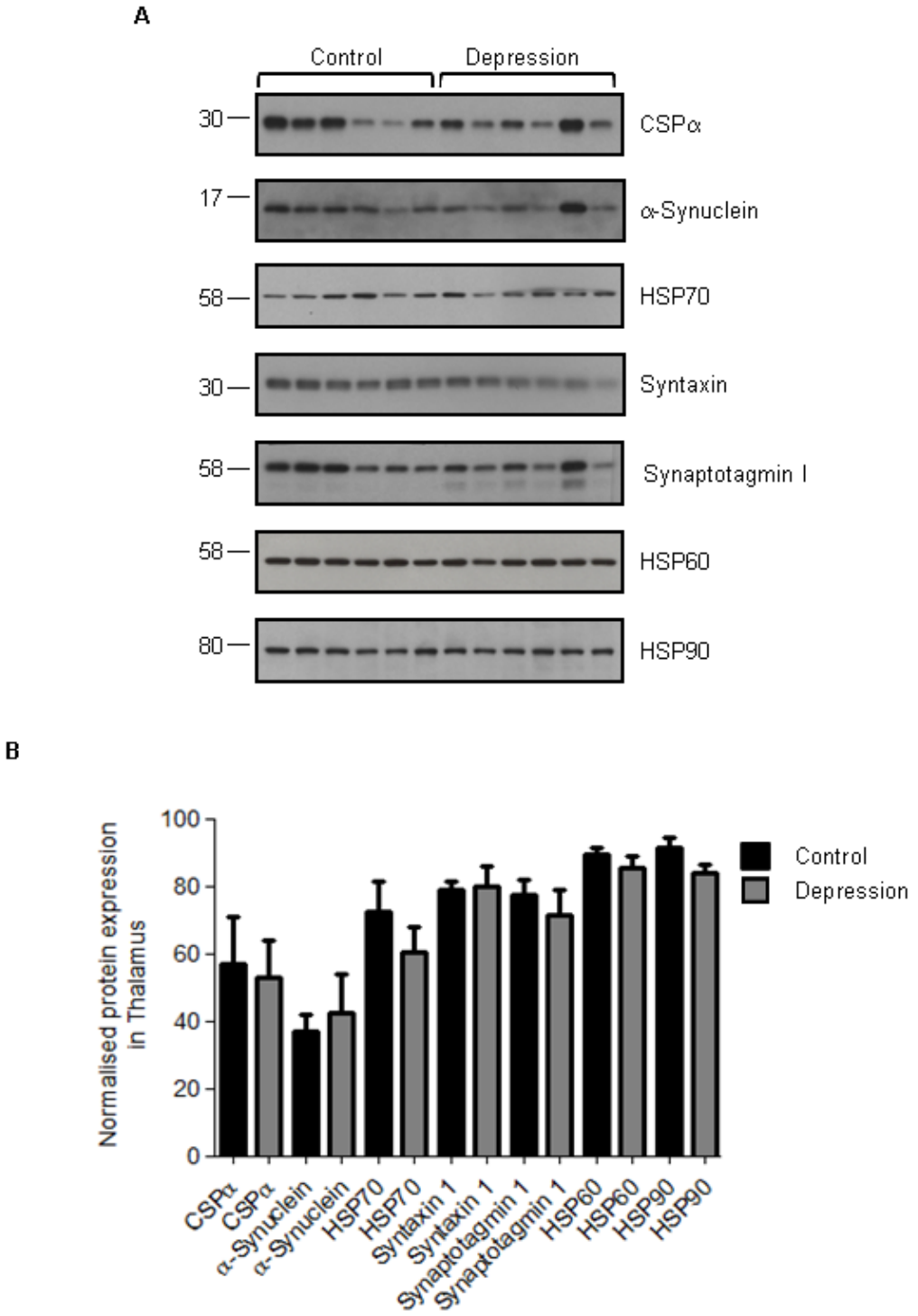

Figure 4.4: Protein expression in Thalamus in depression disorder. Human brain samples were lysed, samples resolved by SDS-PAGE and transferred to nitrocellulose membranes, which were then probed with specific CSPα, α-Synuclein, HSP70, HSP60, HSP90, Synaptotagmin 1 and Syntaxin 1 antibodies. *A*. Shows representative immunoblots. Position of molecular weight standards are shown on the left of panels. *B*. Relative protein expression levels were quantified as described in section 4.2.2. Error bars show the standard error of the mean (n=3). Multiple Student's t-tests revealed no significant difference in the expression of any protein in depression compared to control patients.

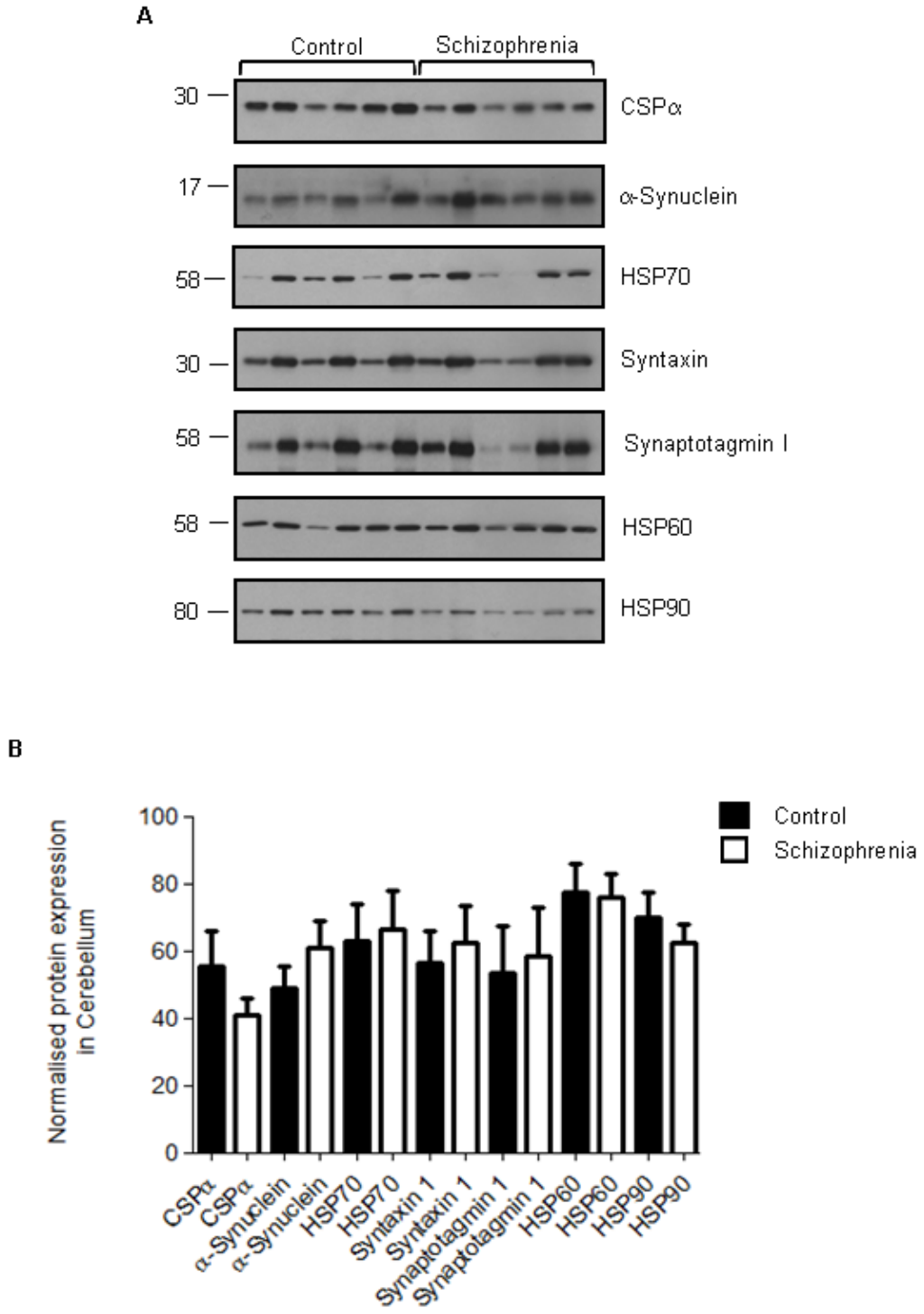

Figure 4.5: Protein expression in Cerebellum in schizophrenia disorder. Human brain samples were lysed, samples resolved by SDS-PAGE and transferred to nitrocellulose membranes, which were then probed with specific CSPα, α-Synuclein, HSP70, HSP60, HSP90, Synaptotagmin 1 and Syntaxin 1 antibodies. *A*. Shows representative immunoblots. Position of molecular weight standards are shown on the left of panels. *B*. Relative protein expression levels were quantified as described in section 4.2.2. Error bars show the standard error of the mean (n=3). Multiple Student's t-tests revealed no significant difference in the expression of any protein in schizophrenia compared to control patients.

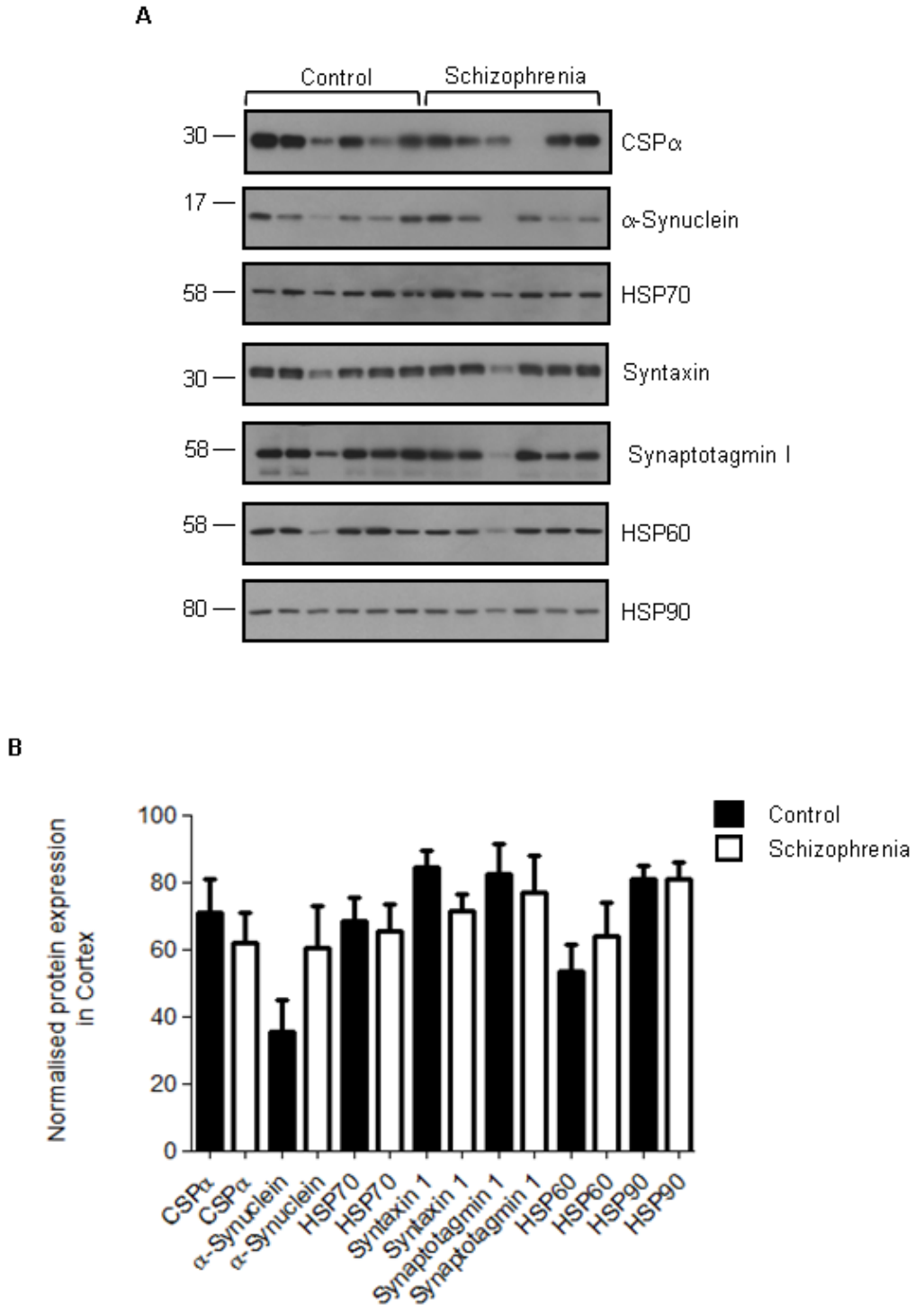

Figure 4.6: Protein expression in Cortex in schizophrenia disorder. Human brain samples were lysed, samples resolved by SDS-PAGE and transferred to nitrocellulose membranes, which were then probed with specific CSPα, α-Synuclein, HSP70, HSP60, HSP90, Synaptotagmin 1 and Syntaxin 1 antibodies. *A*. Shows representative immunoblots. Position of molecular weight standards are shown on the left of panels. *B*. Relative protein expression levels were quantified as described in section 4.2.2. Error bars show the standard error of the mean (n=3). Multiple Student's t-tests revealed no significant difference in the expression of any protein in schizophrenia compared to control patients.

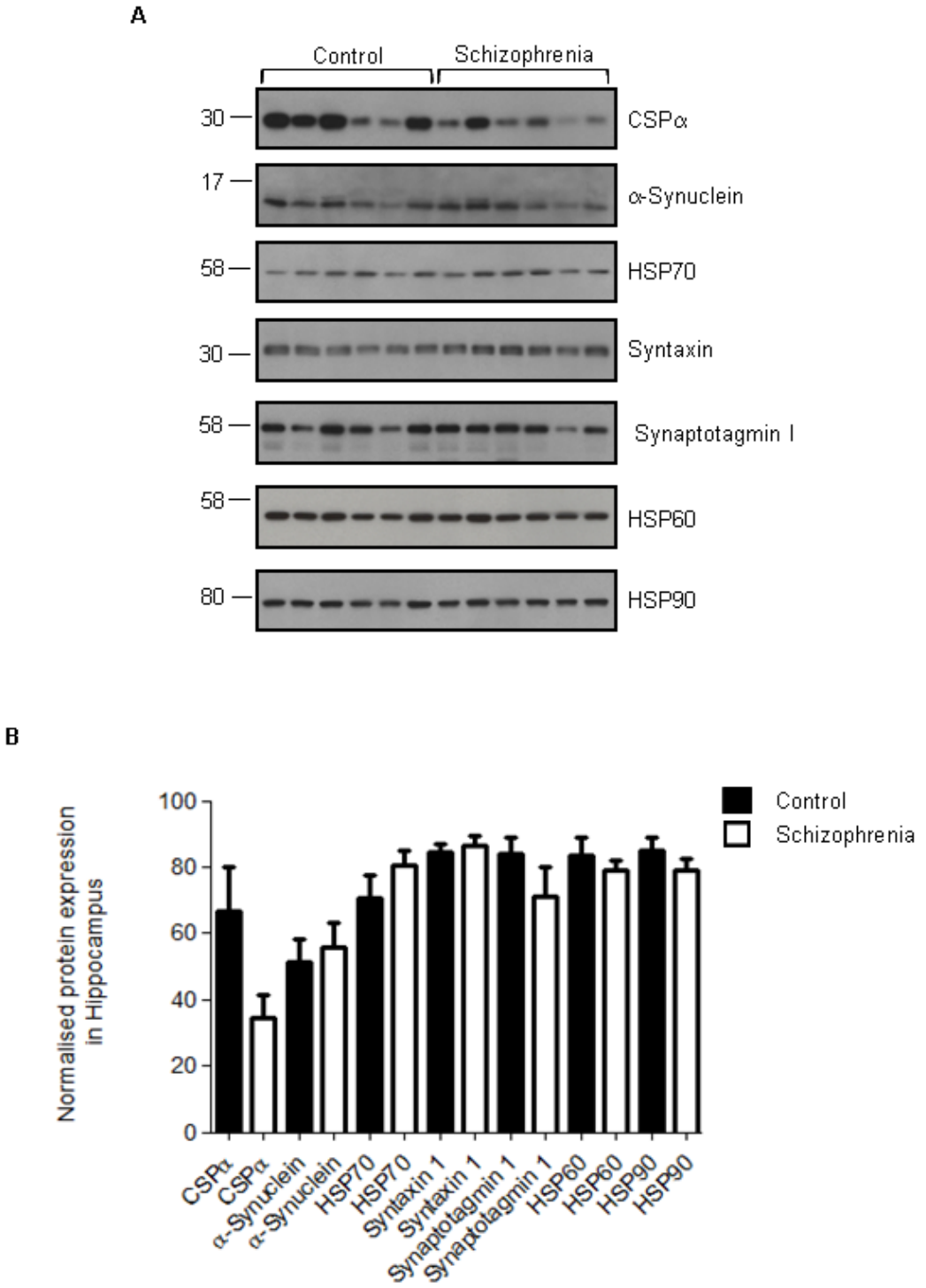

Figure 4.7: Protein expression in Hippocampus in Schizophrenia disorder. Human brain samples were lysed, samples resolved by SDS-PAGE and transferred to nitrocellulose membranes, which were then probed with specific CSPα, α-Synuclein, HSP70, HSP60, HSP90, Synaptotagmin 1 and Syntaxin 1 antibodies. *A*. Shows representative immunoblots. Position of molecular weight standards are shown on the left of panels. *B*. Relative protein expression levels were quantified as described in section 4.2.2. Error bars show the standard error of the mean (n=3). Multiple Student's t-tests revealed no significant difference in the expression of any protein in schizophrenia compared to control patients.

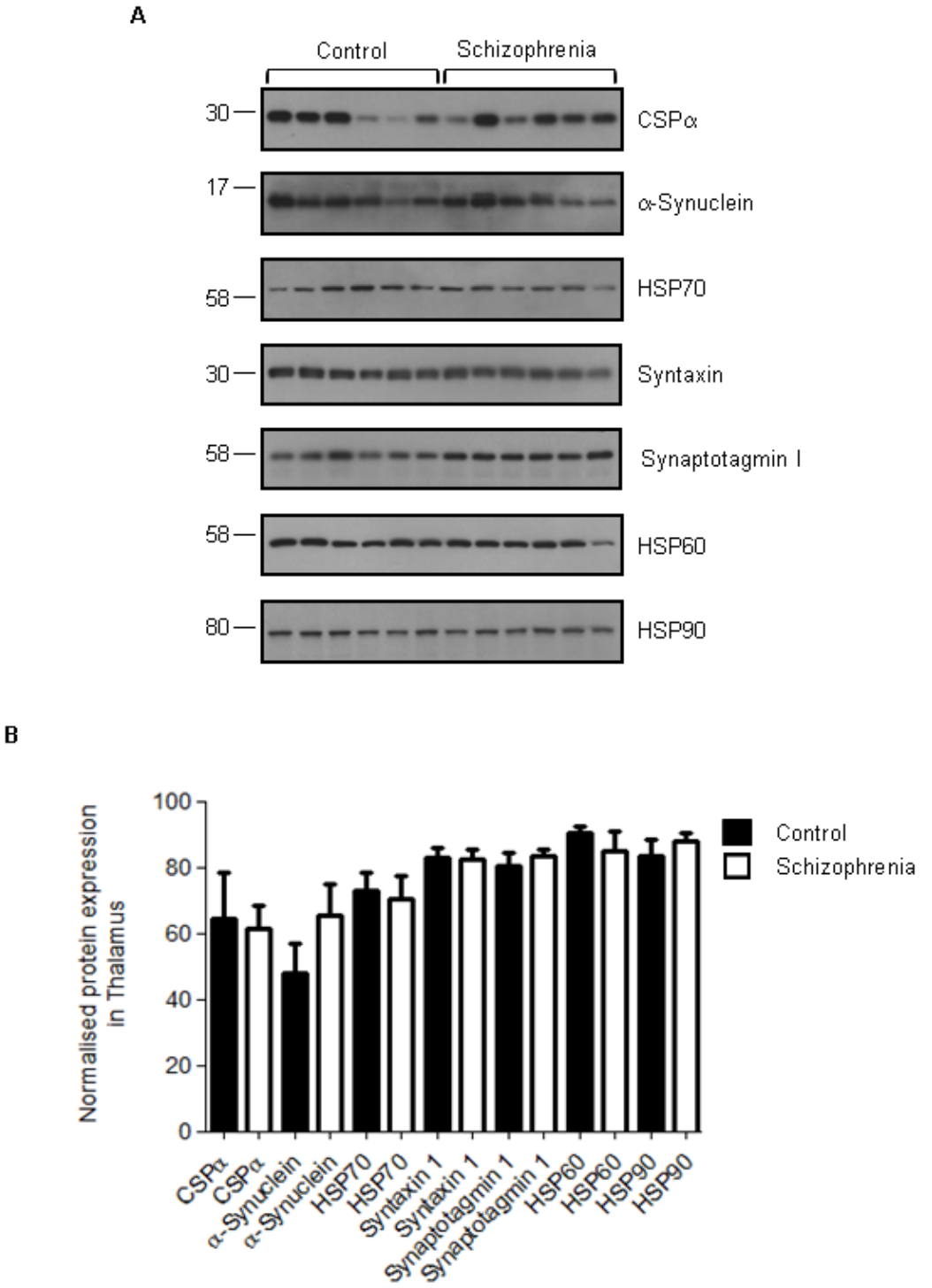

Figure 4.8: Protein expression in Thalamus in Schizophrenia disorder. Human brain samples were lysed, samples resolved by SDS-PAGE and transferred to nitrocellulose membranes, which were then probed with specific CSPα, α-Synuclein, HSP70, HSP60, HSP90, Synaptotagmin 1 and Syntaxin 1 antibodies. *A*. Shows representative immunoblots. Position of molecular weight standards are shown on the left of panels. *B*. Relative protein expression levels were quantified as described in section 4.2.2. Error bars show the standard error of the mean (n=3). Multiple Student's t-tests revealed no significant difference in the expression of any protein in schizophrenia compared to control patients.

Although CSPα mean expression was decreased by ~50% in hippocampus in schizophrenia, this was not found to be significant different (Figure 4.7).

4.2.4 Significant changes in HSP70 and syntaxin expression in bipolar disorder

Analysis of protein expression levels in brain regions of patients with bipolar disorder revealed no significant changes in cerebellum (Figure 4.9) or thalamus (Figure 4.12). However, HSP70 levels were significantly increased in cortex (Figure 4.10, ~2 fold increase; scatter plot shown in Figure 4.10*C*) and hippocampus (Figure 4.11, ~1.8 fold increase; scatter plot shown in Figure 4.11*C*). Interestingly, as with major depression, syntaxin expression was decreased in cortex in bipolar patients (Figure 4.10, ~1.6 fold decrease; scatter plot shown in Figure 4.10*D*).

4.3 Discussion

In this Chapter, the expression levels of CSPα and interacting partners in post-mortem brain samples were examined. Whilst CSPα expression levels were markedly reduced in some brain regions from mental disorder patients (e.g. cortex/depression, hippocampus/schizophrenia and cerebellum/bipolar), these changes did not reach statistical significance. As the sample sizes used (6 patients/condition) were relatively small it would therefore be interesting in future studies to investigate whether CSPα expression is significantly different using larger populations. Interestingly though, significant changes in the expression levels of HSP70 and syntaxin, interacting partners of CSPα (Chamberlain and Burgoyne, 1997a; Chamberlain *et al.*, 2001), were detected in specific disorders and brain regions. HSP70 expression was significantly increased in both the hippocampus ($p<0.005$) and cortex ($p<0.05$) of samples from patients with bipolar disorder. Syntaxin 1 was also perturbed in cortex samples from bipolar patients, showing a significant decrease in expression. Furthermore the levels of this protein were also significantly decreased in samples from patients who had been diagnosed with major depression

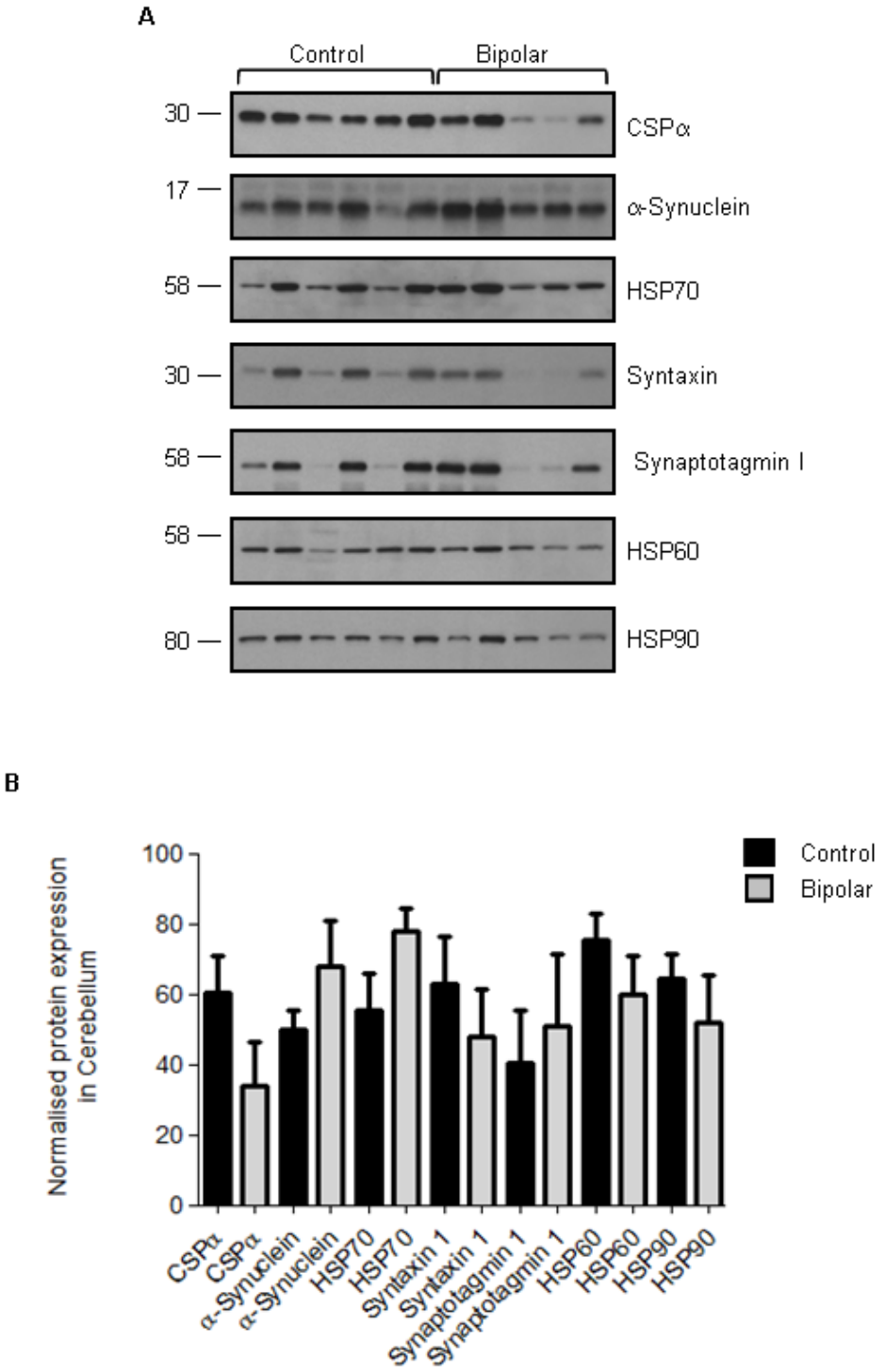

Figure 4.9: Protein expression in Cerebellum in Bipolar disorder. Human brain samples were lysed, samples resolved by SDS-PAGE and transferred to nitrocellulose membranes, which were then probed with specific CSPα, α-Synuclein, HSP70, HSP60, HSP90, Synaptotagmin 1 and Syntaxin 1 antibodies. *A*. Shows representative immunoblots. Position of molecular weight standards are shown on the left of panels. *B*. Relative protein expression levels were quantified as described in section 4.2.2. Error bars show the standard error of the mean (n=3). Multiple Student's t-tests revealed no significant difference in the expression of any protein in bipolar compared to control patients.

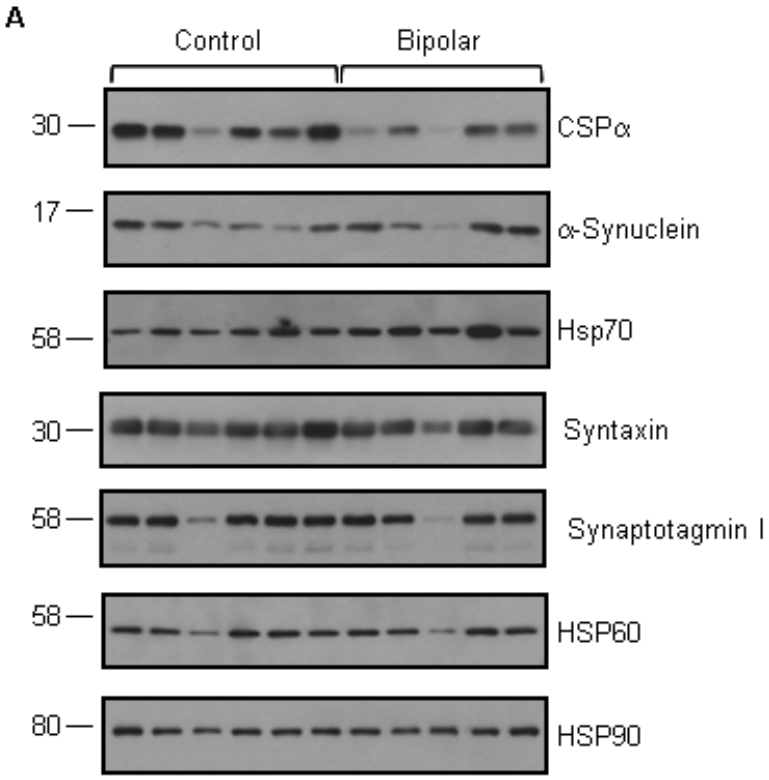
A
Control
Bipolar
30
CSPα
17
α-Synuclein
58
Hsp70
30
Syntaxin
58
Synaptotagmin I
58
HSP60
80
HSP90

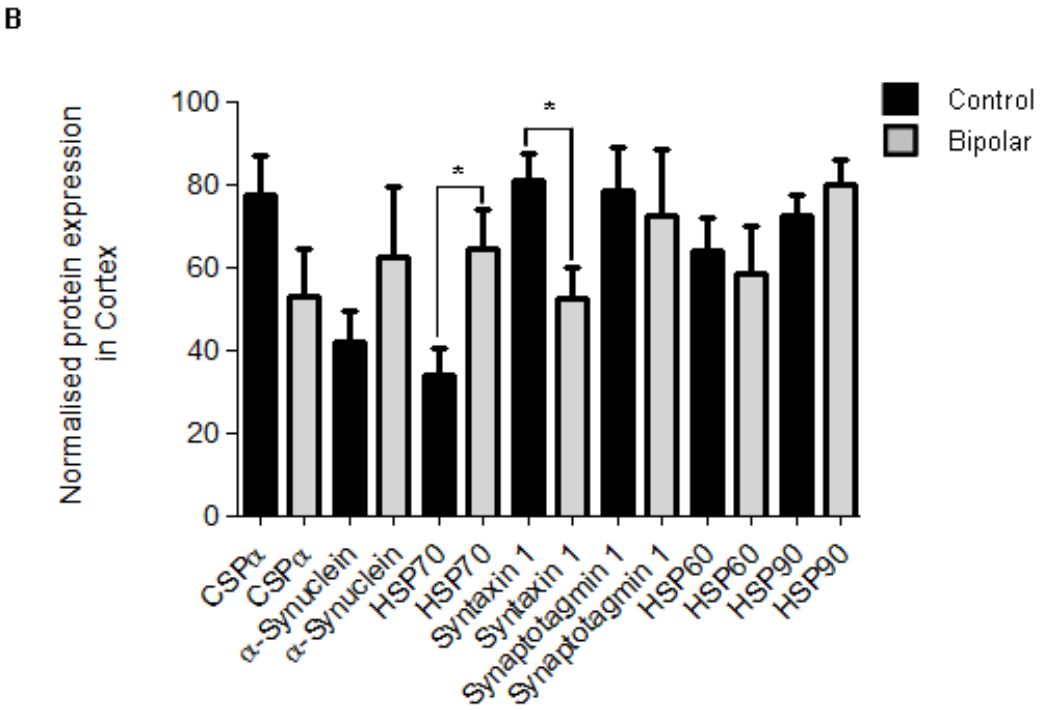
B
Normalised protein expression in Cortex
Control
Bipolar
100
80
60
40
20
0
*
*
CSPα
CSPα
α-Synuclein
α-Synuclein
HSP70
HSP70
Syntaxin 1
Syntaxin 1
Synaptotagmin 1
Synaptotagmin 1
HSP60
HSP60
HSP90
HSP90

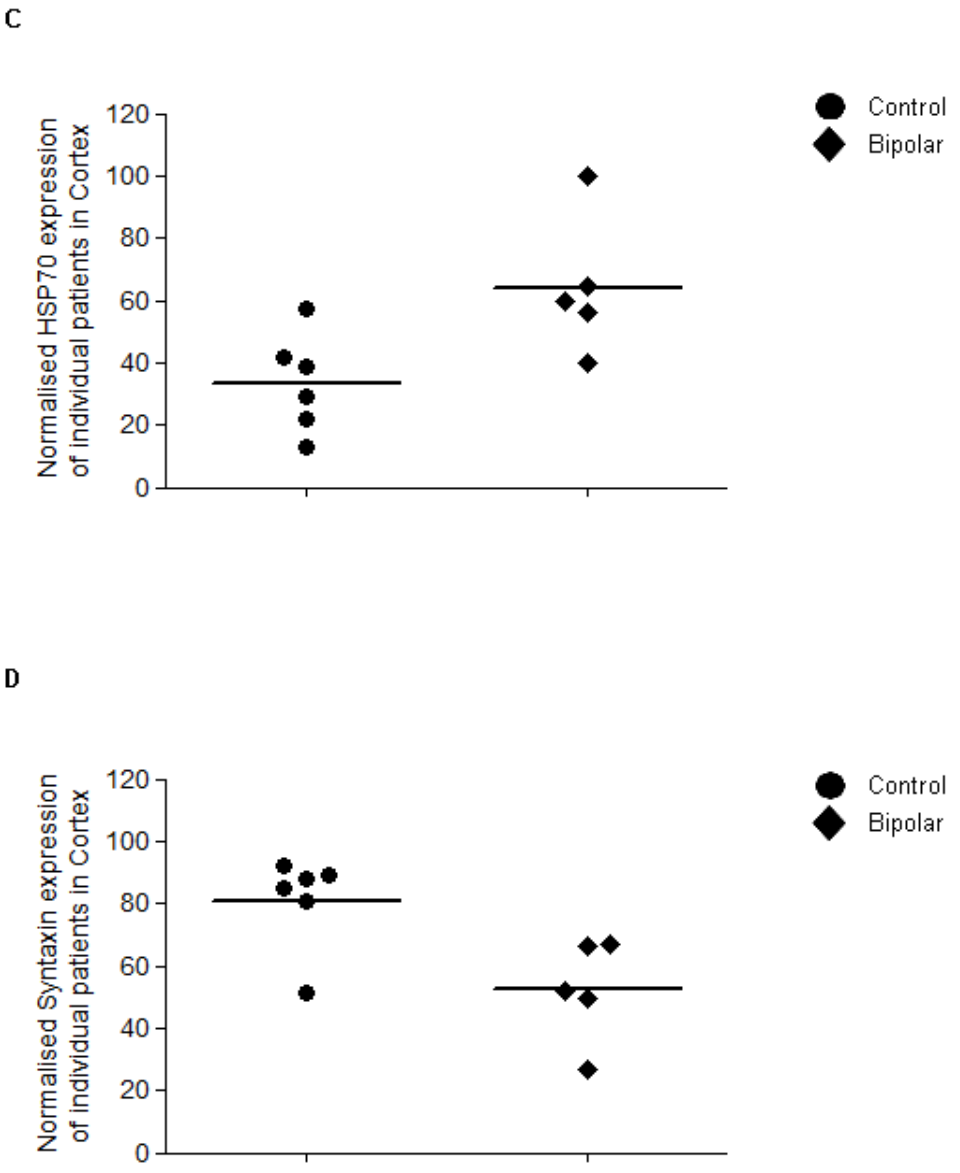

Figure 4.10: Protein expression in Cortex in Bipolar disorder. Human brain samples were lysed, samples resolved by SDS-PAGE and transferred to nitrocellulose membranes, which were then probed with specific CSPα, α-Synuclein, HSP70, HSP60, HSP90, Synaptotagmin 1 and Syntaxin 1 antibodies. *A*. Shows representative immunoblots. Position of molecular weight standards are shown on the left of panels. *B*. Relative protein expression levels were quantified as described in section 4.2.2. Error bars show the standard error of the mean (n=3). * indicates a significant decrease ($p<0.05$) in syntaxin and significant increase in HSP70 expression in bipolar disorder, which was compared to control samples using a Student's t-test. *C-D*. The scatter plots show the normalised HSP70 (*C*) and Syntaxin 1 (*D*) expression levels in cortex of individual bipolar disorder patients.

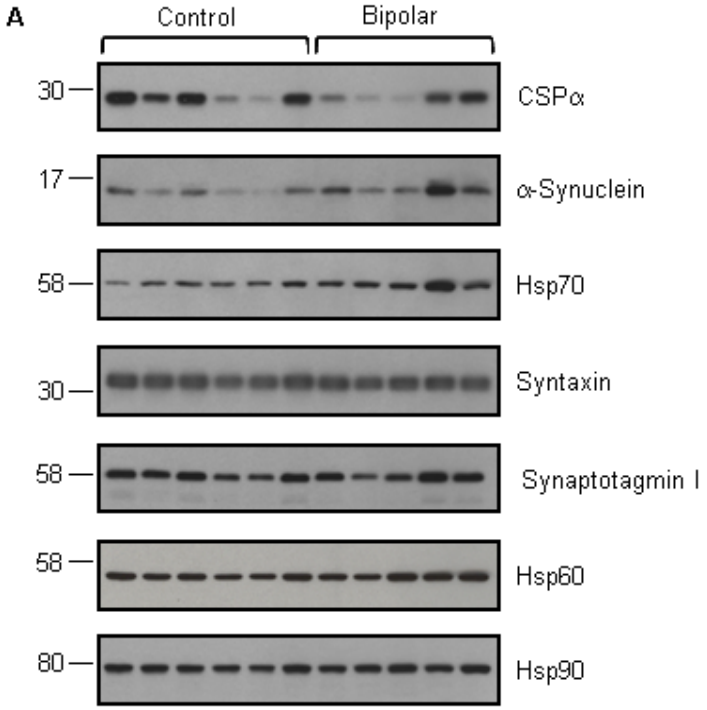
A
Control
Bipolar
30
CSPα
17
α-Synuclein
58
Hsp70
30
Syntaxin
58
Synaptotagmin I
58
Hsp60
80
Hsp90

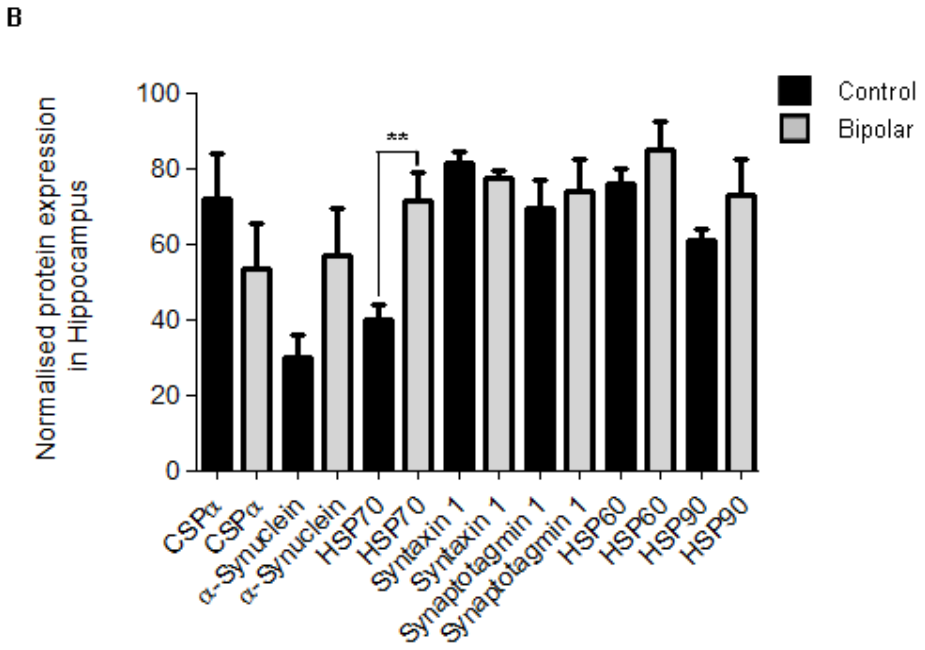
B
Normalised protein expression in Hippocampus
Control
Bipolar
100
80
60
40
20
0
**
CSPα
CSPα
α-Synuclein
α-Synuclein
HSP70
HSP70
Syntaxin 1
Syntaxin 1
Synaptotagmin 1
Synaptotagmin 1
HSP60
HSP60
HSP90
HSP90

C

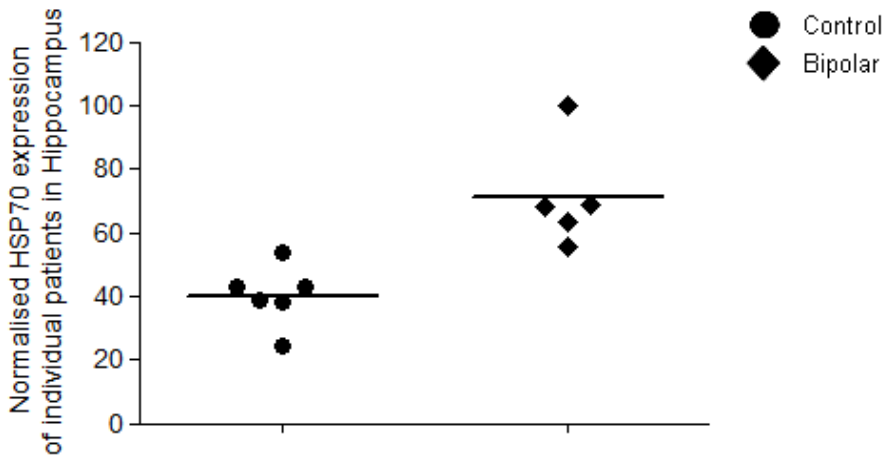

Figure 4.11: Protein expression in Hippocampus in Bipolar disorder. Human brain samples were lysed, samples resolved by SDS-PAGE and transferred to nitrocellulose membranes, which were then probed with specific CSPα, α-Synuclein, HSP70, HSP60, HSP90, Synaptotagmin 1 and Syntaxin 1 antibodies. *A*. Shows representative immunoblots. Position of molecular weight standards are shown on the left of panels. *B*. Relative protein expression levels were quantified as described in section 4.2.2. Error bars show the standard error of the mean (n=3). ** indicates a significant increase ($p<0.005$) in HSP70 expression in bipolar disorder, which was compared to control samples using a Student's t-test. *C*. The scatter plot shows the normalised HSP70 expression levels in hippocampus of individual bipolar disorder patients.

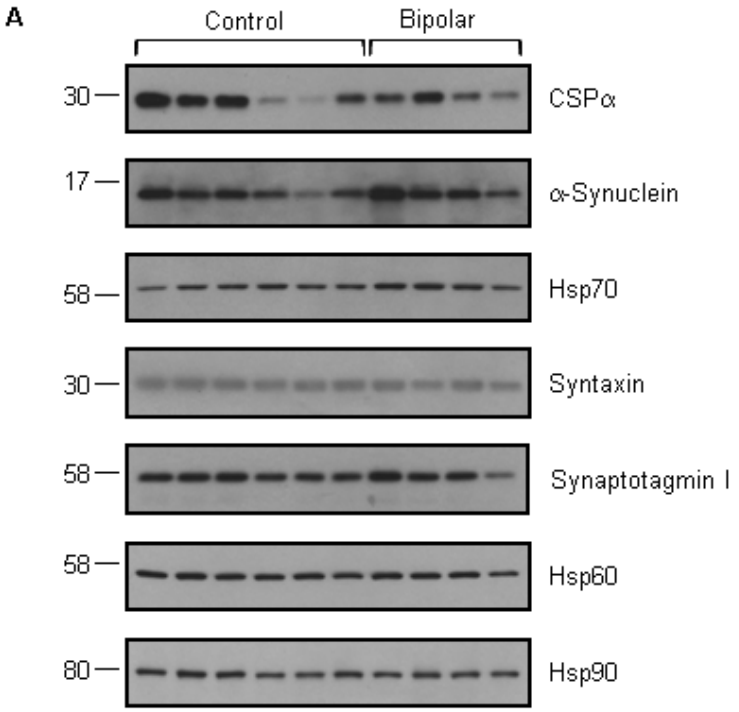
A
Control
Bipolar
30
CSPα
17
α-Synuclein
58
Hsp70
30
Syntaxin
58
Synaptotagmin I
58
Hsp60
80
Hsp90

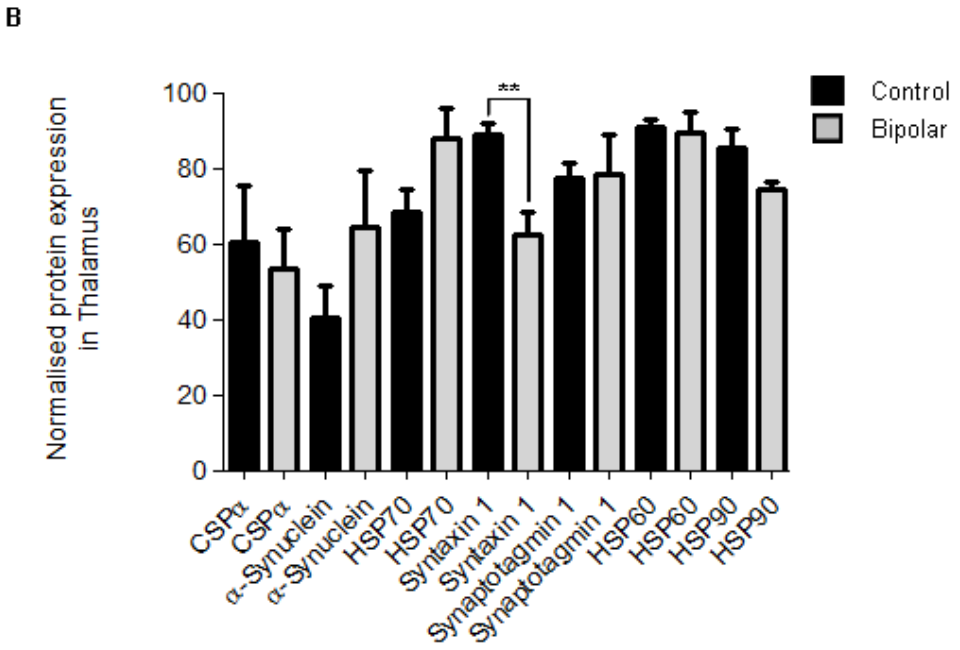
B
Normalised protein expression in Thalamus
100
80
60
40
20
0
**
Control
Bipolar
CSPα
CSPα
α-Synuclein
α-Synuclein
HSP70
HSP70
Syntaxin 1
Syntaxin 1
Synaptotagmin 1
Synaptotagmin 1
HSP60
HSP60
HSP90
HSP90

C

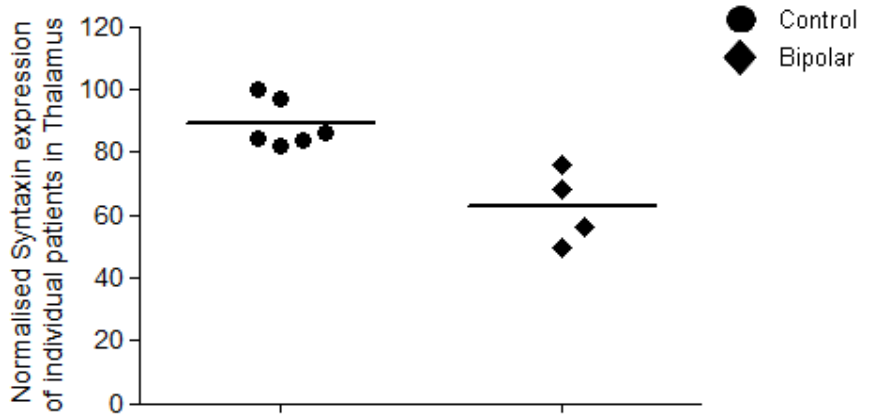

Figure 4.12: Protein expression in Cortex in Bipolar disorder. Human brain samples were lysed, samples resolved by SDS-PAGE and transferred to nitrocellulose membranes, which were then probed with specific CSPα, α-Synuclein, HSP70, HSP60, HSP90, Synaptotagmin 1 and Syntaxin 1 antibodies. *A*. Shows representative immunoblots. Position of molecular weight standards are shown on the left of panels. *B*. Relative protein expression levels were quantified as described in section 4.2.2. Error bars show the standard error of the mean (n=3). * indicates a significant decrease ($p<0.005$) in syntaxin expression in bipolar disorder which was compared to control samples using a Student's t-test. *C*. The scatter plot shows the normalised Syntaxin 1 expression levels in thalamus of the individual bipolar disorder patients.

Importantly, the cortex and hippocampus are the brain regions that are typically affected in depression and bipolar disorder (Nikolaus *et al.*, 2009; Brennaman and Maness, 2010) and are areas responsible for behaviour. Thus, the specific changes seen in HSP70 and syntaxin in these brain regions are of particular interest.

Why are syntaxin and HSP70 levels altered in these disorders? There are several possibilities to explain these observations: (i) expression is affected by genetic mutations; (ii) the proteins are up- or down-regulated as an adaptive response; or (iii) medication taken by the patients has affected the expression of these proteins. HSP70 is a chaperone, which has a multitude of cellular functions, many of which are achieved by interacting with co-chaperones, such as CSPα. HSP70 supports the folding of newly synthesised proteins, subcellular transport of proteins and vesicles, and degradation of unwanted proteins (Bercovich *et al.*, 1997; Frydman, 2001; Schaffitzel *et al.*, 2001; Pratt and Toft, 2003). HSP70 is also up-regulated in response to stress and binds to its protein substrates and stabilises them against aggregation or denaturation. Indeed, HSP70 levels are frequently elevated in multiple forms of cancer (Mosser and Morimoto, 2004) and neurodegenerative diseases, in which protein misfolding can occur as a result of oxidative stress (Kirkegaard *et al.*, 2010). In fact, receantly it has been reported that mitochondrial dysfunction is observed in psychiatric disorders, such as schizophrenia, major depressive and bipolar disorder (Rezin *et al.*, 2009). Mitochondrial dysfunction accounts for either apoptosis or generation of reactive oxygen species (ROS), which leads to oxidative stress and contributes to the pathophysiology of mood disorders (Ozcan *et al.*, 2004; Sarandol *et al.*, 2007). The increased expression of HSP70 specifically in bipolar disorder might therefore point to a difference in cellular stress in this condition compared with major depression and schizophrenia. One interesting aspect of HSP70 is that it forms multiprotein complexes with its co-chaperones (Wall *et al.*, 1994), which are responsible for its activities (Suh *et al.*, 1998; Mayer and Bukau, 2005; Swain *et al.*, 2007). Future work should reveal if its co-chaperones are also affected in mood disorders, such as other J-domain proteins, nucleotide exchange factors (NEFs) and/or tetratricopeptide repeat (TPR)-containing proteins, or heat shock chaperones in general. Due to the fact that oxidative stress contributes to mood disorders it would also be interesting to look at any changes in other stress-related proteins.

Finally, it is particularly important to note that recent work reported that HSP70 levels were raised in patients, who have taken antidepressants (Guest *et al.*, 2004). Unfortunately, here we were not able to obtain any information on patient medication intake.

Bipolar disorder, also known as manic-depressive disorder, is linked to depression, due to the fact that depression is implied after an episode of euphoria (Kruger and Prager, 2007). Therefore it is particularly interesting that syntaxin 1 expression was significantly reduced in cortex in both depression and bipolar disorder (35% and 30% respectively, Figure 4.2 and Figure 4.10). In addition to its essential function in exocytosis, syntaxin has also been shown to interact with serotonin transporters (Haase *et al.*, 2001), which play a critical role in the maintenance of normal serotonin levels and release. Indeed, serotonin secretion has been shown to be abnormal in bipolar disease and major depression. Previous work on post-mortem samples of patients with schizophrenia has shown quantitative abnormalities of syntaxin in cortex (Gabriel *et al.*, 1997; Honer *et al.*, 1997; Honer *et al.*, 2002). In contrast, our results showed no significant change in syntaxin levels in schizophrenic disorder, which nevertheless agree with a more recent publication (Castillo *et al.*, 2010).

It was previously observed that caseine kinase 2 (CK2) levels were decreased in patients with Alzheimer disease and schizophrenia (Aksenova *et al.*, 1991). CK2 has been shown to phosphorylate syntaxin 1 on Ser14 (Hirling and Scheller, 1996; Foletti *et al.*, 2000), and phosphorylation at this site regulates interactions with SNAP25 and Munc18 (Foletti *et al.*, 2000; Castillo *et al.*, 2010). Furthermore it has been reported that regulation of syntaxin 1 by CK2-mediated phosphorylation might play a role in the pathophysiology of schizophrenia, as altered phosphorylation of syntaxin 1 was detected in post-mortem brain samples of patients with schizophrenia disorder (Castillo *et al.*, 2010). Therefore in future studies it would be interesting to look at the phosphorylation status of syntaxin in depression and bipolar disorder.

Mental disorders have been linked to abnormalities in neurotransmitter release and over recent years it has been hypothesised that SNARE proteins, which serve a fundamental molecular mechanism to support neurotransmission (Sollner *et al.*, 1993a; Sollner *et al.*, 1993b) and might be responsible for abnormal neuronal

connectivity, play a role in mental disorders (Jorgensen and Riederer, 1985; Johnston-Wilson *et al.*, 2000; Eastwood and Harrison, 2001). Several publications have suggested that SNAP25 expression is altered in schizophrenia, with levels either decreased (hippocampus) or increased (cortex) (Gabriel *et al.*, 1997; Thompson *et al.*, 1998; Young *et al.*, 1998; Mukaetova-Ladinska *et al.*, 2002; Halim *et al.*, 2003; Thompson *et al.*, 2003a; Thompson *et al.*, 2003b). Meta-Analysis of genome–wide linkage for schizophrenia showed significant linkage to the chromosomal region 20p12.3-11, which also contains SNAP25. Recently two genetic mouse models (hDISC transgenic mice and I67T missense in blind-drunk mutant mouse) have supported the involvement of SNAP25 in schizophrenia (Jeans *et al.*, 2007; Pletnikov *et al.*, 2008).

The data generated in this chapter showed general inconsistency in protein expression levels. All experiments were performed at least three times and six control and disorder patients were compared each time; however, this data is not sufficient to make robust conclusions about any protein and its effect in mental disorders. The only protein profiling that can be done to date is to study pathological processes in human brain in post-mortem brain tissues. This approach however, depends on high-quality representative selection of tissue samples to control for differences related to individuals, post-mortem handling of the tissue, effects of chronic medication, etc. The significant longer post mortem interval in bipolar patients compared to control patients has to be taken in account here. It might be that over time protein levels change due to post-mortem effects rather than disease pathology. Another aspect of our observed non-significant alterations in protein expression levels was probably due to the small number of patients that were analysed. Many examinations of post-mortem patients have been done with a much greater sample size, e.g. between 240 and 280 patients (Pae *et al.*, 2009). Future work potentially has to be done on animal models to fully understand the impact of CSPα and its interacting partners HSP70 and synatxin, as well as changes in individual SNARE proteins and alterations in complex formation. Genetic mouse models, which were linked to schizophrenia, have been used so far (Jeans *et al.*, 2007; Pletnikov *et al.*, 2008), as well as bipolar and major depression models (Jope and Roh, 2006; Zarate *et al.*, 2006). However, to date generating animal models with

mental illnesses is problematic and results are not necessarily reliable. Mental illnesses seem to be uniquely human and cannot be convincingly modelled in animals (Nestler and Hyman, 2010).

CHAPTER FIVE:

EXPRESSION AND LOCALISATION OF THE CYSTEINE STRING PROTEIN ISOFORMS CSPβ AND CSPγ

5.1 Introduction

CSPα has been implicated to be involved in regulated exocytosis, as CSP null *Drosophila* exhibited embryonic lethality, and larvae displayed a defect in evoked presynaptic exocytosis (Umbach *et al.*, 1994; Zinsmaier *et al.*, 1994). Furthermore, CSPα has also been implicated in regulated exocytosis in mammalian cells based on work employing over-expression strategies (Brown *et al.*, 1998; Chamberlain and Burgoyne, 1998; Zhang *et al.*, 1998; Graham and Burgoyne, 2000). Recent work reported that CSPα inactivation reduced the life span of transgenic mice, with no CSPα$^{-/-}$ mice surviving beyond 3 months of age, and caused neurodegeneration of neuromuscular junctions and synapses, suggesting that CSPα has an important neuroprotective function (Fernandez-Chacon *et al.*, 2004). However, no defect in synaptic vesicle exocytosis was evident in Calyx of Held synapses from P9-P11 mice, suggesting that CSPα function is not essential for this membrane fusion pathway.

Two novel CSP isoforms, CSPβ and CSPγ, were recently shown to be expressed in mammals (Evans *et al.*, 2003; Fernandez-Chacon *et al.*, 2004). Expression of these isoforms in mouse brain might explain the lack of an effect on synaptic transmission in CSPα knock out mice, since they might compensate the loss of CSPα. Northern blotting and quantitative real-time PCR however, revealed that CSPβ and CSPγ were only expressed in testis (Evans *et al.*, 2003; Fernandez-Chacon *et al.*, 2004).

Recently a CSPβ antibody was generated against a C-terminal peptide from CSPβ; this antibody specifically identified the β isoform of CSP when recombinant proteins were analysed. Interestingly, this antibody did not detect a protein band corresponding to the size of CSPβ (~ 25 kDa), but it did consistently detect a 100 kDa protein band in both testis and brain (Gundersen *et al.*, 2010). More detailed analysis detected this putative CSPβ band in synaptosomes and synaptic vesicle fractions. This band was proposed to represent an oligomeric from of CSPβ, and a protein band appeared on SDS-PAGE gels, which was the approximate size of monomeric CSPβ, following boiling of cell lysates in a urea-containing buffer. The authors claimed therefore that expression of CSPβ in mouse brain could explain the

lack of an effect on synaptic vesicle exocytosis in CSPα$^{-/-}$ mice. Indeed, overexpression of CSPβ in frog oocytes led to a block of cortical granule exocytosis, and CSPβ was also shown to interact with the HSC70/SGT-complex (Boal *et al.*, 2007; Gundersen *et al.*, 2010), suggesting that CSPβ might regulate exocytosis via the same protein-protein interactions as CSPα.

Fractionations of pancreatic β cells over-expressing CSPβ showed that this isoform is membrane-associated, which is only disrupted by Triton X-100; however [^{3}H]-palmitic acid labelling experiments demonstrated that CSPβ was largely un-palmitoylated, and in immunofluorescence studies CSPβ colocalised with markers (Vti1b) of the trans-Golgi network (Boal *et al.*, 2007).

Thus, if CSPβ is actually expressed in brain, it is unclear whether this protein could compensate for a loss of CSPα expression given the reported different localisations and palmitoylation stati of these two CSP isoforms. Another important issue is whether the relatively modest effect of CSPα knock down on regulated exocytosis in PC12 cells (Chapter 3) is confounded by expression of CSPβ or CSPγ in this cell type.

The aim of this Chapter is to cast light on the possible functional roles of CSPβ and CSPγ by performing a careful characterisation of their expression profiles.

5.2 Result

5.2.1 Characterisation of CSP isoform-specific antibodies

At the time when this work was initiated, there were no published studies that had examined expression of CSPβ and CSPγ at the protein level. To generate a CSPβ antibody rabbits were immunised with the peptide sequences highlighted in the boxed region of Figure 5.1A. The resultant serum was affinity purified individually against each peptide.

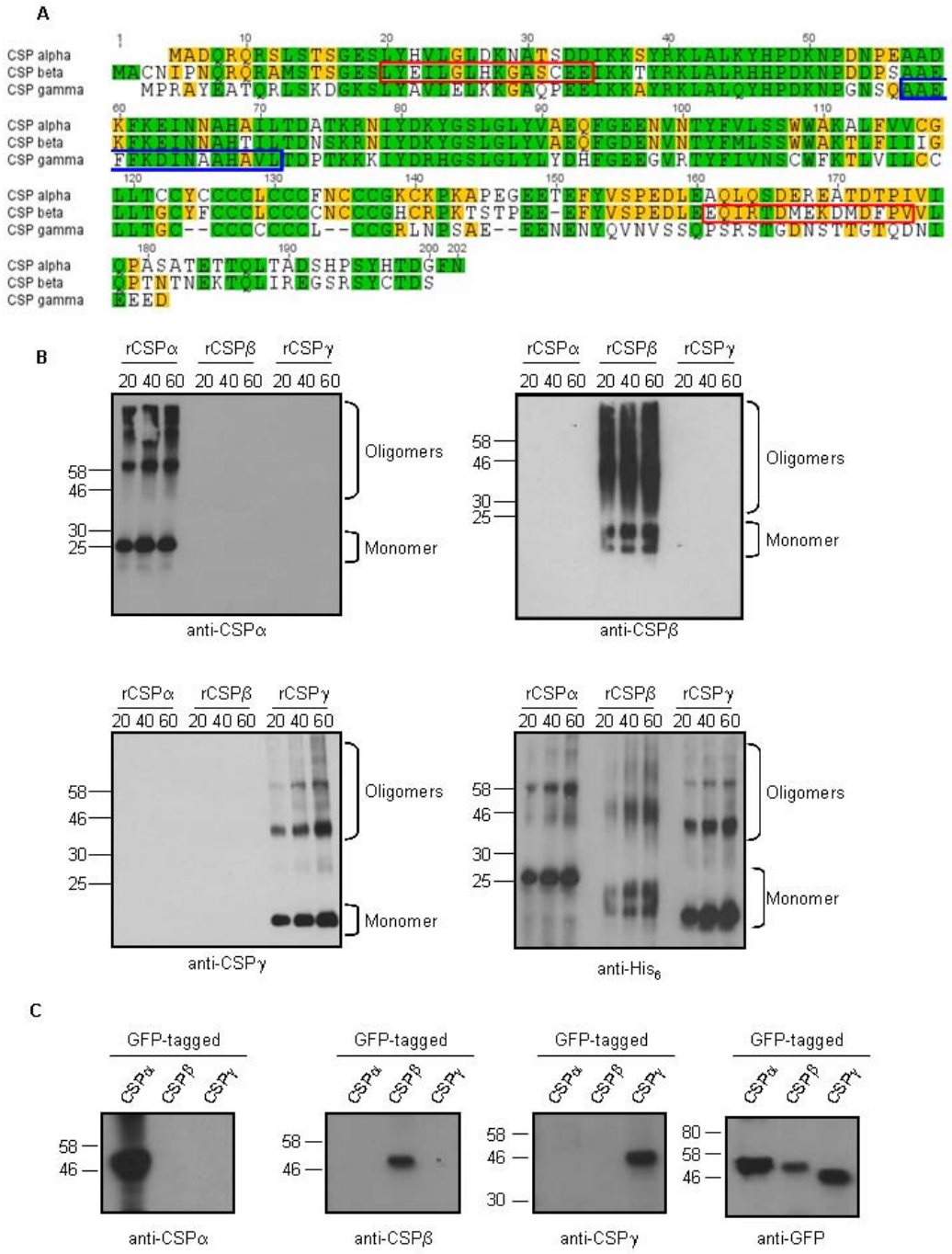

Figure 5.1: Analysis of CSP isoform-specific antibodies. *A*. Alignment of the sequences of rat CSPα, -β and –γ. Conserved amino acids present in all 3 isoforms are coloured green, conserved residues present within 2 isoforms are coloured yellow. The peptides used to generate a CSPβ antibody are outlined with red (CSPβ) and blue (CSPγ) boxes. *B*. Aliquots of His_6-tagged recombinant CSP (rCSP) proteins (20, 40 and 60 ng) were resolved by SDS-PAGE and probed with antibodies against CSPα, CSPβ, CSPγ, and the hexahistidine tags. Positions of CSP monomers and oligomers are indicated. *C*. HEK293T cells grown in 24-well plates were transfected with 1 µg of GFP-tagged CSPs and probed with antibodies against the CSP isoforms or against GFP. The GFP-CSPα fusion protein migrates between the 46 and 58 kDa markers as previously reported (Greaves and Chamberlain, 2006). Positions of molecular mass standards are shown on the left side of all figure panels.

The EQIRTDMEKDMDFPV peptide affinity purified antibody specifically recognised bacterially produced His_6-tagged CSPβ and was not reactive against either His_6-CSPα or His_6-CSPγ (Figure 5.1*B*). In addition, an antiserum was generated against full-length His_6-CSPγ, and this serum was specific for this CSP isoform. The commercial CSPα antibody used in this study was also highly specific for the alpha isoform (Figure 5.1*B*). An anti-His_6 tag antibody was used to demonstrate similar gel-loadings of the His_6-tagged CSP isoforms. The additional higher molecular weight bands that were detected by all antibodies used to probe bacterially expressed proteins (Figure 5.1*B*) represent dimers and higher molecular mass oligomers of CSPs (Swayne *et al.*, 2003; Boal *et al.*, 2004).

The antibody specificity that was observed against bacterially expressed proteins was also reproduced when the antibodies were used to probe lysates of HEK293T cells that had been transfected with EGFP-tagged CSP proteins (Figure 5.1*C*). Here, the GFP antibody was used to confirm broadly similar loadings.

The CSPγ antibody recognised multiple bands when used to probe tissue lysates with no clear indication of which (if any) band was CSPγ. Therefore, this antibody was not used further for tissue expression analysis.

To examine the tissue distribution of the CSPβ protein, lysates were prepared from a panel of rat tissues, resolved on SDS gels and probed with CSPα and CSPβ antibodies. Figure 5.2*A* shows that CSPα is enriched in brain but is also expressed at varying levels in other non-neuronal tissues. In contrast, immunoreactivity against CSPβ was only detected in testis and was absent from brain (Figure 5.2*A*). CSPβ in testis migrated as two bands on SDS gels, one which was the same size as recombinant CSPβ (arrow) and another more prominent higher-molecular mass band (arrowhead). Note that a 100 kDa band similar to that reported by the Gundersen group (2010) was not recognised by this antibody. SNAP23 is ubiquitously expressed, and an antibody against this protein confirmed equal protein loading (Figure 5.2*A*). An antibody against the neuron-specific SNARE protein syntaxin 1A was used to confirm the integrity of brain lysate (Figure 5.2*A*).

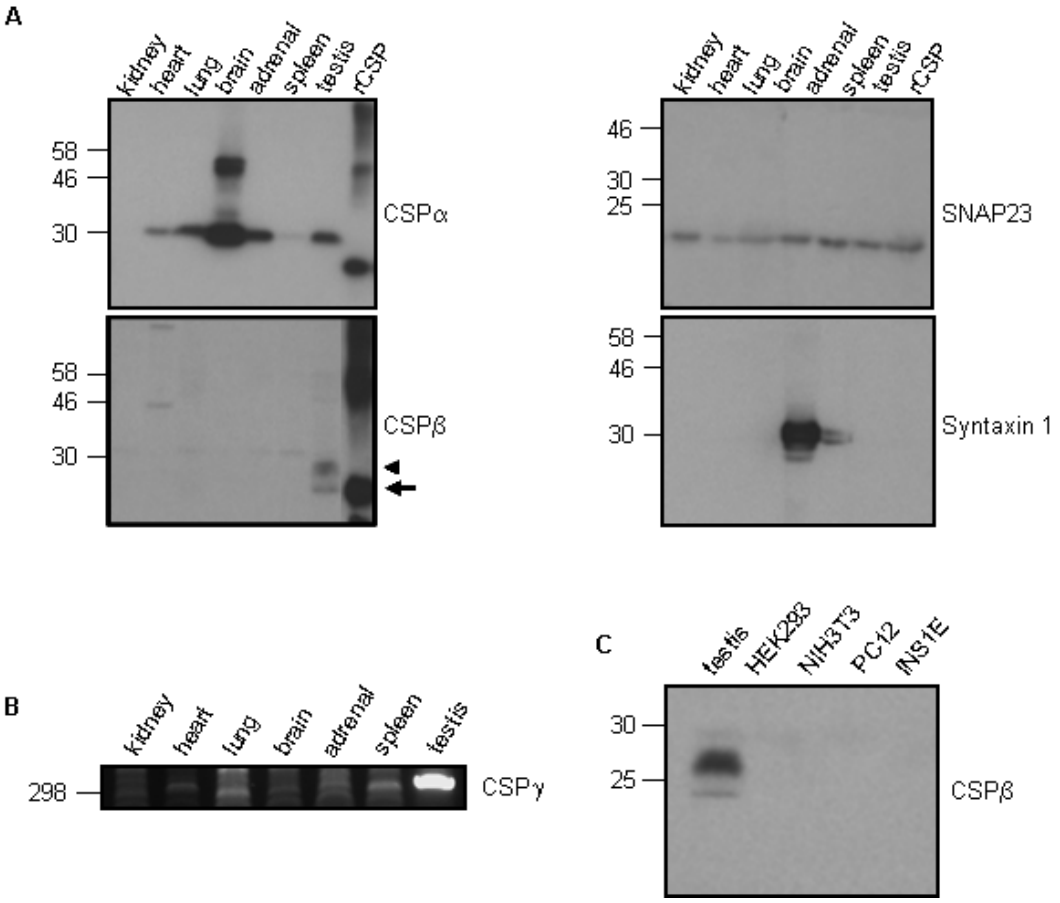

Figure 5.2: Tissue distribution of CSP isoforms. *A*. Rat tissue lysates (10 µg) were resolved by SDS-PAGE and probed with the indicated antibodies; 20 ng of recombinant His_6-CSPα or His_6-CSPβ (rCSP) were used as positive controls. *B*. RNA purified from rat tissues was reverse transcribed to cDNA, and a PCR reaction was run with the appropriate CSPγ oligonucleotide primers (see table 2.3). Position of DNA size standard (in bp) is shown on the left side. *C*. Lysates (10 ng) were prepared from the indicated cell lines, resolved by SDS-PAGE beside a testis lysate, and probed using a CSPβ antibody. Positions of molecular mass standards are shown on left side of panels *A* and *C*.

To examine the tissue distribution of CSPγ, RNA purification, reverse transcription (RT) PCR and standard PCR was used to amplify CSPγ. Figure 5.2*B* shows that CSPγ mRNA was heavily enriched in testis. It was further examined if CSPβ is detectable in common cell lines, such as HEK293, NIH3T3, PC12 and INS1E cells, but no immunoreactivity was detected against CSPβ (Figure 5.2*C*). It is possible that CSPβ is expressed at low levels in specific brain regions (Schmitz *et al.*, 2006) and that a signal might be detected following enrichment of these brain areas. Thus, a panel of samples containing different brain regions isolated from Sprague Dawley rats was obtained from Zyagen (San Diego, California, U.S.A). These samples were resolved by SDS-PAGE and probed with CSPα and CSPβ antibodies, and compared to the signal generated from an aliquot of the appropriate His_6-tagged recombinant CSP isoform. Figure 5.3*A* shows that CSPα was expressed throughout the brain, with enrichment in the hippocampus and the cerebrum. In contrast, no signal was detected with the CSPβ antibody. To confirm the integrity of these commercial samples, a selection of brain areas were isolated from in-house bred Sprague Dawley rats, resolved on SDS-PAGE and probed with CSPα. This analysis showed the pattern of CSPα expression was broadly similar to the commercial samples, for example, with CSPα expression lower in cerebellum than either hippocampus or cerebrum (Figure 5.3*B*). SNAP23 was used to confirm equal protein loading (Figure 5.3*B*).

5.2.2 Membrane-association and palmitoylation of CSPβ

In the following experiments, membrane association and palmitoylation of endogenous CSPβ were examined. In Figure 5.2*A* it was apparent that endogenous CSPβ migrated as two distinct bands. Figure 5.4*A* shows that the upper band detected by the CSPβ antibody (arrowhead in Figure 5.2*A*) co-fractionates with a purified membrane fraction whereas the lower band (arrow in Figure 5.2*A*) is cytosolic.

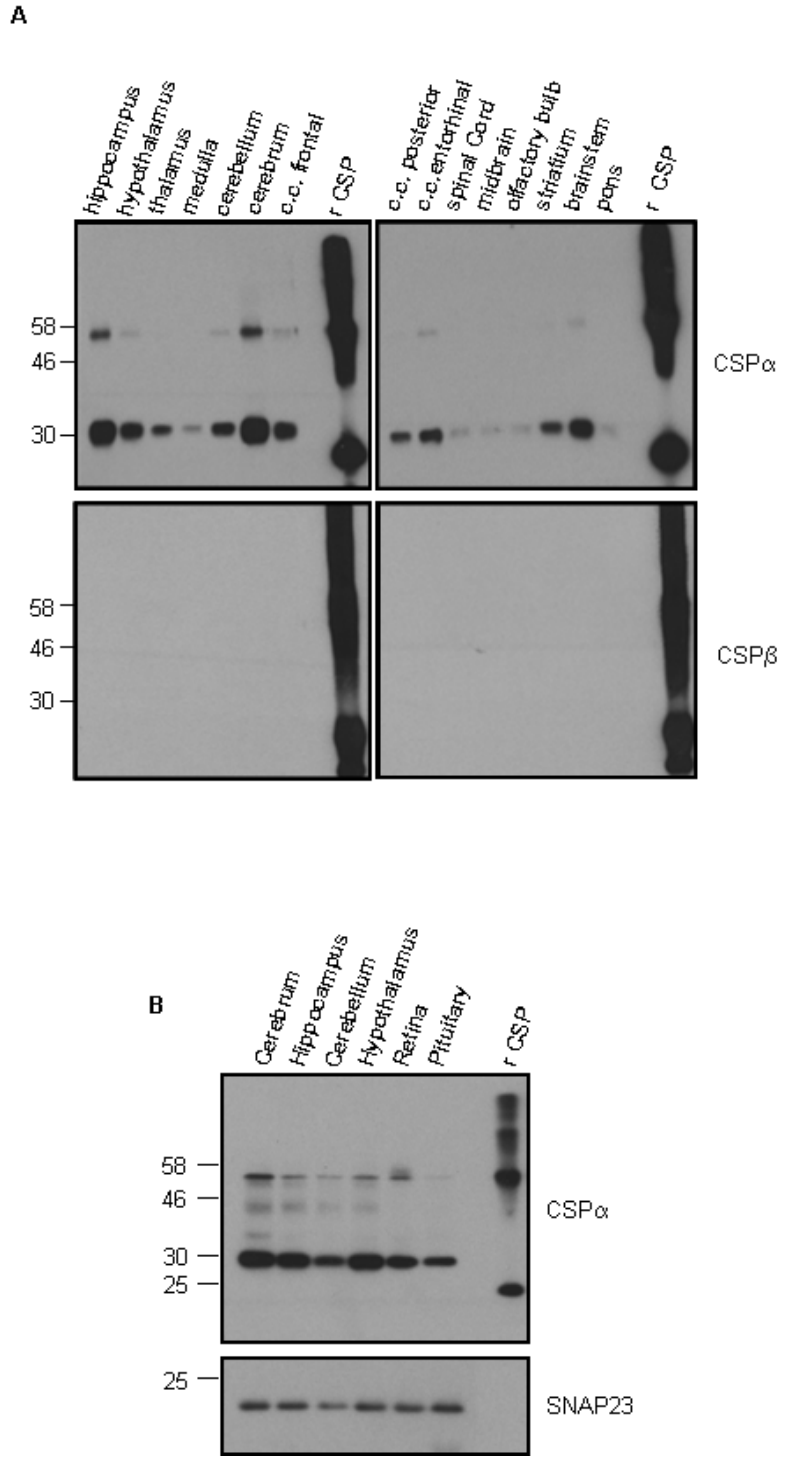

Figure 5.3: CSP expression in brain regions. *A*. Lysates from the various brain regions shown (10 µg), which were obtained from Zyagen Inc., were resolved by SDS-PAGE beside a 20 ng aliquot of His_6-tagged CSPα or CSPβ (rCSP), and were probed with antibodies against CSPα or CSPβ. c.c. denotes the cerebral cortex. *B*. As *A*, except samples were isolated from in-house bred rats. The blots were probed with antibodies against CSPα and SNAP23. Positions of molecular mass markers are shown on the left side of the blots.

Probing these same samples with antibodies recognising GAPDH and HSP70, proteins that have large cytosolic pools, confirmed the efficiency of the fractionation procedure (Figure 5.4*A*). Given that CSPα is extensively palmitoylated, an obvious possibility to explain the increased apparent molecular mass of membrane-associated CSPβ is that this isoform is also highly palmitoylated. To test this possibility, membranes were isolated from testis and incubated overnight in either 1 M hydroxylamine (pH7) to cleave thioester linkages between fatty acids and cysteines, or 1 M Tris (pH7) as a control (Gundersen *et al.*, 1994). Figure 5.4*B* reveals that hydroxylamine treatment decreased the apparent molecular mass of CSPα, as expected and previously reported (Gundersen *et al.*, 1994). Similarly, hydroxylamine caused a marked downward shift in the migration of CSPβ, suggesting that this isoform is also highly palmitoylated. In contrast, no effect on migration of GAPDH was observed confirming that hydroxylamine is not promoting a shift in migration of all proteins (Figure 5.4*B*). Thus, Figure 5.4*A* and 5.4*B* strongly suggest that endogenous CSPβ is predominantly membrane-associated in testis and that this membrane-bound protein is palmitoylated.

A higher-molecular mass band was detected by the CSPβ antibody (above 30 kDa marker) in all tissues (Figure 5.2*A*). Since CSPβ is palmitoylated (Figure 5.4*B*), it was possible that this band represented a differentially palmitoylated form of CSPβ. If this is true, then this band would be predicted to be membrane associated. However, fractionation of spleen revealed that this band was entirely cytosolic, suggesting that this band is not a palmitoylated form of CSPβ and most likely represents a cross-reacting protein.

The observation that endogenous CSPβ is palmitoylated in testis in inconsistent with a previous report suggesting that HA-tagged CSPβ is largely un-palmitoylated when expressed in HIT-T15 pancreatic beta cells (Boal *et al.*, 2007). To determine the extent to which CSPβ is palmitoylated when over-expressed, transfected PC12 cells were fractionated into cytosol and membrane fractions. Figure 5.5*A* shows that the majority of GFP-CSPα was membrane associated and also showed a marked upwards band shift in the membrane fraction, indicating palmitoylation (Figure 5.5*A*,

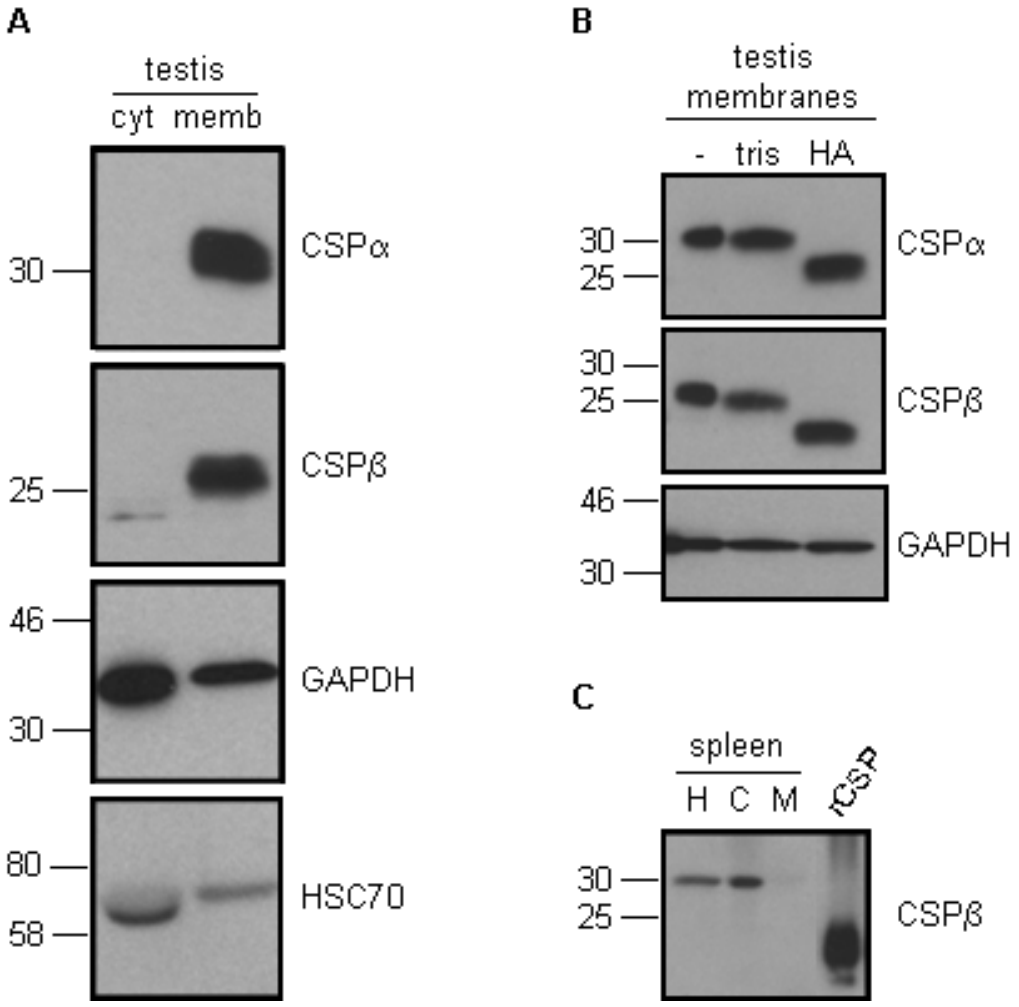

Figure 5.4: Membrane binding and palmitoylation of CSPα. *A*. Rat testis was fractionated into cytosol (cyt) and membrane (memb) fractions which were resolved by SDS-PAGE and probed with the indicated antibodies. *B*. Membranes isolated from testis were untreated (-), or treated with Tris or hydroxylamine (HA), and the samples were probed with the antibodies shown. *C*. Rat spleen was fractionated into cytosol (C) and membrane (M) fractions and resolved by SDS-PAGE beside a spleen homogenate (H) fraction and 20 ng of recombinant His_6-CSPβ (rCSP), and probed with a CSPβ antibody. The positions of molecular mass standards are shown on the left side of each panel.

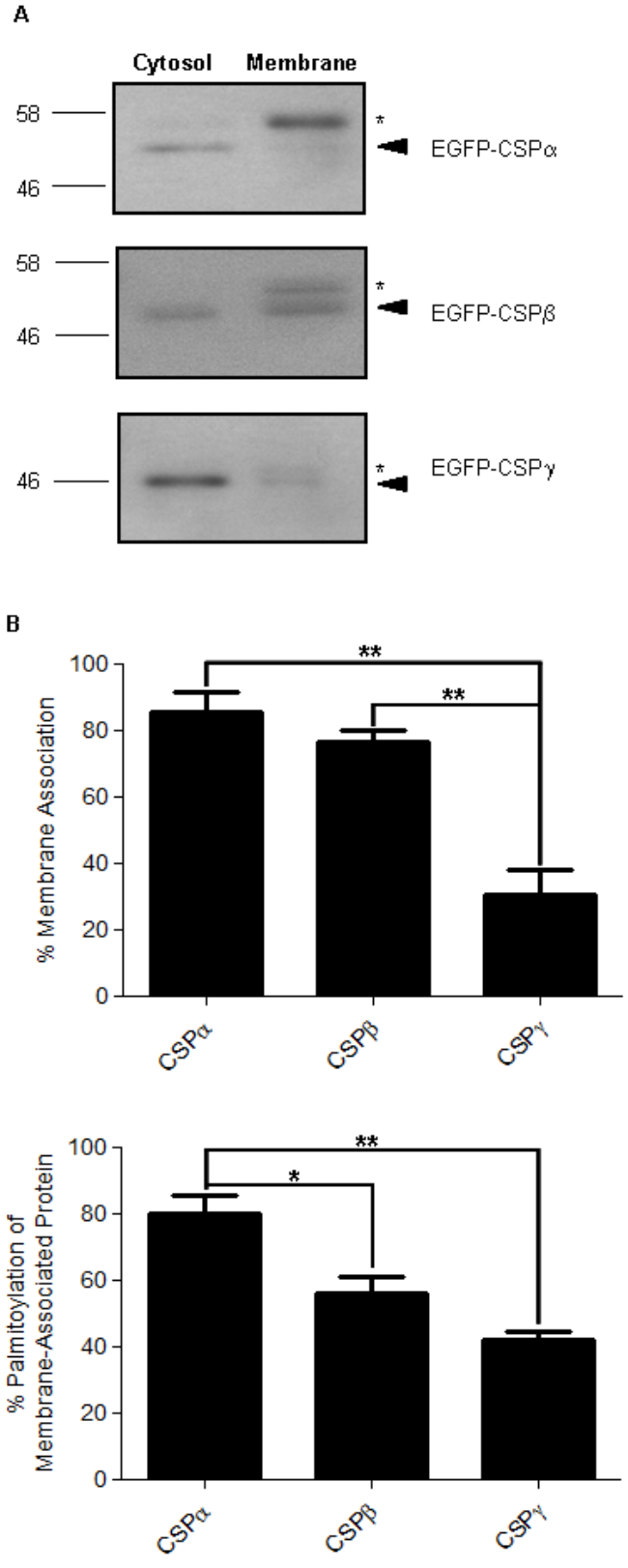

Figure 5.5: Palmitoylation and membrane binding of GFP-tagged CSP isoforms.

Figure 5.5: Palmitoylation and membrane binding of GFP-tagged CSP isoforms. *A*. EGFP-tagged CSPα, CSPβ and CSPγ (1 µg) were transiently transfected into PC12 cells growing on 24-well plates, followed by fractionation into cytosol and membrane fractions, which were resolved by SDS-PAGE. The distribution of the proteins between cytosol and membrane fractions was analysed by immunodetection with a GFP antibody. The arrowheads indicate unpalmitoylated CSP and the asterisks highlight palmitoylated CSP. Positions of molecular mass standards are shown at the left side of all blots. *B*. Quantified data (n=3) for the percent membrane-association (upper panel) and the percent palmitoylation of the membrane-associated protein (lower panel). Membrane binding of CSPα versus CSPγ, and CSPβ versus CSPγ were significantly different (**$p < 0.005$ each). Palmitoylation was also significantly different for CSPα versus CSPβ (*$p < 0.05$), and CSPα versus CSPγ (**$p < 0.005$) as determined by one-way ANOVA.

upper panel, asterisk). However, GFP-CSPβ was found equally in cytosol and membrane fractions, and in membranes was present as both a palmitoylated and an un-palmitoylated form (Figure 5.5*A*, middle panel, arrowhead and asterisk). In contrast, GFP-CSPγ was largely cytosolic and only a small amount was detected in the membrane fraction (Figure 5.5*A*, lower panel), with an indication of palmitoylation (Figure 5.5*A*, low panel, asterisk). Quantitative analysis illustrated that GFP-CSPα and GFP-CSPβ were approximately 80 % membrane associated, whereas only ~ 30 % of GFP-CSPγ was membrane-bound (Figure 5.5*B*, upper panel). Furthermore, GFP-CSPα in the membrane fraction was mainly palmitoylated (~ 80 %); CSPβ however, only displayed ~ 60 % and GFP-CSPγ only ~ 40 % palmitoylation of the membrane-bound pool. Thus, although the expression levels of endogenously expressed CSPβ in testis allow efficient membrane association and palmitoylation, it is clear that tagged forms of CSPβ and CSPγ are less efficiently palmitoylated than CSPα, when the proteins are over-expressed.

As palmitoylation is central to the function of CSPα (Ohyama *et al.*, 2007), chimeric constructs were created in an effort to understand the basis of the different efficiencies of CSPα and CSPβ palmitoylation in PC12 cells. Work from Lang and co-workers has shown that the different configurations of cysteines in the cysteine-string domain of CSPα and CSPβ are not responsible for the observed differences in palmitoylation (Boal *et al.*, 2007). Thus chimeric constructs were generated by interchanging the N-terminal domain of CSPα and CSPβ (CSPα-βNterm and CSPβ-αNterm, Figure5.6*A*). These chimeric constructs were individually transfected into PC12 cells, which were then fractionated into cytosol and membrane fractions. The representative blots (Figure 5.6*B*) and quantified data from several experiments (Figure 5.6*C*) showed that the CSPα-βNterm chimera was significantly decreased in its membrane-association and palmitoylation similar to wild type CSPβ. CSPβ-αNterm however, displayed an increased level of membrane binding and palmitoylation as observed for wild-type CSPα. Thus, the different N-terminal domains of CSPα and CSPβ are important in determining palmitoylation efficiency.

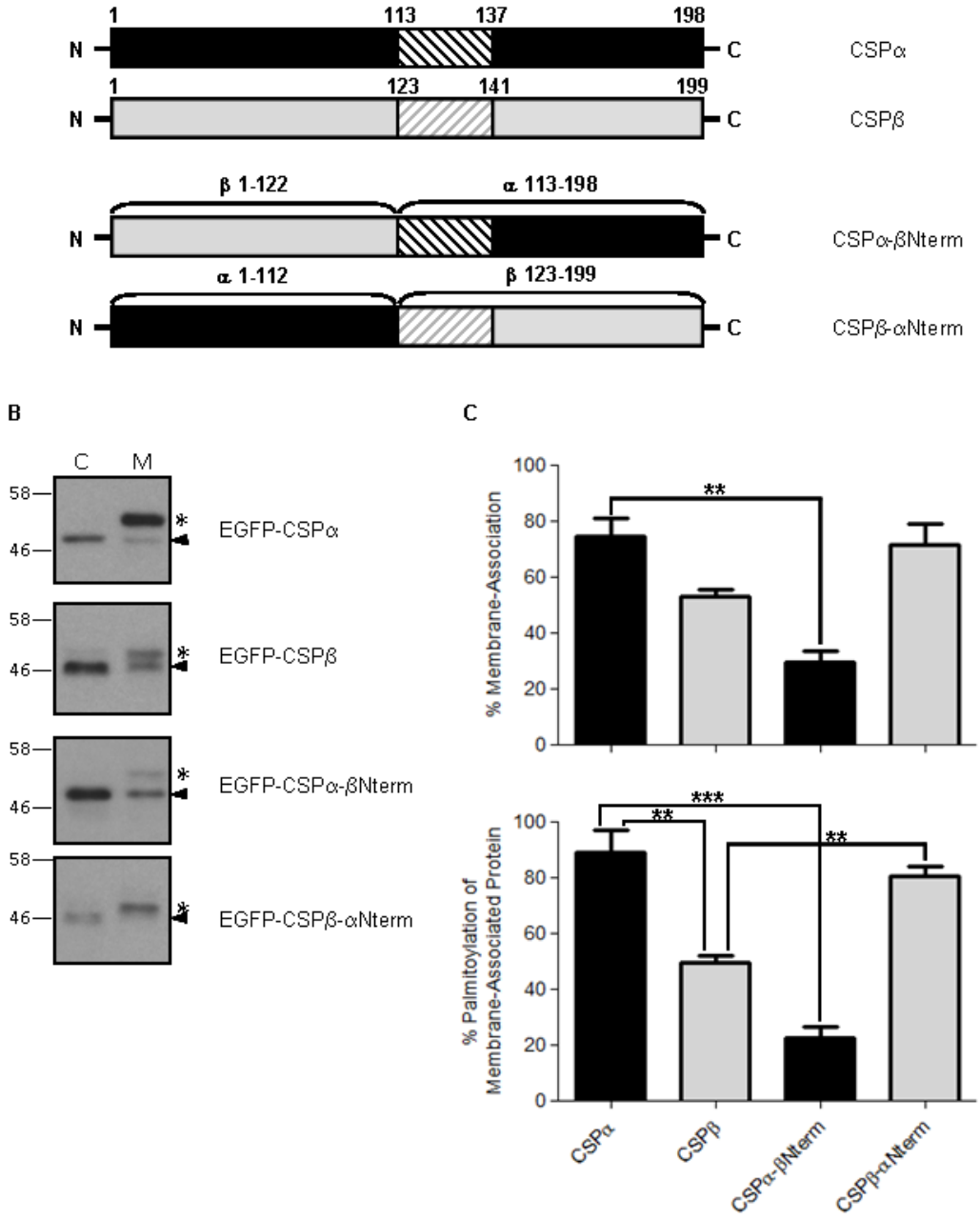

Figure 5.6: Membrane binding and palmitoylation of GFP-tagged CSPα and CSPβ chimeric constructs. *A*. Domain structure of CSPs and representation of the chimeric constructs which were synthesised. The numbers indicate amino acid positions. *B*. CSP constructs were transfected into PC12 cells, which were then fractionated into cytosol (C) and membrane (M) fractions. The distribution of the proteins between cytosol and membrane fractions was determined by immunoblotting with a GFP antibody. The arrowheads denote unpalmitoylated CSP and the asterisks palmitoylated CSP. Positions of molecular mass standards are shown at the left side of all blots. *C*. Quantified data (n=3) for the percent membrane association (upper panel) and the percent palmitoylation of the membrane-associated fraction (lower panel). Membrane binding for CSPα and CSPα-βNterm was significantly different (**p < 0.005). Palmitoylation was also significantly different for CSPα and CSPβ (**p < 0.005), CSPα and CSPα-βNterm (***p < 0.0005), CSPβ and CSPβ-αNterm (**p < 0.005), and CSPβ and CSPα-βNterm (*p < 0.05) as determined by one-way ANOVA.

5.2.3 Localisation of CSPβ and CSPγ in germ cells

To observe whether the three CSP isoforms were equally expressed in testis during development, testis samples from various ages of rat (ranging from post-natal day 8 to 174) were analysed based on protein and mRNA expression. Figure 5.7*A* demonstrates that CSPα is expressed in testis throughout development. Surprisingly though, protein expression of CSPβ was not detected in p22 samples, but was present in p38 samples. SNAP23 detection confirmed equal protein loading. To confirm this developmental switch in CSPβ expression and also to examine CSPγ expression, the mRNA expression profile of all three mammalian CSP isoforms in rat testis was examined by reverse transcriptase PCR (RT-PCR). This analysis confirmed that CSPα is expressed throughout development and that CSPβ expression is detected at p38 but not p22. Interestingly, CSPγ also displayed a development switch in expression, being detected in samples from p22 but not p12 rats. Sexual maturation (puberty) in rats begins between p25 and p33 (Ojeda, 1994a; Hagenauer *et al.*, 2011), and in males this is when spermatogenesis first occurs. As a first step to define the cell types that express CSP proteins in testis, expression was examined in rat sperm samples. Isolation of sperm and testis from two adult male rats and subsequent immunoblotting analysis revealed that CSPα is expressed in mature sperm (Figure 5.8). CSPβ however, could only be detected in the testis fraction.

Testes are comprised of three major cell types, germ (which mature into sperm), Sertoli and Leydig cells. As CSPβ was not detected in mature sperm, it was examined if CSPβ is expressed in rat Leydig (R2C), rat Sertoli (15P-1) or mouse Sertoli (MSC-1) cell lines. These cells where thus fractionated into cytosol and membrane fractions, which were analysed by immunoblotting with CSPα and CSPβ antibodies. Figure 5.9*A* revealed that CSPα was present in the membrane fractions of all cell lines that were analysed. In contrast, CSPβ showed no signal in either Leydig or Sertoli cells; the testis sample was used as a positive control for the immunoblotting procedure. Since no germ cell lines are available and also because cell lines may not express exactly the same proteins as primary cells,

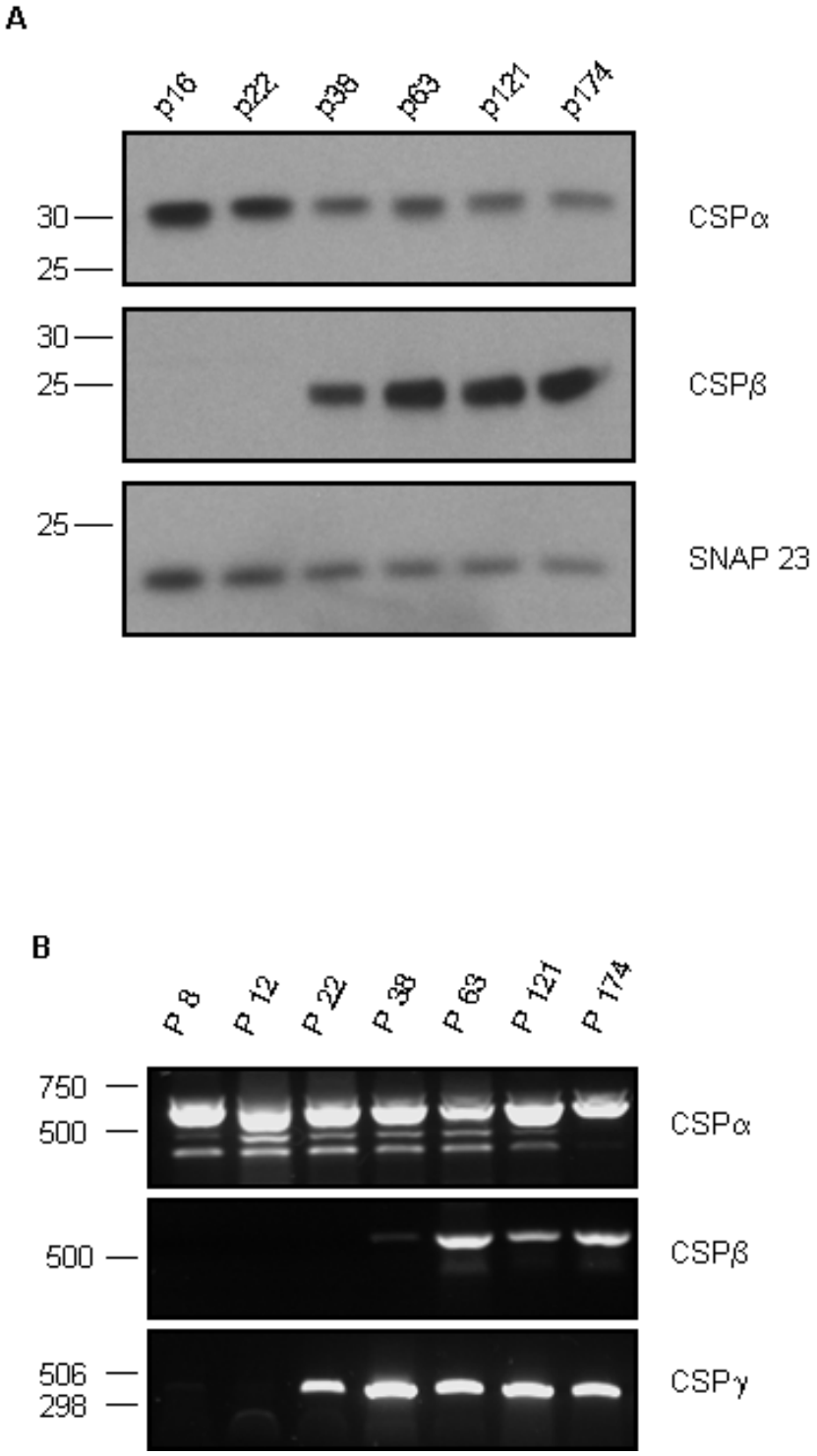

Figure 5.7: Expression of CSP isoforms during testicular maturation. Rat testes were removed at the highlighted post-natal (p) age (in days). *A*. Testes were lysed, resolved by SDS-PAGE and probed with antibodies against CSPα, CSPβ and SNAP23. The position of molecular weight standards (in kDa) are shown on the left side of the blots *B*. RNA was purified from the testes, reverse transcribed to cDNA and a PCR reaction was run with the appropriate CSPα, CSPβ or CSPγ oligonucleotide primers (see table 2.3). Position of DNA size standards (in bp) are shown on the left side.

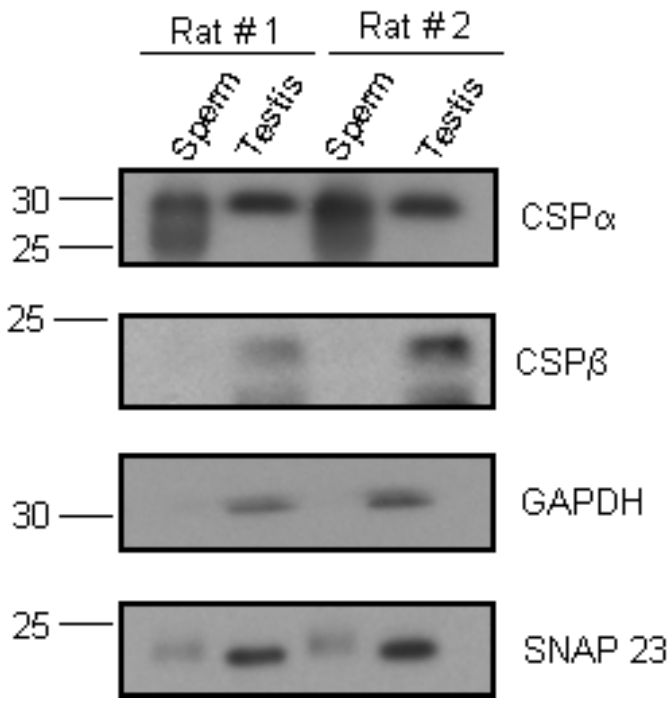

Figure 5.8: Expression of CSP isoforms in sperm. Whole testis and sperm from two adult rats (~ 3 months of age) were isolated, lysed, resolved by SDS-PAGE and probed with the indicated antibodies. Positions of molecular mass standards are shown on the left side of all blots.

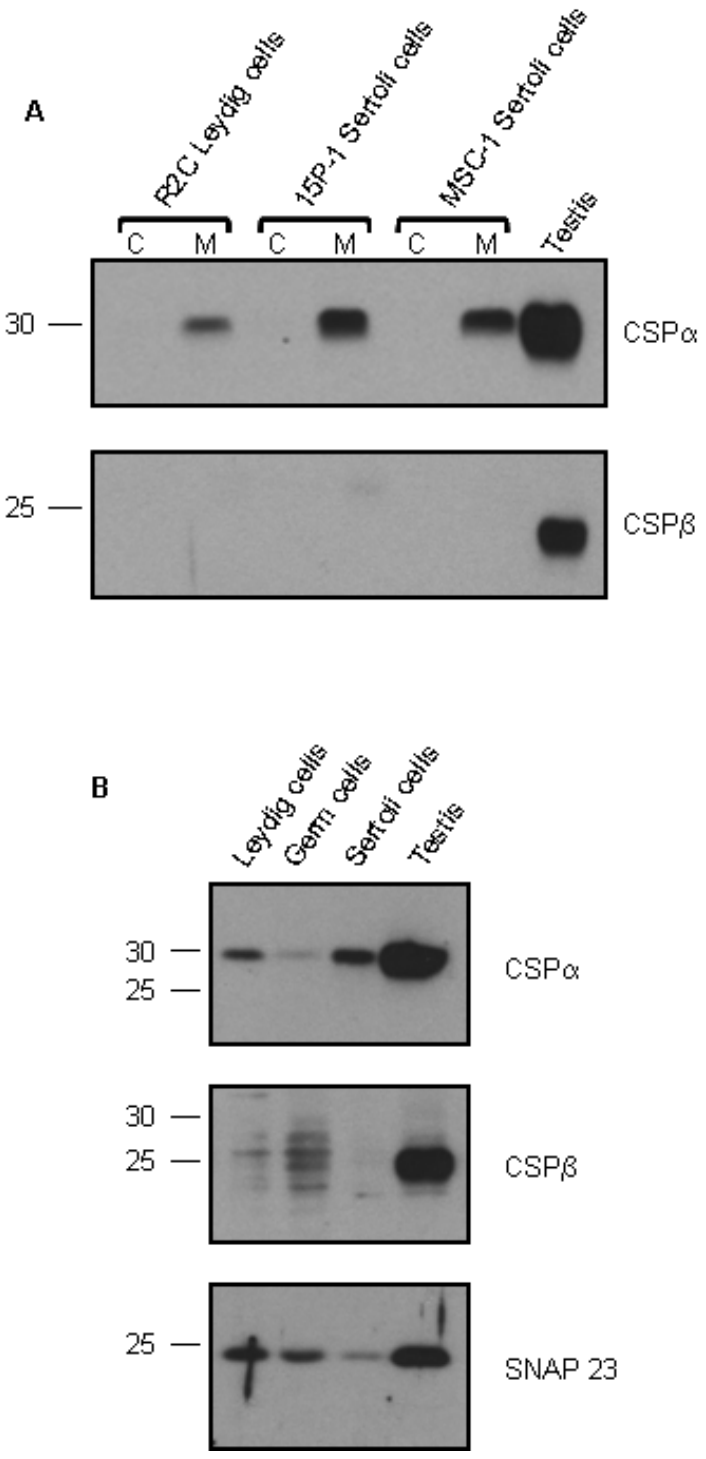

Figure 5.9: Detection of CSP isoforms in Testis cell types. *A*. Rat Leydig (R2C), rat Sertoli (15P-1) and mouse Sertoli (MSC-1) cell lines were fractionated into cytosol (C) and membrane (M) fractions, and resolved by SDS-PAGE and probed with CSPα and CSPβ antibodies. *B*. Testis cell types were isolated as described in (see 2.6.8) (Anway *et al*., 2006), resolved by SDS-PAGE and the distribution of proteins was detected with CSPα, CSPβ and SNAP23 antibodies. Testis samples were used as a positive control. Position of molecular mass standards are shown on the left of all panels.

distinct fractions were purified from testis that contain enrichment of each cell type, using a protocol described in detail by Anway *et al.* (2003) (see methods section). CSPα was detected in all three isolated fractions, but only a low signal was detected in the germ cell-enriched fraction (Figure 5.9*B*). These results for CSPα were also confirmed in Figure 5.10, were immunohistochemical detection of CSPα in testis section demonstrated that CSPα is expressed in every testis cell type. By contrast, CSPβ was mainly present in the germ cell fraction (Figure 5.9*B*). This result suggested that CSPβ might be expressed in germ cells during spermatogenesis but be switched off in mature sperm cells (Figure 5.8). The SNAP23 antibody was used to detect equal protein loading.

The results presented in Figure 5.9 suggest that CSPβ is expressed in germ cells. To confirm this observation and also to examine expression of CSPγ, quantitative real time PCR (qRT-PCR, see 2.3.6) was performed. For this, 3-4 months old *Sprague Dawley* rats were treated with busulphan, which induces apoptosis in germ cells (Choi *et al.*, 2004). Figure 5.11*A* shows that CSPα expression decreased marginally with busulphan, consistent with the data in Figures 5.9 and 5.10, showing weak expression in germ cells. In marked contrast to the expression of CSPα in busulphan-treated mice, CSPβ and CSPγ mRNA expression levels both dropped dramatically and were virtually undetectable in busulphan treated samples (Figure 5.11*B* and 5.11*C*). This finding provides strong evidence that both CSPβ and CSPγ are specifically expressed in germ cells.

The detection of CSPβ and CSPγ in germ cells but not in mature sperm raised the question as to which specific stage during spermatogenesis CSPβ and CSPγ are expressed. Therefore adult mice were given a single injection of busulphan, which initiates apoptosis in spermatogonia within 1 week of treatment followed by a second wave of apoptosis in meiotic spermatocytes after 2 weeks and finally a loss of spermatids between 20 and 30 days, as existing spermatids mature and fail to be replaced (Choi *et al.*, 2004). The mice were sacrificed after 5, 10, 15, 20, 30 and 50 days of busulphan treatment and RNA purified from the testes. qRT-PCR on the corresponding cDNA revealed that CSPβ is robustly expressed following 20 days of

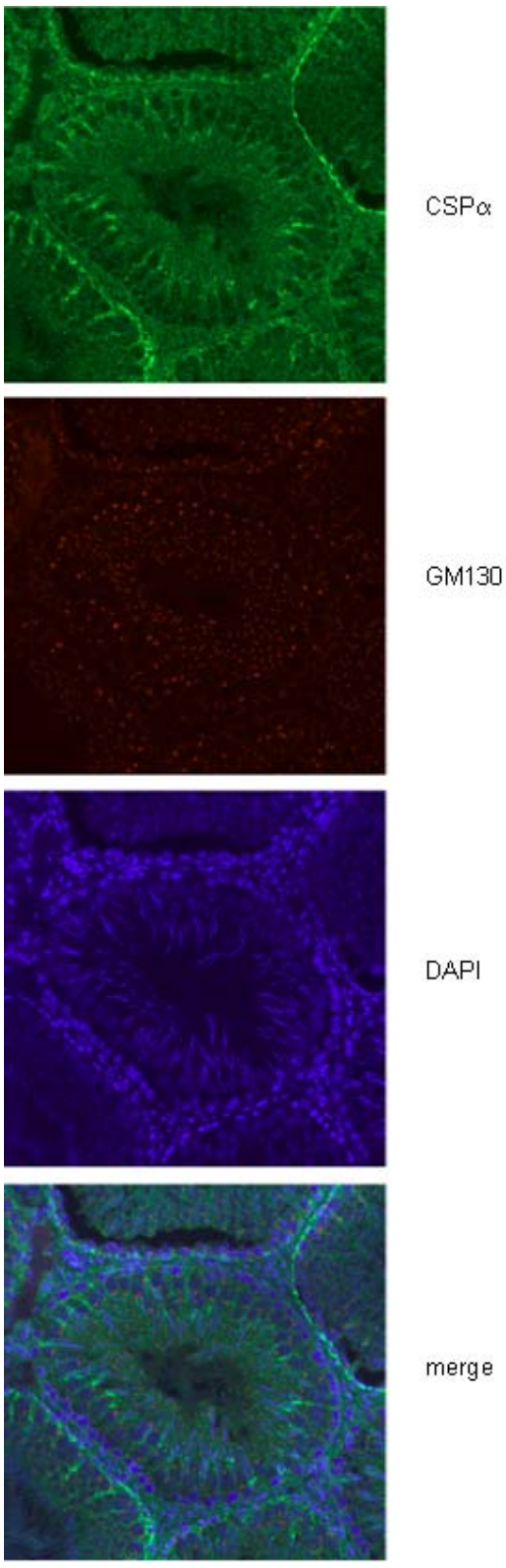

Figure 5.10: Localisation of CSPα in testis slices. 10 µm testis sections taken from a 6 month old rat testis were incubated with CSPα (green) and GM130 (red) antibody, and stained with DAPI (blue) for nuclei detection. The lower panel shows the merged image. *Scale bar*, 100 µm.

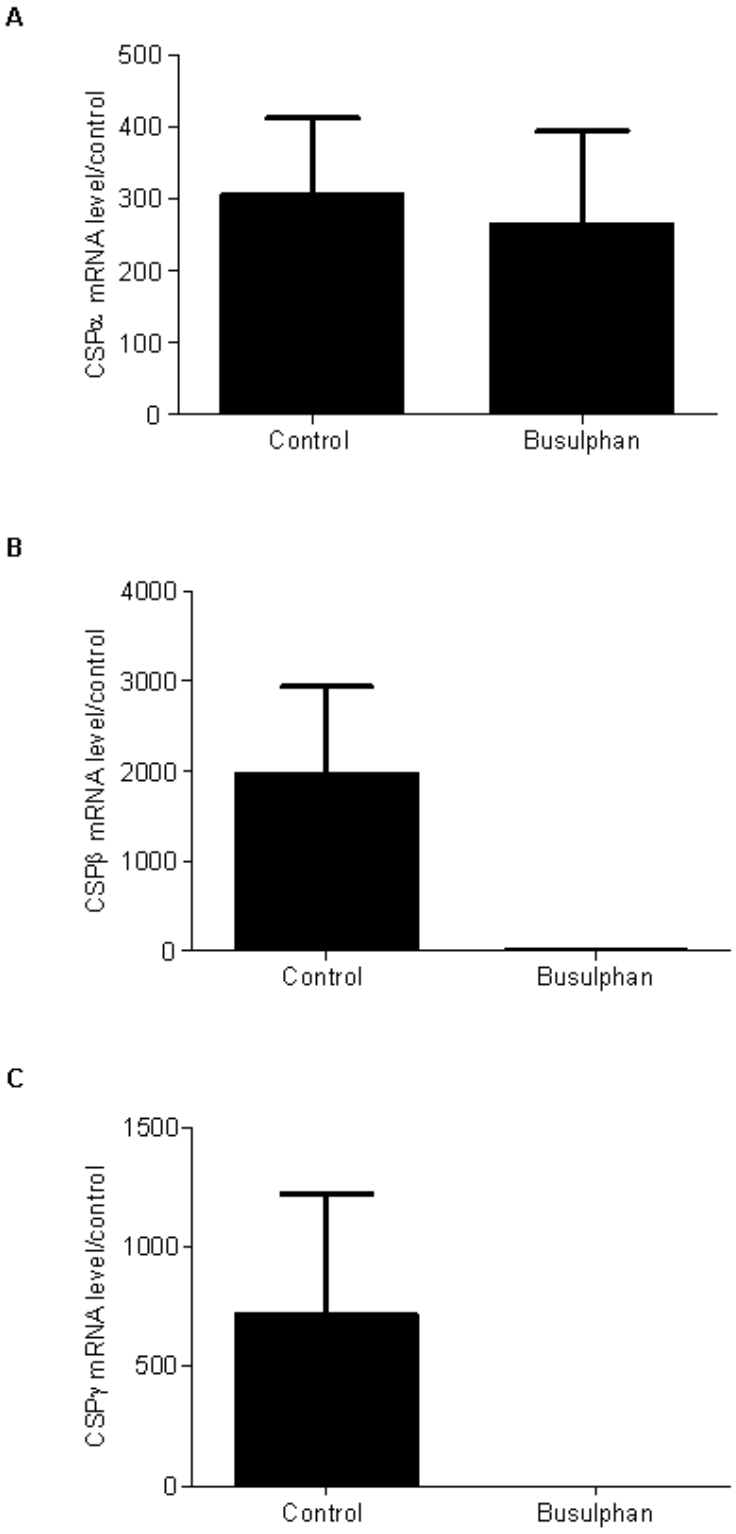

Figure 5.11: Effect of busulphan treatment on CSP expression levels. 5 days after busulphan treatment (30 mg/kg), male rats were sacrificed and their testes were isolated. Testes RNA was purified, reverse transcribed to cDNA and qRT-PCR was performed with the appropriate oligonucleotide primers against each CSP isoform and succinate dehydrogenase (SDH) as an internal control (*A-C*) (see 2.3.6).

busulphan treatment but that expression is lost after 30 days (Figure 5.12*A*). Interestingly, CSPγ expression was reduced after 15 days and almost completely lost after 20 days treatment (Figure 5.12*B*), highlighting a difference in expression profile compared with CSPβ.

5.3 Discussion

The results presented in this chapter demonstrate that CSPβ and CSPγ are highly enriched in rat testis compared with all other rat tissue examined (Figure 5.2*A* and 5.2*B*). This result is consistent with previous analysis of the expression of CSPβ and CSPγ mRNA (Fernandez-Chacon *et al.*, 2004). While there was no detection of CSPβ expression in any brain region tested, it cannot be completely ruled out that levels of this isoform were below the sensitivity of the generated antibody. However, by comparing antibody signal from known concentrations of recombinant CSPs with lysates from selected brain regions (Figure 5.3*A*), it is clear that CSPα is substantially more abundant in brain than CSPβ. The generated antibody did not recognise the high-molecular mass band reported in a recent study (Gundersen *et al.*, 2010). It is not clear why our antibody preparation did not detect this proposed CSPβ oligomeric assembly. This could be due to antibody masking, but it is also possible that the band detected by the Gundersen lab antibody is a cross-reacting protein and not CSPβ.

In testis, CSPβ was mainly membrane-associated. Furthermore, when testis membranes were treated with hydroxylamine, CSPβ underwent a marked band shift, demonstrating that the endogenous form of this CSP isoform is palmitoylated. This observation is in apparent contrast to previous work suggesting that CSPβ is a non-palmitoylated CSP isoform, a conclusion that was based on analyses of CSPβ transfected into pancreatic β cells (Boal *et al.*, 2007).

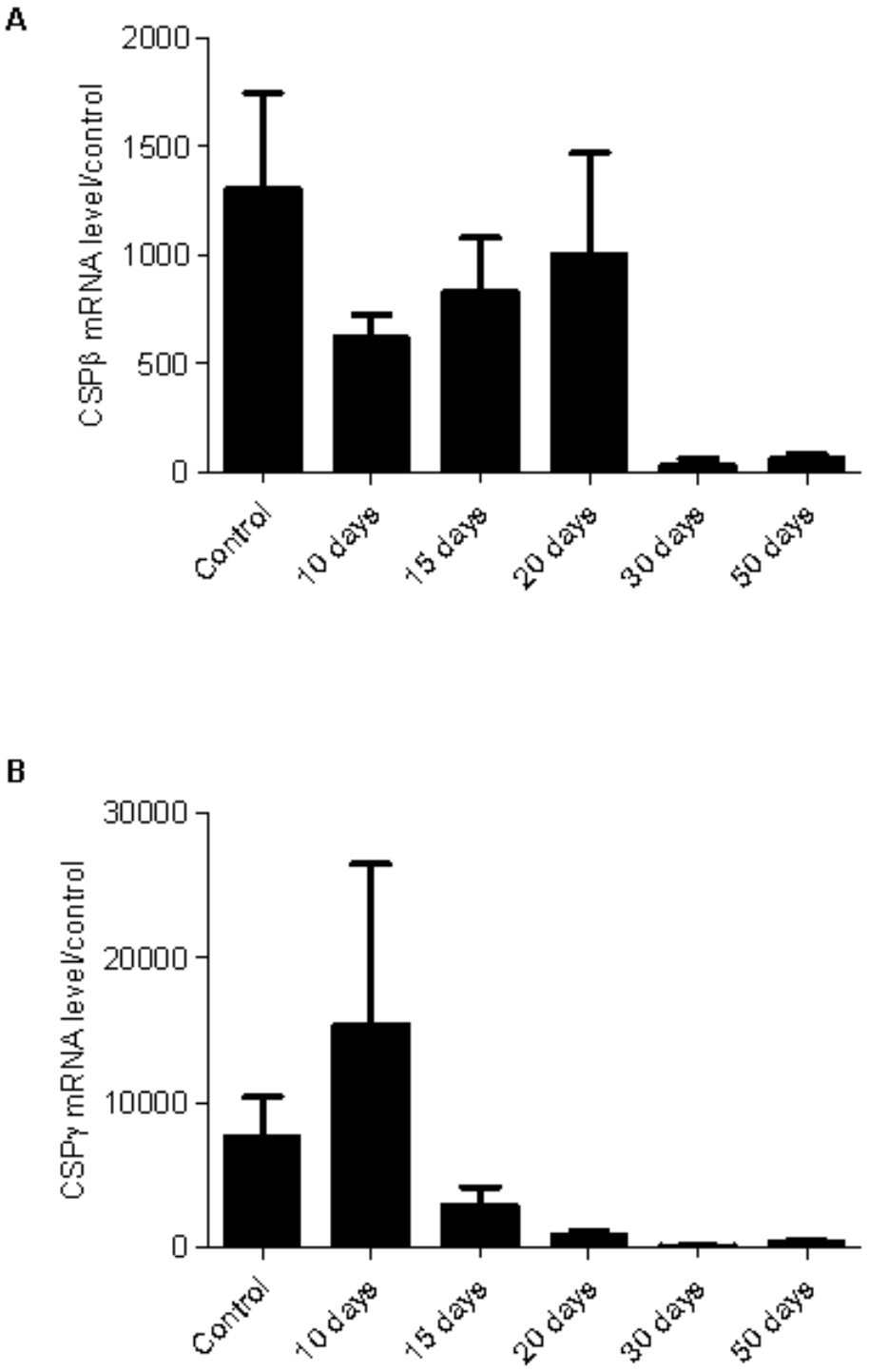

Figure 5.12: Localisation of CSP isoforms in germ cell populations. A single injection of busulphan was given to male mice (30 mg/kg). The mice were sacrificed between 10-50 days after injection and their testes were isolated. The control testes were from animals that had not been treated with busulphan. RNA was purified, reversed transcribed to cDNA and qRT-PCR was performed with the appropriate oligonucleotide primers against each CSP isoform and luciferase as an external control (*A* and *B*) (see 2.3.6).

However, the present work is in accordance with the study of Lang and co-worker, as it was shown that a GFP-CSPβ fusion proteins expressed in PC12 cells also exhibits a reduced efficiency of palmitoylation compared with that of CSPα (Figure 5.5) (Boal *et al.*, 2007). There are two main possibilities that might explain the apparent lack of CSPβ palmitoylation in pancreatic β cells and PC12 cells. (i) Palmitoylation of CSPβ is less efficient than palmitoylation of CSPα, which becomes apparent when proteins are expressed at high levels. (ii) The palmitoyl transferase that palmitoylates CSPβ is expressed at higher levels in testis than in pancreatic β cells or PC12 cells. The first possibility may seem more likely; however, it will be interesting to examine whether different palmitoyl transferases modify CSPα and CSPβ (Greaves *et al.*, 2008).

It is interesting to note that Lang and colleagues employed mutagenic analysis to show that the inefficient palmitoylation of CSPβ in pancreatic β cells was most likely not caused by differences in the cysteine-string domains of CSPα and CSPβ (Boal *et al.*, 2007). In support of these findings, the present study confirmed that switching the entire N-terminal regions of CSPα and CSPβ upstream of the cysteine-string domains, resulted in a loss of CSPα palmitoylation and an increased palmitoylation of CSPβ. These observations suggest that the N-terminal domains of the CSP isoforms regulate palmitoylation efficiency (Figure 5.6*B* and 5.6*C*). This finding is in agreement with recent studies that have shown that palmitoylation of substrate proteins can be influenced by residues that are somewhat displaced from the modified cysteines (Greaves *et al.*, 2009). It was previously shown that amino acids both within and upstream of the cysteine-string domain are important for membrane interaction of CSPα prior to its palmitoylation (Greaves *et al.*, 2008). Thus, it is possible that the different efficiencies of CSPα and CSPβ palmitoylation relate to differences in membrane interaction dynamics of the proteins in their un-palmitoylated forms. Interestingly, CSPγ had an even lower level of membrane binding and palmitoylation than CSPβ; it is possible that these differences in membrane binding/palmitoylation may influence functional properties of the three CSP isoforms.

Expression analysis of the different CSP isoforms in testis samples revealed that CSPβ and CSPγ mRNA display distinct developmental profiles to CSPα, being turned on around the time of sexual maturation in rat (Figure 5.7) (Ojeda, 1994a); CSPα by contrast is constitutively expressed. Furthermore, treatment with busulphan provided strong evidence that CSPβ and CSPγ are specifically localised to germ cells, whereas CSPα is also expressed in other testis cell types (Figure 5.11). The exact expression pattern of the CSP isoforms in mouse germ cells (Figure 5.12*A*), analysed in mice samples treated with busulphan for various periods, suggested that CSPβ and CSPγ are specifically enriched in spermatids and spermatocytes, respectively. This conclusion was made, as the expression pattern is almost the same as seen in the work of O'Shaughnessy *et al.* (2008), where the role of germ cells in regulating Sertoli cell gene expression *in vivo* was examined. Furthermore O'Shaughnessy and colleagues looked at germ cell genes which are predominantly expressed in specific germ cell populations, by treating the mice with busulphan, which destroys fast replicating cells, such as germ cells (Choi *et al.*, 2004; O'Shaughnessy *et al.*, 2008). Furthermore, the expression of CSPγ in spermatocytes supports the results of the mRNA expression profiles of CSPβ and CSPγ during development (Figure 5.7B), where CSPβ expression appears later than expression of CSPγ.

Meiosis is a unique process occurring in germ cells and involves one round of DNA replication followed by two consecutive cell divisions enabling diploid cells to form haploid cells (Cobb and Handel, 1998; Baarends *et al.*, 2001). Spermatocytes are a population of germ cells which undergo a complex process of meiosis requiring many genes and proteins to develop from the diploid spermatocytes to the haploid spermatid (Hermo *et al.*, 2010); since CSPγ was identified in spermatocytes (Figure 5.12*C*), this CSP isoform might be involved in meiosis. The heat shock protein HSP70-2 (mouse) is expressed at high levels during meiosis (Rosario *et al.*, 1992) and chaperones CDC2/cyclin B1 complex formation in spermatocytes (Zhu *et al.*, 1997). This complex is required to trigger the G2/M-phase transition in meiosis I, which is the phase between DNA synthesis and mitosis (Dix *et al.*, 1997). Since it is known that CSPα and CSPβ interact with HSC70/HSP70 as co-chaperones and

activate HSC70/HSP70 ATPase activity, it is possible that CSPγ acts as a co-chaperone for HSP70-2.

In contrast, spermatids undergo several changes to metamorphose into spermatozoa, such as alterations and transformations of organelles, compaction and condensation of the nuclear chromatin and forming of the acrosome, which is partially formed by the Golgi apparatus (Clermont *et al.*, 1994). The area in between the trans face of the Golgi apparatus and the developing acrosome contains vesicular and tubular profiles, which fuse with the acrosome (Burgos and Gutierrez, 1986). Thus, it is possible that CSPβ, which appears to be enriched in spermatids (Figure 5.12*B*), is involved in such membrane fusion reactions, occurring specifically in spermatids. From Figure 5.1*A* it can be seen that CSPα, -β and -γ are most divergent in their C-terminal domains. Thus, it appears likely that these isoforms have evolved to function as common molecular chaperones that likely have distinct substrates that are specified by their C-terminal regions.

In summary, this work is consistent with the notion of CSPβ being enriched in testis and suggests that if this isoform is expressed in brain then it is likely to be at levels substantially lower than that of CSPα. The higher-molecular mass CSPβ band reported by Gundersen and colleagues (Gundersen *et al.*, 2010), was not detected here. However, as the antibody used here was raised against a peptide different from that used by Gundersen *et al.* (2010) to generate their antibody, it is possible that antigen masking prevented detection of this complex.

Furthermore, we were able to localise CSPβ and CSPγ specifically to the germ cell population of spermatocytes and spermatids, respectively. It would be interesting to examine in future studies which organelles the CSP isoforms are localised to in the particular germ cell population and with which proteins they might interact with. CSPβ and CSPγ knock out mice would help to understand to what extend these isoforms are important for fertility and would permit a detailed analysis of the functions of these novel CSP isoforms.

CHAPTER SIX:

LOCALISATION AND MEMBRANE TARGETING OF CSPα IN LEYDIG CELLS

6.1 Introduction

The specific expression of CSPβ and CSPγ in testes suggests a key function for these novel CSP isoforms in this tissue. In addition, the only developmental abnormality that has been reported in CSPα knock out mice is bilateral intra-abdominal cryptorchidism (Fernandez-Chacon *et al.*, 2004), which is the absence of both testes from the scrotum. This observation suggests that CSPα also has an essential function for normal testicular development.

Cryptorchidism occurs frequently in humans, affecting about 12 % of male births (Hutson *et al.*, 1994), and can cause infertility and increases the risks of germ cell tumours (Pettersson *et al.*, 2007). Interestingly, previous work has shown that INSL3 (insulin-like hormone) null mice exhibited bilateral cryptorchidism based on developmental abnormalities of the gubernaculum (Nef and Parada, 1999). INSL3 is specifically expressed in Leydig cells and this cell type also secretes testosterone which is essential for the development of internal and external male genitalia (Shalet, 2009). As CSPα functions in exocytosis and prevents cryptorchidism, one possibility is that CSPα regulates secretion of INSL3.

As a first step towards defining CSPα function in testis, the localisation and targeting of CSPα in R2C cells was investigated; in particular co-distribution with INSL3 was examined. The trafficking, exocytosis, and endocytosis of secretory vesicles and granules has been extensively characterised (Sudhof, 2004), however, the underlying mechanisms whereby proteins are targeted to vesicle membranes are not well defined. To date no motif that might serve as a universal vesicle targeting signal has been characterised. Thus, it has been suggested that different proteins use distinct pathways to be targeted to vesicles and that each vesicle protein controls trafficking through diverse signals (Bonanomi *et al.*, 2006).

CSPα is distributed on vesicles in the majority of mammalian cell types in which it has been studied (Mastrogiacomo *et al.*, 1994b; Braun and Scheller, 1995; Chamberlain *et al.*, 1996; Pupier *et al.*, 1997). Vesicle and granule biogenesis and protein targeting to their limiting membrane has been generally studied in the model neuroendocrine system of PC12 cells. However, overexpression of CSPα in PC12

cells led to an accumulation of CSPα on the plasma membrane (Chamberlain and Burgoyne, 1998), and this mis-targeting made it difficult to determine the features of CSPα that contribute to its targeting in this cell type. In R2C cells, GFP-CSPα displays a very similar distribution to the endogenous protein and thus we have also used this cell line to examine some of the features of CSPα that contribute to vesicle targeting.

6.2 Results

6.2.1 Colocalisation of CSPα and INSL3 in R2C Leydig cells

From the results presented in Chapter 5, it was apparent that CSPα is present in most cell types of the testes. As a first step towards investigating possible functions of CSPα in testes, the localisation of this protein in Sertoli and Leydig cell lines was studied. In both Sertoli cell lines (MSC-1 and 15P-1) and R2C Leydig cells, endogenous and EGFP-CSPα displayed a vesicular localisation. In addition both the endogenous and EGFP-CSPα were present at the plasma membrane and clustered around a perinuclear region in R2C cells. Co-localisation analysis of endogenous and EGFP-CSPα against the trans Golgi network (TGN) marker TGN38 showed that CSPα was clustered in vesicular like structures around the trans Golgi network (Figure 6.1*B*). It was noticeable in R2C cells that the localisation of EGFP-CSPα was very similar to that displayed by the endogenous protein.

Given the possible link between CSPα and INSL3 in cryptorchidism, it was examined if CSPα localisation overlapped with that of INSL3. As no antibodies are available against rat INSL3, INSL3-EGFP was produced and co-transfected into R2C cells with mcherry-CSPα and their distributions examined in live cells using a wide-field fluorescence microscope. The images presented in Figure 6.2 demonstrate that CSPα and INSL3 are co-localised on the same vesicular structure in R2C cells.

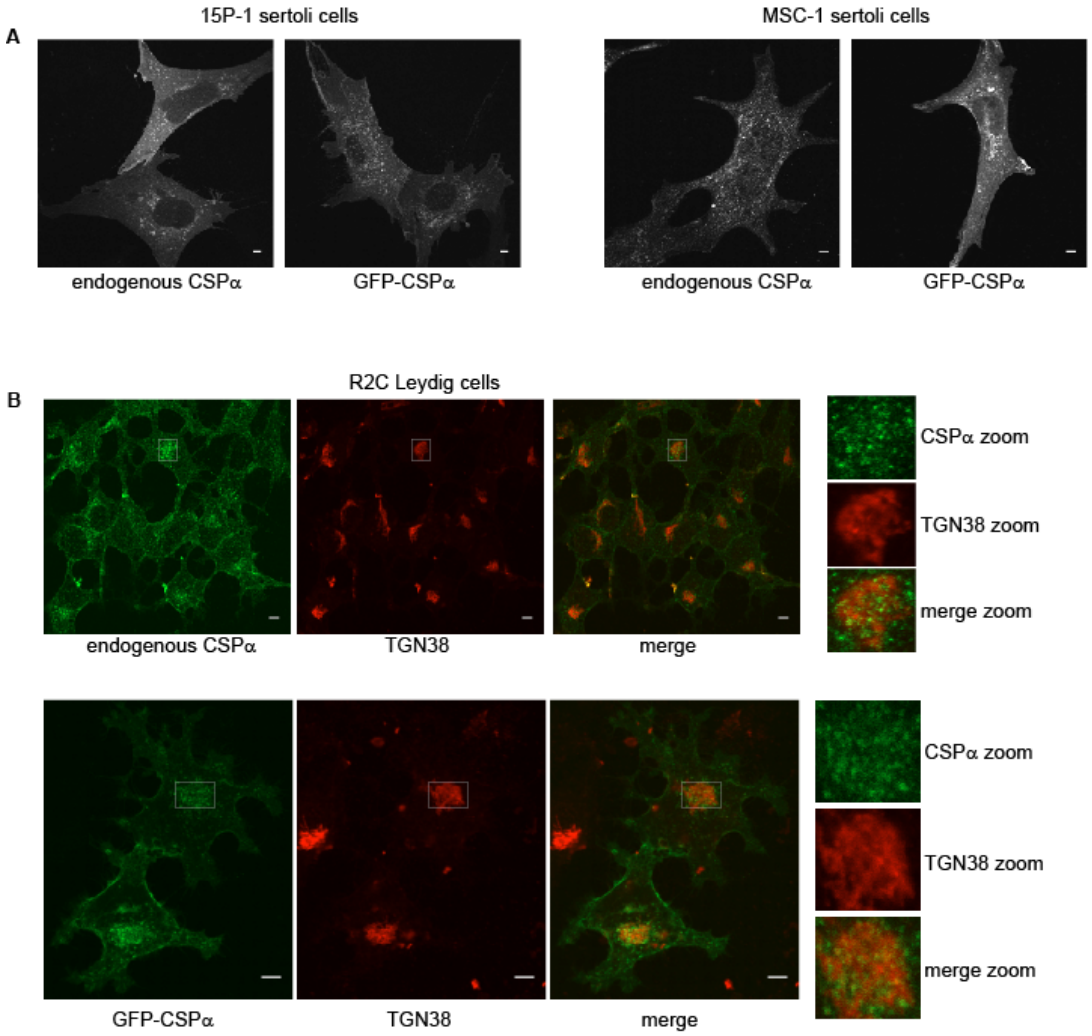

Figure 6.1: Detection of endogenous and over-expressed GFP-tagged CSPα in testis cell types. *A*. Sertoli cells from rat (15P-1) and mouse (MSC-1), were either transfected with EGFP-CSPα or directly fixed, permeabilised and incubated with a polyclonal anti-CSPα antibody to label endogenous CSPα, followed by incubation with an anti-rabbit secondary antibody conjugated to Alexa Fluor 488. *B*. R2C Leydig cells were either transfected with EGFP-CSPα (lower panel) or directly fixed, permeabilised and incubated with a polyclonal anti-CSPα antibody to label endogenous CSPα (upper panel) and a mouse anti-TGN38 antibody to label the trans Golgi network. The cells were then incubated with anti-rabbit and anti-mouse secondary conjugated to Alexa Fluor 488 and Alexa Fluor 543, respectively. The highlighted region of the cell in the images has been enlarged and is shown on the right of the panels. *Scale bar*, 5 µm.

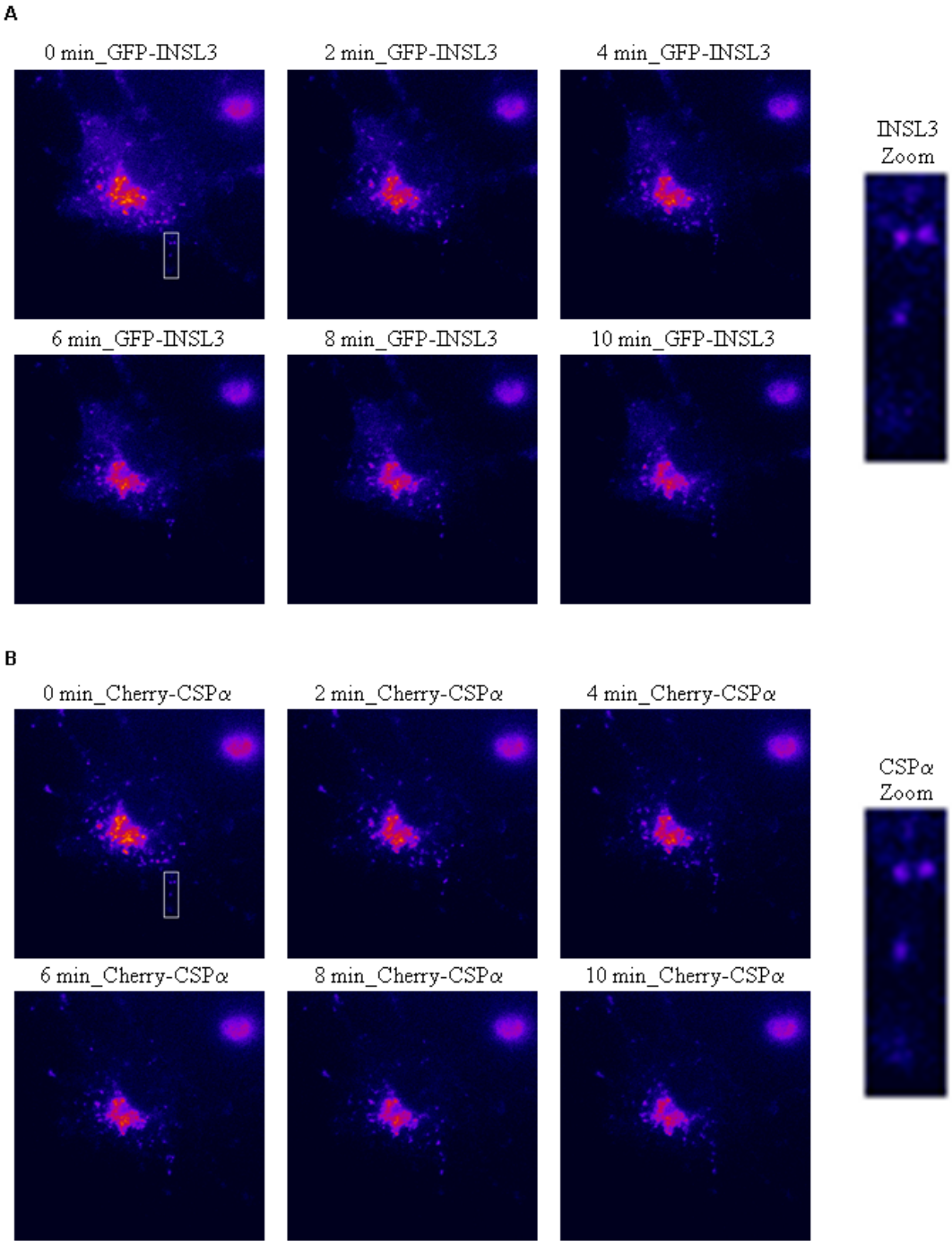

Figure 6.2: CSPα and INSL3 localisation on moving vesicles in R2C Leydig cells. Leydig cells were seeded on 30 mm coverslips and transfected with 0.5 µg of each cherry-CSPα (*A*) and EGFP-INSL3 (*B*). The cells were imaged on an Olympus IX-81 microscope at 60 x magnification over a period of 10 minutes, using microscope settings at 488 nm (EGFP tag) and 562 nm (mCherry tag). Shown are the images taken at 2 minute intervals. The area of interest is highlighted with a white box and enlarged, shown on the right of *A*. and *B*.

6.2.2 Analysis of targeting signals in CSPα

As shown in Figure 6.1, the localisation of EGFP-CSPα and endogenous CSPα are very similar in R2C cells. To date, it has been difficult to study targeting signals present within CSPα as overexpression often leads to mistargeting, for example, in PC12 cells (Chamberlain and Burgoyne, 1998). Thus, we took the opportunity to examine the effect that defined mutations have on CSPα localisation. To alleviate any confounding effects of cell-to-cell variability in CSPα localisation, EGFP-tagged CSPα mutants were co-transfected with mcherry-tagged wild type CSPα to allow a comparison of intracellular localisations to be made in the same cell. Figure 6.3 shows representative images for the localisations of defined N- and C-terminal truncations of EGFP-CSPα. CSPα(1-146) trafficked correctly (as wild type), suggesting that the C-terminus of CSPα does not contain specific signals involved in vesicle/plasma membrane targeting. In contrast, it was found that removal of the N-terminal 69 amino acids (CSPα(70-198)) led to a loss of plasma membrane targeting, although the mutant still co-localised with wild type CSPα on intracellular membranes. The first 69 amino acids contain the majority of the J-domain and the entire N-terminal domain (amino acids 1-14). The loss of plasma membrane localisation could not be attributed to a loss of the N-terminal domain, as a CSPα mutant lacking this domain (CSPα(17-198)) had the same localisation pattern as wild type CSPα (Figure 6.3, right hand panel). All other N-terminal truncations downstream of amino acid 70 displayed the same loss of plasma membrane targeting as the CSPα(70-198) mutant. These findings implicate regions within the J-domain as important for plasma membrane targeting of CSPα in R2C cells, and shows that different features of CSPα differentially regulate targeting to the plasma membrane and intracellular membranes.

The cysteine-string domain of CSPα is extensively palmitoylated and it is possible that this defining feature of CSPα is important for vesicular targeting. To test this idea, R2C cells were co-transfected with mcherry-CSPα wild type and three different cysteine mutants in which specific blocks of cysteines were mutated.

A

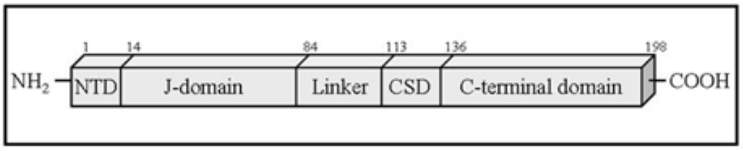

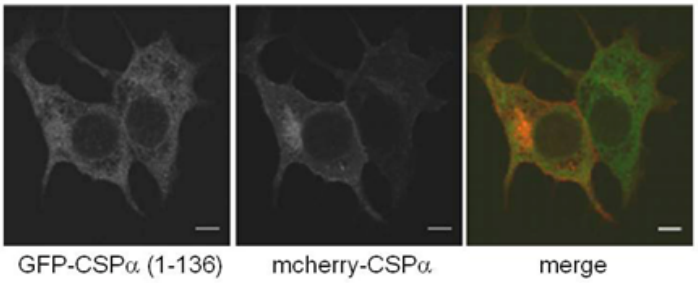

GFP-CSPα (1-136) mcherry-CSPα merge

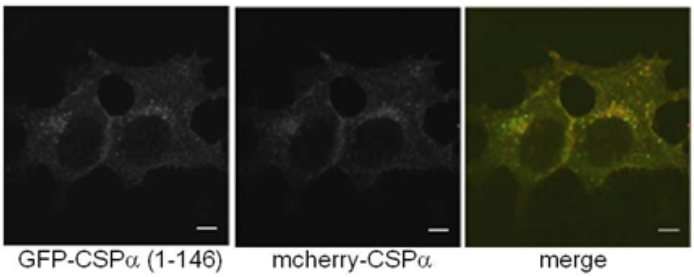

GFP-CSPα (1-146) mcherry-CSPα merge

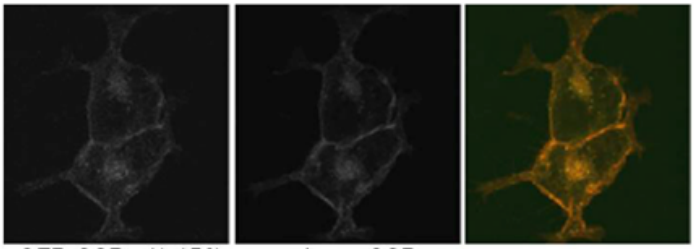

GFP-CSPα (1-156) mcherry-CSPα merge

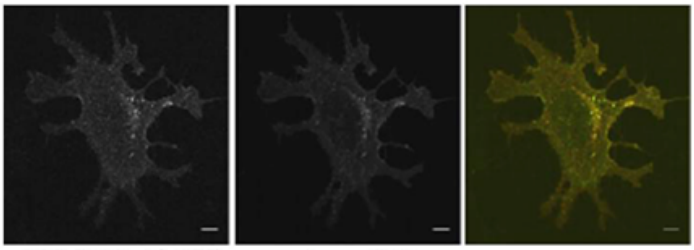

GFP-CSPα (1-166) mcherry-CSPα merge

B

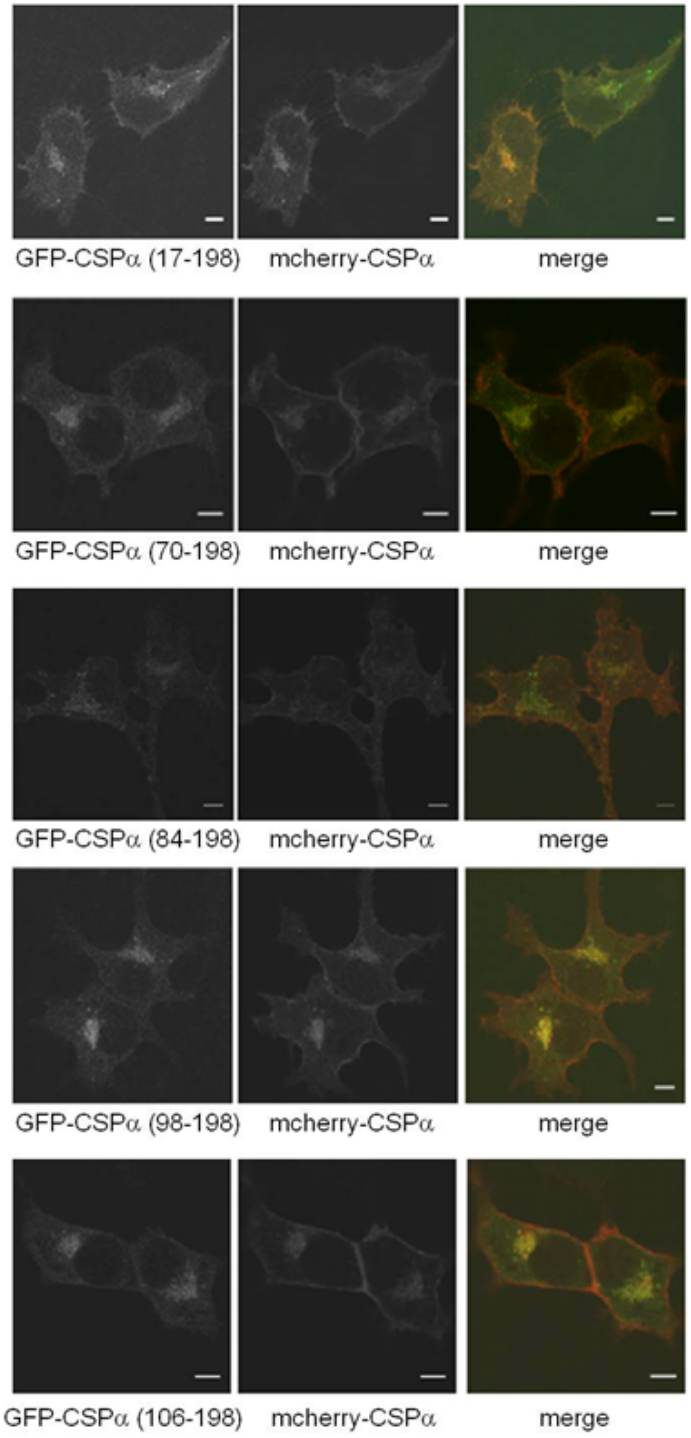

Figure 6.3: Analysis of CSPα targeting in R2C Leydig cells. *A.* Schematic diagram of the domains of mammalian CSPα. The amino acid numbers corresponding to domain boundaries are indicated. R2C Leydig cells were co-transfected with mcherry-CSPα (red) and EGFP-CSPα truncation mutants (green). The C-terminal truncation mutants indicate a truncation from the amino acid indicated, i.e. 1-136, 1-146, 1-156 and 1-166. *B*. The N-terminal truncation mutants indicate a truncation from the amino acid indicated, i.e. 17-198, 70-198, 84-198, 98-198 and 106-198. *Scale bar*, 5 µm.

It was clear from this analysis that the majority of cysteines in the cysteine-string domain were dispensable for intracellular targeting of CSPα (Figure 6.4); we were unable to examine cysteines 4-7, as their mutation blocks membrane binding (Greaves and Chamberlain, 2006).

6.2.3 Successful depletion of CSPα in R2C cells

As a first step towards probing the possible function of CSPα in Leydig cells, the effectiveness of siRNA in blocking CSPα expression in this cell type was examined. Figure 6.5 shows that this cell line is suited to siRNA depletion and CSPα was successfully depleted by 70 %, opening the way for studies probing the function of CSPα in this cell type. Since CSPα has been suggested to play a role in secretion (Umbach *et al.*, 1994; Zinsmaier *et al.*, 1994; Chamberlain and Burgoyne, 1998), it would be of particular interest to examine secretion of INSL3 in CSPα depleted cells.

6.3 Discussion

In this Chapter it was shown that CSPα is localised on mobile vesicles and at the plasma membrane in R2C Leydig cells (Figure 6.2). The vesicles decorated by CSPα showed clustering around the TGN but were clearly distinct from this compartment, as shown by co-localisation analysis against TGN38. As CSPα and INSL3 deletion in mice reveal the same phenotype of cryptorchidism (Nef and Parada, 1999; Fernandez-Chacon *et al.*, 2004), we proposed the hypothesis that cryptorchidism in CSPα null mice may be caused by a loss of INSL3 secretion. As a first step towards examining this, we analysed the localisation of CSPα and INSL3 expressed in R2C cells. It was not only shown that CSPα is localised on mobile vesicles in Leydig cells, but also that this protein is localised on the same vesicles as INSL3 (Figure 6.2), clearly suggesting that CSPα may be involved in the secretion of INSL3. It should be noted that it is not known how INSL3 gets secreted, and whether this is by a constitutive or a regulated exocytosis pathway.

CSPα(wt): **C**GLLT**CC**Y**CCCC**L**CCC**FN**CCC**GK**C**

CSPα(C1-3A): **A**GLLT**AA**Y**CCCC**L**CCC**FN**CCC**GK**C**

CSPα(C8-10S): **C**GLLT**CC**Y**CCCC**L**SSS**FN**CCC**GK**C**

CSPα(11-14S): **C**GLLT**CC**Y**CCCC**L**CCC**FN**SSS**GK**S**

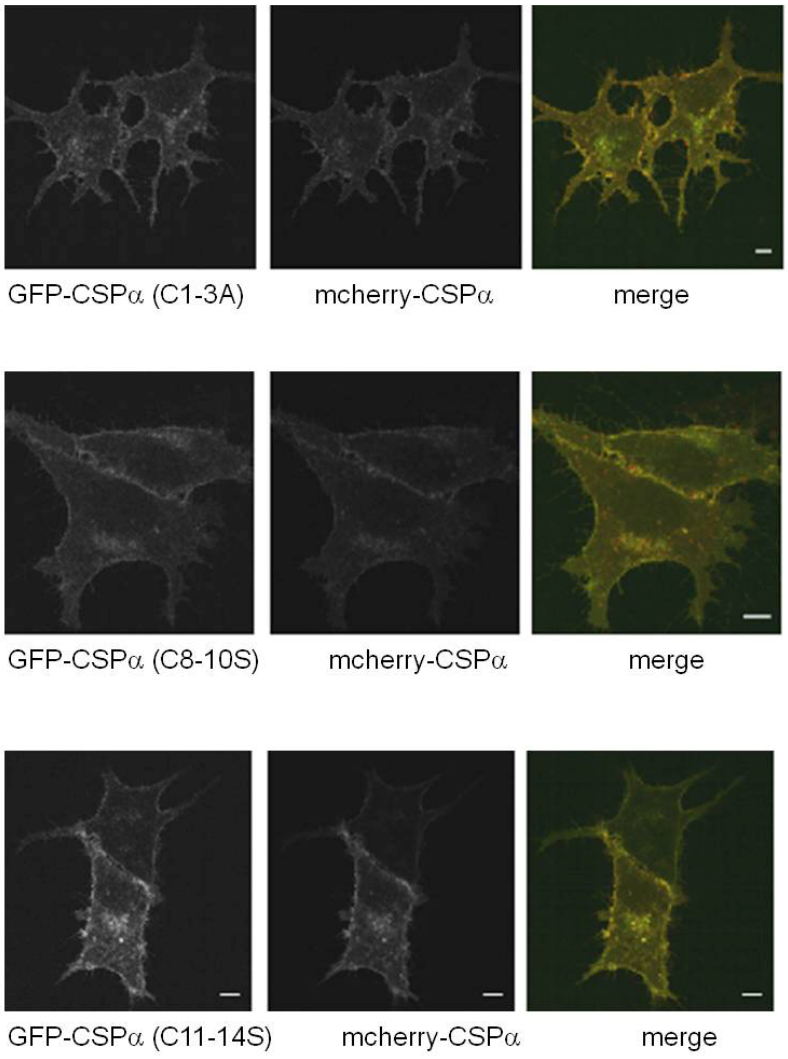

Figure 6.4: Targeting of CSPα cysteine-string domain mutants in R2C Leydig cells. Schematic diagram of the cysteine-string domain of rat CSPα. Cysteine residues are shown in bold and mutations within the cysteine-string domain are highlighted in bold red. R2C Leydig cells were co-transfected with mcherry-CSPα (red) and EGFP-CSPα cysteine-string domain mutants (green). The EGFP-CSPα(C1-3A) mutant has the first 3 cysteines mutated to alanine. EGFP-CSPα(C8-10S) has cysteine residues 8-10 mutated to serines, and EGFP-CSPα(C11-14) has cysteine residues 11-14 mutated to serines. *Scale bar*, 5µm.

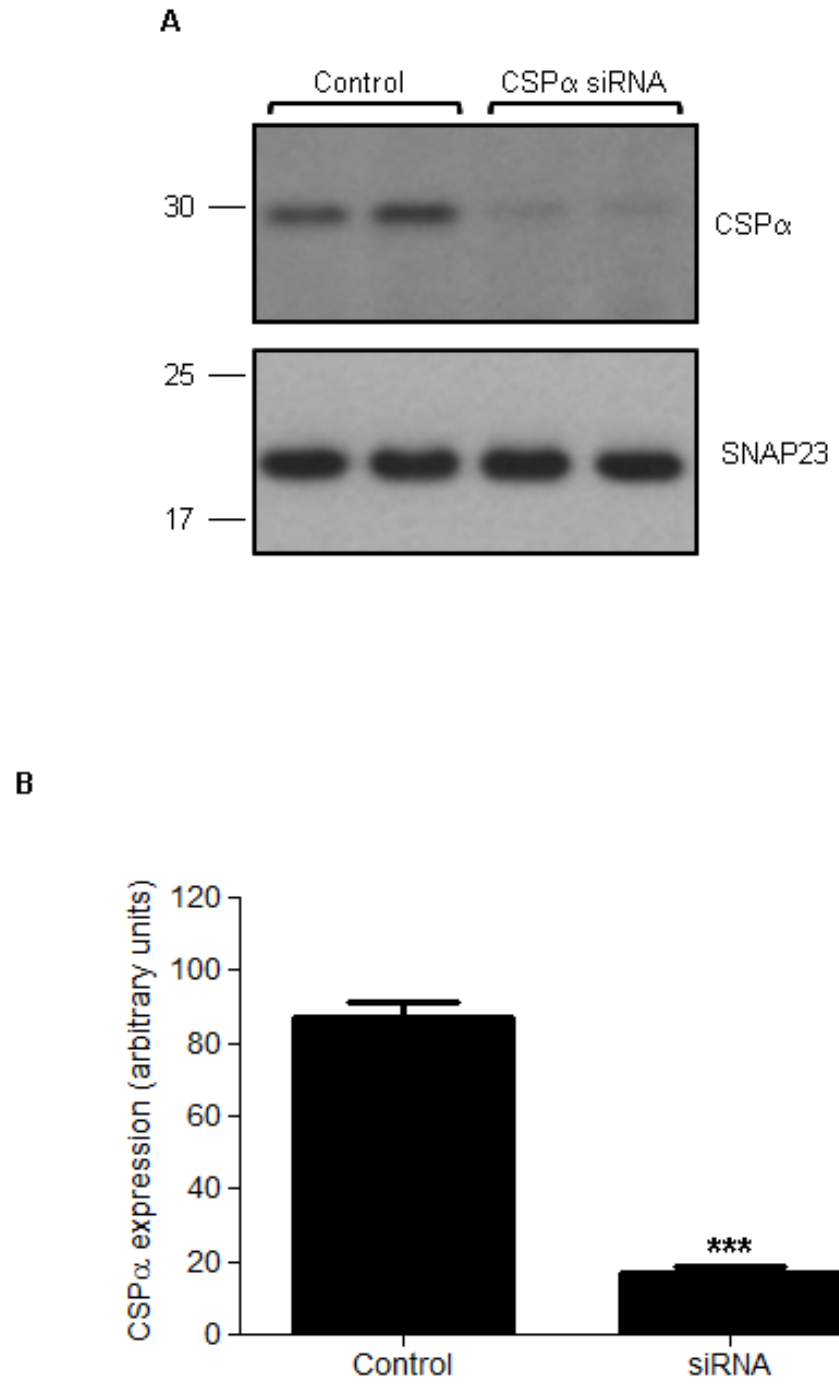

Figure 6.5: siRNA-mediated depletion of CSPα in Leydig cells. *A*. Leydig cells seeded on 24-well plates were incubated with 100 nM of siRNA molecules directed against CSPα or with non-targeting siRNA used as a control for 3 days. Cells were lysed, resolved by SDS-PAGE and protein levels examined by immunoblotting with a CSPα antibody. Position of molecular weight standard is shown on the left. *B*. CSPα levels were quantified in control and siRNA treated cells (n=3) by densitometry. Expression in control cells was arbitrary set to 100 and expression in siRNA-transfected cells is shown relative to this. *** indicates a significant decrease ($p<0.0001$) in CSPα expression compared to control cells as analysed by a Student's t-test.

In future work, we hope to investigate whether CSPα depletion has an effect on INSL3 secretion. Indeed, we have already successfully depleted CSPα using siRNA in Leydig cells. The results showed that CSPα expression can be knocked down by ~ 70 % compared to control (Figure 6.5). This would make it possible to analyse directly in Leydig cells if CSPα is involved in the release of INSL3. However, these assays are presently difficult due to the low transfection efficiency achieved in R2C cells, and it has been difficult to detect INSL3-EGFP expression by immunoblotting. Thus in future work it will be important to optimise protocols for transfection efficiency. If this cannot be overcome, then single cell assays, such as TIRF microscopy, may prove useful to study INSL3 secretion.

In addition to vesicle-like structures, CSPα was also present at the plasma membrane in Leydig cells (Figure 6.1*B*). Importantly, overexpression of EGFP-tagged CSPα appeared to result in exactly the same pattern of localisation as endogenous CSPα (Figure 6.1*B*), which awakened the interest to study CSPα targeting to intracellular membranes, as this has proved difficult in PC12 cells, where over-expressed CSPα mistargets (Chamberlain and Burgoyne, 1998; Greaves and Chamberlain, 2006). It was generally not clear to which intracellular compartment CSPα localised to in R2C cells. Though it looked as if CSPα was located to the trans Golgi network (TGN), enlargement of this area showed that CSPα is not colocalised to the TGN, but instead is present around the TGN on vesicular-like structures.

Analysis of CSPα targeting, using various N- and C-terminal truncation mutants, showed that: (i) the C- terminal domain (146-198) was not required for intracellular targeting, (ii) the N-terminal truncation mutants GFP-CSPα(70-,84-, 98- and 106-198) displayed a loss of plasma membrane targeting, and (iii) mutations in the cysteine string domain did not affect CSPα localisation.

Analyses of the N-terminal mutants demonstrated that an intact J domain is important for plasma membrane targeting, but interestingly not for targeting to intracellular membranes. Further truncation mutants between amino acids 17-70 should be generated to define the precise region which is responsible for plasma membrane binding. If this area is located, point mutations would map out the specific

amino acid(s) that are crucial for plasma membrane binding. In particular it will be interesting to examine if interaction with HSC70 is important for plasma membrane targeting. This could be achieved by studying mutants of the HPD tripeptide in the J-domain. Mutations in the cysteine-string domain of CSPα (CSPα(C1-3A), CSPα(C8-10S) and CSPα(C11-14S)) did not display any obvious difference in localisation on either intracellular membranes or at the plasma membrane compared to wild type CSPα.

CHAPTER SEVEN: CONCLUSION

Despite being identified more than 20 years ago, we still do not have a clear picture of the precise function of CSPα, and indeed there is still debate as to the actual pathway(s) that CSPα regulates. Early work on Drosophila provided strong evidence for an essential function of CSPα in presynaptic neurotransmitter release (Zinsmaier et al., 1994). Later work in mammalian cells also supported a function for CSPα in secretory vesicle exocytosis e.g. (Chamberlain and Burgoyne, 1998). The study describing the generation and analysis of CSPα knockout mice is the one report that does not support the idea that CSPα is an important component of the exocytotic machinery (Fernandez-Chacon et al., 2004). What might be the reason for this apparent inconsistency? It is possible that CSPα null mice develop compensatory mechanisms to overcome the loss of CSPα. There was no compensatory up-regulation of other CSP isoforms or selected key components of the exocytotic machinery. Nevertheless, it is important to recognise that if the function of CSPα is to act as a molecular chaperone that regulates the folding of specific presynaptic proteins then its loss may be easily compensated for by a change in the turnover rate of CSPα substrates. Thus, it would be of significant interest to determine whether the half-life of specific presynaptic proteins is affected by CSPα inactivation.

Given these discrepancies, a major aim of this work was to shed further light on the function(s) of this intriguing family of proteins. As most studies on mammalian systems have used over-expression strategies to study CSP function, the aim here was to examine the effects of CSP depletion in a more controlled system than a knockout mouse. Initially the role of CSPα in regulated exocytosis was examined by knocking down CSPα using siRNA in PC12 cells. Indeed CSPα depletion correlated with a significant decrease in regulated exocytosis, measured using the ^{3}H-dopamine assay and human growth hormone assay. Depletion of CSPα did not affect expression of the SNARE proteins VAMP2 (Leveque *et al.*, 1998; Boal *et al.*, 2004; Weng *et al.*, 2009), syntaxin 1 (Nie *et al.*, 1999; Chamberlain *et al.*, 2001) and SNAP25 (Chandra *et al.*, 2005; Boal *et al.*, 2011; Sharma *et al.*, 2011), which were previously suggested to interact with CSPα. This analysis thus supports the view that CSPα plays an important role in regulated exocytosis. It was unfortunate that the effect on exocytosis was not large enough to pursue rescue experiments using

defined CSPα mutants, as this would have allowed a more detailed characterisation of the domains and putative protein-protein interactions that are important for CSPα function in this pathway. It is likely that a complete depletion of CSPα is needed to obtain a greater inhibition in exocytosis. It will be interesting in future work to perform experiments that test the acute function of CSPα in brain, without possible confounding compensatory effects. One approach to do this could be via injection of recombinant viruses expressing CSPα siRNA into specific rat brain regions followed by electrophysiological analysis of presynaptic exocytosis.

Chemical cross-linking experiments with DSG and EGS showed that upon strong stimulation with ionomycin CSPα interacts with an as yet unknown protein, supporting a function for this protein in a Ca^{2+}-regulated pathway (Chapter 3). It has been difficult to pin down the precise *in vivo* substrates of CSPα but SNAP25 has emerged recently as a protein whose expression is affected by CSPα depletion (Sharma *et al.*, 2011). It is interesting to note that CSPα and SNAP25 are largely separated at an intracellular level. CSPα is present on vesicles and SNAP25 is mainly present at the plasma membrane. Thus, it is possible that CSPα may act on SNAP25 during a short window following synaptic vesicle fusion with the plasma membrane. However there is a small pool of SNAP25 on vesicles and this pool may be affected by CSPα.

It is interesting that CSPα is expressed essentially in every cell type that has been studied to date (Chapter 3). This profile is inconsistent with a single function in regulated exocytosis and suggests that CSPα may have additional, more general, cellular functions. One possibility is that CSPα also functions in constitutive exocytosis pathways (which are present in all cell types). However the analysis performed here did not provide support for this idea. Other possibilities might be that CSPα is involved in additional membrane fusion pathway such as cytokinesis or endosomal trafficking.

Recently two additional CSPα isoforms were identified in mouse and human testis, CSPβ and CSPγ (Evans *et al.*, 2003; Fernandez-Chacon *et al.*, 2004). One consequence of the identification of CSPβ and CSPγ is that they may complicate

analysis of the CSPα knock out mouse (Fernandez-Chacon *et al.*, 2004). However, Fernández-Chacón *et al*. (2004) suggested that expression of CSPβ and CSPγ was mainly restricted to testis with very low levels in brain. Interestingly, a recent study reported the generation of a CSPβ antibody recognising a C-terminal peptide of this protein (Gundersen *et al.*, 2010). Here, we wanted to examine and clarify the functional roles of CSPβ and CSPγ (Chapter 5). Work from Gundersen's group suggested that the lack of effect on exocytosis in CSPα null mice might be explained by compensation by CSPβ. However, our work did not agree with their proposal that CSPβ is expressed in brain as an SDS-resistant oligomeric complex. Studies on tagged versions of CSPβ have provided no evidence to support the idea that CSPβ forms such complexes. Indeed, it is possible that the lower molecular weight band detected by Gundersen following boiling in urea is simply a breakdown product of a cross-reacting 100 kDa protein. By contrast, the antibody generated in our work recognised a protein of the correct size, and failed to recognise the 100 kDa 'complex' described by Gundersen. We are confident that the CSPβ antibody used in this study specifically recognises CSPβ for the following reasons: (i) the band detected is exclusively found in testis in agreement with previous analysis of mRNA expression profiles; and (ii) the protein detected by the antibody is extensively palmitoylated as judged by increased mobility on SDS gels following hydroxylamine treatment. It was disappointing that the antibody raised, specific for recombinant CSPγ, failed to convincingly detect endogenous protein. This might reflect a low expression level of the gamma isoform compared with CSPβ, or that the gamma antibody is less useful for immunoblotting analyses. It would certainly be worthwhile in future studies to invest time to develop a new CSPγ antibody so that the expression profiles of all CSP isoforms could be collectively examined. RT-PCR analysis however, was consistent with the notion that CSPγ is also testis specific.

Interestingly, expression analysis of the different CSP isoforms revealed that CSPβ and CSPγ mRNA display distinct developmental profiles compared to CSPα, which is expressed throughout development. Both isoforms are switched on around the time of sexual maturation in rat (Ojeda, 1994b) (Chapter 5). Treatment with busulphan suggested that CSPβ and CSPγ are localised to germ cells and are specifically

enriched in spermatids and spermatocytes, respectively. CSPα, in contrast, appears to be expressed throughout all testis cell types (germ, Sertoli and Leydig cells). Future work might allow germ cells to be cultured and confocal imaging could reveal exactly where CSPβ and CSPγ are localised in these germ cells, offering an insight into their exact function in spermatids and spermatocytes.

The observed cryptorchidism phenotype of CSPα null mice is intriguing and one possibility is that this relates to a loss or inhibition of testicular molecules such as testosterone or INSL3. There is already genetic evidence showing that INSL3 knockout leads to cryptorchidism in mice (Nef and Parada, 1999) and thus we have focussed recent efforts on this secretory pathway. Interestingly, it was found that CSPα and INSL3 co-localise on mobile vesicles in R2C Leydig cells, suggesting that CSPα might regulate the exocytosis of these vesicles. There is little known about how INSL3 is secreted (constitutive or regulated pathway) or what the intracellular signals would be for secretion (e.g. Ca^{2+}). Thus, it will be important to perform a detailed characterisation of the INSL3 secretory pathway in R2C cells. Importantly, it was shown that siRNA is useful for depleting CSPα expression in these cells, opening up the potential for functional studies. Another interesting angle will be to analyse serum levels of INSL3 and testosterone from $CSP\alpha^{-/-}$ mice to detect if these are any alterations in testosterone or INSL3 levels. Furthermore it would be interesting to test whether the $CSP\alpha^{-/-}$ mice are fertile. A well-characterised pathway of regulated exocytosis is the acrosomal exocytosis in sperm, which is essential for successful fertilisation. As CSPα is expressed in mature sperm, it might be that this isoform has an important function in acrosomal exocytosis. It would be difficult to study fertility in CSPα knockout mice as these mice die at an early age (around puberty) (Fernandez-Chacon *et al.*, 2004); however, fertility could be tested in CSPα knockout mice over-expressing α-synuclein, as these mice have a normal life-span (Chandra *et al.*, 2005). Further obvious experiments would be to examine the effects of CSPβ and CSPγ knockout and how this affects testicular development and fertility. Combined knockouts of CSPα, -β and -γ would provide additional information on the interplay between these isoforms in testis.

R2C cells proved to be a useful system to study targeting of CSPα as EGFP-CSPα showed a very similar localisation to endogenous CSPα. It was interesting that plasma membrane and vesicular targeting of CSPα were able to be separated, the former being dependent upon the N-terminal 70 amino acids. This region of CSPα contains the J-domain and it would prove particularly interesting if the interaction with HSC70 was partly directing the subcellular localisation of CSPα; further work to look at this could involve analysis of CSPα HPD mutants, or CSPα localisation following depletion of HSC70. Alternatively, it might be that the J-domain of CSPα also interacts with other proteins and that these interactions are important for plasma membrane targeting of CSPα. The only other cell type studied to date where CSPα was markedly localised to the plasma membrane was in 3T3-L1 adipocytes (Chamberlain *et al.*, 2001); thus adipocytes and R2C cells may express a common factor that differentially regulates CSPα targeting.

It has been previously reported that there is a link between neurotransmitter release and development of mental disorders (Manji *et al.*, 2001; Sierksma *et al.*, 2010). Furthermore, previous work reported that lithium enhances CSPα gene expression in rat brain (Cordeiro *et al.*, 2000). However, analysis of CSPα expression in post-mortem brain samples of patients with mental disorders displayed a reduction by trend in some brain regions (e.g. cortex/depression, hippocampus/schizophrenia and cerebellum/bipolar), which however, were not statistically significant. HSP70 (hippocampus and cortex in bipolar patients) showed a significant increase in its expression levels. HSP70 supports the folding, subcellular transport and degradation of proteins (Bercovich *et al.*, 1997; Frydman, 2001; Schaffitzel *et al.*, 2001; Pratt and Toft, 2003), and is up-regulated in response to stress (Mosser and Morimoto, 2004; Kirkegaard *et al.*, 2010). The expression level of syntaxin 1 was significantly decreased in the cortex and thalamus in bipolar patients, and cortex in patients with major depression. Serotonin secretion has been shown to be abnormal in bipolar disease and major depression and syntaxin was shown to interact with serotonin transporters. Therefore it is particular interesting that syntaxin 1 expression levels were significantly reduced in cortex of both bipolar and depression disorder. It has been previously shown that CSPα interacts with HSC70 and syntaxin 1

(Chamberlain and Burgoyne, 1997b, a; Chamberlain *et al.*, 2001). However, the data obtained in Chapter 4 showed general inconsistency, which was most likely due to the small sample size (6 patients/condition). Therefore no general conclusions could be made and future work is required with greater sample sizes or preferentially in genetic mouse models.

The presented work supports the idea that CSPα has an important function in regulated exocytosis in neuroendocrine cells. In addition, this investigation has offered an intriguing insight into the expression of CSP isoforms in cells of the testis, and interesting angles for future work will be to examine in more detail whether CSPα is important for secretion of INSL3, and to more finely pinpoint the functions of CSPβ and CSPγ in germ cells. Finally, it should be emphasised that CSPα appears to be ubiquitously expressed and it is currently not clear what 'general' function CSPα might play in all cell types.

BIBLIOGRAPHY

Adler, E.M., Augustine, G.J., Duffy, S.N., and Charlton, M.P. (1991). Alien intracellular calcium chelators attenuate neurotransmitter release at the squid giant synapse. J Neurosci *11*, 1496-1507.

Aksenova, M.V., Burbaeva, G.S., Kandror, K.V., Kapkov, D.V., and Stepanov, A.S. (1991). The decreased level of casein kinase 2 in brain cortex of schizophrenic and Alzheimer's disease patients. FEBS Lett *279*, 55-57.

Ales, E., Tabares, L., Poyato, J.M., Valero, V., Lindau, M., and Alvarez de Toledo, G. (1999). High calcium concentrations shift the mode of exocytosis to the kiss-and-run mechanism. Nat Cell Biol *1*, 40-44.

Amsterdam, J.D. (1998). Selective serotonin reuptake inhibitor efficacy in severe and melancholic depression. J Psychopharmacol *12*, S99-111.

Anway, M.D., Folmer, J., Wright, W.W., and Zirkin, B.R. (2003). Isolation of sertoli cells from adult rat testes: an approach to ex vivo studies of Sertoli cell function. Biol Reprod *68*, 996-1002.

Arnold, C., Reisch, N., Leibold, C., Becker, S., Prufert, K., Sautter, K., Palm, D., Jatzke, S., Buchner, S., and Buchner, E. (2004). Structure-function analysis of the cysteine string protein in Drosophila: cysteine string, linker and C terminus. J Exp Biol *207*, 1323-1334.

Ashton, A.C., and Dolly, J.O. (2000). A late phase of exocytosis from synaptosomes induced by elevated [Ca2+]i is not blocked by Clostridial neurotoxins. J Neurochem *74*, 1979-1988.

Baarends, W.M., van der Laan, R., and Grootegoed, J.A. (2001). DNA repair mechanisms and gametogenesis. Reproduction *121*, 31-39.

Bai, J., and Chapman, E.R. (2004). The C2 domains of synaptotagmin--partners in exocytosis. Trends Biochem Sci *29*, 143-151.

Banerjee, A., Barry, V.A., DasGupta, B.R., and Martin, T.F. (1996). N-Ethylmaleimide-sensitive factor acts at a prefusion ATP-dependent step in Ca2+-activated exocytosis. J Biol Chem *271*, 20223-20226.

Bannan, B.A., Van Etten, J., Kohler, J.A., Tsoi, Y., Hansen, N.M., Sigmon, S., Fowler, E., Buff, H., Williams, T.S., Ault, J.G., Glaser, R.L., and Korey, C.A. (2008). The Drosophila protein palmitoylome: characterizing palmitoyl-thioesterases and DHHC palmitoyl-transferases. Fly (Austin) *2*, 198-214.

Bark, I.C., and Wilson, M.C. (1994). Human cDNA clones encoding two different isoforms of the nerve terminal protein SNAP-25. Gene *139*, 291-292.

Barnard, R.J., Morgan, A., and Burgoyne, R.D. (1997). Stimulation of NSF ATPase activity by alpha-SNAP is required for SNARE complex disassembly and exocytosis. J Cell Biol *139*, 875-883.

Baumert, M., Maycox, P.R., Navone, F., De Camilli, P., and Jahn, R. (1989). Synaptobrevin: an integral membrane protein of 18,000 daltons present in small synaptic vesicles of rat brain. EMBO J *8*, 379-384.

Baumert, M., Takei, K., Hartinger, J., Burger, P.M., Fischer von Mollard, G., Maycox, P.R., De Camilli, P., and Jahn, R. (1990). P29: a novel tyrosine-phosphorylated membrane protein present in small clear vesicles of neurons and endocrine cells. J Cell Biol *110*, 1285-1294.

Beckers, C.J., Block, M.R., Glick, B.S., Rothman, J.E., and Balch, W.E. (1989). Vesicular transport between the endoplasmic reticulum and the Golgi stack requires the NEM-sensitive fusion protein. Nature *339*, 397-398.

Beckmann, R.P., Mizzen, L.E., and Welch, W.J. (1990). Interaction of Hsp 70 with newly synthesized proteins: implications for protein folding and assembly. Science *248*, 850-854.

Begemann, M., Grube, S., Papiol, S., Malzahn, D., Krampe, H., Ribbe, K., Friedrichs, H., Radyushkin, K.A., El-Kordi, A., Benseler, F., Hannke, K., Sperling, S., Schwerdtfeger, D., Thanhauser, I., Gerchen, M.F., Ghorbani, M., Gutwinski, S., Hilmes, C., Leppert, R., Ronnenberg, A., Sowislo, J., Stawicki, S., Stodtke, M., Szuszies, C., Reim, K., Riggert, J., Eckstein, F., Falkai, P., Bickeboller, H., Nave, K.A., Brose, N., and Ehrenreich, H. (2010). Modification of cognitive performance in schizophrenia by complexin 2 gene polymorphisms. Arch Gen Psychiatry *67*, 879-888.

Bennett, M.K., Calakos, N., and Scheller, R.H. (1992). Syntaxin: a synaptic protein implicated in docking of synaptic vesicles at presynaptic active zones. Science *257*, 255-259.

Bennett, M.K., Garcia-Arraras, J.E., Elferink, L.A., Peterson, K., Fleming, A.M., Hazuka, C.D., and Scheller, R.H. (1993). The syntaxin family of vesicular transport receptors. Cell *74*, 863-873.

Bercovich, B., Stancovski, I., Mayer, A., Blumenfeld, N., Laszlo, A., Schwartz, A.L., and Ciechanover, A. (1997). Ubiquitin-dependent degradation of certain protein substrates in vitro requires the molecular chaperone Hsc70. J Biol Chem *272*, 9002-9010.

Betz, A., Okamoto, M., Benseler, F., and Brose, N. (1997). Direct interaction of the rat unc-13 homologue Munc13-1 with the N terminus of syntaxin. J Biol Chem *272*, 2520-2526.

Birnboim, H.C., and Doly, J. (1979). A rapid alkaline extraction procedure for screening recombinant plasmid DNA. Nucleic Acids Res *7*, 1513-1523.

Blasi, J., Chapman, E.R., Link, E., Binz, T., Yamasaki, S., De Camilli, P., Sudhof, T.C., Niemann, H., and Jahn, R. (1993a). Botulinum neurotoxin A selectively cleaves the synaptic protein SNAP-25. Nature *365*, 160-163.

Blasi, J., Chapman, E.R., Yamasaki, S., Binz, T., Niemann, H., and Jahn, R. (1993b). Botulinum neurotoxin C1 blocks neurotransmitter release by means of cleaving HPC-1/syntaxin. Embo J *12*, 4821-4828.

Blatch, G.L., and Lassle, M. (1999). The tetratricopeptide repeat: a structural motif mediating protein-protein interactions. Bioessays *21*, 932-939.

Block, M.R., Glick, B.S., Wilcox, C.A., Wieland, F.T., and Rothman, J.E. (1988). Purification of an N-ethylmaleimide-sensitive protein catalyzing vesicular transport. Proc Natl Acad Sci U S A *85*, 7852-7856.

Blundell, J., Kaeser, P.S., Sudhof, T.C., and Powell, C.M. (2010). RIM1alpha and interacting proteins involved in presynaptic plasticity mediate prepulse inhibition and additional behaviors linked to schizophrenia. J Neurosci *30*, 5326-5333.

Boal, F., Laguerre, M., Milochau, A., Lang, J., and Scotti, P.A. (2011). A charged prominence in the linker domain of the cysteine-string protein Cspalpha mediates its regulated interaction with the calcium sensor synaptotagmin 9 during exocytosis. FASEB J *25*, 132-143.

Boal, F., Le Pevelen, S., Cziepluch, C., Scotti, P., and Lang, J. (2007). Cysteine-string protein isoform beta (Cspbeta) is targeted to the trans-Golgi network as a non-palmitoylated CSP in clonal beta-cells. Biochim Biophys Acta *1773*, 109-119.

Boal, F., Zhang, H., Tessier, C., Scotti, P., and Lang, J. (2004). The variable C-terminus of cysteine string proteins modulates exocytosis and protein-protein interactions. Biochemistry *43*, 16212-16223.

Bonanomi, D., Benfenati, F., and Valtorta, F. (2006). Protein sorting in the synaptic vesicle life cycle. Prog Neurobiol *80*, 177-217.

Bowen, M.E., Weninger, K., Ernst, J., Chu, S., and Brunger, A.T. (2005). Single-molecule studies of synaptotagmin and complexin binding to the SNARE complex. Biophys J *89*, 690-702.

Bracher, A., Kadlec, J., Betz, H., and Weissenhorn, W. (2002). X-ray structure of a neuronal complexin-SNARE complex from squid. J Biol Chem *277*, 26517-26523.

Branks, P.L., and Wilson, M.C. (1986). Patterns of gene expression in the murine brain revealed by in situ hybridization of brain-specific mRNAs. Brain Res *387*, 1-16.

Braun, J.E., and Scheller, R.H. (1995). Cysteine string protein, a DnaJ family member, is present on diverse secretory vesicles. Neuropharmacology *34*, 1361-1369.

Braun, J.E., Wilbanks, S.M., and Scheller, R.H. (1996). The cysteine string secretory vesicle protein activates Hsc70 ATPase. J Biol Chem *271*, 25989-25993.

Brennaman, L.H., and Maness, P.F. (2010). NCAM in neuropsychiatric and neurodegenerative disorders. Adv Exp Med Biol *663*, 299-317.

Brenner, S. (1974). The genetics of Caenorhabditis elegans. Genetics *77*, 71-94.

Broadie, K.S. (1995). Genetic dissection of the molecular mechanisms of transmitter vesicle release during synaptic transmission. J Physiol Paris *89*, 59-70.

Bronk, P., Nie, Z., Klose, M.K., Dawson-Scully, K., Zhang, J., Robertson, R.M., Atwood, H.L., and Zinsmaier, K.E. (2005). The multiple functions of cysteine-string protein analyzed at Drosophila nerve terminals. J Neurosci *25*, 2204-2214.

Bronk, P., Wenniger, J.J., Dawson-Scully, K., Guo, X., Hong, S., Atwood, H.L., and Zinsmaier, K.E. (2001). Drosophila Hsc70-4 is critical for neurotransmitter exocytosis in vivo. Neuron *30*, 475-488.

Brose, N., Petrenko, A.G., Sudhof, T.C., and Jahn, R. (1992). Synaptotagmin: a calcium sensor on the synaptic vesicle surface. Science *256*, 1021-1025.

Brown, H., Larsson, O., Branstrom, R., Yang, S.N., Leibiger, B., Leibiger, I., Fried, G., Moede, T., Deeney, J.T., Brown, G.R., Jacobsson, G., Rhodes, C.J., Braun, J.E., Scheller, R.H., Corkey, B.E., Berggren, P.O., and Meister, B. (1998). Cysteine string protein (CSP) is an insulin secretory granule-associated protein regulating beta-cell exocytosis. EMBO J *17*, 5048-5058.

Bruns, D., and Jahn, R. (1995). Real-time measurement of transmitter release from single synaptic vesicles. Nature *377*, 62-65.

Bryant, N.J., Govers, R., and James, D.E. (2002). Regulated transport of the glucose transporter GLUT4. Nat Rev Mol Cell Biol *3*, 267-277.

Buchanan, G., Ricciardelli, C., Harris, J.M., Prescott, J., Yu, Z.C., Jia, L., Butler, L.M., Marshall, V.R., Scher, H.I., Gerald, W.L., Coetzee, G.A., and Tilley, W.D. (2007). Control of androgen receptor signaling in prostate cancer by the cochaperone small glutamine rich tetratricopeptide repeat containing protein alpha. Cancer Res *67*, 10087-10096.

Burgos, M.H., and Gutierrez, L.S. (1986). The Golgi complex of the early spermatid in guinea pig. Anat Rec *216*, 139-145.

Burgoyne, R.D., and Morgan, A. (2003). Secretory granule exocytosis. Physiol Rev *83*, 581-632.

Burgoyne, R.D., and Morgan, A. (2007). Membrane trafficking: three steps to fusion. Curr Biol *17*, R255-258.

Burke, W.J., Dewan, V., Wengel, S.P., Roccaforte, W.H., Nadolny, G.C., and Folks, D.G. (1997). The use of selective serotonin reuptake inhibitors for depression and psychosis complicating dementia. Int J Geriatr Psychiatry *12*, 519-525.

Burkhardt, P., Hattendorf, D.A., Weis, W.I., and Fasshauer, D. (2008). Munc18a controls SNARE assembly through its interaction with the syntaxin N-peptide. EMBO J *27*, 923-933.

Burnstock, G., and Kennedy, C. (1985). Is there a basis for distinguishing two types of P2-purinoceptor? Gen Pharmacol *16*, 433-440.

Cai, H., Reim, K., Varoqueaux, F., Tapechum, S., Hill, K., Sorensen, J.B., Brose, N., and Chow, R.H. (2008). Complexin II plays a positive role in Ca2+-triggered exocytosis by facilitating vesicle priming. Proc Natl Acad Sci U S A *105*, 19538-19543.

Calakos, N., Bennett, M.K., Peterson, K.E., and Scheller, R.H. (1994). Protein-protein interactions contributing to the specificity of intracellular vesicular trafficking. Science *263*, 1146-1149.

Carr, C.M., and Munson, M. (2007). Tag team action at the synapse. EMBO Rep *8*, 834-838.

Castillo, M.A., Ghose, S., Tamminga, C.A., and Ulery-Reynolds, P.G. (2010). Deficits in syntaxin 1 phosphorylation in schizophrenia prefrontal cortex. Biol Psychiatry *67*, 208-216.

Ceccarelli, B., Hurlbut, W.P., and Mauro, A. (1973). Turnover of transmitter and synaptic vesicles at the frog neuromuscular junction. J Cell Biol *57*, 499-524.

Chae, T.H., Kim, S., Marz, K.E., Hanson, P.I., and Walsh, C.A. (2004). The hyh mutation uncovers roles for alpha Snap in apical protein localization and control of neural cell fate. Nat Genet *36*, 264-270.

Chamberlain, L.H., and Burgoyne, R.D. (1996). Identification of a novel cysteine string protein variant and expression of cysteine string proteins in non-neuronal cells. J Biol Chem *271*, 7320-7323.

Chamberlain, L.H., and Burgoyne, R.D. (1997a). Activation of the ATPase activity of heat-shock proteins Hsc70/Hsp70 by cysteine-string protein. Biochem J *322 (Pt 3)*, 853-858.

Chamberlain, L.H., and Burgoyne, R.D. (1997b). The molecular chaperone function of the secretory vesicle cysteine string proteins. J Biol Chem *272*, 31420-31426.

Chamberlain, L.H., and Burgoyne, R.D. (1998). Cysteine string protein functions directly in regulated exocytosis. Mol Biol Cell *9*, 2259-2267.

Chamberlain, L.H., and Burgoyne, R.D. (2000). Cysteine-string protein: the chaperone at the synapse. J Neurochem *74*, 1781-1789.

Chamberlain, L.H., Graham, M.E., Kane, S., Jackson, J.L., Maier, V.H., Burgoyne, R.D., and Gould, G.W. (2001). The synaptic vesicle protein, cysteine-string protein, is associated with the plasma membrane in 3T3-L1 adipocytes and interacts with syntaxin 4. J Cell Sci *114*, 445-455.

Chamberlain, L.H., Henry, J., and Burgoyne, R.D. (1996). Cysteine string proteins are associated with chromaffin granules. J Biol Chem *271*, 19514-19517.

Chamberlain, L.H., Roth, D., Morgan, A., and Burgoyne, R.D. (1995). Distinct effects of alpha-SNAP, 14-3-3 proteins, and calmodulin on priming and triggering of regulated exocytosis. J Cell Biol *130*, 1063-1070.

Chandra, S., Gallardo, G., Fernandez-Chacon, R., Schluter, O.M., and Sudhof, T.C. (2005). Alpha-synuclein cooperates with CSPalpha in preventing neurodegeneration. Cell *123*, 383-396.

Chapman, E.R. (2008). How does synaptotagmin trigger neurotransmitter release? Annu Rev Biochem *77*, 615-641.

Chapman, E.R., An, S., Barton, N., and Jahn, R. (1994). SNAP-25, a t-SNARE which binds to both syntaxin and synaptobrevin via domains that may form coiled coils. J Biol Chem *269*, 27427-27432.

Chen, X., Lu, J., Dulubova, I., and Rizo, J. (2008). NMR analysis of the closed conformation of syntaxin-1. J Biomol NMR *41*, 43-54.

Chen, X., Tomchick, D.R., Kovrigin, E., Arac, D., Machius, M., Sudhof, T.C., and Rizo, J. (2002). Three-dimensional structure of the complexin/SNARE complex. Neuron *33*, 397-409.

Choi, Y.J., Ok, D.W., Kwon, D.N., Chung, J.I., Kim, H.C., Yeo, S.M., Kim, T., Seo, H.G., and Kim, J.H. (2004). Murine male germ cell apoptosis induced by busulfan treatment correlates with loss of c-kit-expression in a Fas/FasL- and p53-independent manner. FEBS Lett *575*, 41-51.

Clary, D.O., Griff, I.C., and Rothman, J.E. (1990). SNAPs, a family of NSF attachment proteins involved in intracellular membrane fusion in animals and yeast. Cell *61*, 709-721.

Clary, D.O., and Rothman, J.E. (1990). Purification of three related peripheral membrane proteins needed for vesicular transport. J Biol Chem *265*, 10109-10117.

Clermont, Y., Rambourg, A., and Hermo, L. (1994). Connections between the various elements of the cis- and mid-compartments of the Golgi apparatus of early rat spermatids. Anat Rec *240*, 469-480.

Cobb, J., and Handel, M.A. (1998). Dynamics of meiotic prophase I during spermatogenesis: from pairing to division. Semin Cell Dev Biol *9*, 445-450.

Connell, E., Darios, F., Peak-Chew, S., Soloviev, M., and Davletov, B. (2009). N-terminal acetylation of the neuronal protein SNAP-25 is revealed by the SMI81 monoclonal antibody. Biochemistry *48*, 9582-9589.

Coppola, T., and Gundersen, C. (1996). Widespread expression of human cysteine string proteins. FEBS Lett *391*, 269-272.

Corcoran, C., Walker, E., Huot, R., Mittal, V., Tessner, K., Kestler, L., and Malaspina, D. (2003). The stress cascade and schizophrenia: etiology and onset. Schizophr Bull *29*, 671-692.

Cordeiro, M.L., Umbach, J.A., and Gundersen, C.B. (2000). Lithium ions enhance cysteine string protein gene expression in vivo and in vitro. J Neurochem *74*, 2365-2372.

Cousin, M.A. (2009). Activity-dependent bulk synaptic vesicle endocytosis--a fast, high capacity membrane retrieval mechanism. Mol Neurobiol *39*, 185-189.

Cowles, C.R., Emr, S.D., and Horazdovsky, B.F. (1994). Mutations in the VPS45 gene, a SEC1 homologue, result in vacuolar protein sorting defects and accumulation of membrane vesicles. J Cell Sci *107 (Pt 12)*, 3449-3459.

Craxton, M. (2004). Synaptotagmin gene content of the sequenced genomes. BMC Genomics *5*, 43.

Dai, H., Shen, N., Arac, D., and Rizo, J. (2007). A quaternary SNARE-synaptotagmin-Ca2+-phospholipid complex in neurotransmitter release. J Mol Biol *367*, 848-863.

David, D., Sundarababu, S., and Gerst, J.E. (1998). Involvement of long chain fatty acid elongation in the trafficking of secretory vesicles in yeast. J Cell Biol *143*, 1167-1182.

Davletov, B.A., and Sudhof, T.C. (1993). A single C2 domain from synaptotagmin I is sufficient for high affinity Ca2+/phospholipid binding. J Biol Chem *268*, 26386-26390.

Dawson-Scully, K., Bronk, P., Atwood, H.L., and Zinsmaier, K.E. (2000). Cysteine-string protein increases the calcium sensitivity of neurotransmitter exocytosis in Drosophila. J Neurosci *20*, 6039-6047.

de Wit, H., Walter, A.M., Milosevic, I., Gulyas-Kovacs, A., Riedel, D., Sorensen, J.B., and Verhage, M. (2009). Synaptotagmin-1 docks secretory vesicles to syntaxin-1/SNAP-25 acceptor complexes. Cell *138*, 935-946.

Deak, F., Schoch, S., Liu, X., Sudhof, T.C., and Kavalali, E.T. (2004). Synaptobrevin is essential for fast synaptic-vesicle endocytosis. Nat Cell Biol *6*, 1102-1108.

DeBello, W.M., O'Connor, V., Dresbach, T., Whiteheart, S.W., Wang, S.S., Schweizer, F.E., Betz, H., Rothman, J.E., and Augustine, G.J. (1995). SNAP-mediated protein-protein interactions essential for neurotransmitter release. Nature *373*, 626-630.

Deitcher, D.L., Ueda, A., Stewart, B.A., Burgess, R.W., Kidokoro, Y., and Schwarz, T.L. (1998). Distinct requirements for evoked and spontaneous release of neurotransmitter are revealed by mutations in the Drosophila gene neuronal-synaptobrevin. J Neurosci *18*, 2028-2039.

Di Giovanni, G., Di Matteo, V., Pierucci, M., Benigno, A., and Esposito, E. (2006). Central serotonin2C receptor: from physiology to pathology. Curr Top Med Chem *6*, 1909-1925.

DiAntonio, A., Parfitt, K.D., and Schwarz, T.L. (1993). Synaptic transmission persists in synaptotagmin mutants of Drosophila. Cell *73*, 1281-1290.

Dix, D.J., Allen, J.W., Collins, B.W., Poorman-Allen, P., Mori, C., Blizard, D.R., Brown, P.R., Goulding, E.H., Strong, B.D., and Eddy, E.M. (1997). HSP70-2 is required for desynapsis of synaptonemal complexes during meiotic prophase in juvenile and adult mouse spermatocytes. Development *124*, 4595-4603.

Dolphin, A.C. (2006). A short history of voltage-gated calcium channels. Br J Pharmacol *147 Suppl 1*, S56-62.

Drevets, W.C., and Raichle, M.E. (1992). Neuroanatomical circuits in depression: implications for treatment mechanisms. Psychopharmacol Bull *28*, 261-274.

Dufau, M.L. (1988). Endocrine regulation and communicating functions of the Leydig cell. Annu Rev Physiol *50*, 483-508.

Dufau, M.L. (1998). The luteinizing hormone receptor. Annu Rev Physiol *60*, 461-496.

Dulubova, I., Khvotchev, M., Liu, S., Huryeva, I., Sudhof, T.C., and Rizo, J. (2007). Munc18-1 binds directly to the neuronal SNARE complex. Proc Natl Acad Sci U S A *104*, 2697-2702.

Dulubova, I., Sugita, S., Hill, S., Hosaka, M., Fernandez, I., Sudhof, T.C., and Rizo, J. (1999). A conformational switch in syntaxin during exocytosis: role of munc18. EMBO J *18*, 4372-4382.

Eastwood, S.L., and Harrison, P.J. (2001). Synaptic pathology in the anterior cingulate cortex in schizophrenia and mood disorders. A review and a Western blot study of synaptophysin, GAP-43 and the complexins. Brain Res Bull *55*, 569-578.

Eathiraj, S., Pan, X., Ritacco, C., and Lambright, D.G. (2005). Structural basis of family-wide Rab GTPase recognition by rabenosyn-5. Nature *436*, 415-419.

Ebstein, R.P., Lerer, B., Shlaufman, M., and Belmaker, R.H. (1983). The effect of repeated electroconvulsive shock treatment and chronic lithium feeding on the release of norepinephrine from rat cortical vesicular preparations. Cell Mol Neurobiol *3*, 191-201.

Evans, G.J., and Cousin, M.A. (2007). Activity-dependent control of slow synaptic vesicle endocytosis by cyclin-dependent kinase 5. J Neurosci *27*, 401-411.

Evans, G.J., and Morgan, A. (2002). Phosphorylation-dependent interaction of the synaptic vesicle proteins cysteine string protein and synaptotagmin I. Biochem J *364*, 343-347.

Evans, G.J., and Morgan, A. (2003). Regulation of the exocytotic machinery by cAMP-dependent protein kinase: implications for presynaptic plasticity. Biochem Soc Trans *31*, 824-827.

Evans, G.J., Morgan, A., and Burgoyne, R.D. (2003). Tying everything together: the multiple roles of cysteine string protein (CSP) in regulated exocytosis. Traffic *4*, 653-659.

Evans, G.J., Wilkinson, M.C., Graham, M.E., Turner, K.M., Chamberlain, L.H., Burgoyne, R.D., and Morgan, A. (2001). Phosphorylation of cysteine string protein by protein kinase A. Implications for the modulation of exocytosis. J Biol Chem *276*, 47877-47885.

Fasshauer, D., Antonin, W., Margittai, M., Pabst, S., and Jahn, R. (1999). Mixed and non-cognate SNARE complexes. Characterization of assembly and biophysical properties. J Biol Chem *274*, 15440-15446.

Fasshauer, D., Sutton, R.B., Brunger, A.T., and Jahn, R. (1998). Conserved structural features of the synaptic fusion complex: SNARE proteins reclassified as Q- and R-SNAREs. Proc Natl Acad Sci U S A *95*, 15781-15786.

Fernagut, P.O., and Chesselet, M.F. (2004). Alpha-synuclein and transgenic mouse models. Neurobiol Dis *17*, 123-130.

Fernandez-Chacon, R., Konigstorfer, A., Gerber, S.H., Garcia, J., Matos, M.F., Stevens, C.F., Brose, N., Rizo, J., Rosenmund, C., and Sudhof, T.C. (2001). Synaptotagmin I functions as a calcium regulator of release probability. Nature *410*, 41-49.

Fernandez-Chacon, R., Wolfel, M., Nishimune, H., Tabares, L., Schmitz, F., Castellano-Munoz, M., Rosenmund, C., Montesinos, M.L., Sanes, J.R., Schneggenburger, R., and Sudhof, T.C. (2004). The synaptic vesicle protein CSP alpha prevents presynaptic degeneration. Neuron *42*, 237-251.

Fiebig, K.M., Rice, L.M., Pollock, E., and Brunger, A.T. (1999). Folding intermediates of SNARE complex assembly. Nat Struct Biol *6*, 117-123.

Fleming, K.G., Hohl, T.M., Yu, R.C., Muller, S.A., Wolpensinger, B., Engel, A., Engelhardt, H., Brunger, A.T., Sollner, T.H., and Hanson, P.I. (1998). A revised model for the oligomeric state of the N-ethylmaleimide-sensitive fusion protein, NSF. J Biol Chem *273*, 15675-15681.

Foletti, D.L., Lin, R., Finley, M.A., and Scheller, R.H. (2000). Phosphorylated syntaxin 1 is localized to discrete domains along a subset of axons. J Neurosci *20*, 4535-4544.

Foran, P.G., Fletcher, L.M., Oatey, P.B., Mohammed, N., Dolly, J.O., and Tavare, J.M. (1999). Protein kinase B stimulates the translocation of GLUT4 but not GLUT1 or transferrin receptors in 3T3-L1 adipocytes by a pathway involving SNAP-23, synaptobrevin-2, and/or cellubrevin. J Biol Chem *274*, 28087-28095.

Frydman, J. (2001). Folding of newly translated proteins in vivo: the role of molecular chaperones. Annu Rev Biochem *70*, 603-647.

Fujiwara, T., Mishima, T., Kofuji, T., Chiba, T., Tanaka, K., Yamamoto, A., and Akagawa, K. (2006). Analysis of knock-out mice to determine the role of HPC-1/syntaxin 1A in expressing synaptic plasticity. J Neurosci *26*, 5767-5776.

Fukata, M., Fukata, Y., Adesnik, H., Nicoll, R.A., and Bredt, D.S. (2004). Identification of PSD-95 palmitoylating enzymes. Neuron *44*, 987-996.

Gabriel, S.M., Haroutunian, V., Powchik, P., Honer, W.G., Davidson, M., Davies, P., and Davis, K.L. (1997). Increased concentrations of presynaptic proteins in the cingulate cortex of subjects with schizophrenia. Arch Gen Psychiatry *54*, 559-566.

Garcia-Junco-Clemente, P., Cantero, G., Gomez-Sanchez, L., Linares-Clemente, P., Martinez-Lopez, J.A., Lujan, R., and Fernandez-Chacon, R. (2010). Cysteine String Protein-{alpha} Prevents Activity-Dependent Degeneration in GABAergic Synapses. J Neurosci *30*, 7377-7391.

Geppert, M., Bolshakov, V.Y., Siegelbaum, S.A., Takei, K., De Camilli, P., Hammer, R.E., and Sudhof, T.C. (1994a). The role of Rab3A in neurotransmitter release. Nature *369*, 493-497.

Geppert, M., Goda, Y., Hammer, R.E., Li, C., Rosahl, T.W., Stevens, C.F., and Sudhof, T.C. (1994b). Synaptotagmin I: a major Ca2+ sensor for transmitter release at a central synapse. Cell *79*, 717-727.

Gerona, R.R., Larsen, E.C., Kowalchyk, J.A., and Martin, T.F. (2000). The C terminus of SNAP25 is essential for Ca(2+)-dependent binding of synaptotagmin to SNARE complexes. J Biol Chem *275*, 6328-6336.

Giraudo, C.G., Eng, W.S., Melia, T.J., and Rothman, J.E. (2006). A clamping mechanism involved in SNARE-dependent exocytosis. Science *313*, 676-680.

Gleave, T.L., Beechey, R.B., and Burgoyne, R.D. (2001). Cysteine string protein expression in mammary epithelial cells. Pflugers Arch *441*, 639-649.

Goodarzi, M.O., Xu, N., Cui, J., Guo, X., Chen, Y.I., and Azziz, R. (2008). Small glutamine-rich tetratricopeptide repeat-containing protein alpha (SGTA), a candidate gene for polycystic ovary syndrome. Hum Reprod *23*, 1214-1219.

Gordon, D.E., Bond, L.M., Sahlender, D.A., and Peden, A.A. (2010). A targeted siRNA screen to identify SNAREs required for constitutive secretion in mammalian cells. Traffic *11*, 1191-1204.

Graham, M.E., and Burgoyne, R.D. (2000). Comparison of cysteine string protein (Csp) and mutant alpha-SNAP overexpression reveals a role for csp in late steps of membrane fusion in dense-core granule exocytosis in adrenal chromaffin cells. J Neurosci *20*, 1281-1289.

Graham, M.E., Gerke, V., and Burgoyne, R.D. (1997). Modification of annexin II expression in PC12 cell lines does not affect Ca(2+)-dependent exocytosis. Mol Biol Cell *8*, 431-442.

Greaves, J., and Chamberlain, L.H. (2006). Dual role of the cysteine-string domain in membrane binding and palmitoylation-dependent sorting of the molecular chaperone cysteine-string protein. Mol Biol Cell *17*, 4748-4759.

Greaves, J., Prescott, G.R., Fukata, Y., Fukata, M., Salaun, C., and Chamberlain, L.H. (2009). The hydrophobic cysteine-rich domain of SNAP25 couples with downstream residues to mediate membrane interactions and recognition by DHHC palmitoyl transferases. Mol Biol Cell *20*, 1845-1854.

Greaves, J., Salaun, C., Fukata, Y., Fukata, M., and Chamberlain, L.H. (2008). Palmitoylation and membrane interactions of the neuroprotective chaperone cysteine-string protein. J Biol Chem *283*, 25014-25026.

Greene, L.A., and Rein, G. (1977). Release of (3H)norepinephrine from a clonal line of pheochromocytoma cells (PC12) by nicotinic cholinergic stimulation. Brain Res *138*, 521-528.

Greene, L.A., and Tischler, A.S. (1976). Establishment of a noradrenergic clonal line of rat adrenal pheochromocytoma cells which respond to nerve growth factor. Proc Natl Acad Sci U S A *73*, 2424-2428.

Grosshans, B.L., Ortiz, D., and Novick, P. (2006). Rabs and their effectors: achieving specificity in membrane traffic. Proc Natl Acad Sci U S A *103*, 11821-11827.

Guest, P.C., Knowles, M.R., Molon-Noblot, S., Salim, K., Smith, D., Murray, F., Laroque, P., Hunt, S.P., De Felipe, C., Rupniak, N.M., and McAllister, G. (2004). Mechanisms of action of the antidepressants fluoxetine and the substance P

antagonist L-000760735 are associated with altered neurofilaments and synaptic remodeling. Brain Res *1002*, 1-10.

Gundersen, C.B., Kohan, S.A., Souda, P., Whitelegge, J.P., and Umbach, J.A. (2010). Cysteine string protein beta is prominently associated with nerve terminals and secretory organelles in mouse brain. Brain Res *1332*, 1-11.

Gundersen, C.B., Mastrogiacomo, A., Faull, K., and Umbach, J.A. (1994). Extensive lipidation of a Torpedo cysteine string protein. J Biol Chem *269*, 19197-19199.

Gundersen, C.B., and Umbach, J.A. (1992). Suppression cloning of the cDNA for a candidate subunit of a presynaptic calcium channel. Neuron *9*, 527-537.

Gundersen, C.B., Umbach, J.A., and Mastrogiacomo, A. (1996). Cysteine-string proteins: a cycle of acylation and deacylation? Life Sci *58*, 2037-2040.

Haase, J., Killian, A.M., Magnani, F., and Williams, C. (2001). Regulation of the serotonin transporter by interacting proteins. Biochem Soc Trans *29*, 722-728.

Hagenauer, M.H., King, A.F., Possidente, B., McGinnis, M.Y., Lumia, A.R., Peckham, E.M., and Lee, T.M. (2011). Changes in circadian rhythms during puberty in Rattus norvegicus: Developmental time course and gonadal dependency. Horm Behav.

Halim, N.D., Weickert, C.S., McClintock, B.W., Hyde, T.M., Weinberger, D.R., Kleinman, J.E., and Lipska, B.K. (2003). Presynaptic proteins in the prefrontal cortex of patients with schizophrenia and rats with abnormal prefrontal development. Mol Psychiatry *8*, 797-810.

Hanson, P.I., Otto, H., Barton, N., and Jahn, R. (1995). The N-ethylmaleimide-sensitive fusion protein and alpha-SNAP induce a conformational change in syntaxin. J Biol Chem *270*, 16955-16961.

Hanson, P.I., Roth, R., Morisaki, H., Jahn, R., and Heuser, J.E. (1997). Structure and conformational changes in NSF and its membrane receptor complexes visualized by quick-freeze/deep-etch electron microscopy. Cell *90*, 523-535.

Harrison, P.J., and Owen, M.J. (2003). Genes for schizophrenia? Recent findings and their pathophysiological implications. Lancet *361*, 417-419.

Harrison, S.D., Broadie, K., van de Goor, J., and Rubin, G.M. (1994). Mutations in the Drosophila Rop gene suggest a function in general secretion and synaptic transmission. Neuron *13*, 555-566.

Hayashi, T., Yamasaki, S., Nauenburg, S., Binz, T., and Niemann, H. (1995). Disassembly of the reconstituted synaptic vesicle membrane fusion complex in vitro. EMBO J *14*, 2317-2325.

He, P., Southard, R.C., Chen, D., Whiteheart, S.W., and Cooper, R.L. (1999). Role of alpha-SNAP in promoting efficient neurotransmission at the crayfish neuromuscular junction. J Neurophysiol *82*, 3406-3416.

Heckmann, M., Adelsberger, H., and Dudel, J. (1997). Evoked transmitter release at neuromuscular junctions in wild type and cysteine string protein null mutant larvae of Drosophila. Neurosci Lett *228*, 167-170.

Hermo, L., Pelletier, R.M., Cyr, D.G., and Smith, C.E. (2010). Surfing the wave, cycle, life history, and genes/proteins expressed by testicular germ cells. Part 1: background to spermatogenesis, spermatogonia, and spermatocytes. Microsc Res Tech *73*, 241-278.

Hesketh, J.E., Nicolaou, N.M., Arbuthnott, G.W., and Wright, A.K. (1978). The effect of chronic lithium administration on dopamine metabolism in rat striatum. Psychopharmacology (Berl) *56*, 163-166.

Hess, D.T., Slater, T.M., Wilson, M.C., and Skene, J.H. (1992). The 25 kDa synaptosomal-associated protein SNAP-25 is the major methionine-rich polypeptide in rapid axonal transport and a major substrate for palmitoylation in adult CNS. J Neurosci *12*, 4634-4641.

Hirling, H., and Scheller, R.H. (1996). Phosphorylation of synaptic vesicle proteins: modulation of the alpha SNAP interaction with the core complex. Proc Natl Acad Sci U S A *93*, 11945-11949.

Holz, R.W., Bittner, M.A., Peppers, S.C., Senter, R.A., and Eberhard, D.A. (1989). MgATP-independent and MgATP-dependent exocytosis. Evidence that MgATP primes adrenal chromaffin cells to undergo exocytosis. J Biol Chem *264*, 5412-5419.

Honer, W.G., Falkai, P., Bayer, T.A., Xie, J., Hu, L., Li, H.Y., Arango, V., Mann, J.J., Dwork, A.J., and Trimble, W.S. (2002). Abnormalities of SNARE mechanism proteins in anterior frontal cortex in severe mental illness. Cereb Cortex *12*, 349-356.

Honer, W.G., Falkai, P., Young, C., Wang, T., Xie, J., Bonner, J., Hu, L., Boulianne, G.L., Luo, Z., and Trimble, W.S. (1997). Cingulate cortex synaptic terminal proteins and neural cell adhesion molecule in schizophrenia. Neuroscience *78*, 99-110.

Hong, H.K., Chakravarti, A., and Takahashi, J.S. (2004). The gene for soluble N-ethylmaleimide sensitive factor attachment protein alpha is mutated in hydrocephaly with hop gait (hyh) mice. Proc Natl Acad Sci U S A *101*, 1748-1753.

Hong, W. (2005). SNAREs and traffic. Biochim Biophys Acta *1744*, 120-144.

Huntwork, S., and Littleton, J.T. (2007). A complexin fusion clamp regulates spontaneous neurotransmitter release and synaptic growth. Nat Neurosci *10*, 1235-1237.

Hutson, J.M. (1985). A biphasic model for the hormonal control of testicular descent. Lancet *2*, 419-421.

Hutson, J.M., Baker, M., Terada, M., Zhou, B., and Paxton, G. (1994). Hormonal control of testicular descent and the cause of cryptorchidism. Reprod Fertil Dev *6*, 151-156.

Inoue, A., Obata, K., and Akagawa, K. (1992). Cloning and sequence analysis of cDNA for a neuronal cell membrane antigen, HPC-1. J Biol Chem *267*, 10613-10619.

Ishizuka, T., Saisu, H., Odani, S., and Abe, T. (1995). Synaphin: a protein associated with the docking/fusion complex in presynaptic terminals. Biochem Biophys Res Commun *213*, 1107-1114.

Ishizuka, T., Saisu, H., Suzuki, T., Kirino, Y., and Abe, T. (1997). Molecular cloning of synaphins/complexins, cytosolic proteins involved in transmitter release, in the electric organ of an electric ray (Narke japonica). Neurosci Lett *232*, 107-110.

Jahn, R., Hanson, P.I., Otto, H., and Ahnert-Hilger, G. (1995). Botulinum and tetanus neurotoxins: emerging tools for the study of membrane fusion. Cold Spring Harb Symp Quant Biol *60*, 329-335.

Jahn, R., and Scheller, R.H. (2006). SNAREs--engines for membrane fusion. Nat Rev Mol Cell Biol *7*, 631-643.

Jahn, R., and Sudhof, T.C. (1999). Membrane fusion and exocytosis. Annu Rev Biochem *68*, 863-911.

Jarvis, S.E., Magga, J.M., Beedle, A.M., Braun, J.E., and Zamponi, G.W. (2000). G protein modulation of N-type calcium channels is facilitated by physical interactions between syntaxin 1A and Gbetagamma. J Biol Chem *275*, 6388-6394.

Jeans, A.F., Oliver, P.L., Johnson, R., Capogna, M., Vikman, J., Molnar, Z., Babbs, A., Partridge, C.J., Salehi, A., Bengtsson, M., Eliasson, L., Rorsman, P., and Davies, K.E. (2007). A dominant mutation in Snap25 causes impaired vesicle trafficking, sensorimotor gating, and ataxia in the blind-drunk mouse. Proc Natl Acad Sci U S A *104*, 2431-2436.

Jin, H., Wu, H., Osterhaus, G., Wei, J., Davis, K., Sha, D., Floor, E., Hsu, C.C., Kopke, R.D., and Wu, J.Y. (2003). Demonstration of functional coupling between gamma -aminobutyric acid (GABA) synthesis and vesicular GABA transport into synaptic vesicles. Proc Natl Acad Sci U S A *100*, 4293-4298.

Jocelyn, H.D., and Setchell, B.P. (1972). Regnier de Graaf on the human reproductive organs. An annotated translation of Tractatus de Virorum Organis Generationi Inservientibus (1668) and De Mulierub Organis Generationi Inservientibus Tractatus Novus (1962). J Reprod Fertil Suppl *17*, 1-222.

Johansson, J.U., Ericsson, J., Janson, J., Beraki, S., Stanic, D., Mandic, S.A., Wikstrom, M.A., Hokfelt, T., Ogren, S.O., Rozell, B., Berggren, P.O., and Bark, C. (2008). An ancient duplication of exon 5 in the Snap25 gene is required for complex neuronal development/function. PLoS Genet *4*, e1000278.

Johnson, R.D., Oliver, P.L., and Davies, K.E. (2008). SNARE proteins and schizophrenia: linking synaptic and neurodevelopmental hypotheses. Acta Biochim Pol *55*, 619-628.

Johnston-Wilson, N.L., Sims, C.D., Hofmann, J.P., Anderson, L., Shore, A.D., Torrey, E.F., and Yolken, R.H. (2000). Disease-specific alterations in frontal cortex brain proteins in schizophrenia, bipolar disorder, and major depressive disorder. The Stanley Neuropathology Consortium. Mol Psychiatry *5*, 142-149.

Jope, R.S., and Roh, M.S. (2006). Glycogen synthase kinase-3 (GSK3) in psychiatric diseases and therapeutic interventions. Curr Drug Targets *7*, 1421-1434.

Jorgensen, O.S., and Riederer, P. (1985). Increased synaptic markers in hippocampus of depressed patients. J Neural Transm *64*, 55-66.

Kato, T. (2007). Molecular genetics of bipolar disorder and depression. Psychiatry Clin Neurosci *61*, 3-19.

Katz, B. (1969). The Release of Neurotransmitter Substances. Liverpool University Press.

Kelly, R.B. (1985). Pathways of protein secretion in eukaryotes. Science *230*, 25-32.

Kennedy, S.H. (2008). Core symptoms of major depressive disorder: relevance to diagnosis and treatment. Dialogues Clin Neurosci *10*, 271-277.

Kerem, E., Corey, M., Kerem, B.S., Rommens, J., Markiewicz, D., Levison, H., Tsui, L.C., and Durie, P. (1990). The relation between genotype and phenotype in cystic fibrosis--analysis of the most common mutation (delta F508). N Engl J Med *323*, 1517-1522.

Khvotchev, M., Dulubova, I., Sun, J., Dai, H., Rizo, J., and Sudhof, T.C. (2007). Dual modes of Munc18-1/SNARE interactions are coupled by functionally critical binding to syntaxin-1 N terminus. J Neurosci *27*, 12147-12155.

Kibble, A.V., Barnard, R.J., and Burgoyne, R.D. (1996). Patch-clamp capacitance analysis of the effects of alpha-SNAP on exocytosis in adrenal chromaffin cells. J Cell Sci *109 (Pt 9)*, 2417-2422.

Kirkegaard, T., Roth, A.G., Petersen, N.H., Mahalka, A.K., Olsen, O.D., Moilanen, I., Zylicz, A., Knudsen, J., Sandhoff, K., Arenz, C., Kinnunen, P.K., Nylandsted, J., and Jaattela, M. (2010). Hsp70 stabilizes lysosomes and reverts Niemann-Pick disease-associated lysosomal pathology. Nature *463*, 549-553.

Kruger, S., and Prager, P. (2007). [Bipolar disorders: the disease of extreme emotions]. MMW Fortschr Med *149 Suppl 2*, 56-59.

Laemmli, U.K. (1970). Cleavage of structural proteins during the assembly of the head of bacteriophage T4. Nature *227*, 680-685.

Langer, T., Lu, C., Echols, H., Flanagan, J., Hayer, M.K., and Hartl, F.U. (1992). Successive action of DnaK, DnaJ and GroEL along the pathway of chaperone-mediated protein folding. Nature *356*, 683-689.

Lee, M.T., Mishra, A., and Lambright, D.G. (2009). Structural mechanisms for regulation of membrane traffic by rab GTPases. Traffic *10*, 1377-1389.

Leveque, C., Pupier, S., Marqueze, B., Geslin, L., Kataoka, M., Takahashi, M., De Waard, M., and Seagar, M. (1998). Interaction of cysteine string proteins with the alpha1A subunit of the P/Q-type calcium channel. J Biol Chem *273*, 13488-13492.

Link, E., Edelmann, L., Chou, J.H., Binz, T., Yamasaki, S., Eisel, U., Baumert, M., Sudhof, T.C., Niemann, H., and Jahn, R. (1992). Tetanus toxin action: inhibition of neurotransmitter release linked to synaptobrevin proteolysis. Biochem Biophys Res Commun *189*, 1017-1023.

Littleton, J.T., Stern, M., Schulze, K., Perin, M., and Bellen, H.J. (1993). Mutational analysis of Drosophila synaptotagmin demonstrates its essential role in Ca(2+)-activated neurotransmitter release. Cell *74*, 1125-1134.

Liu, F.H., Wu, S.J., Hu, S.M., Hsiao, C.D., and Wang, C. (1999). Specific interaction of the 70-kDa heat shock cognate protein with the tetratricopeptide repeats. J Biol Chem *274*, 34425-34432.

Llinas, R., Steinberg, I.Z., and Walton, K. (1981). Relationship between presynaptic calcium current and postsynaptic potential in squid giant synapse. Biophys J *33*, 323-351.

Lowe, A.W., Madeddu, L., and Kelly, R.B. (1988). Endocrine secretory granules and neuronal synaptic vesicles have three integral membrane proteins in common. J Cell Biol *106*, 51-59.

Lu, Q., AtKisson, M.S., Jarvis, S.E., Feng, Z.P., Zamponi, G.W., and Dunlap, K. (2001). Syntaxin 1A supports voltage-dependent inhibition of alpha1B Ca2+ channels by Gbetagamma in chick sensory neurons. J Neurosci *21*, 2949-2957.

Magga, J.M., Jarvis, S.E., Arnot, M.I., Zamponi, G.W., and Braun, J.E. (2000). Cysteine string protein regulates G protein modulation of N-type calcium channels. Neuron *28*, 195-204.

Maggi, A., and Enna, S.J. (1980). Regional alterations in rat brain neurotransmitter systems following chronic lithium treatment. J Neurochem *34*, 888-892.

Malhi, G.S., Green, M., Fagiolini, A., Peselow, E.D., and Kumari, V. (2008). Schizoaffective disorder: diagnostic issues and future recommendations. Bipolar Disord *10*, 215-230.

Manji, H.K., Drevets, W.C., and Charney, D.S. (2001). The cellular neurobiology of depression. Nat Med *7*, 541-547.

Marz, K.E., Lauer, J.M., and Hanson, P.I. (2003). Defining the SNARE complex binding surface of alpha-SNAP: implications for SNARE complex disassembly. J Biol Chem *278*, 27000-27008.

Mastrogiacomo, A., Evans, C.J., and Gundersen, C.B. (1994a). Antipeptide antibodies against a Torpedo cysteine-string protein. J Neurochem *62*, 873-880.

Mastrogiacomo, A., and Gundersen, C.B. (1995). The nucleotide and deduced amino acid sequence of a rat cysteine string protein. Brain Res Mol Brain Res *28*, 12-18.

Mastrogiacomo, A., Parsons, S.M., Zampighi, G.A., Jenden, D.J., Umbach, J.A., and Gundersen, C.B. (1994b). Cysteine string proteins: a potential link between synaptic vesicles and presynaptic Ca2+ channels. Science *263*, 981-982.

Matthew, W.D., Tsavaler, L., and Reichardt, L.F. (1981). Identification of a synaptic vesicle-specific membrane protein with a wide distribution in neuronal and neurosecretory tissue. J Cell Biol *91*, 257-269.

Mayer, M.P., and Bukau, B. (2005). Hsp70 chaperones: cellular functions and molecular mechanism. Cell Mol Life Sci *62*, 670-684.

McFerran, B.W., and Guild, S.B. (1996). The roles of adenosine 3',5'-cyclic monophosphate-dependent protein kinase A and protein kinase C in stimulus-secretion coupling in AtT-20 cells. J Mol Endocrinol *16*, 133-140.

McGlashan, T.H., and Fenton, W.S. (1991). Classical subtypes for schizophrenia: literature review for DSM-IV. Schizophr Bull *17*, 609-632.

McMahon, H.T., Missler, M., Li, C., and Sudhof, T.C. (1995). Complexins: cytosolic proteins that regulate SNAP receptor function. Cell *83*, 111-119.

McRory, J.E., Rehak, R., Simms, B., Doering, C.J., Chen, L., Hermosilla, T., Duke, C., Dyck, R., and Zamponi, G.W. (2008). Syntaxin 1A is required for normal in utero development. Biochem Biophys Res Commun *375*, 372-377.

Medine, C.N., Rickman, C., Chamberlain, L.H., and Duncan, R.R. (2007). Munc18-1 prevents the formation of ectopic SNARE complexes in living cells. J Cell Sci *120*, 4407-4415.

Melia, T.J., Jr. (2007). Putting the clamps on membrane fusion: how complexin sets the stage for calcium-mediated exocytosis. FEBS Lett *581*, 2131-2139.

Miller, L.C., Swayne, L.A., Chen, L., Feng, Z.P., Wacker, J.L., Muchowski, P.J., Zamponi, G.W., and Braun, J.E. (2003). Cysteine string protein (CSP) inhibition of N-type calcium channels is blocked by mutant huntingtin. J Biol Chem *278*, 53072-53081.

Misura, K.M., Scheller, R.H., and Weis, W.I. (2000). Three-dimensional structure of the neuronal-Sec1-syntaxin 1a complex. Nature *404*, 355-362.

Morales, M., Ferrus, A., and Martinez-Padron, M. (1999). Presynaptic calcium-channel currents in normal and csp mutant Drosophila peptidergic terminals. Eur J Neurosci *11*, 1818-1826.

Morgan, A., and Burgoyne, R.D. (1992). Interaction between protein kinase C and Exo1 (14-3-3 protein) and its relevance to exocytosis in permeabilized adrenal chromaffin cells. Biochem J *286 (Pt 3)*, 807-811.

Morgan, A., and Burgoyne, R.D. (1995a). Is NSF a fusion protein? Trends Cell Biol *5*, 335-339.

Morgan, A., and Burgoyne, R.D. (1995b). A role for soluble NSF attachment proteins (SNAPs) in regulated exocytosis in adrenal chromaffin cells. EMBO J *14*, 232-239.

Morgan, A., Dimaline, R., and Burgoyne, R.D. (1994). The ATPase activity of N-ethylmaleimide-sensitive fusion protein (NSF) is regulated by soluble NSF attachment proteins. J Biol Chem *269*, 29347-29350.

Morgan, A., Wilkinson, M., and Burgoyne, R.D. (1993). Identification of Exo2 as the catalytic subunit of protein kinase A reveals a role for cyclic AMP in Ca(2+)-dependent exocytosis in chromaffin cells. EMBO J *12*, 3747-3752.

Mosser, D.D., and Morimoto, R.I. (2004). Molecular chaperones and the stress of oncogenesis. Oncogene *23*, 2907-2918.

Mruk, D.D., and Cheng, C.Y. (2004). Sertoli-Sertoli and Sertoli-germ cell interactions and their significance in germ cell movement in the seminiferous epithelium during spermatogenesis. Endocr Rev *25*, 747-806.

Mukaetova-Ladinska, E.B., Hurt, J., Honer, W.G., Harrington, C.R., and Wischik, C.M. (2002). Loss of synaptic but not cytoskeletal proteins in the cerebellum of chronic schizophrenics. Neurosci Lett *317*, 161-165.

Murphy, T.V., Prountzos, C., Kotsonis, P., Iannazzo, L., and Majewski, H. (1999). Structural determinants of phorbol ester binding in synaptosomes: pharmacokinetics and pharmacodynamics. Eur J Pharmacol *381*, 77-84.

Murthy, V.N., and De Camilli, P. (2003). Cell biology of the presynaptic terminal. Annu Rev Neurosci *26*, 701-728.

Natochin, M., Campbell, T.N., Barren, B., Miller, L.C., Hameed, S., Artemyev, N.O., and Braun, J.E. (2005). Characterization of the G alpha(s) regulator cysteine string protein. J Biol Chem *280*, 30236-30241.

Nef, S., and Parada, L.F. (1999). Cryptorchidism in mice mutant for Insl3. Nat Genet *22*, 295-299.

Neher, E., and Sakaba, T. (2008). Multiple roles of calcium ions in the regulation of neurotransmitter release. Neuron *59*, 861-872.

Nestler, E.J., and Hyman, S.E. (2010). Animal models of neuropsychiatric disorders. Nat Neurosci *13*, 1161-1169.

Neuwald, A.F. (1999). The hexamerization domain of N-ethylmaleimide-sensitive factor: structural clues to chaperone function. Structure *7*, R19-23.

Nicholson, K.L., Munson, M., Miller, R.B., Filip, T.J., Fairman, R., and Hughson, F.M. (1998). Regulation of SNARE complex assembly by an N-terminal domain of the t-SNARE Sso1p. Nat Struct Biol *5*, 793-802.

Nie, Z., Ranjan, R., Wenniger, J.J., Hong, S.N., Bronk, P., and Zinsmaier, K.E. (1999). Overexpression of cysteine-string proteins in Drosophila reveals interactions with syntaxin. J Neurosci *19*, 10270-10279.

Nikolaus, S., Antke, C., and Muller, H.W. (2009). In vivo imaging of synaptic function in the central nervous system: II. Mental and affective disorders. Behav Brain Res *204*, 32-66.

Nonet, M.L., Grundahl, K., Meyer, B.J., and Rand, J.B. (1993). Synaptic function is impaired but not eliminated in C. elegans mutants lacking synaptotagmin. Cell *73*, 1291-1305.

Nonet, M.L., Saifee, O., Zhao, H., Rand, J.B., and Wei, L. (1998). Synaptic transmission deficits in Caenorhabditis elegans synaptobrevin mutants. J Neurosci *18*, 70-80.

Noordman, Y.E., Jansen, P.A., and Hendriks, W.J. (2006). Tyrosine-specific MAPK phosphatases and the control of ERK signaling in PC12 cells. J Mol Signal *1*, 4.

Novick, P., Field, C., and Schekman, R. (1980). Identification of 23 complementation groups required for post-translational events in the yeast secretory pathway. Cell *21*, 205-215.

Novick, P., and Schekman, R. (1979). Secretion and cell-surface growth are blocked in a temperature-sensitive mutant of Saccharomyces cerevisiae. Proc Natl Acad Sci U S A *76*, 1858-1862.

Nutt, D.J. (2006). The role of dopamine and norepinephrine in depression and antidepressant treatment. J Clin Psychiatry *67 Suppl 6*, 3-8.

O'Shaughnessy, P.J., Hu, L., and Baker, P.J. (2008). Effect of germ cell depletion on levels of specific mRNA transcripts in mouse Sertoli cells and Leydig cells. Reproduction *135*, 839-850.

Ohyama, T., Verstreken, P., Ly, C.V., Rosenmund, T., Rajan, A., Tien, A.C., Haueter, C., Schulze, K.L., and Bellen, H.J. (2007). Huntingtin-interacting protein 14, a palmitoyl transferase required for exocytosis and targeting of CSP to synaptic vesicles. J Cell Biol *179*, 1481-1496.

Ojeda, S.R., Urbanski, H.F. (1994a). Puberty in the rat. The Physiology of Reproduction *Raven*, 543-409.

Ojeda, S.R., Urbanski, H.F. (1994b). Puberty in the rat. The Physiology of Reproduction *2*, 363-409.

Olson, A.L., Knight, J.B., and Pessin, J.E. (1997). Syntaxin 4, VAMP2, and/or VAMP3/cellubrevin are functional target membrane and vesicle SNAP receptors for insulin-stimulated GLUT4 translocation in adipocytes. Mol Cell Biol *17*, 2425-2435.

Oyler, G.A., Higgins, G.A., Hart, R.A., Battenberg, E., Billingsley, M., Bloom, F.E., and Wilson, M.C. (1989). The identification of a novel synaptosomal-associated protein, SNAP-25, differentially expressed by neuronal subpopulations. J Cell Biol *109*, 3039-3052.

Ozcan, M.E., Gulec, M., Ozerol, E., Polat, R., and Akyol, O. (2004). Antioxidant enzyme activities and oxidative stress in affective disorders. Int Clin Psychopharmacol *19*, 89-95.

Pabst, S., Hazzard, J.W., Antonin, W., Sudhof, T.C., Jahn, R., Rizo, J., and Fasshauer, D. (2000). Selective interaction of complexin with the neuronal SNARE complex. Determination of the binding regions. J Biol Chem *275*, 19808-19818.

Pae, C.U., Drago, A., Mandelli, L., De Ronchi, D., and Serretti, A. (2009). TAAR 6 and HSP-70 variations associated with bipolar disorder. Neurosci Lett *465*, 257-261.

Palade, G. (1975). Intracellular aspects of the process of protein synthesis. Science *189*, 867.

Payne, A.H., and Youngblood, G.L. (1995). Regulation of expression of steroidogenic enzymes in Leydig cells. Biol Reprod *52*, 217-225.

Pereira-Leal, J.B., and Seabra, M.C. (2001). Evolution of the Rab family of small GTP-binding proteins. J Mol Biol *313*, 889-901.

Perin, M.S., Fried, V.A., Mignery, G.A., Jahn, R., and Sudhof, T.C. (1990). Phospholipid binding by a synaptic vesicle protein homologous to the regulatory region of protein kinase C. Nature *345*, 260-263.

Pettersson, A., Richiardi, L., Nordenskjold, A., Kaijser, M., and Akre, O. (2007). Age at surgery for undescended testis and risk of testicular cancer. N Engl J Med *356*, 1835-1841.

Pevsner, J., Hsu, S.C., Braun, J.E., Calakos, N., Ting, A.E., Bennett, M.K., and Scheller, R.H. (1994). Specificity and regulation of a synaptic vesicle docking complex. Neuron *13*, 353-361.

Pfeffer, S.R. (2001). Rab GTPases: specifying and deciphering organelle identity and function. Trends Cell Biol *11*, 487-491.

Pfeffer, S.R. (2005). Structural clues to Rab GTPase functional diversity. J Biol Chem *280*, 15485-15488.

Pletnikov, M.V., Ayhan, Y., Nikolskaia, O., Xu, Y., Ovanesov, M.V., Huang, H., Mori, S., Moran, T.H., and Ross, C.A. (2008). Inducible expression of mutant human DISC1 in mice is associated with brain and behavioral abnormalities reminiscent of schizophrenia. Mol Psychiatry *13*, 173-186, 115.

Poage, R.E., Meriney, S.D., Gundersen, C.B., and Umbach, J.A. (1999). Antibodies against cysteine string proteins inhibit evoked neurotransmitter release at Xenopus neuromuscular junctions. J Neurophysiol *82*, 50-59.

Podszywalow-Bartnicka, P., Kosiorek, M., Piwocka, K., Sikora, E., Zablocki, K., and Pikula, S. (2010). Role of annexin A6 isoforms in catecholamine secretion by PC12 cells: distinct influence on calcium response. J Cell Biochem *111*, 168-178.

Poodry, C.A., and Edgar, L. (1979). Reversible alteration in the neuromuscular junctions of Drosophila melanogaster bearing a temperature-sensitive mutation, shibire. J Cell Biol *81*, 520-527.

Poulain, B., Molgo, J., and Thesleff, S. (1995). Quantal neurotransmitter release and the clostridial neurotoxins' targets. Curr Top Microbiol Immunol *195*, 243-255.

Powell, C.M., Schoch, S., Monteggia, L., Barrot, M., Matos, M.F., Feldmann, N., Sudhof, T.C., and Nestler, E.J. (2004). The presynaptic active zone protein RIM1alpha is critical for normal learning and memory. Neuron *42*, 143-153.

Pratt, W.B., and Toft, D.O. (2003). Regulation of signaling protein function and trafficking by the hsp90/hsp70-based chaperone machinery. Exp Biol Med (Maywood) *228*, 111-133.

Pupier, S., Leveque, C., Marqueze, B., Kataoka, M., Takahashi, M., and Seagar, M.J. (1997). Cysteine string proteins associated with secretory granules of the rat neurohypophysis. J Neurosci *17*, 2722-2727.

Radyushkin, K., El-Kordi, A., Boretius, S., Castaneda, S., Ronnenberg, A., Reim, K., Bickeboller, H., Frahm, J., Brose, N., and Ehrenreich, H. (2010). Complexin2 null mutation requires a 'second hit' for induction of phenotypic changes relevant to schizophrenia. Genes Brain Behav *9*, 592-602.

Ranjan, R., Bronk, P., and Zinsmaier, K.E. (1998). Cysteine string protein is required for calcium secretion coupling of evoked neurotransmission in drosophila but not for vesicle recycling. J Neurosci *18*, 956-964.

Ravichandran, V., Chawla, A., and Roche, P.A. (1996). Identification of a novel syntaxin- and synaptobrevin/VAMP-binding protein, SNAP-23, expressed in non-neuronal tissues. J Biol Chem *271*, 13300-13303.

Rebois, R.V., Reynolds, E.E., Toll, L., and Howard, B.D. (1980). Storage of dopamine and acetylcholine in granules of PC12, a clonal pheochromocytoma cell line. Biochemistry *19*, 1240-1248.

Reim, K., Mansour, M., Varoqueaux, F., McMahon, H.T., Sudhof, T.C., Brose, N., and Rosenmund, C. (2001). Complexins regulate a late step in Ca2+-dependent neurotransmitter release. Cell *104*, 71-81.

Reim, K., Wegmeyer, H., Brandstatter, J.H., Xue, M., Rosenmund, C., Dresbach, T., Hofmann, K., and Brose, N. (2005). Structurally and functionally unique complexins at retinal ribbon synapses. J Cell Biol *169*, 669-680.

Resh, M.D. (2006). Use of analogs and inhibitors to study the functional significance of protein palmitoylation. Methods *40*, 191-197.

Rezin, G.T., Amboni, G., Zugno, A.I., Quevedo, J., and Streck, E.L. (2009). Mitochondrial dysfunction and psychiatric disorders. Neurochem Res *34*, 1021-1029.

Richards, D.A., Guatimosim, C., and Betz, W.J. (2000). Two endocytic recycling routes selectively fill two vesicle pools in frog motor nerve terminals. Neuron *27*, 551-559.

Rickman, C., Jimenez, J.L., Graham, M.E., Archer, D.A., Soloviev, M., Burgoyne, R.D., and Davletov, B. (2006). Conserved prefusion protein assembly in regulated exocytosis. Mol Biol Cell *17*, 283-294.

Rickman, C., Medine, C.N., Bergmann, A., and Duncan, R.R. (2007). Functionally and spatially distinct modes of munc18-syntaxin 1 interaction. J Biol Chem *282*, 12097-12103.

Rickman, C., Medine, C.N., Dun, A.R., Moulton, D.J., Mandula, O., Halemani, N.D., Rizzoli, S.O., Chamberlain, L.H., and Duncan, R.R. (2010). t-SNARE protein conformations patterned by the lipid micro-environment. J Biol Chem.

Rizzoli, S.O., and Betz, W.J. (2005). Synaptic vesicle pools. Nat Rev Neurosci *6*, 57-69.

Rizzoli, S.O., and Jahn, R. (2007). Kiss-and-run, collapse and 'readily retrievable' vesicles. Traffic *8*, 1137-1144.

Rosario, M.O., Perkins, S.L., O'Brien, D.A., Allen, R.L., and Eddy, E.M. (1992). Identification of the gene for the developmentally expressed 70 kDa heat-shock protein (P70) of mouse spermatogenic cells. Dev Biol *150*, 1-11.

Roth, D., and Burgoyne, R.D. (1994). SNAP-25 is present in a SNARE complex in adrenal chromaffin cells. FEBS Lett *351*, 207-210.

Rothman, J.E., and Orci, L. (1992). Molecular dissection of the secretory pathway. Nature *355*, 409-415.

Royle, S.J., and Lagnado, L. (2003). Endocytosis at the synaptic terminal. J Physiol *553*, 345-355.

Ruiz, R., Casanas, J.J., Sudhof, T.C., and Tabares, L. (2008). Cysteine string protein-alpha is essential for the high calcium sensitivity of exocytosis in a vertebrate synapse. Eur J Neurosci *27*, 3118-3131.

Russell, L.D., Warren, J., Debeljuk, L., Richardson, L.L., Mahar, P.L., Waymire, K.G., Amy, S.P., Ross, A.J., and MacGregor, G.R. (2001). Spermatogenesis in Bclw-deficient mice. Biol Reprod *65*, 318-332.

Sakisaka, T., Meerlo, T., Matteson, J., Plutner, H., and Balch, W.E. (2002). Rab-alphaGDI activity is regulated by a Hsp90 chaperone complex. EMBO J *21*, 6125-6135.

Salaun, C., Greaves, J., and Chamberlain, L.H. (2010). The intracellular dynamic of protein palmitoylation. J Cell Biol *191*, 1229-1238.

Sarandol, A., Sarandol, E., Eker, S.S., Erdinc, S., Vatansever, E., and Kirli, S. (2007). Major depressive disorder is accompanied with oxidative stress: short-term antidepressant treatment does not alter oxidative-antioxidative systems. Hum Psychopharmacol *22*, 67-73.

Satokata, I., Benson, G., and Maas, R. (1995). Sexually dimorphic sterility phenotypes in Hoxa10-deficient mice. Nature *374*, 460-463.

Sawada, K., Young, C.E., Barr, A.M., Longworth, K., Takahashi, S., Arango, V., Mann, J.J., Dwork, A.J., Falkai, P., Phillips, A.G., and Honer, W.G. (2002). Altered immunoreactivity of complexin protein in prefrontal cortex in severe mental illness. Mol Psychiatry *7*, 484-492.

Schaffitzel, E., Rudiger, S., Bukau, B., and Deuerling, E. (2001). Functional dissection of trigger factor and DnaK: interactions with nascent polypeptides and thermally denatured proteins. Biol Chem *382*, 1235-1243.

Schaub, J.R., Lu, X., Doneske, B., Shin, Y.K., and McNew, J.A. (2006). Hemifusion arrest by complexin is relieved by Ca2+-synaptotagmin I. Nat Struct Mol Biol *13*, 748-750.

Scheufler, C., Brinker, A., Bourenkov, G., Pegoraro, S., Moroder, L., Bartunik, H., Hartl, F.U., and Moarefi, I. (2000). Structure of TPR domain-peptide complexes: critical elements in the assembly of the Hsp70-Hsp90 multichaperone machine. Cell *101*, 199-210.

Schiavo, G., Benfenati, F., Poulain, B., Rossetto, O., Polverino de Laureto, P., DasGupta, B.R., and Montecucco, C. (1992). Tetanus and botulinum-B neurotoxins block neurotransmitter release by proteolytic cleavage of synaptobrevin. Nature *359*, 832-835.

Schiavo, G., Rossetto, O., Catsicas, S., Polverino de Laureto, P., DasGupta, B.R., Benfenati, F., and Montecucco, C. (1993). Identification of the nerve terminal targets of botulinum neurotoxin serotypes A, D, and E. J Biol Chem *268*, 23784-23787.

Schiavo, G., Stenbeck, G., Rothman, J.E., and Sollner, T.H. (1997). Binding of the synaptic vesicle v-SNARE, synaptotagmin, to the plasma membrane t-SNARE, SNAP-25, can explain docked vesicles at neurotoxin-treated synapses. Proc Natl Acad Sci U S A *94*, 997-1001.

Schikorski, T., and Stevens, C.F. (2001). Morphological correlates of functionally defined synaptic vesicle populations. Nat Neurosci *4*, 391-395.

Schmidt, B.Z., Watts, R.J., Aridor, M., and Frizzell, R.A. (2009). Cysteine string protein promotes proteasomal degradation of the cystic fibrosis transmembrane conductance regulator (CFTR) by increasing its interaction with the C terminus of Hsp70-interacting protein and promoting CFTR ubiquitylation. J Biol Chem *284*, 4168-4178.

Schmitz, F., Tabares, L., Khimich, D., Strenzke, N., de la Villa-Polo, P., Castellano-Munoz, M., Bulankina, A., Moser, T., Fernandez-Chacon, R., and Sudhof, T.C. (2006). CSPalpha-deficiency causes massive and rapid photoreceptor degeneration. Proc Natl Acad Sci U S A *103*, 2926-2931.

Schoch, S., Deak, F., Konigstorfer, A., Mozhayeva, M., Sara, Y., Sudhof, T.C., and Kavalali, E.T. (2001). SNARE function analyzed in synaptobrevin/VAMP knockout mice. Science *294*, 1117-1122.

Schou, M. (1997). Forty years of lithium treatment. Arch Gen Psychiatry *54*, 9-13; discussion 14-15.

Schubert, D., Heinemann, S., Carlisle, W., Tarikas, H., Kimes, B., Patrick, J., Steinbach, J.H., Culp, W., and Brandt, B.L. (1974). Clonal cell lines from the rat central nervous system. Nature *249*, 224-227.

Schubert, D., and Klier, F.G. (1977). Storage and release of acetylcholine by a clonal cell line. Proc Natl Acad Sci U S A *74*, 5184-5188.

Schultz, J., Doerks, T., Ponting, C.P., Copley, R.R., and Bork, P. (2000). More than 1,000 putative new human signalling proteins revealed by EST data mining. Nat Genet *25*, 201-204.

Schulze, K.L., Littleton, J.T., Salzberg, A., Halachmi, N., Stern, M., Lev, Z., and Bellen, H.J. (1994). rop, a Drosophila homolog of yeast Sec1 and vertebrate n-Sec1/Munc-18 proteins, is a negative regulator of neurotransmitter release in vivo. Neuron *13*, 1099-1108.

Schwarz, T.L. (1994). Genetic analysis of neurotransmitter release at the synapse. Curr Opin Neurobiol *4*, 633-639.

Schweizer, F.E., Dresbach, T., DeBello, W.M., O'Connor, V., Augustine, G.J., and Betz, H. (1998). Regulation of neurotransmitter release kinetics by NSF. Science *279*, 1203-1206.

Schweizer, F.E., and Ryan, T.A. (2006). The synaptic vesicle: cycle of exocytosis and endocytosis. Curr Opin Neurobiol *16*, 298-304.

Scott, C.E., Abdullah, L.H., and Davis, C.W. (1998). Ca2+ and protein kinase C activation of mucin granule exocytosis in permeabilized SPOC1 cells. Am J Physiol *275*, C285-292.

Scott, H.M., Mason, J.I., and Sharpe, R.M. (2009). Steroidogenesis in the fetal testis and its susceptibility to disruption by exogenous compounds. Endocr Rev *30*, 883-925.

Seabra, M.C., Mules, E.H., and Hume, A.N. (2002). Rab GTPases, intracellular traffic and disease. Trends Mol Med *8*, 23-30.

Seagar, M., Leveque, C., Charvin, N., Marqueze, B., Martin-Moutot, N., Boudier, J.A., Boudier, J.L., Shoji-Kasai, Y., Sato, K., and Takahashi, M. (1999). Interactions between proteins implicated in exocytosis and voltage-gated calcium channels. Philos Trans R Soc Lond B Biol Sci *354*, 289-297.

Seeman, P., and Lee, T. (1975). Antipsychotic drugs: direct correlation between clinical potency and presynaptic action on dopamine neurons. Science *188*, 1217-1219.

Segev, N. (2001). Ypt/rab gtpases: regulators of protein trafficking. Sci STKE *2001*, re11.

Shalet, S.M. (2009). Normal testicular function and spermatogenesis. Pediatr Blood Cancer *53*, 285-288.

Sharma, M., Burre, J., and Sudhof, T.C. (2011). CSPalpha promotes SNARE-complex assembly by chaperoning SNAP-25 during synaptic activity. Nat Cell Biol *13*, 182.

Shen, J., Tareste, D.C., Paumet, F., Rothman, J.E., and Melia, T.J. (2007). Selective activation of cognate SNAREpins by Sec1/Munc18 proteins. Cell *128*, 183-195.

Sheng, Z.H., Westenbroek, R.E., and Catterall, W.A. (1998). Physical link and functional coupling of presynaptic calcium channels and the synaptic vesicle docking/fusion machinery. J Bioenerg Biomembr *30*, 335-345.

Shirane, M., and Nakayama, K.I. (2006). Protrudin induces neurite formation by directional membrane trafficking. Science *314*, 818-821.

Sierksma, A.S., van den Hove, D.L., Steinbusch, H.W., and Prickaerts, J. (2010). Major depression, cognitive dysfunction and Alzheimer's disease: is there a link? Eur J Pharmacol *626*, 72-82.

Silver, P.A., and Way, J.C. (1993). Eukaryotic DnaJ homologs and the specificity of Hsp70 activity. Cell *74*, 5-6.

Simpson, L.L. (1989). Botulinum Neurotoxins and Tetanus Toxin. Academic Press, New York.

Siolas, D., Lerner, C., Burchard, J., Ge, W., Linsley, P.S., Paddison, P.J., Hannon, G.J., and Cleary, M.A. (2005). Synthetic shRNAs as potent RNAi triggers. Nat Biotechnol *23*, 227-231.

Sollner, T., Bennett, M.K., Whiteheart, S.W., Scheller, R.H., and Rothman, J.E. (1993a). A protein assembly-disassembly pathway in vitro that may correspond to sequential steps of synaptic vesicle docking, activation, and fusion. Cell *75*, 409-418.

Sollner, T., Whiteheart, S.W., Brunner, M., Erdjument-Bromage, H., Geromanos, S., Tempst, P., and Rothman, J.E. (1993b). SNAP receptors implicated in vesicle targeting and fusion. Nature *362*, 318-324.

Sorensen, J.B., Nagy, G., Varoqueaux, F., Nehring, R.B., Brose, N., Wilson, M.C., and Neher, E. (2003). Differential control of the releasable vesicle pools by SNAP-25 splice variants and SNAP-23. Cell *114*, 75-86.

Staunton, D.A., Deyo, S.N., Shoemaker, W.J., Ettenberg, A., and Bloom, F.E. (1982). Effects of chronic lithium on enkephalin systems and pain responsiveness. Life Sci *31*, 1837-1840.

Sudhof, T.C. (1995). The synaptic vesicle cycle: a cascade of protein-protein interactions. Nature *375*, 645-653.

Sudhof, T.C. (2004). The synaptic vesicle cycle. Annu Rev Neurosci *27*, 509-547.

Sudhof, T.C., Baumert, M., Perin, M.S., and Jahn, R. (1989). A synaptic vesicle membrane protein is conserved from mammals to Drosophila. Neuron *2*, 1475-1481.

Suh, W.C., Burkholder, W.F., Lu, C.Z., Zhao, X., Gottesman, M.E., and Gross, C.A. (1998). Interaction of the Hsp70 molecular chaperone, DnaK, with its cochaperone DnaJ. Proc Natl Acad Sci U S A *95*, 15223-15228.

Surprenant, A., Buell, G., and North, R.A. (1995). P2X receptors bring new structure to ligand-gated ion channels. Trends Neurosci *18*, 224-229.

Sutton, R.B., Fasshauer, D., Jahn, R., and Brunger, A.T. (1998). Crystal structure of a SNARE complex involved in synaptic exocytosis at 2.4 A resolution. Nature *395*, 347-353.

Swain, J.F., Dinler, G., Sivendran, R., Montgomery, D.L., Stotz, M., and Gierasch, L.M. (2007). Hsp70 chaperone ligands control domain association via an allosteric mechanism mediated by the interdomain linker. Mol Cell *26*, 27-39.

Swayne, L.A., Blattler, C., Kay, J.G., and Braun, J.E. (2003). Oligomerization characteristics of cysteine string protein. Biochem Biophys Res Commun *300*, 921-926.

Takamori, S., Holt, M., Stenius, K., Lemke, E.A., Gronborg, M., Riedel, D., Urlaub, H., Schenck, S., Brugger, B., Ringler, P., Muller, S.A., Rammner, B., Grater, F., Hub, J.S., De Groot, B.L., Mieskes, G., Moriyama, Y., Klingauf, J., Grubmuller, H., Heuser, J., Wieland, F., and Jahn, R. (2006). Molecular anatomy of a trafficking organelle. Cell *127*, 831-846.

Tang, J., Maximov, A., Shin, O.H., Dai, H., Rizo, J., and Sudhof, T.C. (2006). A complexin/synaptotagmin 1 switch controls fast synaptic vesicle exocytosis. Cell *126*, 1175-1187.

Tao-Cheng, J.H., Du, J., and McBain, C.J. (2000). Snap-25 is polarized to axons and abundant along the axolemma: an immunogold study of intact neurons. J Neurocytol *29*, 67-77.

Teng, F.Y., Wang, Y., and Tang, B.L. (2001). The syntaxins. Genome Biol *2*, REVIEWS3012.

Thompson, P.M., Egbufoama, S., and Vawter, M.P. (2003a). SNAP-25 reduction in the hippocampus of patients with schizophrenia. Prog Neuropsychopharmacol Biol Psychiatry *27*, 411-417.

Thompson, P.M., Kelley, M., Yao, J., Tsai, G., and van Kammen, D.P. (2003b). Elevated cerebrospinal fluid SNAP-25 in schizophrenia. Biol Psychiatry *53*, 1132-1137.

Thompson, P.M., Sower, A.C., and Perrone-Bizzozero, N.I. (1998). Altered levels of the synaptosomal associated protein SNAP-25 in schizophrenia. Biol Psychiatry *43*, 239-243.

Thonberg, H., Scheele, C.C., Dahlgren, C., and Wahlestedt, C. (2004). Characterization of RNA interference in rat PC12 cells: requirement of GERp95. Biochem Biophys Res Commun *318*, 927-934.

Tobaben, S., Thakur, P., Fernandez-Chacon, R., Sudhof, T.C., Rettig, J., and Stahl, B. (2001). A trimeric protein complex functions as a synaptic chaperone machine. Neuron *31*, 987-999.

Tobaben, S., Varoqueaux, F., Brose, N., Stahl, B., and Meyer, G. (2003). A brain-specific isoform of small glutamine-rich tetratricopeptide repeat-containing protein binds to Hsc70 and the cysteine string protein. J Biol Chem *278*, 38376-38383.

Toda, M., and Abi-Dargham, A. (2007). Dopamine hypothesis of schizophrenia: making sense of it all. Curr Psychiatry Rep *9*, 329-336.

Tooze, S.A., Martens, G.J., and Huttner, W.B. (2001). Secretory granule biogenesis: rafting to the SNARE. Trends Cell Biol *11*, 116-122.

Treiser, S.L., Cascio, C.S., O'Donohue, T.L., Thoa, N.B., Jacobowitz, D.M., and Kellar, K.J. (1981). Lithium increases serotonin release and decreases serotonin receptors in the hippocampus. Science *213*, 1529-1531.

Trimble, W.S., Cowan, D.M., and Scheller, R.H. (1988). VAMP-1: a synaptic vesicle-associated integral membrane protein. Proc Natl Acad Sci U S A *85*, 4538-4542.

Tsai, J., and Douglas, M.G. (1996). A conserved HPD sequence of the J-domain is necessary for YDJ1 stimulation of Hsp70 ATPase activity at a site distinct from substrate binding. J Biol Chem *271*, 9347-9354.

Tucker, W.C., Edwardson, J.M., Bai, J., Kim, H.J., Martin, T.F., and Chapman, E.R. (2003). Identification of synaptotagmin effectors via acute inhibition of secretion from cracked PC12 cells. J Cell Biol *162*, 199-209.

Umbach, J.A., and Gundersen, C.B. (1997). Evidence that cysteine string proteins regulate an early step in the Ca2+-dependent secretion of neurotransmitter at Drosophila neuromuscular junctions. J Neurosci *17*, 7203-7209.

Umbach, J.A., Saitoe, M., Kidokoro, Y., and Gundersen, C.B. (1998). Attenuated influx of calcium ions at nerve endings of csp and shibire mutant Drosophila. J Neurosci *18*, 3233-3240.

Umbach, J.A., Zinsmaier, K.E., Eberle, K.K., Buchner, E., Benzer, S., and Gundersen, C.B. (1994). Presynaptic dysfunction in Drosophila csp mutants. Neuron *13*, 899-907.

Valtorta, F., Meldolesi, J., and Fesce, R. (2001). Synaptic vesicles: is kissing a matter of competence? Trends Cell Biol *11*, 324-328.

van de Goor, J., Ramaswami, M., and Kelly, R. (1995). Redistribution of synaptic vesicles and their proteins in temperature-sensitive shibire(ts1) mutant Drosophila. Proc Natl Acad Sci U S A *92*, 5739-5743.

Verhage, M., Maia, A.S., Plomp, J.J., Brussaard, A.B., Heeroma, J.H., Vermeer, H., Toonen, R.F., Hammer, R.E., van den Berg, T.K., Missler, M., Geuze, H.J., and Sudhof, T.C. (2000). Synaptic assembly of the brain in the absence of neurotransmitter secretion. Science *287*, 864-869.

Voets, T., Toonen, R.F., Brian, E.C., de Wit, H., Moser, T., Rettig, J., Sudhof, T.C., Neher, E., and Verhage, M. (2001). Munc18-1 promotes large dense-core vesicle docking. Neuron *31*, 581-591.

Wall, D., Zylicz, M., and Georgopoulos, C. (1994). The NH2-terminal 108 amino acids of the Escherichia coli DnaJ protein stimulate the ATPase activity of DnaK and are sufficient for lambda replication. J Biol Chem *269*, 5446-5451.

Wang, H.Y., and Friedman, E. (1989). Lithium inhibition of protein kinase C activation-induced serotonin release. Psychopharmacology (Berl) *99*, 213-218.

Wang, Y., and Tang, B.L. (2006). SNAREs in neurons--beyond synaptic vesicle exocytosis (Review). Mol Membr Biol *23*, 377-384.

Washbourne, P., Thompson, P.M., Carta, M., Costa, E.T., Mathews, J.R., Lopez-Bendito, G., Molnar, Z., Becher, M.W., Valenzuela, C.F., Partridge, L.D., and Wilson, M.C. (2002). Genetic ablation of the t-SNARE SNAP-25 distinguishes mechanisms of neuroexocytosis. Nat Neurosci *5*, 19-26.

Weber, T., Parlati, F., McNew, J.A., Johnston, R.J., Westermann, B., Sollner, T.H., and Rothman, J.E. (2000). SNAREpins are functionally resistant to disruption by NSF and alphaSNAP. J Cell Biol *149*, 1063-1072.

Weber, T., Zemelman, B.V., McNew, J.A., Westermann, B., Gmachl, M., Parlati, F., Sollner, T.H., and Rothman, J.E. (1998). SNAREpins: minimal machinery for membrane fusion. Cell *92*, 759-772.

Weidman, P.J., Melancon, P., Block, M.R., and Rothman, J.E. (1989). Binding of an N-ethylmaleimide-sensitive fusion protein to Golgi membranes requires both a soluble protein(s) and an integral membrane receptor. J Cell Biol *108*, 1589-1596.

Weng, N., Baumler, M.D., Thomas, D.D., Falkowski, M.A., Swayne, L.A., Braun, J.E., and Groblewski, G.E. (2009). Functional role of J domain of cysteine string protein in Ca2+-dependent secretion from acinar cells. Am J Physiol Gastrointest Liver Physiol *296*, G1030-1039.

White, S.R., and Lauring, B. (2007). AAA+ ATPases: achieving diversity of function with conserved machinery. Traffic *8*, 1657-1667.

Whiteheart, S.W., Griff, I.C., Brunner, M., Clary, D.O., Mayer, T., Buhrow, S.A., and Rothman, J.E. (1993). SNAP family of NSF attachment proteins includes a brain-specific isoform. Nature *362*, 353-355.

Wimmer, C., Hohl, T.M., Hughes, C.A., Muller, S.A., Sollner, T.H., Engel, A., and Rothman, J.E. (2001). Molecular mass, stoichiometry, and assembly of 20 S particles. J Biol Chem *276*, 29091-29097.

Xu, T., Ashery, U., Burgoyne, R.D., and Neher, E. (1999). Early requirement for alpha-SNAP and NSF in the secretory cascade in chromaffin cells. EMBO J *18*, 3293-3304.

Xue, M., Reim, K., Chen, X., Chao, H.T., Deng, H., Rizo, J., Brose, N., and Rosenmund, C. (2007). Distinct domains of complexin I differentially regulate neurotransmitter release. Nat Struct Mol Biol *14*, 949-958.

Xue, M., Stradomska, A., Chen, H., Brose, N., Zhang, W., Rosenmund, C., and Reim, K. (2008). Complexins facilitate neurotransmitter release at excitatory and inhibitory synapses in mammalian central nervous system. Proc Natl Acad Sci U S A *105*, 7875-7880.

Young, C.E., Arima, K., Xie, J., Hu, L., Beach, T.G., Falkai, P., and Honer, W.G. (1998). SNAP-25 deficit and hippocampal connectivity in schizophrenia. Cereb Cortex *8*, 261-268.

Young, J.W., Zhou, X., and Geyer, M.A. (2010). Animal models of schizophrenia. Curr Top Behav Neurosci *4*, 391-433.

Yu, R.C., Jahn, R., and Brunger, A.T. (1999). NSF N-terminal domain crystal structure: models of NSF function. Mol Cell *4*, 97-107.

Zarate, C.A., Jr., Singh, J., and Manji, H.K. (2006). Cellular plasticity cascades: targets for the development of novel therapeutics for bipolar disorder. Biol Psychiatry *59*, 1006-1020.

Zhang, H., Kelley, W.L., Chamberlain, L.H., Burgoyne, R.D., and Lang, J. (1999). Mutational analysis of cysteine-string protein function in insulin exocytosis. J Cell Sci *112 (Pt 9)*, 1345-1351.

Zhang, H., Kelley, W.L., Chamberlain, L.H., Burgoyne, R.D., Wollheim, C.B., and Lang, J. (1998). Cysteine-string proteins regulate exocytosis of insulin independent from transmembrane ion fluxes. FEBS Lett *437*, 267-272.

Zhang, H., Peters, K.W., Sun, F., Marino, C.R., Lang, J., Burgoyne, R.D., and Frizzell, R.A. (2002a). Cysteine string protein interacts with and modulates the maturation of the cystic fibrosis transmembrane conductance regulator. J Biol Chem *277*, 28948-28958.

Zhang, H., Schmidt, B.Z., Sun, F., Condliffe, S.B., Butterworth, M.B., Youker, R.T., Brodsky, J.L., Aridor, M., and Frizzell, R.A. (2006). Cysteine string protein monitors late steps in cystic fibrosis transmembrane conductance regulator biogenesis. J Biol Chem *281*, 11312-11321.

Zhang, X., Kim-Miller, M.J., Fukuda, M., Kowalchyk, J.A., and Martin, T.F. (2002b). Ca2+-dependent synaptotagmin binding to SNAP-25 is essential for Ca2+-triggered exocytosis. Neuron *34*, 599-611.

Zhu, D., Dix, D.J., and Eddy, E.M. (1997). HSP70-2 is required for CDC2 kinase activity in meiosis I of mouse spermatocytes. Development *124*, 3007-3014.

Zinsmaier, K.E., Eberle, K.K., Buchner, E., Walter, N., and Benzer, S. (1994). Paralysis and early death in cysteine string protein mutants of Drosophila. Science *263*, 977-980.

Zinsmaier, K.E., Hofbauer, A., Heimbeck, G., Pflugfelder, G.O., Buchner, S., and Buchner, E. (1990). A cysteine-string protein is expressed in retina and brain of Drosophila. J Neurogenet *7*, 15-29.